PhD-FSTM-2025-099
The Faculty of Science, Technology and Medicine

DISSERTATION

Defence held on 21/10/2025 in Esch-sur-Alzette

to obtain the degree of

DOCTEUR DE L'UNIVERSITÉ DU LUXEMBOURG

EN BIOLOGIE

by

Félicia JEANNELLE
Born on 17 May 1997 in Langres (France)

NORADRENERGIC DYSFUNCTION AND ASTROCYTE HETEROGENEITY ALONG THE LOCUS COERULEUS-HIPPOCAMPUS AXIS IN ALZHEIMER'S DISEASE AND RELATED DEMENTIA

Dissertation defence committee

Prof. Dr. Michel Mittelbronn, Dissertation Supervisor
Professor, University of Luxembourg, Luxembourg

Prof. Dr. Stephanie Kreis (Chair)
Professor, University of Luxembourg, Luxembourg

Prof. Dr. Rejko Krüger
Professor, University of Luxembourg, Luxembourg

Prof. Dr. Dietmar Rudolf Thal
Professor, KU Leuven, Belgium

Prof. Dr. Pierre Magistretti
Professor, King Abdullah University of Science and Technology, Kingdom of Saudi Arabia

Noradrenergic Dysfunction and Astrocyte Heterogeneity along the Locus Coeruleus-Hippocampus Axis in Alzheimer's Disease and Related Dementia

A PhD Dissertation by

Félicia JEANNELLE

Doctor of Biology

Submitted to the University of Luxembourg

Doctoral School in Science and Engineering (DSSE)

Doctoroal Program in Systems and Molecular Biomedicine

Dissertation defence committee

Prof. Dr. Michel Mittelbronn, Dissertation Supervisor

Professor, University of Luxembourg, Luxembourg

Prof. Dr. Stephanie Kreis (Chair)

Professor, University of Luxembourg, Luxembourg

Prof. Dr. Rejko Krüger

Professor, University of Luxembourg, Luxembourg

Prof. Dr. Dietmar Rudolf Thal

Professor, KU Leuven, Belgium

Prof. Dr. Pierre Magistretti

Professor, King Abdullah University of Science and Technology, Kingdom of Saudi Arabia

Funded by

Luxembourg National Research Fund

Affidavit / Statement of originality

I declare that this thesis:

- is the result of my own work. Any contribution from any other party, and any use of generative artificial intelligence technologies have been duly cited and acknowledged;
- is not substantially the same as any other that I have submitted, and;
- is not being concurrently submitted for a degree, diploma or other qualification at the University of Luxembourg or any other University or similar institution except as specified in the text.

With my approval I furthermore confirm the following:

- I have adhered to the rules set out in the University of Luxembourg's Code of Conduct and the Doctoral Education Agreement (DEA)[1], in particular with regard to Research Integrity.
- I have documented all methods, data, and processes truthfully and fully.
- I have mentioned all the significant contributors to the work.
- I am aware that the work may be screened electronically for originality.

I acknowledge that if any issues are raised regarding good research practices based on the review of the thesis, the examination may be postponed pending the outcome of any investigation of such issues. If a degree was conferred, any such subsequently discovered issues may result in the cancellation of the degree.

Approved on 2025-07-29

[1] If applicable (DEA is compulsory since August 2020)

“ […] que trépasse si je faiblis !”

– Godefroy Amaury de Malefète, comte de Montmirail, d’Apremont et de Papincourt.

Acknowledgments

I would like to express my deepest gratitude to everyone who has supported me over the past four years, beginning with the University of Luxembourg and the Luxembourg National Research Fund for supporting my PhD studies and for giving me the opportunity to attend conferences and summer schools to present my project.

I am sincerely grateful to the patients and their families, whose generosity and participation make research progress possible. My thoughts are also with all the little mice that played an essential role in helping me advance this project.

I would like to express my greatest gratitude to my co-supervisor, Dr. David Bouvier, without whom this project would not have been possible. Thank you so much for having guided me throughout this PhD journey. Your infallible passion and dedication for your work were very inspiring and always pushed me to give the best of myself. You have undoubtedly passed on your passion for the most beautiful cell type in the brain to me! Thank you for everything.

Special thanks go to Dr. Tony Heurtaux, my first internship supervisor and thesis advisor, who inspired me to pursue a career in research. You were, and still are, a great inspiration to me, both professionally and personally, with your endless enthusiasm, joy and kindness. Thank you for having being here during all these years, never far away.

I am also profoundly thankful to my PhD supervisor, Prof. Michel Mittelbronn, who gave me the opportunity to join the team and trusted me with this PhD project. Thank you for your continuous support, for your advice and for the instructive discussions we shared.

I would like to thank my CET members, Dr. Lasse Sinkonnen and Prof. Matthew Holt for providing me with their insightful advice and encouraging feedback during my PhD. I would also like to acknowledge the jury members of my defence committee, Prof. Dietmar Thal, Prof. Pierre Magistretti, Prof. Stephanie Kreis and Prof. Rejko Krüger, for taking the time to evaluate and examine my thesis.

I want to thank my colleagues from the NCPR group David, Mónica, Sophie, Zahraa, Denis, Céline and Morgane and all the past members of the LCNP group for your support and all your advice. Thank you Gaël for your amazing work with our data and especially for your patience. Thank you Jay and Ziad for having being here, replying to my (sometimes stupid) questions and making (sometimes stupid) jokes! Thank you Sonja, Camille and Lorraine for all your "senior" and precious PhD, scientific and

technical advice. A big thank you to the Immuno Girls and the entire diagnostic team of the LNS for your endless help!

My deepest thank you goes to Sophie and Mónica, my Girls who are doing experiments, for your infallible support, your kindness, your patience, your precious friendship and, of course, for the gossips! You made this PhD journey much easier and funnier and I don't have enough words to thank you for that!

Un énorme merci à mes parents qui m'ont permis d'en arriver là, pour avoir cru en moi jusqu'au bout et pour toutes ces heures au téléphone qui m'ont été, et me le sont toujours, si précieuses. Je ne vous dirai jamais assez merci pour tout ! Evidemment, un grand merci à ma grande sœur, mes grands frères, mes nièces et neveux, ainsi que les compagnes et compagnons, pour être là, toujours présents, que ça soit à 500 mètres ou à 600 km ! Merci du fond du cœur.

Aux copains, merci pour votre compréhension, votre patience mais aussi votre soutien, désolée si j'ai posé des lapins, et à tout vite pour trinquer à tout ce que j'ai raté ces dernier(e)s mois/années.

Enfin, mille et une fois merci à mon soutien de tous les jours, Romain François, qui n'a jamais failli à sa mission de supporter aux premières loges. Ta patience admirable, tes encouragements, ton réconfort et ton toi tout entier m'ont été indispensables pour arriver jusqu'ici. J'espère pouvoir être toujours là pour toi comme tu l'as été pour moi. Merci pour tout.

Thank you all!!

Table of Contents

List of Abbreviations

Aβ	Amyloid-beta
Ace	Angiotensin I converting enzyme
Ace 2	Angiotensin converting enzyme 2
AD	Alzheimer's disease
ADHD	Attention-deficit/hyperactivity disorder
ADRA1A	Adrenoceptor Alpha 1A
ADRA2C	Adrenoceptor Alpha 2C
ALDH1L1	Aldehyde dehydrogenase 1 family member L1
ALDH7A1	Aldehyde dehydrogenase 7 family member 1
APOE	Apolipoprotein
APP	Amyloid precursor protein
AQP4	Aquaporine 4
BBB	Blood-brain-barrier
CA	Cornu ammonis
Ca^{2+}	Calcium
Camk4	Calcium/calmodulin dependent protein kinase IV
cAMP	Cyclic adenosine monophosphate
Cartpt	CART prepropeptide
CBS	Cystathionine Beta-Synthase
cIHC	Chromogenic immunohistochemistry
CNS	Central nervous system
CSF	Cerebrospinal fluid
CTL	Control
DA	Dopamine
DAA	Diseased-associates astrocytes
DAB	3,3'-diaminobenzidine
DG	Dentate gyrus
DLB	Dementia with Lewy bodies
DMEM	Dulbecco's Modified Eagle Medium
EC	Entorhinal cortex

EOAD	Early-onset AD
FBS	Fetal bovine serum
FFPE	Formalin-fixed paraffin-embedded
GABA	Gamma-aminobutyric acid
GBA	Glucocerebrosidase
GFAP	Glial Fibrillary Acidic Protein
GLAST	Glutamate aspartate transporter
GM-CSF	Granulocyte-macrophage colony-stimulating factor
GPC5	Glypican 5
GSH	Glutathione
H_2S	Hydrogen sulfide
Hcy	Homocystein
HHcy	Hyperhomocysteinemia
Hmox1	Heme oxygenase 1
IFNγ	Interferon-gamma
IL1β	Interleukine 1-beta
IL-3	Interleukine 3
LB	Lewy body
LBD	Lewy body dementia
LC	Locus coeruleus
LN	Lewy neurites
LRKK2	Leucine Rich-Repeat Kinase 2
LTP	Long-term potentiation
MACS	Magnetic cell sorting
MAPT	Microtubule-associated protein tau
MCI	Mild cognitive impairment
MCP1	Monocyte chemotactic protein-1
MHC	Major histocompatibility complex
MS	Multiple sclerosis
NA	Noradrenaline
NFT	Neurofibrillary tangles
NDD	Neurodegenerative diseases

Nqo1	NAD(P)H quinone dehydrogenase 1
NSD-ISS	Neuronal α-synuclein disease integrated staging system
OPCs	Oligodendrocyte progenitor cells
PD	Parkinson's disease
PDD	Parkinson's disease with dementia
PFA	Paraformaldehyde
PFC	Prefrontal cortex
PHC	Parahippocampal cortex
PHF	Paired-helical filaments
PINK1	PTEN-induced kinase 1
PRKN	Parkin
PSEN	Presenilin
PSD95	Post-Synaptic Density Protein 95
pTau	Hyperphosphorylated tau
ROS	Reactive oxygen species
Rpl27	Ribosomal protein L27
S100b	S100 calcium binding protein B
Scg2	Secretogranin II
SNCA	Synuclein alpha
Sod3	Superoxide dismutase 3
SPARC	Secreted protein acidic and rich in cysteine
Srxn1	Sulfiredoxin-1
TDP-43	TAR DNA-binding protein 43
TNFα	Tumor necrosis alpha
TSP	Thrombospondin
VGAT	Vesicular GABA Transporter
VGLUT1	Vesicular Glutamate Transporter 1
VMAT2	Vesicular Monoamine Transporter 2
WHO	World Health Organization

List of Tables

List of Figures

List of Publications & Manuscripts

Jeannelle F. Miranda de la Maza M., Hammer G.P, Schreiner S., Mittelbronn M., Bouvier D.S. Selective expression of astrocyte markers identifies GPC5 as a subtype-specific signature in Alzheimer's disease and related dementias. 2025. https://doi.org/10.1101/2025.08.19.671074. *BioRxiv.*

Jeannelle F. Miranda de la Maza M., Schreiner S., Hammer G.P, Heurtaux T., Muller A., Mittelbronn M., Bouvier D.S. Noradrenaline modulation of astrocytic molecular signatures is disrupted in Alzheimer's and Parkinson's dementia. 2025. *Ready to submit*.

Fixemer S.*, Miranda de la Maza M.*, Hammer G. P., **Jeannelle F.**, Schreiner S., Gérardy J-J., Boluda S., Mirault D., Mechawar N., Mittelbronn M., Bouvier D.S. Microglia aggregates define distinct immune and neurodegenerative niches in Alzheimer's disease hippocampus. *Acta Neuropathologica.* 2025; 10.1007/s00401-025-02857-8. *(not included in the thesis)*

Mencke P., Ohnmacht J., **Jeannelle F.**, Ries A., Miranda de la Maza M., Ullrich M., Massart F., Mulica P., Badanjak K., Hanss Z., Rybicki A., Antony P., Delcambre S., Arena G., Cruciani G., Jarazo J., Gavotto F., Jaeger C., Ewen A., Pacheco M.P., Brenner D., Schwamborn J-C., Sauter T., Sinkkonen L., Dittmar G., Bouvier D.S., Meiser J., Gruenewald A., Bonifati V., Platten M., Krueger R., Boussaad I. DJ-1 mediates regulation of metabolism and immune response in Parkinsons' disease astrocytes and Glioblastoma cells. *BioRxiv* (preprint). 2024; 10.1101/2024.10.31.621212. *(not included in the thesis)*

Bouvier D.S., Fixemer S., Heurtaux T., **Jeannelle F.**, Frauenknecht K.B.M, Mittelbronn M. The multifaceted neurotoxicity of astrocytes in ageing and age-related neurodegenerative diseases: a translational perspective. *Front. Physiol*. 2022; 10.3389/fphys.2022.814889.

Abstract

Neurodegenerative diseases (NDDs) such as Alzheimer's disease (AD) and Parkinson's disease (PD) represent an increasing economic and medical challenge due to the ageing population and a partial understanding of the detrimental mechanisms. These age-related disorders share several pathological hallmarks such as abnormal intra- and extracellular misfolded protein aggregation. Yet, the implication of astrocytes, one of the major glial cell types with key physiological functions (e.g. maintenance of brain homeostasis, neuroprotection, etc.), and their relationship to early noradrenergic system deterioration still need to be further investigated. After decades on the sidelines, recent research has revealed the significant contribution of astrocytes to the progression of neurodegeneration. They are known to change their properties and react to brain insults, with exhibiting a spectrum of reactive responses which may become toxic under certain conditions. Noradrenaline (NA) is a strong modulator of astrocytes and has potent anti-inflammatory and anti-oxidative effects on these cells. Interestingly, it has been shown that an alteration of the noradrenergic system affects glial cells in AD and PD. However, how NA system disruption affects astrocyte function and responses in such disorders is still poorly understood. Furthermore, the astrocytic heterogeneity is increasingly recognised, since astrocytes exhibit notable diversity in morphologies, properties and functionality between and within brain regions. Nevertheless, their heterogeneity is still poorly considered as a factor of regional vulnerability and/or in the progression of NDDs. This PhD thesis addressed two crucial aspects of astrocyte implication in NDDs pathophysiology. The first study provides a detailed characterisation of the heterogeneity of the hippocampal astrocytes and their distribution within the hippocampus of healthy individuals as well as patients with AD and PD with dementia (PDD). Using a high-content neuropathological approach involving chromogenic immunohistochemistry and digital pathology, we discovered specific distribution patterns of astrocyte markers, suggesting the existence of distinct subpopulations with region-specific vulnerabilities and molecular signatures. In addition, we also emphasise the importance of incorporating new markers in order to capture the full astrocytic response to neurodegeneration. The second study provides a comprehensive understanding of the modulatory role of NA on astrocyte physiology and responses. By combining bulk RNA sequencing on primary mouse astrocytes with RT-qPCR, cytokine assays and digital pathology analyses on *post-mortem* brain samples, we demonstrated that NA influences core astrocyte functions, and that the expression of NA-

sensitive genes in hippocampal astrocytes is severely altered in NDDs. Our results suggest that the intimate relationship between the noradrenergic system and the astrocytes affords a significant phenotypic control of the astrocytes by NA and may be drastically impacted in disease. NA deprivation might lead to altered astrocyte roles and impaired neuroprotection, thus enhancing pathology progression.

Part I: Scope & Outline

Alzheimer's disease (AD) and Parkinson's disease (PD) are the most common age-related neurodegenerative diseases (NDDs) and the main causes of dementia. They share many cognitive symptoms and cellular changes, including progressive cognitive decline.

A few decades ago, astrocytes, one of the main glial cell types in the brain, started to attract the attention of the scientific community due to their potential active roles in neurodegeneration. However, their exact implication remains poorly understood and underestimated. Recent single-cell and single-nucleus transcriptomic analyses have revealed the highly complex heterogeneity of mouse astrocytes that guides their phenotypes and responses (Green et al. 2024; Habib et al. 2020). These analyses have also shown that astrocyte subpopulations change their signatures in disease states. However, whether human astrocyte heterogeneity may be involved in regional-vulnerability and disease progression remains poorly understood.

NDDs are also characterised by degeneration of the locus coeruleus (LC), a small brainstem nucleus comprising noradrenaline (NA)-producing neurons, leading to a progressive alteration of the noradrenergic system. The LC innervates several brain regions including the hippocampus, a crucial brain structure for memory processes. Hence, the LC-NA system has been shown to play a pivotal role in processes such as arousal, anxiety, learning and memory as well as neuronal survival and neuroinflammation. Indeed, NA is a potent modulator of neurons and glial cells, especially astrocytes, regulating their phenotypes and responses. Interestingly, it has been demonstrated that altering the NA system affects glial cells in AD and PD (Zorec et al. 2018; Evans et al. 2024a; Yao et al. 2015; Braun et al. 2014). This suggests that NA deprivation could be a factor in impaired neuroprotection and neurodegeneration progression. While the alteration of the NA system has been proposed as a cause of NDDs, it remains unclear whether LC alteration and NA depletion drive the onset of cognitive and behavioural phenotypes.

The overarching goals of my PhD project were twofold: (**i**) to define the multifaceted responses of astrocytic subgroups in the hippocampus of AD and PD with dementia (PDD) patients, and (**ii**) to characterise the modulatory role of NA on astrocyte phenotype and responses *in vitro*, under both homeostatic and inflammatory conditions. This study was performed to improve our understanding of the astrocytic heterogeneity in disease context, as well as the impact of NA deprivation on astrocytes and its consequences on memory-associated brain regions, particularly the hippocampus. Therefore, we took advantage of our large collection of *post-mortem* samples from non-demented individuals, AD

and PDD patients to investigate the noradrenergic system and the astrocyte heterogeneity across neurodegenerative conditions.

The results of the current project are presented in ***Part IV*** across **chapters I** (preprint in BioRxiv) and **II** (ready-to-submit) and discussed in ***Part V***, followed by final conclusions and perspectives in ***Part VI***. The multifaceted identity of the astrocytes in ageing and NDDs is reviewed in ***Part IV***, **Chapter III**, published in Frontiers in Physiology.

Part IV: Chapter I – Manuscript I – In this chapter, I present the manuscript entitled "GPC5 expression highlights astrocytic heterogeneity and divergent hippocampal responses in Alzheimer's and Parkinson's Dementia". In this article, we highlighted the degree of astrocyte heterogeneity in the hippocampus of healthy individuals and investigated whether this heterogeneity is affected in AD and PDD patients. We identified a new astrocytic subtype, the GPC5-positive astrocytes, with specific molecular signature and responses to neurodegeneration. We also proposed the use of multiple astrocytic markers such as AQP4, ALDH1L1 and ALDH7A1 for monitoring astrocyte changes in disease states.

Part IV: Chapter II – Manuscript II – This chapter concerns the manuscript entitled "Noradrenaline modulation of astrocytic molecular signatures is disrupted in Alzheimer's and Parkinson's dementia", in which the main findings of the characterisation of the NA effect on astrocyte phenotype and responses are described. This article also shows the molecular signatures of astrocytes to DA exposure. We also investigated the expression of NA-sensitive genes in the hippocampus of healthy, AD and PDD cases.

Part IV: Chapter III – Manuscript III – This chapter presents the manuscript entitled "The multifaceted neurotoxicity of the astrocytes in ageing and age-related neurodegenerative diseases: a translational perspective", in which we reviewed astrocyte responses in ageing and NDDs from a translational perspective. In addition, we discussed how reactive astrocytes become neurotoxic and whether they could be interesting therapeutic targets.

Part II: Introduction

"*I am writing to share a story with you, specifically for you. My hope is that it will help you understand your patients along with their spouses and caregivers a little more. And as for the research you do, perhaps this will add a few more faces behind the why you do what you do.*" – Susan Schneider Williams in her letter "The terrorist inside my husband's brain", wife of Robin Williams who severely suffered from Lewy Body Dementia (Williams 2016). This letter is a meaningful testament to the importance of our research for patients with neurodegenerative diseases and, above all, for their beloved ones. Despite centuries of inquiry into the complexities of the brain, and decades of dedicated research into neurodegeneration, many aspects remain poorly understood and continue to challenge the development of effective diagnostic tools and therapeutic strategies. To understand brain processes in health and disease, it is crucial to take a multi-layered point of view that encompasses cellular physiology, responses and interactions. This doctoral project makes a scientific contribution by characterising astrocytes identities and responses in both homeostatic and diseased states and their relationship to one of the most potent neuromodulators, the noradrenaline.

1. Age-related neurodegenerative diseases and associated dementia

Neurodegenerative diseases (NDDs) represent a heterogeneous group of neurological disorders characterised by a progressive loss of neurons in the central nervous system (CNS) or peripheral nervous system. These diseases, including Alzheimer's disease (AD), Parkinson's disease (PD) and dementia with Lewy body (DLB), share multiple hallmarks such as, among others, the deposition of pathological protein aggregates, altered neuronal networks and neuroinflammation (**Figure 1**), all leading to dementia. Dementia is a syndrome described as a progressive and irreversible cognitive decline that interferes with daily life and independence. Nowadays, over 55 million people worldwide are affected by dementia, including around 7,500 people in Luxembourg, with numbers expected to triple to 150 million by 2050, according to the World Health Organization (WHO).

AD is the main cause of dementia, accounting for 60-70% of cases, followed by DLB. Both diseases, as well as PD, are defined by a prodromal phase that can begin up to 20 years prior to diagnosis and during which time no notable but still identifiable symptoms (from medical records) are present (e.g. mild cognitive impairment, sleep deprivation, constipation) (Mellergaard et al. 2023; Roos et al. 2022). If only 5-15% of cases have a genetic cause, the vast majority of AD, DLB and PD cases are sporadic, resulting from a complex interplay of ageing, lifestyle and environmental factors in addition to genetic

susceptibility (without a familial pattern). The sporadic form, the causes of which are still not understood, poses an exceptional challenge to the scientific community whose struggles to develop therapies that not only alleviate symptoms or slow down disease progression, but also that have the potential to halt the disease. Multidisciplinary research is crucial for unravelling the causes of neurodegeneration, understanding the mechanisms behind these diseases, and ultimately, identifying potential targets for novel biomarkers or therapeutic strategies.

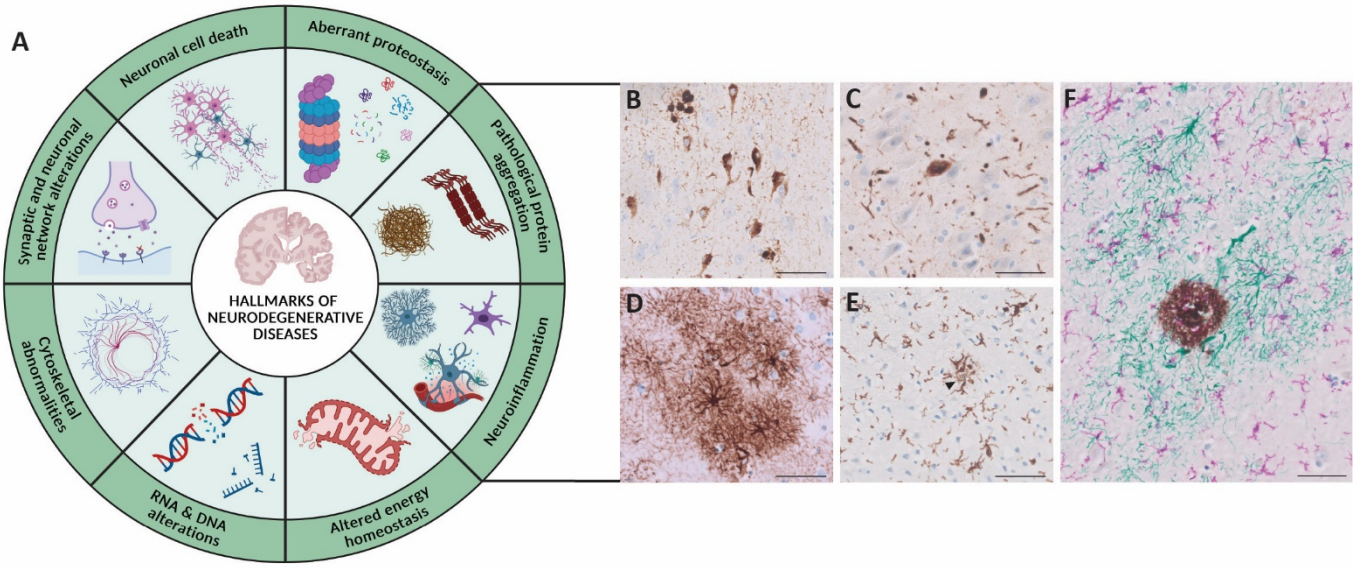

Figure 1: Pathological hallmarks of neurodegenerative diseases and evidence from the human hippocampus.

A *The last decades of translational and clinical research allow to identify eight NDDs hallmarks shared by AD, DLB and PD. Adapted from Wilson et al., 2023 (Wilson et al. 2023) and created with BioRender.* ***B-F*** *Representative IHC of pathological hallmarks from post-mortem FFPE brain samples.* ***B*** *In AD, AT8 (DAB) stains phospho-tau and labels flame-shaped neurofibrillary tangles enwrapping pyramidal neurons.* ***C*** *Anti-pSyn staining (DAB) in the CA3 of a patient with PDD.* ***D*** *GFAP staining (DAB) in AD hippocampus reveals hypertrophic astrocytes.* ***E*** *Iba1 (DAB) labels microglia that can be found in small clusters (full arrow) in AD hippocampus.* ***F*** *Multiplex IHC revealing an Aβ plaque (4G8, DAB) surrounded by a reactive glial net composed of hypertrophic astrocytes (GFAP, green) and activated microglia (Iba1, purple) in the AD hippocampus. Scale bars: 50 µm. Own microscopic images.*

1.1. Alzheimer's and Parkinson's disease: distinct disorders with common threads.

In 1906, Prof. Alois Alzheimer described for the first time the clinical case of Auguste Deter who suffered from an "unusual illness of the cerebral cortex" ("*Eine eigenartige Erkrankung der Hirnrinde*"), which later became known as AD. In his clinical report, A. Alzheimer depicted a progressive cognitive impairment with hallucinations, delusions and psychosocial alterations, highlighting a rapid loss of memory and a severe disorientation in time and space. His *post-mortem* analysis described an evenly atrophic brain as well as neurofibrillary tangles replacing neurons (Stelzmann et al. 1995).

PD, by contrast, was first clinically documented by James Parkinson in his 1817 essay, " An Essay on the Shaking Palsy", in which he described "*involuntary tremulous motion, with lessened muscular power, in parts not in action and even when supported […] the senses and intellects being uninjured*" (Parkinson 2002). Today, PD is recognised as a complex neurodegenerative disorder that includes not only motor symptoms, but also a wide range of non-motor features. As a result, two different forms of PD have been identified (Sezgin et al. 2019): PD with mild cognitive impairment (PD-MCI) and PD with dementia (PDD), which, alongside AD, will be the focus of this thesis manuscript. PDD is classified as a Lewy body dementia (LBD), together with DLB, and clinically characterised by fluctuating cognition (e.g. variations in attention and alertness) and behavioural changes (e.g. apathy, anxiety), parkinsonian motor symptoms (e.g. bradykinesia, rest tremor or rigidity), visual hallucinations and disruption of sleep-wake cycles, that might precede severe cognitive impairment (Sezgin et al. 2019).

Hence, these NDDs share several clinical features: while cognitive impairment is a relatively common feature in patients with PD (Riedel et al. 2010; Fang et al. 2020), some parkinsonian symptoms are also observed in individuals diagnosed with AD (Wilson et al. 2000; Ono et al. 2025). However, despite these overlapping hallmarks, AD and PDD exhibit substantial pathological heterogeneity.

At the genetic level, distinct gene mutations are responsible for the development of AD or PD(D) phenotypes. Familial forms of AD, also known as early-onset AD (EOAD), are genetically inherited from rare, highly penetrant mutations in the amyloid precursor protein (*APP*), presenilin 1 (*PSEN1*) and presenilin 2 (*PSEN2*) genes (Andrews et al. 2023). Genetic variants responsible for developing familial PD forms include mutations in *PRKN* (encoding Parkin), *SNCA* (encoding Synuclein Alpha), *PINK1* (encoding PTEN-induced kinase 1), and *LRKK2* (encoding Leucine Rich-Repeat Kinase 2) genes, among others (Funayama et al. 2023). There are additional genetic risk factors that are specifically involved in the development of cognitive impairment in PD, including mutations in *GBA* (encoding

Glucocerebrosidase), *MAPT* (encoding Microtubule-associated protein tau) and *APOE* (encoding Apolipoprotein) genes (Sezgin et al. 2019).

The neuropathological basis of AD mainly involves changes in the medial temporal cortex and the neocortical association areas. Such alterations underlie the characteristic impairment in episodic memory of patients with AD. In PDD patients, subcortical nuclei as well as frontal and parietal lobes are predominantly affected by the deposition of misfolded protein aggregates (see Part III, 1.2. "Misfolded proteins in AD and PD(D)"), thus affecting executive, attentional and visuospatial functions (Park et al. 2011). Although the neuropathological substrate of PD is very similar to that of PDD, the progression of the pathology differs, affecting only the brainstem and limbic areas without impacting the neocortex (Walker et al. 2019).

The next section outlines the neuropathology of AD and PDD, focusing on amyloid, tau and □-synuclein mechanisms.

1.2. Misfolded protein pathologies in AD and PDD.

One of the most extensively studied pathological hallmarks of AD and PDD is the aggregation of misfolded proteins.

In AD, this includes amyloid plaques and tau tangles and neurites (**Figure 1B, F**). Amyloid plaques are extracellular deposits consisting of fibrillary aggregates of amyloid β (Aβ) (Masters et al. 1985). Aβ is a by-product of the sequential cleavage of the neuronal, highly expressed APP by β- and γ-secretases. APP can be processed via two different pathways: the non-amyloidogenic and the amyloidogenic pathways. The non- amyloidogenic pathway involves α-secretase-mediated APP cleavage, that generates soluble N-terminal fragments (APPsα, APPsβ), and prevents Aβ production. In contrast, the amyloidogenic pathway is mediated by β-secretase cleavage and generates Aβ peptides. Indeed, APP processing produces membrane-associated C terminal fragments (CTFα, CTFβ) that are further cleaved by the γ-secretase into monomeric Aβ peptides (Guo et al. 2012). It is hypothesised that mis-regulation of APP cleavage and/or impaired clearance of APP generate excessive Aβ peptides that are prone to aggregating into oligomers and fibrils, and ultimately Aβ plaques (Guo et al. 2012; Hampel et al. 2021). The histology of Aβ plaques has been extensively studied, resulting in the establishment of a classification based on plaque morphology. This classification distinguishes between diffuse and neuritic plaques, among others. Diffuse plaques are ill-defined deposits with blurred borders, whereas neuritic plaques, also known as dense-core or focal plaques, are well-defined structures characterised

by a central dense, spherical mass surrounded by a corona of dystrophic neurites and neural cell processes (Dickson and Vickers 2001; Bussière et al. 2004; D'Andrea and Nagele 2010; Jellinger 2020). The formation and accumulation of these plaques follow spatiotemporal dynamics. Aβ deposition evolves through five phases starting first in the neocortex (frontal, temporal, parietal and occipital cortices; Thal phase 1), then affecting allocortical regions (e.g. hippocampus, entorhinal cortex, amygdala; Thal phase 2), diencephalic nuclei and basal ganglia (e.g, putamen, caudate nucleus, striatum; Thal phase 3), brainstem nuclei and medulla oblongata (Thal phase 4) and finally the cerebellum, additional brainstem nuclei (e.g. locus coeruleus) and the pons (Thal phase 5) (Thal et al. 2002; Walker 2020) .

The accumulation of hyperphosphorylated MAPT in the cell body and processes of neurons forms the neurofibrillary tangles (NFTs) and dystrophic neurites (or neuropil threads) typical of AD (Bancher et al. 1989; Braak and Braak 1988). In disease, abnormally hyperphosphorylated tau (pTau) is present in the cytosol where it inhibits the assembly of microtubules and therefore promotes the disruption of the cytoskeleton (Iqbal et al. 2009). pTau is also prone to self-aggregation forming oligomers, paired-helical filaments (PHFs), also known as pretangles, NFTs (mature tangles), and ultimately ghost tangles (dead NFT-bearing neurons that is degrading) (Guo et al. 2017). Tau pathology also evolves into different stages, appearing first in the brainstem, including the locus coeruleus, and spreading towards the transentorhinal regions (Braak NFT stage I), the entorhinal cortex (Braak NFT stage II) and the limbic brain areas (e.g. hippocampus, amygdala, perirhinal cortex) (Braak NFT stage III). In Braak NFT stage IV and V, it affects the superior temporal gyrus and the neocortex, respectively. Finally, tau pathology accumulates in primary cortical areas (Braak NFT stage VI) (Braak and Braak 1991; Thal et al. 2025).
Based on these different Aβ and NFT stages, the neuropathological assessment of AD staging is now standardised using the ABC score. This score represents the following: A–amyloid pathology (Thal phases); B–tau pathology (Braak staging); and C–neuritic plaques (C = CERAD, Consortium to Establish a Registrery for Alzheimer's Disease) (**Table 9**).

PDD pathophysiology involves the presence of α-synuclein (α-syn) inclusions, such as Lewy bodies (LBs) and Lewy neurites (LNs) in neuronal cell bodies and processes, respectively (**Figure 1 C**). Under pathological states, α-syn is susceptible to extensive post-translational modifications, such as phosphorylation. This leads to conformational changes that result in α-syn misfolding, and ultimately the formation of pre-fibrillar aggregates and highly toxic oligomers (Arias-Carrión et al. 2025). LBs and

LNs are preliminary composed of phosphorylated α-Syn aggregates. Two types of LBs have been reported in the literature: brainstem LBs, defined by an acidophilic central core and a pale-stained halo mainly observed in the substantia nigra and the locus coeruleus; and cortical LBs which are irregularly shaped, do not have a core neither a halo, and are mainly found in cortical layers V and VI and limbic brain areas, especially the amygdala (Perry et al. 1990; Outeiro et al. 2019). The mechanisms underlying the propagation of α-syn pathology appear to be more complex and less understood than those governing the spread of Aβ and NFTs. Although the majority of cases follows a rostral-caudal propagation pattern, different staging systems have been developed to assess α-syn distribution in LBD brain, including the Newcastle-McKeith criteria (McKeith et al. 2017a) and the modified version by Leverenz and colleagues (Leverenz et al. 2008), the Braak staging system (Braak et al. 2003), the unified staging of Beach and colleagues (Beach et al. 2009), and the newly proposed "neuronal α-synuclein disease integrated staging system" (NSD-ISS) (Simuni et al. 2024a; Dam et al. 2024) (**Figure 2**).

These key hallmark lesions are fundamental to the neuropathological assessment of *post-mortem* brains affected by AD or PDD. However, these misfolded protein pathologies are not mutually exclusive and often co-occur across NDD cases, thus referred to as cerebral multimorbidity (Jellinger and Attems 2015; Rahimi and Kovacs 2014). In fact, the presence of only one distinct lesion type, that defines a pure pathology, is the exception rather than the rule. Indeed, multiple *post-mortem* studies reported AD patients with LB deposition (Uchikado et al. 2006), TDP-43 inclusions (Meneses et al. 2021) and severe cerebrovascular lesions (Jellinger and Attems 2005; Iadecola and Gottesman 2018); and LBD cases with strong Aβ and tau pathology accompanied by cerebrovascular diseases (Sarro et al. 2017; Jellinger 2021). Even though the co-occurrence of misfolded protein pathologies is now widely accepted, the mechanisms behind regional vulnerability and neurodegeneration are still being elucidated.

NIAA ABC SCORE

SCORE	"**A**" – Amyloid pathology (Thal phase)	"**B**" – Tau pathology (Braak and Braak NFT stage)	"**C**" – Neuritic plaques (CERAD score)
0	0	None	None
1	1 or 2	I or II	Sparse
2	3	III or IV	Moderate
3	4 or 5	V or VI	Frequent

Table 1: National Institute on Aging-Alzheimer's Association (NIAA) ABC score for evaluating neuropathological changes in patients with AD. Adapted from Montine et al., 2011 (Montine et al. 2012); Kautzky et al., 2018 (Kautzky et al. 2018).

A

BrainNet Europe protocol

Brain areas	Medulla		Pons		Midbrain	Basal forebrain		Hippocampus		Gyrus cinguli	Temporal cortex	Frontal cortex	Parietal cortex
Anatomical region	dmV	irx	LC	R	SN	nbM	AC	CA2	TOcx	Grey matter	Grey matter	Grey matter	Grey matter
Braak stage	1	1	2	2	3	3	4	3	4	5	5	6	6
McKeith type	BRAINSTEM					LIMBIC						NEOCORTICAL	
Amygdala predominant							AC predominant						
Lesion type requested	LNs and/or (brainstem) LBs						LBs	LNs	(cortical) LBs				

B

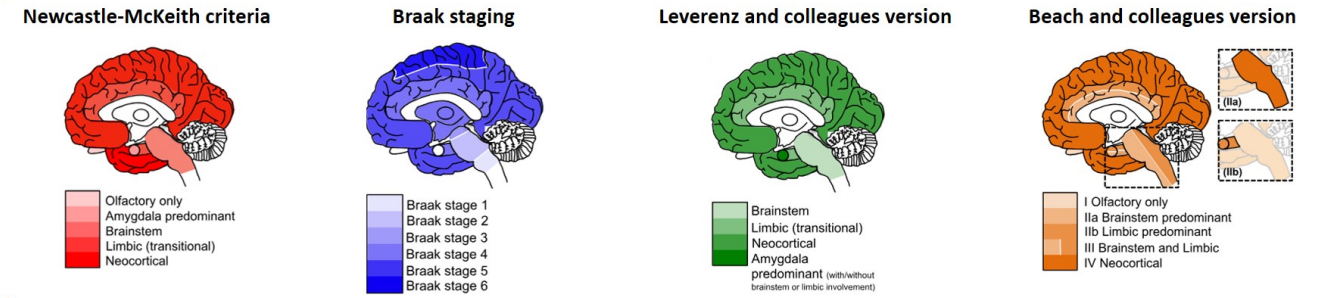

C

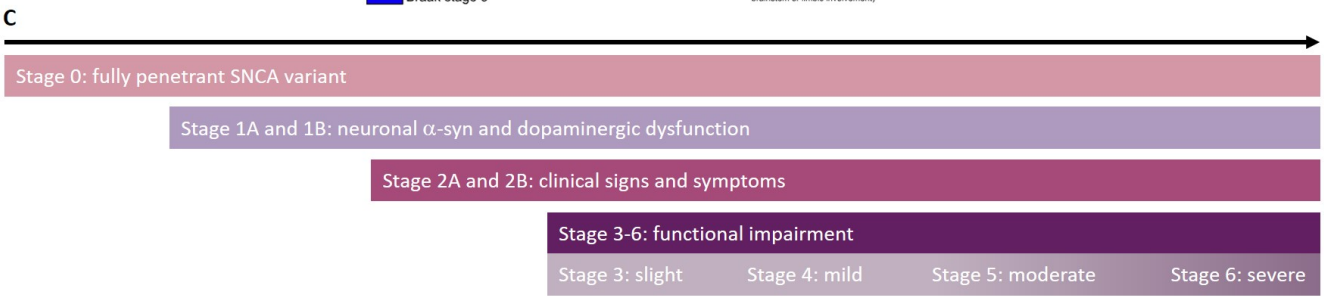

Figure 2: Staging criteria of a-Synuclein deposition in LBD brains.

A, B *The BrainNet Europe protocol has been proposed by BrainNet Europe consortium to assess the deposition of aSyn in different brain regions, using Braak stage and Newcastle-McKeith type. To meet the criteria for a Braak stage, only one of the designated regions must be affected with one of the requested lesion types (LBs or LNs). To be classified as McKeith brainstem, limbic or neocortical type, at least one of the brainstem (medulla, pons or midbrain), limbic (basal forebrain, hippocampus, gyrus cingula or temporal cortex) or neocortical (frontal or parietal cortex) regions, respectively, needs to be affected with LBs or LNs. In the amygdala (AC)-predominant type, LBs are found either exclusively in the*

AC or occur more abundantly in the AC compared to the brainstem regions. Modified criteria and staging systems have been proposed for cases where α-syn pathology is limited to the amygdala (Leverenz et al.), or the olfactory bulb (Beach et al.), or follows a limbic-predominant pathway without affecting the brainstem (Beach et al.). ***C*** *Neuronal α-synuclein disease integrated staging system (NSD-ISS) framework. Abbreviations: dmV, dorsal motor nucleus of vagus; irx, intermediate reticular zone; LC, locus coeruleus; R, raphe; SN, substantia nigra; nbM, nucleus basalis of Meynert; TOcx, temporo-occipital cortex. Adapted from Alafuzoff et al., 2009 (Alafuzoff et al. 2009); Outeiro et al., 2019 (Outeiro et al. 2019) and Simuni et al., 2024 (Simuni et al. 2024b).*

1.3. The hippocampus vulnerability as a core driver of memory impairment

The hippocampus is a crucial brain structure located in the medial temporal lobe supporting memory and learning processes (**Figure 3**). Named after its seahorse-like shape (from the Ancient Greek "hippos" – *horse*, "kampos" – *sea creature*), the hippocampus is formed by the infoldings of the dentate gyrus (DG), Cornu Ammonis (CA1, CA2, CA3 and CA4) and subiculum. The latter is continuous with the entorhinal area and the parahippocampal cortex (Duvernoy 2005). The hippocampus is the brain center of memory being involved in different forms of memory, including spatial (navigation and orientation), episodic (personal experience) and semantic (factual knowledge) memories (Ekstrom and Hill 2023; Eichenbaum 2017; Duff et al. 2020). Hippocampal processing is supported by multiple cellular connections. It notably involves the trisynaptic loop (or the polysynaptic pathway) that connects the entorhinal cortex to the DG. In turn, the granular cells of the DG projects to CA3 pyramidal neurons that send a large collateral projection to the CA1 pyramidal neurons, and finally output to subiculum (Duvernoy 2005). Moreover, the hippocampus is indirectly connected to specific components of the limbic system such as the amygdala and the thalamus thanks to its central position within the Papez circuit that links the subiculum and the entorhinal cortex to the mammillary bodies of the hypothalamus (Willis and Haines 2018).

Given its critical role in cognition, the slightest disturbance can have disastrous consequences for cognitive functions. The hippocampus is particularly vulnerable to pathological processes, and hippocampal atrophy is a hallmark of age-related NDDs**,** particularly AD. Indeed, the hippocampus and the cortex both undergo severe shrinkage alongside ventricle enlargement. This results in progressive cognitive impairments with disability in memory formation and retrieval, affecting first the episodic memory, closely followed by spatial and semantic memories (Jahn 2013). While mechanisms behind neurodegeneration is extensively studied across different NDDs, the cell-type-specific mechanisms

underlying selective hippocampal vulnerability remain unclear, particularly how ageing, the primary shared risk factor, interacts with these processes to drive region- and disease-specific vulnerability.

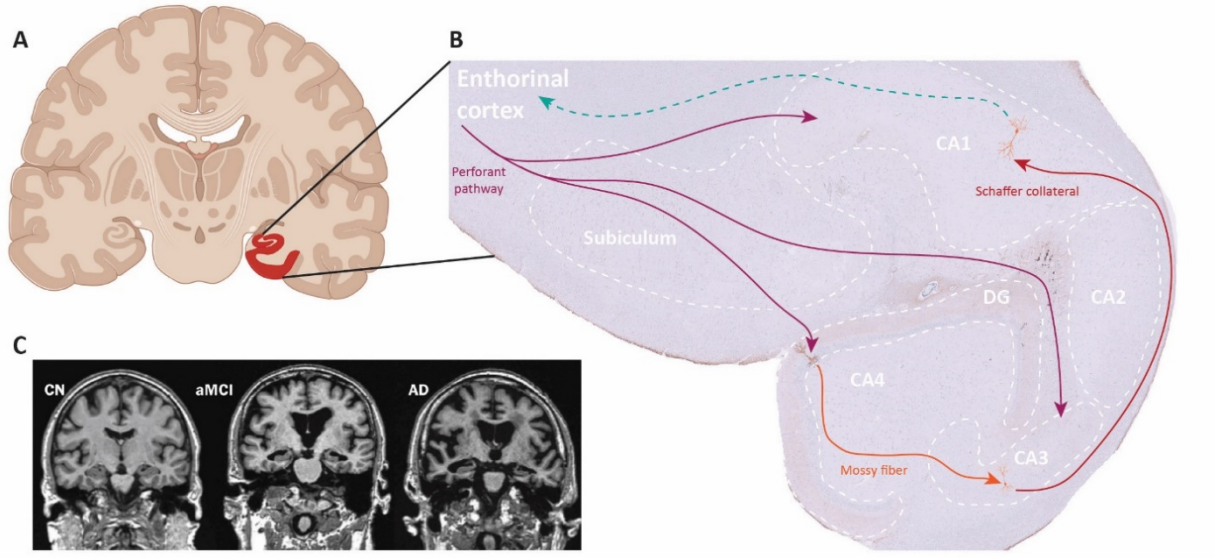

Figure 3: The human hippocampus in health and disease.

A *Coronal view of the healthy human brain revealing the hippocampal area.* ***B*** *Histological representation of the main hippocampal subregions (white dashed lines) through which the trisynaptic circuit projects. Axons from entorhinal cortex (EC) send projection to the DG through the perforant pathway (purple arrow). The DG relays the information to the pyramidal neurons in the CA3 via mossy fibers (orange arrow). In turn, the CA3 neurons projects to CA1 pyramidal cells through the Schaffer collateral. CA1 neurons send back information into deep-layer neurons of the EC (cyan dashed arrow). CA3 and CA1 pyramidal neurons also receive direct projections from the EC (purple arrows).* ***C*** *Structural MRI acquisitions in cognitively normal (CN), amnestic mild cognitive impairment (aMCI) and AD individuals show brain atrophy notably visible with brain shrinkage and ventricles enlargement. Image from Vemuri and Jack, 2010 (Vemuri and Jack 2010). Created with BioRender and Illustrator.*

2. Astrocytes, the star cells of the brain

In 1858, the term *neuroglia* ("*Nervenkitt*") is for the first time introduced to the scientific community by Rudolf Virchow who described a connective substance filling spaces between neurons, a kind of biological glue or scaffold (Kettenmann and Verkhratsky 2008). By the end of the 19th century, it had become clear that this material was composed of distinct cells with their own nuclei, and the term of *astrocyte* is finally introduced by Michael von Lenhossék in 1895 (von Lenhossék and Mills 1895). Among the key scientists in astrocyte characterisation was Ramón y Cajal, who developed a microscopic method using gold chloride sublimate. This allowed him to visualise and describe the star-shaped cells that we know now as astrocytes (y Cajal 1913). His illustrations and descriptions revealed their intricate processes and close relationships with neurons and blood vessels, forming the basis of our modern understanding of astrocyte morphology and spatial organisation (**Figure 4**).

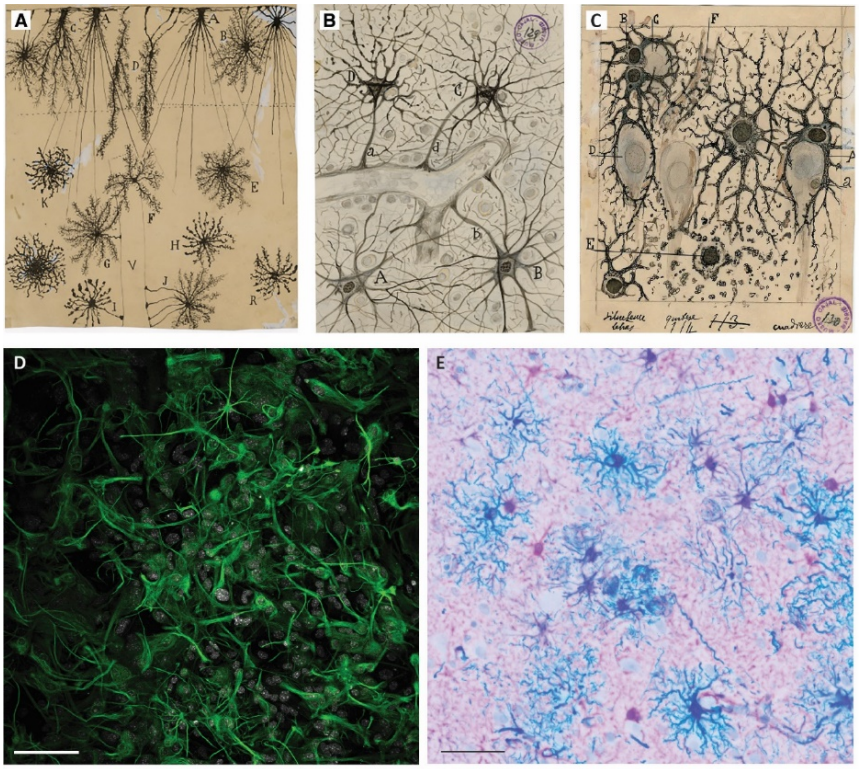

Figure 4: Astrocytes over a century of discovery: from initial descriptions to modern observations.

A-C *Using different staining methods, including the Golgi method, Santiago Ramón y Cajal was able to observe and draw astrocytes in detail from the human brain.* ***A*** *Representation of Golgi-impregnated human astroglia across cortical layers.* ***B*** *Drawing of perivascular astrocytes.* ***C*** *In this drawing, Ramón y Cajal depicted hippocampal astrocytes wrapping around pyramidal neurons. (These images are part*

of the Cajal Legacy collection at the Cajal Institute of the Spanish Research Council (CSIC) in Madrid, Spain. © CSIC 2017). ***D–E*** *Nowadays, we routinely use immunofluorescence and chromogenic immunohistochemistry for such observations.* ***D*** *3D confocal image of primary mouse astrocytes stained with GFAP (green) and DAPI (white).* ***E*** *Multiplex chromogenic immunohistochemistry image of human cortical astrocytes astrocytes stained with GFAP (teal) and ALDH1L1 (purple). Scale bars:* ***D*** *100 µm;* ***E*** *50 µm.* ***D*** *and* ***E:*** *Own microscopic images.*

2.1. The core roles of the astrocytes in the healthy brain

Astrocytes are a very large population of glial cells in the CNS, accounting for approximately 20 to 40% of all brain cells (Khakh and Sofroniew 2015), supporting CNS development, homeostasis and function (**Figure 5**). During development of the mammalian brain and throughout adulthood, astrocytes have a critical position in which their intimate interactions with neurons allow active communication and orchestrate the development of neuronal circuits. Several *in vitro* studies showed that astrocytes guide the formation, the maturation, but also the pruning of synapses by secreting synaptogenic factors. Thrombospondins, hevins, secreted protein acidic and rich in cysteine (SPARC), and glypicans are such astrocyte-secreted synaptogenic molecules that interact with synaptic binding partners, thus enabling connectivity and circuit refinement (Christopherson et al. 2005; Kucukdereli et al. 2011; Clarke and Barres 2013). In the mature brain, astrocyte modulate synaptic plasticity and transmission. The tripartite synapse is a real proof of concept of the crucial role of astrocytes in synaptic processes. Because of their intricate arborisation and ramifications, they can enwrap the synaptic terminal to sense the synaptic cleft milieu. This allows them to respond to released neurotransmitters, notably glutamate and gamma-aminobutyric acid (GABA), via high-affinity transporters such as the glutamate aspartate transporter (GLAST), to prevent excitotoxicity (Rothstein et al. 1996) and fine-tune synaptic activity (Hahn et al. 2015). Moreover, astrocytes release various neuroactive molecules named gliotransmitters, such as D-serine, adenosine and ATP that influence neuronal signalling and contribute to the regulation of synaptic plasticity and long-term potentiation (LTP) (Ota et al. 2013). Although far more complex, such processes lay the foundations for memory formation and learning processes. Indeed, these glial cells, and especially hippocampal astrocytes, are recognised as being involved in learning and memory processes. They are able to contribute to different forms of memory, such as working and spatial memory, as well as recognition and contextual memory (Escalada et al. 2024). Moreover, by integrating and computing neural signals, they play a central role in decision-making (Wang et al. 2017; Kofuji and Araque 2021). Emerging evidence also implicates astrocytes in the

regulation of circadian rhythms (Hastings et al. 2023). Indeed, they can influence the timing of neuronal activity in the suprachiasmatic nucleus via glutamate and ATP signalling, indicating the involvement of astrocytes in initiating and sustaining complex behaviour (Tso et al. 2017; Brancaccio et al. 2019).

Astrocytes are essential for brain homeostasis that is necessary for optimal synaptic transmission. They are notably central to ion homeostasis to maintain the ionic environment necessary for proper neuronal firing. For example, they are key in buffering the extracellular potassium via specific channels, such as Kir4.1 that is enriched in astrocytic branches enwrapping blood vessels and synapses (McNeill et al. 2021). Moreover, astrocytes play a crucial role in water homeostasis, notably through aquaporin 4 (AQP4), a water channel highly expressed in perivascular astrocytic endfeet. AQP4 facilitates bidirectional water transport, thus mediating a tonic water efflux, which is essential for maintaining osmotic balance to support cellular equilibrium in the brain (Pham et al. 2024). Being a key component of the glymphatic system, AQP4 plays a crucial role in clearing interstitial waste and soluble proteins (Iliff et al. 2012; Nagelhus and Ottersen 2013). Furthermore, astrocytes are an integral part of the vascular unit. Indeed, astrocytic endfeet form a critical interface between the parenchyma and the vasculature. Thus, astrocytes contribute to the development and maintenance of the blood-brain-barrier (BBB). *In vitro* studies reported that astrocytes promote the development of BBB properties in endothelial cells notably by regulating the expression of tight junction proteins (Tao-Cheng et al. 1987; Tontsch and Bauer 1991). Hence, astrocytes are ideally positioned to actively participate in the controlling of the cerebral blood flow. Indeed, they have been reported to regulate the neurovascular coupling by detecting neuronal activity and releasing vasoactive molecules (e.g. prostaglandins, nitric oxide, ATP) onto cerebral vessels, thus changing vascular diameter and *in fine*, regulating the cerebrovascular tone (Metea and Newman 2006; Gordon et al. 2008; MacVicar and Newman 2015). Ultimately, through all these interactions, astrocytes are responsible for and critical to neuronal metabolic support. They support neurons notably via the astrocyte-neuron lactate shuttle wherein astrocytes metabolise glucose to lactate, which is then shuttled to neurons to fuel oxidative phosphorylation, providing most or all ATP necessary for neuronal energetic metabolism (Pellerin and Magistretti 1994; Bélanger et al. 2011). It is also worth noting that astrocyte glycogen and glutamine are additional sources of metabolic support for neurons, the glycogen resource being modulated by certain neurotransmitters such as noradrenaline (Sorg and Magistretti 1992). Hence, such metabolic support is fundamental for neuronal activity and survival, and consequently for cognition, particularly for learning and memory processes (Roumes et al. 2023).

In addition, astrocytes are actively involved in neuroprotection. Indeed, they efficiently respond to oxidative stress through the upregulation of specific antioxidant pathways, such as Nrf2-Keap1-ARE pathway (Heurtaux et al. 2022). They can also develop antioxidant activity, including the synthesis and release of glutathione precursors and the detoxification of reactive oxygen species (ROS) (Chen et al. 2020). Additionally, astrocyte are potent modulators of the inflammatory immune response in the CNS, notably by releasing a cocktail of pro- and anti-inflammatory cytokines (IL6, IL33, IL10, etc.) and chemokines (CXCL10, CXCL12, CCL2, etc.) in response to injury or infection. Through these signalling molecules, astrocytes might recruit immune cells and support BBB integrity. Moreover, growing evidence indicate a key role of astrocytes in antigen presentation and interaction with T cells. Indeed, they have been reported to express major histocompatibility complex class II (MHC II) but also co-stimulatory molecules (CD80, CD86, CD40), suggesting a potential role in antigen-specific T cell activation (Rostami et al. 2020; Beretta et al. 2025). However, these mechanisms behind astrocyte immune modulatory function remains still unclear. Crucially, astrocytes can engulf and degrade extracellular Aβ and tau aggregates (Thal et al. 2000; Kim et al. 2024; Reid et al. 2025). Through phagocytic activity and/or receptor-mediated processes (e.g. TLRs, LDLR), in addition to the expression of Aβ-/tau-degrading enzymes (e.g. NEP, IDE, HMGCS2) (Mohamed and Posse De Chaves 2011; Mulder et al. 2012; Bouvier and Murai 2015; Reid et al. 2025), they play an active role in the clearance of such pathological protein aggregates. Importantly, astrocytes responses to CNS injury or any other abnormal stimuli involve a bidirectional communication with microglia, the immune cells of the brain. Indeed, astrocyte are known to influence microglia states and function through releasing signalling molecules. This is the case of interleukine-3 (IL-3) secreted by astrocytes that has been shown to induce transcriptomic, morphological and functional reprogramming in microglia to modulate their immune response, enhance their motility and facilitate microglia barrier formation and A clearance (McAlpine et al. 2021). In turn, microglia signalling (e.g. C1q, IL1β, Tnfα) also shape astrocyte responses by triggering either resting or reactive states. Overall, astrocyte–microglia communication forms a bidirectional signalling axis that fine-tunes neuroimmune balance. Through these interactions, astrocytes can either amplify or restrain microglial-mediated inflammation, making this crosstalk a central mechanism in coordinating neuroprotective responses and preserving brain homeostasis.

This chapter summarises some of the diverse functions of astrocytes and highlights their fundamental role in maintaining brain homeostasis. Their central position suggests that astrocytes play a significant role in the pathogenesis of NDDs, although their implication is still widely underestimated and poorly

understood. Moreover, astrocyte research over the last decade has revealed a remarkable astrocyte heterogeneity, which also explains the diversity of functions described above. This heterogeneity makes it even more difficult to characterise and understand astrocyte implication in ageing and disease processes. Therefore, it is fundamental to deeper investigate astrocyte diversity and their potential influence in the onset and/or progression of neurodegeneration.

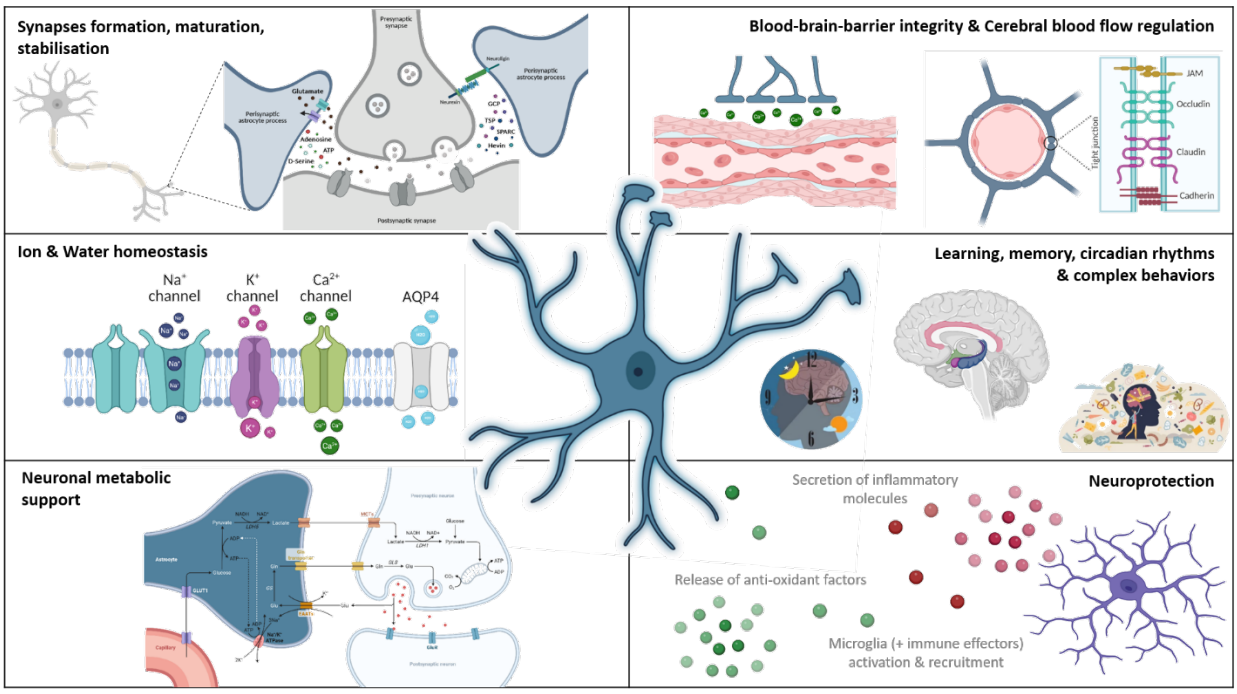

Figure 5: The multifaceted functions of astrocytes: examples of core roles in the CNS.

Astrocytes support synapse formation and maturation by secreting thrombospondins (TSP), glypicans (GPC), hevins and SPARC in the synaptic cleft; and synapse stabilisation and homeostasis by releasing gliotransmitters (D-serine, ATP, adenosine) and uptaking excess glutamate that might cause excitotoxicity. They are responsible for ion and water homeostasis and supply neurons with energetic resources. They also support the formation of tight junctions, such as cadherin, claudin, occluding and junctional adhesion molecules (JAM) and maintain epithelial cells for an efficient BBB integrity. They regulate the cerebral blood flow by influencing contraction of the smooth muscle tissue through the release of Ca^{2+} ions. Astrocytes are widely involved in memory and learning processes, in the circadian regulation of metabolism, energy, behaviour, etc., but also in developing complex behaviour, such as feeding behaviour. Together with microglia, astrocytes are fundamental to CNS neuroprotection. Created with BioRender.

2.2. Astrocytic heterogeneity within a conventionally defined homogeneous cell type

Although these cells have traditionally been considered a functionally homogeneous population, it is now more widely appreciated that they exhibit a notable panel of morphologies, properties, and functionality between, but also within, brain regions (Holt 2023). Initially, astrocytes were defined by their star-shaped morphology, which rapidly evolved into a more advanced classification by Albert von Kölliker and William Lloyd Andriezen, who described protoplasmic and fibrous astrocytes located in the grey and white matter, respectively (Verkhratsky and Parpura 2010a). However, investigation on astrocyte morphologies revealed other astrocytic subtypes and differences between rodents and primate astrocytes (**Figure 6**). By comparing rodents and human astrocytes, Oberheim and colleagues showed that human astrocytes exhibit a greater morphological complexity and heterogeneity (Oberheim et al. 2009). Human protoplasmic astrocyte, defined by highly branched, bushy processes, are larger with a greater number of processes than the rodent counterparts. However, they show a similar non-overlapping organisation in both species. Given their wide distribution across the grey matter, protoplasmic astrocytes are largely involved in the functions described above (**Part III, section 2.1**) (Tabata 2015). In humans, as in rodents and nonhuman primates, fibrous astrocytes are remarkably larger than protoplasmic astrocytes. They are characterised by a morphology with fewer fine bulbous processes, reflecting the reduced presence of synapses in white matter, and longer, straighter branches. Interestingly, they show a higher expression of GFAP than protoplasmic astrocytes. Although their functions are not clear yet, these cells appear to be primarily adapted for structural support (Oberheim et al. 2009; Tabata 2015). The primate brain also contains interlaminar astrocytes, which were first described by William Lloyd Andriezen in 1893 as *caudate neuroglial fibre cells*. These cells were studied in depth and characterised by Colombo and his colleagues hundreds of years later (Colombo et al. 1995; 1997; Colombo and Reisin 2004). Interlaminar astrocytes project straight and poorly ramified processes, sometimes arborising a few varicosities loaded with GFAP+ material, into the cortical grey matter, terminating in layers II to IV and frequently ending on capillaries. Given their close contact with the microvasculature of the brain, these astrocytes might be involved in the coordination of the blood flow. A second astrocytic subtype that is primate-specific have been discovered by Oberheim and colleagues and is designated as varicose projection (VP) astrocytes. This GFAP+ astrocyte subtype is mainly localised in the cortical layers V and VI, extending shorter and more spiny processes than protoplasmic astrocytes. In addition, they project within deep cortical layers one to five unbranched processes, each a few millimetre-long, containing many varicosities (Oberheim et al. 2009; Sosunov et al. 2014). These varicosities suggest specialised structures or

compartmentalisation of cellular components, but their exact function and significance remain unclear. A recent study showed that VP astrocytes are *in vitro* inducible by the presence of proinflammatory cytokines (Ciani et al. 2025). Moreover, Ciani and colleagues demonstrated through their quantification data an increase in the density of this astrocytic subtype in patients with AD, PD and multiple sclerosis (MS), suggesting that VP astrocytes are a reactive phenotype that appears in response to pathological states (Ciani et al. 2025).

In addition to these complex and specific morphologies, there are also specialised astrocytic populations enriched in distinct brain regions. The Müller glial cells is a subtype of radially polarised astrocytes localised in the retina that contributes to retinal structure and homeostasis, supporting functioning and metabolism of retinal neurons (Bringmann et al. 2009; Reichenbach and Bringmann 2013). The Bergmann glia, another example of specialised astrocytic subtype, is localised in the cerebellar cortex where it exhibits a complex polarised morphology with very long processes. These cells are in close interaction with the Purkinje cells, the neuronal output cells of the cerebellar cortex, and are fundamental for ion homeostasis, synapse plasticity and stability, metabolic functions and neuroprotection (De Zeeuw and Hoogland 2015).

In addition to this remarkable morphological diversity, astrocytes also exhibit very diverse molecular signatures. Investigations into single-cell RNA sequencing over the last decade have shed light on the molecular heterogeneity of these cells and highlighted new astrocyte signatures. Habib and colleagues described a population of disease-associated astrocytes (DAAs) that appears at early disease stage and increases in abundance with disease progression (Mathys et al. 2019; Habib et al. 2020; Green et al. 2024). They described these DAAs as a GFAP-high population with a unique molecular profile and exclusively found in AD. They also identified a homeostatic population of astrocytes in a low-GFAP state that expresses a unique set of genes and whose number decreases consistently with AD progression, alongside a corresponding increase in DAAs. Thus, such studies indicate an important diversity of astrocyte responses in disease conditions. Indeed, reactive astrocyte populations are highly dynamic and have been shown to adopt distinct profiles such as proliferative versus non-proliferative, or neurotoxic versus neuroprotective profiles (Zamanian et al. 2012; Liddelow et al. 2017; Hasel et al. 2021). Furthermore, some studies showed that the intrinsic signalling activity of the astrocytes to

disease conditions is highly heterogeneous, which partly explains such functional differences (Qin et al. 2023).

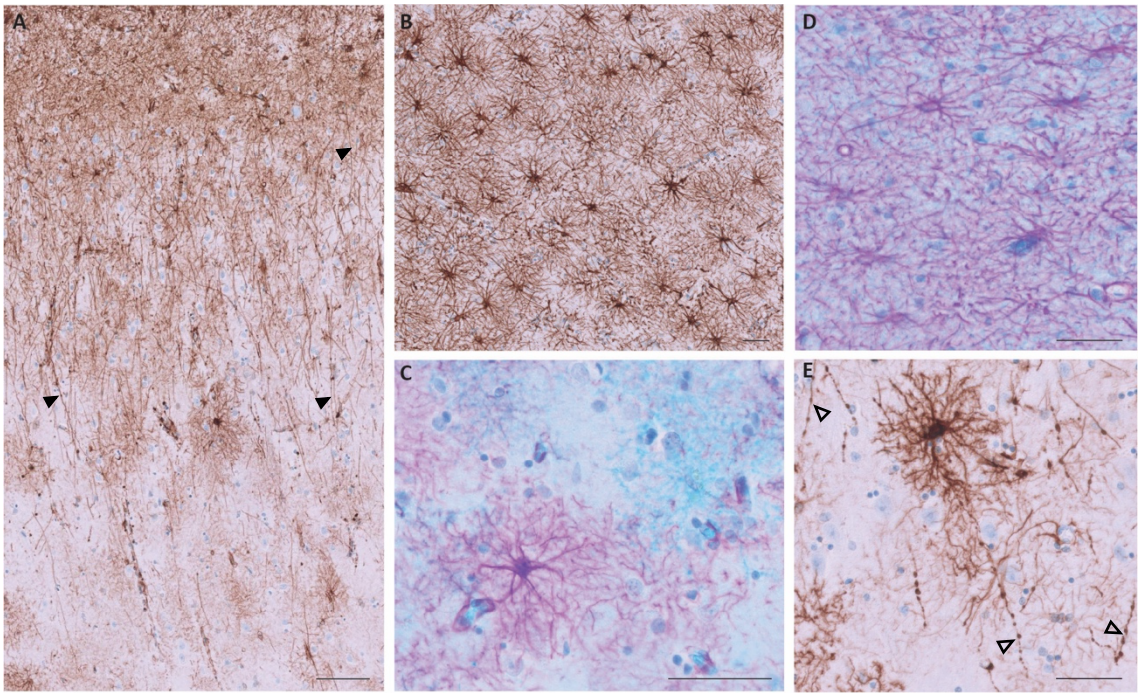

Figure 6: Representative examples of astrocyte morphological diversity.

*The human brain is a veritable niche hosting diverse and complex astrocytic morphologies: (**A**) interlaminar astrocytes (GFAP, DAB, brown) and their very long processes projecting across cortical layers (full arrows); (**B-C**) protoplasmic astrocytes (B: GFAP, DAB, brown; C: GFAP in purple, AQP1 in teal) with a bushy and very ramified morphology; (**D**) fibrous astrocytes and their long and straight branches; and (**E**) varicose projections astrocytes with varicosities along extended processes (empty arrows). Scalebars: **A** 100 µm, **B-E** 50 µm. Own microscopy images.*

2.3. Astrocyte responses in neurodegenerative diseases

The multifacets of astrocyte neurotoxicity and the astrocyte involvement in ageing and NDDs are thoroughly discussed in the following review (**manuscript III, Part IV, Chapter III**):

The Multifaceted Neurotoxicity of Astrocytes in Ageing and Age-Related Neurodegenerative Diseases: A Translational Perspective

David S. Bouvier [1,2,3], Sonja Fixemer [2,3], Tony Heurtaux [3,4], Félicia Jeannelle [1,3], Katrin B. M. Frauenknecht [1,3,5] and Michel Mittelbronn [1,2,3,6,7,8*]*

1 National Center of Pathology (NCP), Laboratoire National de Santé (LNS), Dudelange, Luxembourg, 2 Luxembourg Center of Systems Biomedicine (LCSB), University of Luxembourg (UL), Belvaux, Luxembourg, 3 Luxembourg Center of Neuropathology (LCNP), Dudelange, Luxembourg, 4 Systems Biology Group, Department of Life Sciences and Medicine (DLSM), University of Luxembourg, Belvaux, Luxembourg, 5 Institute of Neuropathology, Medical Center of the Johannes Gutenberg University Mainz, Mainz, Germany, 6 Department of Cancer Research (DOCR), Luxembourg Institute of Health (LIH), Luxembourg, Luxembourg, 7 Faculty of Science, Technology, and Medicine (FSTM), University of Luxembourg, Esch-sur-Alzette, Luxembourg, 8 Department of Life Sciences and Medicine (DLSM), University of Luxembourg, Esch-sur-Alzette, Luxembourg

3. The noradrenergic system: from modulation to degeneration

Noradrenaline (NA), also known as norepinephrine (NE), has been suggested as a byproduct of tyrosine degradation in 1939 by Hermann Blaschko and Peter Holtz, but its role in the body has been discovered by the physiologist Ulf van Euler in 1945 (Euler 1946). Finally, it is Marthe Vogt who investigated and made a detailed map of the NA distribution in the dog brain and showed its uneven distribution across the brain (Vogt 1954).

3.1. The noradrenergic system: from a small brainstem nucleus to a brain-wide system

The forebrain noradrenergic system originates in the locus coeruleus (LC), a small brainstem nucleus located in the dorsal pontine tegmentum (**Figure 7**). Despite its very small size, the LC widely projects noradrenergic (NA) efferences throughout the entire brain following three main NA pathways: the cortical/ascendant pathway, including projections to the amygdala, hippocampus, and prefrontal cortex (PFC); the spinal pathway (or descendent) that projects to brainstem nuclei (e.g. nervus vagus); and the cerebellar pathway, connecting both cerebellar cortex and nuclei (Foote et al. 1983; Ordway et al. 2007; Hussain et al. 2025). With such large-scale projections, the NA system exerts extensive modulatory influence on physiological as well as cognitive processes. Indeed, through the cortical pathway, the NA system has been shown to be involved in learning, memory, attention/arousal and sleep processes (Berridge and Waterhouse 2003; Aston-Jones and Cohen 2005; Ordway et al. 2007; Roozendaal 2007; Sara 2009; O'Donnell et al. 2012; Mather and Harley 2016; Mercan and Heneka 2022; Hussain et al. 2025).

The LC is the main source of NA in the CNS, a catecholaminergic neurotransmitter synthesised by the NA neurons. These neurons are identifiable by a darkly pigmentation due to neuromelanin (**Figure 7**), a byproduct of both dopamine (DA) and NA that binds metal ions (Zucca et al. 2006; Clewett et al. 2016). NA is synthesised from tyrosine, which is converted into dihydroxyphenylalanine (DOPA) by the

tyrosine hydroxylase, and then into DA by the DOPA decarboxylase. DA is finally converted into NA by the dopamine β-hydroxylase within NA neurons. NA is then released either via classical synaptic transmission into the synaptic cleft or by volume transmission via axonal varicosities. The latter enables a broad, paracrine-like mode of signalling that can influence a wide range of cellular targets beyond synapses, including astrocytes, microglia, and endothelial cells of the neurovascular unit (Stone and Ariano 1989; Marien et al. 2004; Vizi et al. 2010; O'Donnell et al. 2012; Pan et al. 2025). Indeed, all these cell types express various noradrenergic receptors belonging to the α1-, α2- and β-adrenergic receptor families, to which NA binds with the highest, lowest and intermediate affinity, respectively (Ordway et al. 2007). These three main receptor families are further divided into three subtypes each: α1A, α1B, α1D; α2A, α2B, α2C and β1, β2, β3. Through these G protein-coupled receptors, NA exerts either stimulatory (via α1 coupled to Gq proteins or β-adrenergic receptors coupled to Gs proteins) or inhibitory (via α2-adrenergic receptors coupled to Gi proteins) effects on cell signalling (Ordway et al. 2007; O'Donnell et al. 2012; Mercan and Heneka 2022; Hussain et al. 2025).

The following section will briefly summarise the noradrenergic signalling within the aforementioned cell types, before describing more precisely the intimate relationship between the NA system and astrocytes.

3.2. Noradrenergic signalling in neurons, glia and brain immune cells

NA is a potent modulator of neuronal circuits signalling through the three above mentioned adrenergic receptor families. Indeed, α1-adrenergic receptors (α1-ARs) are mainly expressed by the postsynaptic terminals located in various brain regions, including the LC, DG, amygdala, cerebral cortex, olfactory bulb and thalamus, and mainly perform excitatory actions. Notably in the PFC, activation of these receptors may increase glutamate release, inducing persistent firing activity. The α2-AR subtypes are found both pre- and postsynaptic, notably in the LC, amygdala and hypothalamus, mainly exerting inhibitory effects. Similar to α1-ARs, β-ARs are mainly expressed at postsynaptic sites and promote inhibitory actions. Through these receptors, NA can regulate both excitatory and inhibitory transmission, thus shaping neuronal circuit activities and contributing to cognitive functions, including attention, learning and memory processes (Mercan and Heneka 2022; Hussain et al. 2025; O'Donnell et al. 2012).

Glial cells are also key targets of the noradrenergic system and are highly responsive to NA. For example, oligodendrocyte precursor cells (OPCs) express α1-AR and activation of α1A-AR subtype by

NA binding has been shown in mice to stimulate OPCs proliferation (Lu et al. 2023) and promote their differentiation into myelinating oligodendrocytes (Fiore et al. 2023). Thus, NA is an important regulator of OPCs fate.

The modulatory effect of NA on astrocytes physiology will be detailed in the following section.

Finally, NA is also a potent modulator of microglia, the resident immune cells of the brain. Indeed, NA is well recognised for its anti-inflammatory effects on microglia, notably by signalling through β-ARs. This includes the down-regulation of the expression of pro-inflammatory genes (e.g. *MCP, iNOS, COX2*) and reduced secretion of pro-inflammatory cytokines (e.g. TNFα, IL-6) and chemokines (e.g. CCL2, CCL5) (Heneka et al. 2010; Zou et al. 2021; Durcan et al. 2025). NA was also reported to reduce the IFNγ-dependent upregulation of MHCII antigens (Loughlin et al. 1993; Gutiérrez et al. 2022), thus mediating microglial immune response. Furthermore, NA has been shown to increase microglia phagocytosis and migration (Heneka et al. 2010; Feinstein et al. 2016; Mercan and Heneka 2019; Durcan et al. 2025). NA was also found to promote process retraction in both resting and activated microglia through α2a- and β2-ARs activation, thereby modulating cell motility and reducing microglial surveillance as well as synaptic plasticity (Stowell et al. 2019; Gyoneva and Traynelis 2013; Liu et al. 2019).

Hence, NA is a potent neuromodulator that finely tunes the activity and interactions of all brain cell types to maintain CNS homeostasis and adaptability. However, all the mechanisms behind these modulatory effects are still not fully understood.

3.3. Astrocyte-noradrenergic signalling: a modulatory interface

Astrocytes are deeply integrated into this neuromodulatory architecture. Indeed, they express all families of noradrenergic receptors enabling them to respond dynamically to fluctuations in extracellular NA levels (Hertz et al. 2004; O'Donnell et al. 2012; Ding et al. 2013; Wahis and Holt 2021; Pan et al. 2025). Activation of these receptors leads to an increase of intracellular calcium (Ca^{2+}) and cAMP, thus stimulating multiple effector mechanisms and influencing key astrocytic functions (Duffy and MacVicar 1995; Bekar et al. 2008; Hertz et al. 2010; Paukert et al. 2014; Wahis and Holt 2021; Bogdanović Pristov et al. 2025). Indeed, NA has been demonstrated to control the glycogen breakdown and synthesis in astrocytes to provide neurons with lactate, and thus supporting neuronal metabolism (Sorg and Magistretti 1992; Fink et al. 2021). NA is also known as a vasoactive neurotransmitter that contributes to astrocyte-mediated vasoconstriction. Indeed, Mulligan and MacVicar reported that NA increases significantly intracellular Ca^{2+} in astrocyte endfeet, leading to arteriole constriction (Mulligan

and MacVicar 2004). In addition to its potent vasoconstrictive properties, NA has been recently shown to promote glymphatic fluid transport and brain clearance during sleep (Hauglund et al. 2025). These crucial functions might be partly supported by astrocyte endfeet that have been proposed to function as “valves” promoting glymphatic flow in perivascular spaces and averting backward flow (Bork et al. 2023; Gan et al. 2023; Bellier et al. 2025). Moreover, Chen and colleagues have recently demonstrated the critical role of astrocytic AQP4 in glymphatic exchange and clearance (W. Chen et al. 2025). Importantly, recent research has revealed that NA-mediated astrocyte activity is critical for synaptic regulation and behavioural outcomes. Indeed, NA has been shown to act via astrocytic purinergic signalling to influence passive behaviour state in zebrafish by modulating neuronal excitation (A. B. Chen et al. 2025). Conjointly, studies in mice and zebrafish showed that NA shapes synaptic dynamics via astrocytic signalling, specifically through astrocytic α1A-ARs, and, *in fine*, modulates synaptic strength (A. B. Chen et al. 2025; Lefton et al. 2025). Such neuromodulation has been reported to contribute to specific memory processes (e.g. astrocytic cAMP elevations) during vigilance state in awake mice (Oe et al. 2020). Interestingly, NA is known to induce morphological changes in astrocytes through β-ARs via elevation of intracellular cAMP (Vardjan et al. 2014; Sherpa et al. 2016). These microstructural changes mainly affect astrocytic leaflets (or perisynaptic astrocyte processes) regulating the astrocytic coverage of the synapse, thus influencing synaptic transmission (Henneberger et al. 2020; Zorec 2025). In addition, Guttenplan and colleagues have recently shown in drosophila that tyramine, a functional analog of NA, “gates” astrocytic responsiveness to other neurotransmitters such as DA, implying that NA does not merely activate astrocytes, but also reprograms their functional state (Guttenplan et al. 2025).

Importantly, NA is a potent modulator of brain inflammation by regulating the expression of inflammatory genes in endothelial (Feinstein et al. 2002) and glial cells, including microglia (Dello Russo et al. 2004; Schlachetzki et al. 2010; Ishii et al. 2015; Zou et al. 2021) and astrocytes (Madrigal et al. 2009; Hinojosa et al. 2013; Laureys et al. 2014). This modulatory effect has been shown *in vitro* to be mediated mainly through β-ARs and validated in AD mouse models in which the pharmacological blockade of these receptors potentiates neuroinflammation (Ardestani et al. 2017; Evans et al. 2020; 2024b). Such antagonistic effect increases the expression of proteins involved in inflammation, such as TNFα and IL1β in both astrocytes and microglia, NOS2 in astrocytes mainly, and adhesion molecules (e.g. ICAM-1) in astrocytes and brain endothelial cells. It also increases the expression of genes related to class II major histocompatibility complexes (MHC II) in brain endothelial cells (Feinstein et al. 2016). Furthermore, LC lesion in PD rodent models was associated with exacerbated neuroinflammation in

addition to an increased sensitivity of nigrostriatal DA cells to damage and degeneration (Fornai et al. 1999; Song et al. 2019; Af Bjerkén et al. 2019). By contrast, some studies have demonstrated that NA stimulates the expression and release of anti-inflammatory factors, including astrocytic MCP-1 (monocyte chemotactic protein-1, or CCL2), IL-10, IL-1 receptor antagonists (e.g. IL-1ra, IL-R2), and GM-CSF (granulocyte-macrophage colony-stimulating factor, recognised for its anti-inflammatory and neuroprotective properties) (Ağaç et al. 2018).

Moreover, NA plays a crucial role in neuronal protection against oxidative stress (Troadec et al. 2001). Indeed, *in vitro* studies showed that NA increases the intracellular concentration of glutathione (GSH) in astrocytes through the stimulation of β3-ARs (Yoshioka et al. 2016; 2021). GSH is a key factor of the antioxidant machinery that protects cells against oxidative damage notably by scavenging and detoxifying intra- and extracellular ROS (Pérez-Sala and Pajares 2023). The astrocytic GSH is essential for providing neighbouring neurons with the fundamental precursors needed to synthesise neuronal GSH, thereby supporting neurons in their response to oxidative stress (Dringen and Arend 2025). The antioxidant properties of NA has been validated *in vivo* in a PD mouse model in which LC lesion exacerbated oxidative stress associated with reduced pools of GSH and glutathione peroxidase as well as an increased lipid peroxidation (Song et al. 2019; Hou et al. 2019).

3.4. Selective vulnerability: the noradrenergic system in neurodegenerative disorders

The LC is a highly vulnerable structure sensitive to brain insults. This can be explained by its exposed location in close proximity to the fourth ventricle, accentuating its exposure to inflammatory molecules and toxins that might circulate in the cerebrospinal fluid (Matchett et al. 2021). Importantly, there is growing consensus that the LC is among the earliest sites of pathology in AD, with tau pathology and neuronal loss occurring well before overt cognitive symptoms emerge (German et al. 1992; Braak and Del Tredici 2011; Braak et al. 2011; Theofilas et al. 2017; Gilvesy et al. 2022; Bueichekú et al. 2024; Hary et al. 2025). *In vivo* evidences showed a spread of tau pathology in AD mice from the LC to the forebrain, underlying the selective vulnerability of the LC to AD pathogenesis (Kang et al. 2020; Iba et al. 2015). Similarly, early LC degeneration is observed in other disorders such as PDD (Bertrand et al. 1997; Sun et al. 2023) and DLB (Szot et al. 2006; Železníková et al. 2025), underscoring the potential unifying role of NA system disruption in (Zarow et al. 2003; Weinshenker 2018; Jacobs et al. 2020; Matchett et al. 2021). Notably, in AD, loss of rostral LC neurons, which predominantly innervate the hippocampus, is particularly pronounced and may underlie early memory deficits characteristic of the disease (Theofilas et al. 2017; Gutiérrez et al. 2022; Bae et al. 2025).

Moreover, the vulnerability of the NA neurons can be partly explained by impairment of the "metabolic coupling" between astrocytes and LC neurons. Indeed, secreted NA induces astrocytes to release L-lactate, which in turn excites LC neurons and stimulates the further release of NA, thus supporting extra energy demand and enhanced metabolic activity of LC neurons (Tang et al. 2014; Vardjan et al. 2018). Hence, the disruption of the excitation-energy coupling might accentuate the vulnerability of the LC neurons (Zorec 2025). In addition, hyperactivation of LC neurons accompanied by mitochondrial dysfunction and subsequent oxidative stress (Sanchez-Padilla et al. 2014; Wang et al. 2020), as well as heavy metal accumulation (Ehrenberg et al. 2025), are additional crucial factors that render the LC vulnerable to neurodegeneration.

3.5. Disruption of the glial cell-noradrenergic crosstalk as a key factor in the progression of neurodegeneration.

Given its involvement in fundamental functions and its modulatory effect, the early depletion of NA due to LC degeneration is believed to trigger widespread dysregulation of astrocytic, microglial and neuronal activity and responses in NDDs, contributing to progressive cognitive impairment (Weinshenker 2008). Several studies reported detrimental effects of NA depletion notably on microglia responses to disease states. Heneka and colleagues demonstrated an increase of microglia activation, accompanied with astrocyte reactivity, in NA-depleted APP transgenic mice (Heneka et al. 2006). They also showed that NA deprivation induces deficit of microglial phagocytosis and reduces the recruitment of these cells to Aβ plaques. This was accompanied with increased levels of extracellular Aβ deposition in the hippocampus and frontal cortex. Conversely, pharmacological rescue of NA levels prevents the decrease in phagocytosis and migration of microglia, thereby restoring Aβ clearance (Heneka et al. 2010). Moreover, chronic depletion of NA levels has been reported in APP transgenic mice to increase neuroinflammation in NA-targeted brain regions, including hippocampus and cortex. This neuroinflammation was characterised by an elevation of pro-inflammatory cytokines and contributed to early impaired neuronal functions and increased cognitive deficits (Heneka et al. 2006). In addition, activated microglia induced by LC lesion have been shown to release superoxide and some other forms of ROS, thereby increasing oxidative stress in neurons before they degenerate (Song et al. 2019).

As explained above (see Part III, 3.3. " Astrocyte-noradrenergic signalling: a modulatory interface"), chronic NA depletion also severely affect astrocytes with a loss of their homeostatic roles, adopting

neurotoxic phenotypes that contributes to inflammation, oxidative stress, and neuronal dysfunction (Braun et al. 2014; Bouvier et al. 2022; Escartin et al. 2021; Hinojosa et al. 2013). However, despite growing recognition of these processes, the molecular mechanisms by which NA shapes astrocyte responses during disease remain incompletely understood.

Therefore, this thesis presents a comprehensive characterisation of astrocytic changes and the impact of NA deprivation on their phenotype and responses in NDDs.

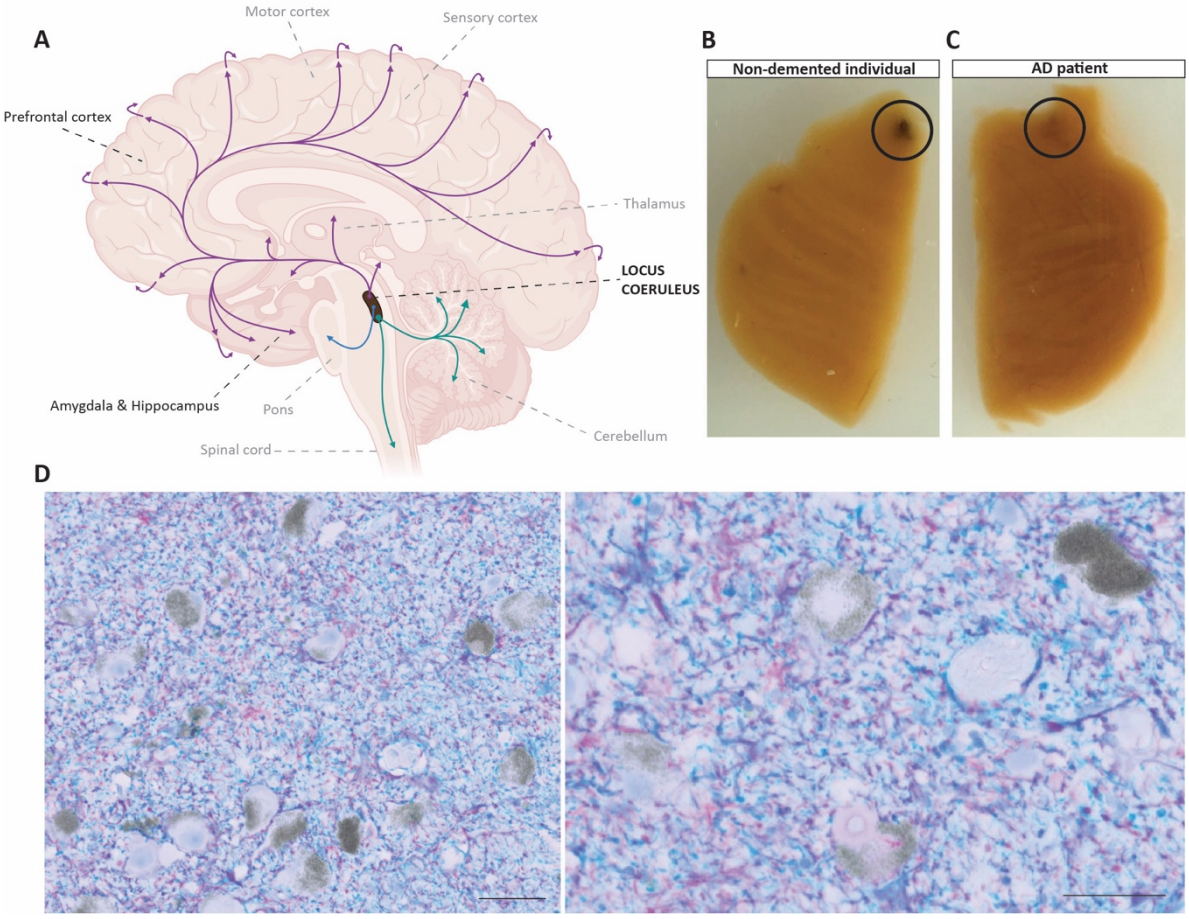

Figure 7: The locus coeruleus is an early vulnerable brain region in NDDs.

***A** The LC is a small brainstem nucleus that projects NA efferences throughout the CNS. The localisation of NA neurons within the LC reflects their projection destination: neurons from the rostral part of the LC project to the forebrain regions (purple); middle LC neurons to the pons (blue) and caudal LC neurons to the cerebellum and the spinal cord (green). Adapted from (Matchett et al. 2021). Created with*

BioRender. ***B*** *Macroscopic image of the LC from a non-demented individual. The LC (circle) appears darkly pigmented due to the presence of neuromelanin.* ***C*** *In AD patients, the LC (circle) is significantly depigmented due to a loss of neuromelanin, reflecting neurodegeneration.* ***D*** *Multiplex cIHC of pigmented LC neurons among GFAP+ (teal) and GPC5+ (purple) astrocytes. Scale bars: 50 μm. Own macro- and microscopic images.*

Part III: Material & Methods

1. Material

Table 2: Primary cells

Primary cells	Tissue	Mouse strain	Source	Manuscript
Primary mouse astrocytes	Cerebrum	Crl:CD-1 (1-3 days old pups)	Charles-River, France	II
Primary mouse microglia	Cerebrum	Crl:CD-1 (1-3 days old pups)	Charles-River, France	II

Table 3: Post-mortem human samples

Post-mortem human samples	Brain regions	Sample storage	Source	Manuscript
Non-demented control (CTL)	Hippocampus; Locus coeruleus; Prefrontal cortex; Amygdala	FFPE; PFA-fixed; frozen	Douglas-Bell Canada Brain Bank; GIE-Neuro-CEB biobank; The Netherlands Brain Bank	I, II
Alzheimer's disease (AD)		FFPE; PFA-fixed; frozen	Douglas-Bell Canada Brain Bank; GIE-Neuro-CEB biobank; The Netherlands Brain Bank	I, II
Parkinson's disease with dementia (PDD)		FFPE	The Netherlands Brain Bank	I, II

Table 4: Cell culture media and solutions

Cell culture media and solutions	Source	Manuscript
DMEM 10% (= DMEM, 10% (v/v) FBS, 100 U/mol Penicillin, 10 mg/ml Streptomycin)	Gibco	II
DMEM	Gibco	II

Table 5: Chemicals and recombinant proteins

Chemicals and recombinant proteins	Reference	Source	Manuscript
Noradrenaline	A9512	Sigma-Aldrich	II
Dopamine	H8502	Sigma-Aldrich	II
Murine TNFα	315-01A	PeproTech	II
Murine IL1β	211-11B	PeproTech	II
Murine IFNγ	315-05	PeproTech	II

Table 6: Antibodies

Antibodies	Reference	Source	Manuscript
PRIMARY ANTIBODIES			
Rabbit polyclonal anti-ALDH1L1	HPA050139	Sigma	I, II
Rabbit polyclonal anti-ALDH7A1	HPA023296	Sigma	I
Mouse monoclonal anti-AQP4	AMAb90537	Sigma	I, II
Mouse monoclonal anti-β-Amyloid	800712	BioLegend	I
Rabbit polyclonal BACE2	HPA035416	Sigma	II
Rabbit polyclonal anti-CBS	HPA001223	Sigma	II
Rabbit monoclonal anti-GFAP	760-4345	Ventana Medical Systems	I, II
Guinea-pig polyclonal anti-GFAP	173004	SynapticSystem	II
Rabbit polyclonal anti-GPC5	HPA040152	Sigma	I
Rabbit polyclonal SPARC	HPA003020	Sigma	II
Mouse monoclonal anti-phospho Synuclein – clone 81A (Ser129)	MABN826	Millipore	II
Rabbit polyclonal anti-phospho tau – pS396	44-752G	Thermo Fisher Scientific	I
Mouse monoclonal anti-phospho tau – AT8 (Ser202, Thr205)	MN1020	Thermo Fisher Scientific	I, II
Rabbit polyclonal anti-VGAT	HPA058859	Sigma	I
Rabbit polyclonal anti-VGLUT1	HPA063679	Sigma	I
Mouse monoclonal Vimentin	05278139001	Ventana Medical Systems	II
Mouse monoclonal anti-VMAT2	TA500506	Origene	II
SECONDARY ANTIBODIES			
DISCOVERY OmniMap anti-Rb HRP	760-4311	Roche	I, II
DISCOVERY OmniMap anti-Ms HRP	760-4310	Roche	I, II
DISCOVERY CM DAB kit	760-159	Roche	I, II
DISCOVERY Purple Kit	760-229	Roche	I, II
DISCOVERY Teal HRP kit	760-247	Roche	I, II
Discovery Green HRP kit	08478295001	Roche	I, II
Donkey anti-guinea pig Alexa Fluor 647	706-605-148	Jackson ImmunoResearch Labs	II
Donkey anti-rabbit Alexa Fluor 555	A-31572	Invitrogen	II
Donkey anti-rat Alexa Fluor 488	A21208	Life Technologies	II

Table 7: Primers

siRNA and primers	Sequence	Source	Manuscript
Ace2 primers (NM_ 001130513)	F: 5'-GAC-AAC-TTC-TTG-ACA-GCC-CA-3' R: 5'-CAA-CAG-CTT-CAT-GGA-ACC-CT-3'	Eurogentec	II
Camk4 primers (NM_ 009793)	F: 5'-ATG-CAA-ACA-GAA-GGG-GAC-C-3' R: 5'-ATG-TTC-GGG-TGT-GAG-AGA-CG-3'	Eurogentec	II
Cartpt primers (NM_ 013732)	F: 5'-ACA-TCT-ACT-CTG-CCG-TGG-AT-3' R: 5'-GCT-TCG-ATC-TGC-AAC-ATA-GCG-3'	Eurogentec	II
Cxcl10 primers (NM_ 021274.2)	F: 5'-TGCTGCCGTCATTTTCTGCCTC-3' R: 5'-AGCTTCCCTATGGCCCTCATTCTC-3'	Eurogentec	II
Igf1 primers (NM_010512)	F: 5'- CTC TGC TTG CTC ACC TTC-3' R: 5'- CAA CAC TCA TCC ACA ATG C-3'	Eurogentec	II
Rpl27 primers (NM_011289.3)	F: 5'-TGG-GCA-AGA-AGA-AGA-TCG-CCA-AG-3' R: 5'-TTC-AAA-GCT-GGG-TCC-CTG-AAC-AC-3'	Eurogentec	II
Scg2 primers (NM_009129.3)	F: 5'-AGA-TGA-AAC-GTT-CAG-GGC-AG-3' R: 5'-CCC-ACA-GCA-TTC-ACT-AAC-CT-3'	Eurogentec	II
Sod3 primers (NM_011435.3)	F: 5'-GCC-TTC-TTG-TTC-TAC-GGC-TTG-CTA-C-3' R: 5'-GCG-TGT-CGC-CTA-TCT-TCT-CAA-CC-3'	Eurogentec	II
Tnfa primers (NM_013693.3)	F: 5'-GCA-CAG-AAA-GCA-TGA-TCC-GCG-AC-3' R: 5'-TGA-GAA-GAG-GCT-GAG-ACA-TAG-GCA-C-3'	Eurogentec	II

Table 8: Kits

Kits	Source	Manuscript
MACS® isolation kit (autoMACS® Rinsing Solution, MACS® BSA stock solution, MACS LS separation columns)	Miltenyi	II
innuPREP RNA Mini kit 2.0	IST Innuscreen GmbH	II
ImProm-II(TM) Reverse Transcription System	Promega	II

2. Methods

Table 9: Methods

Methods	Manuscript
Magnetic Cell Sorting (MACS)	II
siRNA-mediated knock-down	II
RNA extraction, reverse transcription, qPCR and RNA-sequencing	II
Immunoblotting	II
Immunohistochemistry and microscopy	I, II
Digital pathology	I, II

Part IV: Results

3. CHAPTER I – GPC5 expression highlights astrocytic heterogeneity and divergent hippocampal responses in Alzheimer's and Parkinson's Dementia.

3.1. Introduction

Astrocytes, one of the main glial cell types in the CNS, play crucial roles in brain development, homeostasis, and function. In response to injury or disease, they undergo reactive changes, making astrocyte reactivity a biomarker of neuroinflammation and a potential indicator of NDDs (Liddelow et al. 2017; Pelkmans et al. 2024; Luijerink et al. 2024). While GFAP emerged as a promising CSF and plasma biomarker to assess astrocyte reactivity (Benedet et al. 2021; Abdelhak et al. 2022; Lin et al. 2023; Liu et al. 2023; Gogishvili et al. 2025), its capacity to reflect parenchymal heterogeneity remains debated (Chiotis et al. 2023; Edison 2024; Youn et al. 2025). Indeed, increasing evidence challenges the traditional view of astrocytes as a homogeneous population, highlighting their diverse morphologies, functions, and region-specific subtypes. Single-cell studies further reveal that astrocytic responses to pathology are markedly heterogeneous as well. Despite this, the astrocyte heterogeneity is still poorly considered as a factor in the onset and/or progression of neurodegeneration. Therefore, we believe that characterising astrocyte heterogeneity in both healthy and diseased brains is crucial to understanding how specific subtypes shift their phenotype and whether they are involved in disease progression. To this purpose, we mapped and quantified established and emerging astrocytic markers (GFAP, ALDH1L1, AQP4, GPC5, ALDH7A1) across hippocampi of cognitively non-impaired elderly individuals (CTLs) as well as AD and PDD patients, using chromogenic immunohistochemistry (cIHC) and digital pathology.

3.2. Personal contributions

For this paper, I conducted the study under the supervision of Dr David Bouvier and with the technical support of my colleagues Mónica Miranda de la Maza, Sophie Schreiner and Dr. Gaël Hammer. Below are listed my personal contributions:

- FFPE sample slicing, cIHC staining and imaging;
- HALO quantification
- Data analysis and visualisation

- Production and design of the below listed figures submitted for this manuscript, except figure 1D (designed by Sophie Schreiner).
    - Figure 1 (A-C, E), Figure 2 (A-G), Figure 3 (A-J), Figure 4 (A-O), Figure 5 (A-G), Figure 6 (A-E);
    - Supplementary figure 1 (A-E), Supplementary figure 2, Supplementary figure 3 (A-E), Supplementary figure 4 (A-B), Supplementary figure 5 (A-F); Supplementary figure 6 (A-B);
- Drafting and final writing of the manuscript (with the support of Dr David Bouvier);
- Editing and reviewing of the final manuscript;
- Details of each author's individual contributions are provided in the author contribution section at the end of the manuscript.

3.3. Original manuscript I

GPC5 expression highlights astrocytic heterogeneity and divergent hippocampal responses in Alzheimer's and Parkinson's Dementia

Félicia Jeannelle[1], Mónica Miranda de la Maza[2], Gaël Paul Hammer[1], Sophie Schreiner[1], Dominique Mirault[4], Naguib Mechawar[4], Netherlands Brain Bank[5], Michel Mittelbronn[1,2,3,6], David S. Bouvier[1]

Author affiliations :

[1] National Center of Pathology (NCP), Laboratoire national de santé (LNS), Dudelange, Luxembourg.

[2] Department of Infection and Immunity (DII), Luxembourg Institute of Health (LIH), Belval, Luxembourg.

[3] Luxembourg Centre for Systems Biomedicine (LCSB), University of Luxembourg, Belval, Luxembourg.

[4] Douglas Mental Health University Institute, Department of Psychiatry, McGill University, Montreal, Quebec, Canada.

[5]Netherlands Institute for Neuroscience, Amsterdam, the Netherlands Brain Bank

[6]Department of Life Science and Medicine (DLSM), University of Luxembourg, Belval, Luxembourg.

Correspondence to: Dr. David S. Bouvier
Laboratoire national de santé (LNS)
1, Rue Louis Rech
L-3555 Dudelange
Email: David.Bouvier@lns.etat.lu

Number of Figures: 6
Number of Supplementary Files: 7
Number of Pages: 42

ABSTRACT

Astrocytes are central to central nervous system (CNS) homeostasis and memory consolidation. They also display remarkably heterogeneous morphological phenotypes, functions and molecular profiles between and within distinct regions of the human brain. Yet, their role in regional vulnerability in neurodegenerative diseases (NDDs) remains poorly understood. To elucidate this subregional heterogeneity of astrocytes in the hippocampus and parahippocampal cortex and its implication for neurodegeneration, we employed high-content neuropathology, integrating chromogenic immunohistochemistry (cIHC) and digital pathology, to map and quantify the expression of functional astrocytic markers (GFAP, ALDH1L1, AQP4, GPC5 and ALDH7A1) of healthy individuals, of patients with Alzheimer's disease (AD) or Parkinson's disease with dementia (PDD). We found that astrocytic markers followed distinct expression patterns in AD and PDD. In AD, GFAP was strongly reduced in specific hippocampal regions, whereas AQP4 was increased and GPC5 expression, although regionally stable, was locally associated with amyloid and tau pathology. In PDD, astrocytic responses were characterized by selective decreases in ALDH1L1 and ALDH7A1, with GFAP and GPC5 remaining largely unaffected. Notably, GFAP and GPC5 expression delineated distinct astrocytic subtypes that were differentially distributed across hippocampal subfields and showed specific responses to AD and PD pathologies. These findings provide new insights into the landscape of astrocytic heterogeneity in the human hippocampus and beyond, revealing disease- and region-specific astrocytic signatures. Importantly, they underscore the value of incorporating novel markers such as GPC5 to fully capture astrocytic diversity and to better understand astrocyte contributions to neurodegeneration.

INTRODUCTION

Astrocytes are glial cells of the central nervous system (CNS) essential for its development, homeostasis and function. It is estimated that they constitute between 20% and 40% of all brain cells (Khakh and Sofroniew 2015) performing critical roles in the regulation of synapse formation and plasticity (Perea et al. 2009; Eroglu and Barres 2010; Sancho et al. 2021) ; neurotransmitter clearance and ion homeostasis (Sancho et al. 2021), as well as neuroprotection (Bouvier et al. 2022). Astrocytes are also an integral component of the neurovascular unit contributing to blood-brain barrier function (Díaz-Castro et al. 2023; MacVicar and Newman 2015) and neuronal metabolic support (Bélanger et al. 2011). They are actively involved in key physiological processes including blood flow regulation (Díaz-Castro et al. 2023; Mulligan and MacVicar 2004), glymphatic clearance (Silva et al. 2021; Das et al. 2023), responses to inflammation (Fisher and Liddelow 2024a) and oxidative stress (Chen et al. 2020), and circadian rhythm regulation (Hastings et al. 2023). Moreover, they integrate and compute neural signals suggesting a central role in decision-making (Wang et al. 2017; Kofuji and Araque 2021). In the hippocampus, a brain region crucial for learning and memory, astrocytes contribute to different forms of memory, including working, spatial and contextual memory (Escalada et al. 2024). Although astrocytes perform a variety of homeostatic and protective functions, they are known to alter their properties in response to brain insults, displaying a range of severity in their reactive profile. Reactive astrocytes can be toxic under certain conditions (Rothhammer and Quintana 2015; Liddelow and Barres 2017; Escartin et al. 2021; Lawrence et al. 2023). A reactive astrocytic phenotype is commonly assessed using markers such as glial fibrillary acidic protein (GFAP), which remains the most widely used astrocyte marker (Liddelow and Barres 2017; Luijerink et al. 2024), alongside aldehyde dehydrogenase 1 family member L1 (ALDH1L1), aquaporin 4 (AQP4), S100 calcium-binding protein beta (S100β), excitatory amino acid transporter 1/2 (EAAT1/2 ; GLAST and GLT1), and connexin 43 (Cx43) (Jurga et al. 2021). GFAP in cerebrospinal fluid (CSF) and blood has also emerged as a promising biomarker for neurodegenerative diseases (NDDs) such as Alzheimer's disease (AD) (Benedet et al. 2021; Abdelhak et al. 2022; Lin et al. 2023; Liu et al. 2023; Gogishvili et al. 2025). However, its correlation with parenchymal astrocytic changes is still being debated (Chiotis et al. 2023; Youn et al. 2025). Questions are being raised about the development of astrocyte-specific positron emission tomography (PET) tracers that would capture the complexity of their changes and internal heterogeneity (Edison 2024). Although it is widely accepted that astrocytes exhibit notable differences in morphology, properties, and functionality between and within brain regions, this heterogeneity is still poorly understood in the context of onset or progression of brain diseases. Furthermore, the astrocyte-to-neuron ratio is higher

in humans than in other species, and human astrocytes exhibit even greater morphological and molecular complexity and heterogeneity (Oberheim et al. 2009; Vasile et al. 2017). Astrocytes are traditionally defined by a star-shaped morphology in grey matter but specialised subtypes exist throughout the CNS. These include the fibrous astrocytes of the white matter (Verkhratsky and Parpura 2010b), the Müller glia which is a subtype of radially polarised astrocytes localised in the retina, the Bergmann glia in the cerebellar cortex which display a complex polarised morphology with very long processes (Farmer and Murai 2017; Baldwin et al. 2024), as well as the glia limitans, the interlaminar astrocytes and the varicose projection astrocytes found in the superficial cortical layers of the human brain (Oberheim et al. 2012; Falcone et al. 2021; Ciani and Falcone 2024; Hasel et al. 2025). Studies using single-cell transcriptomics have further highlighted new astrocyte signatures. Disease-associated astrocytes (DAAs) appear at an early stage of AD, increase as the disease progresses and may therefore be a key factor in disease progression (Mathys et al. 2019; Green et al. 2024; Habib et al. 2020). Habib et al. described the DAAs as a GFAP-high population with a unique molecular profile in an AD mouse model and human samples. They also identified a low-GFAP state population expressing a distinct set of genes, including glypican 5 (*Gpc5)*, a membrane-associated heparan sulfate proteoglycan. Therefore, given the profound molecular and functional diversity of astrocytes, it is crucial to characterize their heterogeneity to better understand how specific subsets shift their phenotype and contribute to disease progression.

In this study, we investigate astrocyte heterogeneity in the hippocampus of healthy individuals, and patients with NDD such as AD, and Parkinson's disease with dementia (PDD) patients. Using chromogenic immunohistochemistry (cIHC) and digital pathology, we assessed the expression and distribution of canonical and emerging astrocytic markers such as GFAP, AQP4, ALDH1L1, alongside aldehyde dehydrogenase 7 family member A1 (ALDH7A1) and GPC5. Our comprehensive profiling approach revealed marker-specific patterns of astrocyte distribution, suggesting the presence of distinct subpopulations with region-specific vulnerabilities and molecular signatures. Our findings highlight the limitations of relying only on traditional markers such as GFAP and underscore the importance of incorporating novel markers such as GPC5 to better capture the heterogeneity of human astrocytes and their roles in NDDs.

MATERIALS AND METHODS

Human brain samples

Post-mortem formalin-fixed paraffin embedded (FFPE) hippocampal and cortical tissues were obtained from The Netherlands Brain Bank (NBB, Amsterdam, The Netherlands), the Douglas-Bell Canada Brain Bank (Douglas Mental Health University Institute, Montreal, QC, Canada), and the GIE-Neuro-CEB biobank (Groupe Hospitalier Pitié-Salpêtrière, Paris, France). Research involving these samples was conducted with approval from the respective ethic committees of these institutions, as well as the University of Luxembourg (ERP 16-037 and 21-009).

Neuropathological assessments were carried out by specialized neuropathologists at the brain banks, following standardized criteria including Braak (Braak and Braak 1991; Braak et al. 2003), ABC (Montine et al. 2012) and McKeith (McKeith 2006) staging, based on the presence of Aβ plaques, neurofibrillary tangles (NFTs), and α-synuclein pathology.

FFPE hippocampal and cortical samples include age-matched non-demented CTLs (n= 8), AD (n= 9) and PDD patients (n=10). Age at death, *post-mortem* delay (PMD), sex and staging of the human subjects are listed in Supplementary Table 1.

Immunohistochemistry (IHC)

FFPE hippocampal and cortical tissue blocs were sectioned at 5 µm thickness using a standard microtome and mounted on Dako FLEX IHC-coated slides (Cat# K8020, Agilent). The sections were then dried at 60 °C for at least one hour before undergoing automated staining on a Dako Omnis Immunostainer (Agilent). Antigen retrieval was performed using heat-induced epitope retrieval (HIER) with high- or low-pH buffer solutions (EnVisionTMFLEX Target Retrieval Solution, Cat# K8004 and Cat# K8005, respectively) for 30 min at 97 °C.

Primary antibodies (anti-ALDH1L1 Cat# HPA050139 and anti-AQP4 Cat# AMAb90537) were prepared in EnVisionTMFLEX antibody diluent (Cat# K8006), with specific concentrations provided in Supplementary Table 2. The sections were incubated with primary antibodies for one hour at room temperature (RT), followed by 54isualization using a horseradish peroxidase (HRP)/3,3'-diaminobenzidine (DAB) detection system (EnVisionTMFLEX Detection Kit, Cat# K8000). Counterstaining was performed using hematoxylin (Cat# GC808), after which the slides were dehydrated through ethanol washes and mounted.

Multiplex chromogenic IHC (cIHC)

For experiments conducted using the Ventana Discovery Ultra automated IHC and *in situ* hybridisation (ISH) platform (Roche Ventana Medical Systems, Tucson, AZ, USA), 5 µm sections from FFPE tissue blocs were mounted onto hydrophilic adhesion slides (Matsunami TOMO®, Cat# TOM-1190). Slides were dried as previously described. All reagents were provided within the system as per Roche Diagnostics' recommendations, and washing steps were carried out using Reaction Buffer (Cat# 950-300). Antibody concentrations used in the assays are detailed in Supplementary Table 2.

For both single and multiplex IHC, counterstaining was performed using haematoxylin II (Cat# 790-2208) and bluing reagent (Cat# 760-2039), each incubated for 4 min. Following staining, all slides underwent washing, dehydration through a graded alcohol series, and were coverslipped.

For single-plex cIHC, sections were first deparaffinised at 69 °C in EZ Prep solution (Cat# 950-102) for 8 min, repeated across three cycles. HIER was carried out at 95 °C for 40 min using Cell Conditioning 1 (CC1, Cat# 950-224). To block endogenous peroxidase and non-specific protein interactions, sections were incubated with Chromomap (CM) inhibitor at 37 °C for 8 min. Primary antibodies (anti-ALDH1L1 Cat# HPA050139, anti-ALDH7A1 Cat# HPA023296, anti-AQP4 Cat# AMAb90537, anti-GFAP Cat# 760-4345, anti-GPC5 Cat# HPA040152, anti-VGAT Cat# HPA058859 and anti-VGLUT1 Cat# HPA063679) were automatic and manually applied after dilution in EnVisionTMFLEX buffer, respectively. Incubation with primary antibodies lasted 60 min, followed by detection using OmniMap anti-Rb (Cat# 760-4311) or OmniMap anti-Ms (Cat# 760–4310) for 16 min. This was followed by sequential incubations of H_2O_2 CM (4 min), DAB CM (8 min), and Copper CM (4 min), all from the Discovery CM DAB kit (Cat# 760-159). All multiplex protocols (two- to three-plex) shared a common initial sequence, including deparaffinization, HIER using CC1, and blocking with the Discovery inhibitor, unless otherwise specified. In the two-plex combinations (GPC5/GFAP, GPC5/ALDH1L1, ALDH1L1/GFAP, AQP4/GFAP, GPC5/AQP4, ALDH7A1/GPC5, ALDH7A1/GFAP, ALDH1L1/ALDH7A1, GPC5/AT8 and GPC5/pS396) following deparaffinization and HIER, one drop of Discovery inhibitor (Cat# 760-4840) was applied for 8 min. Subsequently, primary antibodies including anti-GPC5, anti-ALDH1L1, anti-ALDH7A1 and anti-AQP4 were incubated for 60 min. These were developed using OmniMap anti-Rb or OmniMap anti-Ms HRP for 16 min, followed by a chromogenic reaction using Discovery Purple and H_2O_2 Purple from the Discovery Purple Kit (Cat# 760-229), with 4 min and 32 min of incubation, respectively. Between each staining cycle, heat-mediated antibody denaturation (100 °C for 24 min) was performed using Cell Conditioning 2 (CC2) reagent (Cat# 950-223) to dissociate primary antibody-HRP complexes and prevent cross-reactivity with residual HRP. Next, anti-GFAP, anti-ALDH1L1, anti-ALDH7A1, anti-

phospho tau AT8 (Cat# MN1020), anti-phospho tau pS396 (Cat# 44-752G), anti-GPC5, and anti-AQP4 were applied for 48 min (anti-GFAP) or 60 min (all others). Detection involved signal amplification with OmniMap anti-Rb or anti-Ms HRP for 16 min, followed by chromogenic development with either Discovery Teal HRP chromophore (Cat# 760-247) or Discovery Green HRP chromophore (Cat# 08478295001), involving a 4-min incubation with Teal/Green HRP Substrate, 32 min with Teal/Green HRP H_2O_2, and 16 min with Teal/Green HRP Activator.

The three-plex protocols (4G8/GPC5/GFAP; pSYN/GPC5/GFAP) were carried out as follows: anti-4G8 (Cat# 800712) or anti-pSYN (Cat# MABN826) were incubated for 1 hour and 32 min, amplified with OmniMap anti-Ms HRP for 16 min, and revealed using Discovery CM DAB according to the single-plex IHC method. After denaturation, anti-GPC5 was applied for 60 min, followed by OmniMap anti-Rb HRP for 16 min and chromogenic detection with Discovery Purple. Finally, anti-GFAP was incubated for 48 min, followed by signal amplification using OmniMap anti-Rb HRP for 16 min and development using either Discovery Teal HRP or Discovery Green HRP.

Brightfield Microscopy

Brightfield imaging of chromogenic stained FFPE sections was conducted using a Leica DM2000 LED microscope equipped with 5X, 10X, 20X, 40X and 63X objectives, along with a Leica DMC2900 camera (Leica Microsystems). Additionally, high-throughput whole-slide scanning was performed using the IntelliSite Ultra Fast Scanner (Philips). In certain analysis, if needed, images were also acquired using the HALO® image analysis platform (Indica Labs, version 3.6).

Digital pathology and statistical analysis

Analysis of cIHC images were performed using the HALO® image analysis platform (Indica Labs, version 3.6). The areas of the hippocampus, which was manually segmented into five subregions (dentate gyrus (DG), Cornu Ammonis 4 (CA4), CA3, CA1/CA2, and subiculum as well as the parahippocampal cortex were measured. GFAP, AQP4, ALDH1L1, ALDH7A1 and GPC5-positive areas were quantified using the HALO® area quantification module. Comparisons of stained area percentages were conducted using Wilcoxon test with R Studio software (Supplementary File 1– Supplementary Excel 1).

R2 Genomics platform database analysis

The *gfap* and *gpc5* genes, which showed a positive correlation, were extracted from the R2 Genomics platform (https://r2.amc.nl/) from a dataset (n=173) of cognitively unimpaired individuals in the Alzheimer's Disease Research Center (Brain-ADRC) Cotman (253 – MAS5.0 – u133p2) regrouping four brain regions: the hippocampus, the entorhinal cortex, the post-central gyrus and the superior frontal gyrus (GSE48350). To further refine astrocyte-relevant targets, we integrated data from the Brain RNA-seq (https://brainrnaseq.org/) and Human Protein Atlas (https://www.proteinatlas.org/) databases, selecting genes associated with astrocyte identity or function. The 500 most highly correlated genes for *gfap* or *gpc5* were then subjected to STRING pathway enrichment analysis (https://string-db.org), with the four most prevalent Kyoto Encyclopedia of Genes and Genomes (KEGG) pathways reported graphically.

RESULTS

GFAP and AQP4 reveal heterogeneous, spatially restricted astrocyte subpopulations in the human hippocampus, in contrast to the homogeneous distribution of the pan-astrocytic marker ALDH1L1.

To assess the distribution, composition, and morphology of astrocytes within the human hippocampus in the context of NDDs, we first evaluated the spatial expression patterns of three commonly used astrocytic markers – GFAP, AQP4, and ALDH1L1 – in the hippocampus. cIHC was performed on FFPE sections from 8 cognitively normal elderly donors (CTL) (mean age at death: 89 years, 5 females, 3 males) for each marker. The DAB-stained area was measured using HALO® software and analysed for each hippocampal subfield DG, CA4, CA3, CA1/CA2, subiculum and parahippocampal cortex (PHC) (Fig. 1A-E).

While GFAP, AQP4 and ALDH1L1 were all expressed throughout the hippocampus, each marker revealed distinct astrocyte features (Fig. 1). Staining for GFAP, the most used marker for visualizing the astrocyte cytoskeleton, showed a heterogeneous expression pattern across hippocampal subfields and layers (Fig. 1Aa-d). Within the CA and subiculum regions, GFAP expression was the highest in the oriens, molecular and radiatum layers (Fig. 1Ab-d). However, in the pyramidal layer, GFAP staining was more sparse, almost patchy, with some areas clearly devoid of GFAP+ astrocytes (Fig. 1Ac). There was no significant difference in relative GFAP expression between subfields and PHC, even though it was lower in CA1/CA2 and the subiculum (Fig. 1E). The staining of AQP4, a water channel protein enriched in the perivascular endfeet and the membrane of the astrocytes, showed higher intensity in the DG and CA4, and denser labeling in the molecular layer of CA compared to the radiatum and pyramidal layers (Fig. 1Be-h). In the subiculum, AQP4 was sparsely distributed within the pyramidal layer, in contrast to the polymorphic and molecular layers, which displayed a high density of AQP4+ cells (Fig. 1Bh). The relative expression of AQP4 was significantly higher in the DG and CA4 compared to other hippocampal subfields (Fig. 1E). ALDH1L1 staining, which detects a cytoplasmic astrocytic enzyme, exhibited a broader expression than GFAP throughout the hippocampus, showing a uniform astrocyte density across subfields (Fig. 1Ci-l). Its relative expression was also similar across hippocampal subfields (Fig. 1E). These results suggest that ALDH1L1 is a broader astrocyte marker.AQP4 is expressed unevenly by hippocampal astrocytes with predominant expression polarized towards blood vessels, whereas GFAP defines subsets of astrocytes with distinct spatial distributions.

Glypican 5 is expressed by a distinct astrocyte subpopulation in the human hippocampus.

Given the observed astrocytic heterogeneity, we hypothesized the existence of subpopulations not fully captured by GFAP. To explore this, we investigated the expression of glypican 5 (GPC5) previously linked to $GFAP_{LOW}$ astrocyte population in single cell transcriptomic analysis (Habib et al. 2020). GPC5 expression was assessed in hippocampal regions from the same cohort of *post-mortem* CTL samples.

GPC5 showed a more discrete and spatially restricted expression pattern throughout the hippocampus (Fig. 2A-E). Quantitative analysis confirmed its limited surface coverage across hippocampal subfields relative to the broader expression observed with GFAP, AQP4 and ALDH1L1 (mean expression in total hippocampus: GFAP= 64.73%; AQP4= 77.58%; ALDH1L1= 74.38%; GPC5= 2.97%) (Fig. 2F, Supplementary File 1– Supplementary Excel 1). GPC5 was most prominently expressed in the DG, particularly in the outer two-thirds of the molecular layer (SM 2/3) where its diffuse staining resembled synaptic labelling. Well-defined GPC5+ astrocytes were observed in CA4 (Fig. 2B). In the CA subfields, GPC5 displayed a laminar distribution, characterised by a higher proportion of GPC5+ astrocytes in the molecular and oriens layers, compared to the radiatum and pyramidal layers (Fig. 2C-D). In the subiculum, GPC5+ astrocytes exhibited complex branching, although a few GPC5+ neurons were also detected (Fig. 2E). Given the synaptogenic properties of GPC5 (Bosworth et al. 2023; Salas et al. 2024a), we further investigated whether GPC5 expression is associated with excitatory and inhibitory synapses in the DG. The diffuse staining of GPC5 In the DG overlapped with VGAT (vesicular GABA transporter) but not VGLUT (vesicular glutamate transporter) staining, labelling inhibitory and excitatory synapses, respectively (Fig. 2G). Next, we investigated the presence of GPC5+ astrocytes in the PHC and prefrontal cortex (PFC). In the PHC, GPC5 overall expression was significantly lower than that of GFAP, AQP4 and ALDH1L1 (Supplementary Fig. 1A-E). In the PFC, GPC5+ astrocytes were sparsely distributed, with enrichment in layers I–III and VI (Supplementary Fig. 2).

GPC5 labels distinct astrocyte subsets with a shared core identity

To explore potential functional differences between GFAP+ and GPC5+ astrocyte populations, we identified genes positively correlated with either *gfap* or *gpc5* across four brain regions (hippocampus, entorhinal cortex, post-central gyrus, and superior frontal gyrus) from cognitively unimpaired individuals in the Alzheimer's Disease Research Center (Brain-ADRC) Cotman dataset (n=173) using the R2 Genomics platform. This analysis revealed both marker-specific gene sets and a core set of genes that were correlated with the expression of both *gfap* and *gpc5* (Fig. 3A). Astrocyte-relevant genes included *cd44* and *st6galnac3* for GFAP+ astrocytes, and *slc1a4* and *erbb4* for GPC5+

astrocytes. A set of canonical astrocytic genes; *slc1a2*, *slc1a3*, *aldh1l1*, *aqp4*, *aldh7a1*, and *apoe;* was shared between both groups, supporting the hypothesis of a common core identity. To infer biological differences, we subjected the first 500 positively correlated genes for each group to STRING pathway enrichment analysis (https://string-db.org). GFAP-associated genes were enriched for KEGG pathways including regulation of the actin cytoskeleton and TGF-β signalling, while GPC5-correlated genes showed enrichment in fatty acid degradation and glycine, serine and threonine metabolism, pointing to distinct functional programs between these astrocyte subsets (Fig. 3B-C).

To further investigate the complex identity of hippocampal astrocytes, we first performed multiplex cIHC for GFAP combined with AQP4 (n=3) or ALDH1L1 (n=5) or ALDH7A1 (n=5) in CTL *post-mortem* samples. Co-staining for GFAP and AQP4 revealed that GFAP+ astrocytes were also AQP4+ such as in the CA4 or DG with a spectrum of AQP4 intensity. In the CA3 to CA1 subfields, GFAP+/AQP4+ astrocytes were often adjacent to AQP4+ single positive cells. In the subiculum and the PHC we observed a mosaic pattern of GFAP+/AQP4+ astrocytes alongside single positive cells for either AQP4 or GFAP (Fig. 3D, Supplementary Fig. 3A). GFAP/ALDH1L1 co-staining in the hippocampus and PHC confirmed that ALDH1L1 is a broader marker than GFAP, with numerous astrocytes stained only for ALDH1L1 whereas GFAP astrocytes were predominantly ALDH1L1+/GFAP+ double-positive (Fig. 3E, Supplementary Fig. 3B). ALDH7A1 showed a uniform expression throughout the hippocampus, with surface coverage comparable of ALDH1L1 (Supplementary Fig. 4A). Combined with ALDH1L1 (n=4), co-staining confirmed that the two markers were expressed by hippocampal astrocytes in an overlapping manner, with almost all of them being ALDH7A1+/ALDH1L1+ (Supplementary Fig. 4B). Duplex staining of ALDH7A1 and GFAP (n=6) revealed that almost all GFAP+ astrocytes expressed ALDH7A1 (Fig. 3F). Furthermore, many astrocytes expressed ALDH7A1 with low or undetectable levels of GFAP.

We next multiplexed GPC5 in combination with GFAP (n=6), AQP4 (n=3), ALDH1L1 (n=5) or ALDH7A1 (n=4) in CTL hippocampal samples. Duplex staining with GPC5 and GFAP revealed a spectrum of profiles among astrocytes, with cells that were either single-positive for GPC5 or GFAP, or double-positive for GPC5 and GFAP. Importantly, they were expressing GFAP at various levels ranging from GPC5/$GFAP_{LOW}$ to GPC5/$GFAP_{HIGH}$ mainly in the CA4 and the molecular layer of the CA, but also in the glia limitans and the first layer of the PHC (Fig. 3G, Supplementary Fig. 3C). Co-staining for GPC5 and AQP4 showed double-positive AQP4+/GPC5+ astrocytes in the CA4 region, and few in the molecular layer of the CA. We also observed double-positive AQP4+/GPC5+ cells in the second layer of the PHC with many single AQP4+ astrocytes (Fig. 3H, Supplementary Fig. 3D). ALDH1L1 or ALDH7A1 were both labelling all GPC5+ astrocytes in the hippocampus (Fig. 3I-J, Supplementary Fig. 3E).

These observations highlight the molecular heterogeneity of hippocampal astrocytes. ALDH1L1 and ALDH7A1 are more ubiquitous markers, whereas GFAP, AQP4 and GPC5 delineate distinct astrocyte subpopulations in terms of identity, localisation and numbers, suggesting a continuum of astrocyte phenotypes. This underscores the importance of using a broader panel of astrocyte markers to gain a more comprehensive understanding of astrocyte responses in the context of NDDs.

Astrocyte markers are differently affected in AD and PDD.

To investigate disease-associated alterations in astrocyte subtypes, we performed cIHC and quantified DAB-stained area for GFAP, AQP4, ALDH1L1, ALDH7A1 and GPC5 in *post-mortem* hippocampal sections from individuals with AD (n=9, average age at death: 73.4 years, 6 females, 3 males) and PDD (GFAP, AQP4, ALDH1L1 and GPC5: n=10, average age at death: 74.6 years, 5 females, 5 males; ALDH7A1: n=8, average age at death: 73.8 years, 3 females, 5 males), compared to CTLs. All markers tested followed a specific pattern across disease groups and hippocampal subfields (Fig. 4A-O). GFAP expression was significantly reduced in AD relative to CTLs and PDD in DG, CA4 and CA3. In CA1/CA2, GFAP intensity was decreased in both AD (p value=0.07) and PDD (p value=0.04) cases. Despite the reduced staining, we observed focal areas of intense GFAP expression. In some of these areas in AD, GFAP+ astrocytes displayed a hypertrophic appearance polarised towards presumed amyloid-β plaques, especially in CA1. We also found clusters of astrocytes expressing high level of GFAP in PDD (Fig. 4A-C). AQP4 expression, however, was significantly increased in AD compared to both CTLs and PDD in CA3, CA1/CA2 and subiculum. In PDD, the distribution of AQP4 was comparable to CTL cases to the exception of CA4 (p value=0.03) showing significant lower levels (Fig. 4D-F). Expression of ALDH1L1 was significantly decreased in both AD and PDD. In AD cases, the decrease was more prominent in DG, CA4, CA3 and PHC, whereas in PDD the decrease was significant for all subfields and PHC. In both AD and PDD, we observed a general reduction of ALDH1L1 intensity in the astrocyte arborisation (Fig. 4G-I). ALDH7A1 followed the general ALDH1L1 pattern, showing a significant and strong reduction in PDD cases globally, with the strongest decrease seen in the CA3, CA1/CA2, subiculum and PHC subregions. There was a significant decrease in the subiculum and PHC of AD cases (Fig. 4J-L). Finally, GPC5 expression displayed a specific expression pattern, remaining stable across diseases. Besides, we observed a decrease of GPC5 expression in DG of AD patients (p value=0.07), mainly due to the loss of a more diffuse staining in the molecular layer. Nevertheless, GPC5+ astrocytes exhibited a partially altered spatial organisation in AD, appearing more scattered and forming small clusters across the hippocampus. GPC5+ astrocyte adopted a spectrum of morphologies, ranging from

thin to very enlarged phenotypes. Furthermore, we observed plaque-like and tangle-like morphologies labelled by a more diffuse GPC5 staining (Fig. 4M-O).

To further characterize whether the pattern of astrocyte identity is affected by neurodegeneration, we next used multiplex cIHC to co-stain pairs (n=3 GFAP/AQP4; n=6 GFAP/ALDH1L1; n=6 GFAP/ALDH7A1; n=6 GPC5/GFAP; n=3 GPC5/AQP4; n=6 GPC5/ALDH1L1; n=6 GPC5/ALDH7A1) of astrocyte markers in AD hippocampal samples. We observed a broader range of AQP4 and GFAP expression in the AQP4+/GFAP+ population, from low to very high intensity. AQP4 was also found to be associated with Aβ plaques (Fig. 5A, Supplementary Fig. 5A). The mosaic pattern of GFAP, AQP4, ALDH1L1 and ALDH7A1 expression found in the subiculum and PHC of CTLs was largely preserved in AD (Supplementary Fig. 5A-C). By combining GPC5 with GFAP, we observed a variety of profiles, a high proportion of single-positive GFAP, some GFAP+/GPC5+ cells displaying GFAP intensity ranging from low to high; and a small number of single-positive GPC5 cells. GPC5+/GFAP+ cells exhibited various morphologies, ranging from very elongated to enlarged. In the hippocampus as well as the PHC, GPC5+ astrocytes forming nets around Aβ plaques were all positive for GFAP (ranging from low to very high level) but were less frequent than single GFAP+ astrocytes (Fig. 5D, Supplementary Fig. 5D). GPC5 staining also revealed tangle-like structures near GPC5+ astrocytes, often double stained by GFAP forming then a kind of astrocyte tangle mesh (Fig. 5D). The relationship between GPC5+ astrocytes and AQP4, ALDH1L1 and ALDH7A1 remained the same as in CTLs (Fig. 5E-G). Multiplexed cIHC of GPC5 with AQP4, ALDH1L1 or ALDH7A1 in the hippocampus and PHC revealed plaques surrounded by double-positive astrocytes (Fig. 5E-G; supplementary Fig. 5E-G). Although ALDH1L1 expression was reduced in AD, it was still present in double-positive GPC5+/ALDH1L1+ cells.

Taken together, our data revealed that each astrocyte marker follow a distinct alteration pattern across disease types, also dependant of the subregional anatomy. We also report that GFAP+ and GPC5+ astrocytes are differentially impacted by neurodegeneration. Overall, GFAP expression is severely decreased in AD hippocampal samples opposed to the increase of AQP4. GPC5 expression largely persists. Both GFAP and GPC5 may be focally involved in Alzheimer's pathology. Broader astrocyte markers, such as ALDH1L1 and ALDH7A1, are also affected in AD and PDD, with a more significant reduction observed in PDD.

GPC5+ astrocytes are associated with amyloid and tau pathology but not with synuclein pathology.

Based on the above observation of regrouped GPC5+ astrocytes around putative amyloid-□ plaques, we next decided to investigate whether GPC5+ astrocytes were associated with pathological

hallmarks of AD and PDD (Salas et al. 2024b; Green et al. 2024). To this end, we examined the association of GPC5+ astrocytes with amyloid-β (Aβ), tau or α-synuclein pathology in *post-mortem* samples from AD and PDD patients. To evaluate the misfolded protein pathologies in AD samples, we co-stained markers of amyloid (4G8) and tau (AT8 or pS396) pathology with GPC5. Duplex staining with 4G8 (n=3) confirmed the frequent association, but not systematic, of GPC5+ astrocytes with Aβ plaques across hippocampal subfields and PHC (Fig. 6A). GPC5 was also found diffuse in the core. Other clusters of GPC5+ astrocytes were again found within the pyramidal layer alongside tangle-like structures positive for GPC5 (Fig. 6A). The triplex staining 4G8, GPC5 and GFAP (n=8) confirmed that GPC5+/GFAP+ are often associated with Aβ plaques across hippocampal subfields and PHC (Fig. 6B). We decided to extended our analysis to the PFC (n=3), where amyloid-β might accumulate prior to the hippocampus (Thal et al. 2002). As expected, the PFC exhibited a higher amyloid burden compared to the hippocampus, and this was accompanied by a marked presence of single GPC5+ astrocytes, particularly in proximity to Aβ plaques. These cells were observed to be polarised towards diffuse, non-cored and dense core Aβ plaques (Almeida et al. 2025). Some exhibited hypertrophic morphology and invaded the boundaries of the plaques. GFAP+ astrocytes were present, albeit to a lesser extent than in the hippocampus. Hypertrophic GPC5+/GFAP+ double-positive astrocytes were mostly observed close to Aβ plaques (Supplementary Fig. 6).

To investigate the relationship between GPC5 and tau tangles, we double-stained tissue sections for GPC5 and either AT8 (n = 3) or pS396 (n = 3). These are two markers of different stages of tau tangle maturation: AT8 is more general, whereas pS396 is more specific to advanced stages (Augustinack et al. 2002; Fixemer et al. 2025). GPC5+ astrocytes were frequently found near AT8+ tangles. However, there was no overlap with diffuse GPC5 (Fig. 6C). Double staining with pS396 revealed that pS396 tangles were frequently stained with GPC5 and were often surrounded by GPC5+ astrocytes (Fig. 6D).

In PDD samples stained for GPC5, GFAP and pSYN (pSYN 81A), we found no clear association between GPC5+ astrocytes, Lewy bodies or neurites. However, we did observe some dysmorphic GFAP+ astrocytes, some of which exhibited intracellular accumulation of phosphorylated α-synuclein (Fig. 6E). Overall, our data revealed that GPC5+/GFAP+ astrocytes can be associated with amyloid deposition or tau tangle maturation in AD. These results support the idea that GPC5+ astrocytes are a distinct subtype of astrocytes in terms of both spatial distribution and response to pathology. They may engage at different stages of disease progression.

DISCUSSION

For a long time, astrocytes have been considered a functionally uniform population, however accumulating evidence now highlights their extensive regional and molecular heterogeneity. Recent transcriptomic studies revealed astrocyte subtypes with distinct molecular profiles in different brain regions of mice (Chai et al. 2017; Batiuk et al. 2020; Viana et al. 2023; Bocchi et al. 2025). Still, how this diversity manifests in the human brain, and its potential involvement in the onset or progression of NDDs remains poorly defined. In this study, we present a systematic characterisation of astrocyte heterogeneity in the human hippocampus, integrating chromogenic immunohistochemistry and quantitative digital pathology in both non-demented control and disease contexts (AD and PDD). Our results provide a comparative mapping of canonical and subtype-specific astrocytic markers across hippocampal subfields and of the PHC in aged human brains. Notably, we demonstrate that astrocyte identity is more accurately captured through combinatorial marker analysis rather than through reliance on a single marker such as GFAP, which limits the resolution of astrocytic phenotyping (Escartin et al. 2021; Zimmer et al. 2024). We distinguish astrocytic subtypes across a spectrum of phenotypes, which are mainly characterised by the degree of expression of GFAP and GPC5. These subtypes have divergent spatial distributions in healthy and pathological conditions.

GFAP identifies a large subgroup of astrocytes and is widely decreased in AD but not in PDD.

By mapping GFAP+ astrocytes in the healthy human hippocampus, we show that GFAP labels only a subset of astrocytes, exhibiting subfield-specific expression with a more sparse and patchy distribution particularly within the pyramidal layers of CA1/CA2 and CA3, as well as in the subiculum. However, these GFAP-negative or low parenchyma territories are not devoid of astrocytes, as they are populated by ALDH1L1+ and ALDH7A1+ astrocytes, as well as AQP4+ astrocytes to a lesser extent. Similar observations were made in the PHC, where GFAP expression varies across cortical layers. These findings demonstrate the necessity of moving beyond single-marker definitions of astrocyte identity (Escartin et al. 2021; Sofroniew and Vinters 2010). GFAP negative or $GFAP_{LOW}$ astrocytes are not unique to human and have been found in the CA1 radiatum layer of the adult rat (Walz and Lang 1998) or mouse (Habib et al. 2020) hippocampus. The patchy distribution of GFAP, confirmed in eGFP-GFAP mice (Nolte et al. 2001), has led to the development of more inclusive astrocyte reporter models using markers such as ALDH1L1 (Cahoy et al. 2008; Srinivasan et al. 2016; Yang et al. 2011) which we show here also offer broader coverage in the human hippocampus. Strikingly, we observe a pronounced decrease in GFAP expression in the hippocampus of AD patients but not in PDD. The decrease is more pronounced

in DG, CA4 and CA3 which are the subfields with the highest GFAP expression in CTLs. These results appear to contradict prior studies reporting GFAP upregulation in AD animal models (Kamphuis et al. 2012; Olsen et al. 2018) and AD patient (Simpson et al. 2010; Phillips et al. 2024) brains. However, the brain samples analysed in our study reflect advanced stages of disease, and the reported increase in GFAP expression may represent earlier, transient astrocytic responses that precede severe neurodegeneration. This interpretation aligns with *in vivo* PET imaging studies of astrocyte reactivity. Using a new astrocyte-specific PET tracer (11C BU99008), Livingston et al. reported that astrocyte reactivity peaks in the early stages of AD, but declines during the later stages, suggesting a shift from a reactive to a potentially functionally impaired astrocytic phenotype (Livingston et al. 2022). Notably, Mohammed et al., employing the same tracer, found no significant differences in astrocyte reactivity between individuals with Parkinson's disease dementia and age-matched controls (Mohamed et al. 2022), which is consistent with our own findings and supports the hypothesis that astrocytic activation in neurodegeneration is disease- and stage-specific. Despite the overall reduction of GFAP in late-stage AD, we still observed GFAP+ astrocytes closely associated with Aβ plaques. Our recent work supports that human GFAP+ astrocytes contribute to the formation of glial-immune hotspots around Aβ plaques, linking them to hippocampal deterioration and broader disease progression (Fixemer et al. 2025), providing direct validation of mechanisms previously described in AD mouse models (Huang et al. 2024; Mallach et al. 2024).

AQP4 expression is increased in AD while ALDH1L1 and ADH7A1 ones are decreased in PDD.

AQP4 plays critical roles in maintaining water homeostasis and ensuring an efficient glymphatic clearance (Nagelhus and Ottersen 2013). Alteration of the glymphatic system is associated with ageing (Kress et al. 2014; Hsiao et al. 2023) and NDDs (McKnight et al. 2021; Liu et al. 2024; Carotenuto et al. 2022; Zeppenfeld et al. 2017). Alteration of AQP4 expression and perivascular localization has been reported in AD models (Ishida et al. 2022; Xu et al. 2015; Pedersen et al. 2023) as well as in patients (Zeppenfeld et al. 2017), resulting in a dysfunctional glymphatic system that affects Aβ and tau clearance (MohanaSundaram et al. 2024), contributing to cognitive impairment (Xu et al. 2015). Our data show a strong increase of AQP4 expression in AD confirming astrocyte dysfunction associated with the neurovascular and glymphatic system; highlighting AQP4 as a potential therapeutic target for AD.
Surprisingly PDD samples that were mostly preserved from GFAP and AQP4 changes showed a subregional decrease of both ALDH1L1 and ALDH7A1. An imbalance of ALDH1L1 could potentially disrupt folate metabolism in the brain, a process that is known to be altered in PD (Bou Ghanem et al.

2024; Doddaballapur et al. 2025). Also known as Antiquitin, ALDH7A1 plays a critical role in regulating adult hippocampal neurogenesis, learning and memory processes (Yan et al. 2024). Mutations in ALDH7A1 are linked to pyridoxine-dependent epilepsy (PDE), a condition marked by cognitive impairment, making it a promising target (Yan et al. 2024; Coughlin and Gospe 2023; Salih et al. 2024). In the human brain, ALDH7A1 expression has been observed in cortical astrocytes of young adults and colocalized with GFAP (Jansen et al. 2014). Conditional deletion of ALDH7A1 in astrocytes induces spontaneous seizures in mice in a pyridoxine-dependent manner and is accompanied by impaired dendritic spine development and cognitive deficits. Loss of ALDH7A1 also leads to the dysregulation of the MGP (matrix Gla protein) gene in astrocytes, which potentially disrupts extracellular matrix (ECM) homeostasis (Wu et al. 2025). ECM remodelling is relevant to both astrocyte function, AD and PD progression (Jones and Bouvier 2014; Yang et al. 2024; Jacobson and Song 2024). These findings suggest that ALDH7A1 alterations may also contribute to astrocyte dysfunction in various neurodegenerative conditions.

The various patterns of GFAP, AQP4, ALDH1L1, and ALDH7A1 across conditions overall indicates a partial or severe loss of astrocyte homeostatic signatures in the advanced stages of AD and PDD. These results reveal significant differences in astrocytic signatures that appear to be related to the disease and the anatomical distribution and suggest that different underlying cellular mechanisms are involved in these pathologies (Song et al. 2009; van den Berge et al. 2012).

GPC5 astrocytes constitute a subgroup with unique disease signature.

GPC5 belongs to the glypican family of GPI-anchored heparan sulphate proteoglycans (GPC1–GPC6) and is widely expressed in the mammalian brain throughout development and adulthood (Filmus et al. 2008). Among these, GPC5 is notably expressed by human astrocytes and has been associated with synapse maturation and maintenance (Bosworth et al. 2023). Moreover, GPC5 expression has been reported to be dysregulated in various NDDs, including fronto-temporal dementia (Marsan et al. 2023), multiple sclerosis (Schirmer et al. 2019) and AD (Salas et al. 2024a; Lau et al. 2020). This suggests a broad role of GPC5 in brain pathology. In healthy hippocampus, the expression of GPC5 is relatively low compared to that of GFAP, AQP4, ALDH1L1 and ALDH7A1. However, it displays distinct laminar distributions across the CA subfields that differ from the pattern of GFAP. We also observed a strong, diffuse GPC5 immunoreactivity in the molecular layer 2/3 of the DG, overlapping with VGAT+ inhibitory synapses in CTL and preserved in PDD. This pattern is markedly changed in AD. Given GPC5's role in synapse regulation, changes in its expression could influence synaptic dysfunction and neuronal

hyperexcitability (Bosworth et al. 2023; Salas et al. 2024a). Reduced GPC5 expression in the DG could then significantly impact the hippocampal neuronal circuitry. The spatial organization of GPC5+ astrocytes in AD differed from age-matched controls, especially in the CA1/CA2, PHC as well as in the PFC of AD patients where they can form clusters toward Aβ plaques or be found close to tangles. Given the association of GPC5 expression with homeostatic astrocytic signatures (Green et al. 2024; Habib et al. 2020; Saliu and Zhao 2024; Dai et al. 2023), our finding suggest that GPC5+ astrocytes represent a protective subtype. Our data highlight the heterogeneity of the astrocyte cluster forming reactive glial nets (RGNs) (Bouvier et al. 2016) with microglia, which may differ over time and in different anatomical regions. Interestingly we have also found a more diffuse staining of GPC5 localised in amyloid plaque core and tangles. Glypicans such as GPC1 and GPC4 are intimately involved in the amyloid plaque formation (Williamson et al. 1996) and are found in diffuse and core plaques (Van Horssen et al. 2002). GPC5 has recently been found to be associated with AD brain proteome and plaques in CRDN8 AD mouse model and humans (Levites et al. 2024). Based on our results, GPC5+/GFAP+ astrocytes may release GPC5 in the vicinity of the plaque. Similarly, we found GPC5 in tangles, which are often surrounded by GPC5+ /GFAP+ astrocytes. The presence of diffuse GPC5 around tangles is associated with small invasive processes of GFAP, seemingly forming an astrocyte tangle mesh. This distribution is potentially associated with the severity of tau pathology and appears to be linked to specific types of tangles identified by the pS396 antibody but not the AT8 antibody.

Overall, our findings on human hippocampal and cortical astrocytes support the notion that astrocyte identity and response evolve along the spatial and temporal trajectory of AD pathology (Serrano-Pozo et al. 2024) and that astrocyte metabolism and function are partially dysregulated in late PD (Derevyanko et al. 2025).

Limitations of the study

This study has several limitations. First, our cohort includes limited number of patient brain samples, which may affect the generalizability of our findings. Second, our analysis focused primarily on tissues representing advanced stages of the disease. Validation in larger and independent cohorts is therefore necessary. Additional studies are needed to assess astrocyte diversity and vulnerability in other key regions implicated in disease.

Conclusion

In summary, our study highlights the significant heterogeneity of astrocytes in the human hippocampus, challenging the near-exclusive reliance on GFAP to define these cells to date. We propose the use of multiple markers such as AQP4, ALDH1L1 and ALDH7A1 for observing changes in the overall distribution and number of astrocytes in healthy and diseased brains. Our results revealed marker-specific patterns of astrocyte distribution, suggesting the presence of distinct subpopulations with region-specific vulnerabilities and molecular signatures. We identified two distinct astrocyte subpopulations based on their expression of GFAP and/or GPC5, exhibiting different responses to neurodegeneration. This work advances the field by demonstrating that astrocyte heterogeneity in the human hippocampus is not merely a static regional characteristic but is dynamically shaped by disease type and stage (Edison 2024). These insights underscore the importance of incorporating astrocytic diversity into models of NDD pathogenesis and highlight new avenues for targeted therapeutic strategies.

DECLARATIONS

Ethics approval

Use of human brain *post-mortem* samples for research was approved by the respective Ethic Panels of the Douglas-Bell Canada Brain Bank (Douglas Mental Health University Institute, Montreal, QC, Canada), the Netherlands Brain Bank (Netherlands Institute for Neuroscience, Amsterdam) and the GIE-Neuro-CEB biobank (Groupe Hospitalier Pitié-Salpêtrière, Paris, France) as well as of the University of Luxembourg (ERP 16-037 and 21-009).

Data availability

Raw data is available on request.

Consent for publication

All authors have consented for the publication of manuscript.

Declaration of interests

The authors report no competing interests.

Funding

This work was supported by the Espoir-en-tête Rotary-International awards (to DSB) and the Luxembourg National Research Fund (FNR: PEARL P16/BM/11192868 and NCER13/BM/11264123 (to MM)). FJ and SSc were supported by the AFR program of the Luxembourg National Research Found through the grants AFR15735457 and AFR17129900. MMM was supported by the PRIDE program of the Luxembourg National Research Found through the grant PRIDE21/16749720/NEXTIMMUNE2.

Acknowledgments

We thank the brain donors and their family for their support of the project.

Author contributions

DSB conceived and supervised the study. FJ, MMM and SSc performed the experiments. FJ, MMM, SSc and GH produced and analyzed the statistical data. FJ, Ssc and DSB prepared the figures. DM, NM and NBB provided cohort of human brain samples and neuropathological reports. FJ, MMM, MM and DSB.

FIGURE LEGENDS

Figure 1: Distribution of astrocyte markers GFAP, AQP4 and ALDH1L1 across the hippocampus of healthy aging brain.

Representative IHC of (**A**) GFAP, (**B**) AQP4 and (**C**) ALDH1L1 expression in control hippocampus. **A** GFAP expression (DAB, brown) differs between hippocampal subfields with a strong density of GFAP+ astrocytes in (**a**) DG and CA4. GFAP+ astrocytes in the (**b**) CA3, (**c**) CA1 and (**d**) subiculum shows a patchy distribution, especially in the pyramidal layer (stratum pyramidale, SPy). In the subiculum, we distinguished two types of GFAP+ astrocytes: cells with high levels of GFAP ($GFAP_{HIGH}$, full lines) and cells with low GFAP expression ($GFAP_{LOW}$, dashed lines). **B** AQP4 (DAB, brown) is highly expressed in astrocytes of the (**e**) DG/CA4, (**f**) CA3 and stratum moleculare of the CA compared to (**g**) CA1 and (**h**) subiculum. **C** ALDH1L1 (DAB, brown) is widely expressed by hippocampal astrocytes across all hippocampal subfields (**i-l**). **D** Digital pathology workflow used for digital pathology quantification. **E** The relative expression of GFAP and ALDH1L1 is stable across the hippocampal subfields whereas APQ4 expression is the lowest in the CA3 and CA1/CA2. n= 8; statistical analysis: Wilcoxon test, * $p<0.05$, ** $p<0.005$, *** $p<0.0005$ (case #8). **DG**, dentate gyrus; **SM**, stratum moleculare; **SO**, stratum oriens; **SPy**, stratum pyramidale; **SR**, stratum radiatum. Scale bars: low magnification, 500 μm; high magnification (**a–l**) 50 μm.

Figure 2: Glypican 5 is selective to spatially restricted subgroups of astrocytes in the hippocampus.

A-E cIHC reveals the expression of GPC5 by astrocytes in the healthy hippocampus. **A** GPC5 (DAB, brown) expression is enriched in specific layers of the hippocampus subfields (case #5). **B** GPC5 labels many well-defined astrocytes of the CA4 but is diffuse in the DG (case #6). **C** GPC5+ astrocytes of the CA3 are mainly observed in the stratum moleculare (case #6). **D** In the CA1, the radiatum and pyramidal layers showed low density of GPC5+ astrocytes compared to the stratum moleculare (case #6). **E** In the subiculum, GPC5 labels many astrocytic branches and stains a few neurons (asterisk) (case #12). **F** GPC5 expression is uniformly distributed across the hippocampal subfields, although the DG contains high levels of diffused GPC5. n= 8; statistical analysis: Wilcoxon test, * $p<0.05$, ** $p<0.005$, *** $p<0.0005$. **G** Representative IHC staining (DAB, brown) of VGAT, GPC5 and VGLUT1 in the healthy DG show an enrichment of GPC5 in VGAT positive areas (case #2). **SG**, stratum granulosum; **SM 1/3**, inner stratum moleculare; **SM 2/3**, outer stratum moleculare. Scale bars: **A** 500 μm; **B-E** 50 μm; **G** 50 μm.

Figure 3: GFAP and GPC5 reveal subtypes of astrocytes.

A-C *Gfap* and *gpc5*-associated signatures in the R2 human brain bulk RNA-seq database**.** Gene expression positively correlated (p value cutoff: 0.05 FDR) with *gfap* and *gpc5* were extracted from the GSE48350 dataset (173 normal brain samples, 4 brain regions) in the R2: Genomics analysis and visualization platform. **A** The Venn diagram shows a shared astrocytic signature between *gfap* and *gpc5* correlates as well as unique associations. **B-C** Functional signatures associated with (**B**) *gfap* or (**C**) *gpc5*. The top 500 genes with the strongest positive correlation with *gfap* or *gpc5* revealed specific KEGG pathway enrichment. **D** The multiplex cIHC for GFAP (green) and AQP4 (purple) reveals a large number of GFAP+/AQP4+ double-positive astrocytes (dark purple, full arrows), which are found amongst AQP4+ cells (white arrows) (case #9). **E** Co-staining of GFAP (green) and ALDH1L1 (purple) shows a widespread expression of ALDH1L1 across the astrocyte population through the hippocampal layers. In contrast, GFAP labels only specific subgroups of astrocytes that co-express ALDH1L1 (dark purple, full arrows) (case #9). **F** ALDH7A1 (purple) is widely expressed by hippocampal astrocytes. GFAP+ astrocytes (green) also co-express ALDH7A1 (dark purple, full arrows) (case #9). **G** Co-staining of GFAP and GPC5 highlights single-positive astrocytes for either GFAP (teal, empty arrows) or GPC5 (purple, white arrows). It also reveals double-positive GFAP+/GPC5+ astrocytes (full arrows) (cases #2 and #9). **H** Co-staining of GPC5 (purple) and AQP4 (teal) revealed double-positive GPC5+/AQP4+ cells (dark blue, full arrows) (case #9). **I** GPC5+ astrocytes also express ALDH1L1 (dark blue, full arrows) (case #16). **J** GPC5+ astrocytes are positive for ALDH7A1 (dark blue, full arrows) (case #12). White arrows identify single positive astrocytes. **DG**, dentate gyrus. Scale bars: **D** 50 μm; **E** low magnification: 100 μm, high magnification: 50 μm; **F** 50 μm; **G** left panel – low magnification 100 μm, – high magnification 50 μm; right panel 50 μm; **H-I** 50 μm; **J** low magnification 100 μm, high magnification 50 μm.

Figure 4: Differential alterations of astrocytes markers in AD and PDD.

A-B GFAP+ astrocytes (DAB, brown) display a dysmorphic morphology in AD and PDD hippocampi and form cluster of cells reminiscent of reactive glial nets in AD (A) and reactive gliosis in PDD (B) (AD case #31; PDD case #43). **C** The quantitative analysis of GFAP expression in the different hippocampal subfields of patients with AD and PDD (surface coverage area of the DAB staining) shows a strong decrease of GFAP in the DG, CA4 and CA3 of AD cases, and only in the CA1/CA2 of PDD patients. N= 8 CTL, n= 9 AD, n= 11 PDD. **D-F** AQP4 (DAB, brown) is highly expressed by astrocytes in both AD and PDD and is even significantly increased in the CA3, CA1/CA2 and subiculum of patients with AD (AD case #27; PDD case #34). N= 8 CTL, n= 9 AD, n= 10 PDD. **G-H** ALDH1L1 expression (DAB, brown) is generally decreased among astrocytes, which appear to have less complex arborisation. Its relative expression is

affected in the DG, CA4 and CA3 of AD cases and overall decreased in all hippocampal subfields in PDD (AD case #27; PDD case #35). n= 8 CTL, n= 9 AD, n= 10 PDD. **J-K** ALDH7A1 expression (DAB, brown) is decreased in disease notably in the CA3, CA1/CA2 and PHC in PDD and in the subiculum in both AD and PDD patients (AD case #26; PDD case #34). n= 8 CTL, n= 9 AD, n= 8 PDD. **M-O** GPC5 expression (DAB, brown) remains stable across disease conditions. **M** In AD, GPC5 labeling reveals secreted GPC5 concentrated in potential amyloid β plaques (zoom-in). **N** In PDD, the distribution pattern of GPC5+ is similar to that of the CTL but it also shows enlarged and potentially reactive astrocytes (zoom-in) (AD case #26; PDD case #40). n= 8 CTL, n= 9 AD, n= 10 PDD. Statistical analysis: Wilcoxon test, * $p<0.05$, ** $p<0.005$, *** $p<0.0005$. Scale bars: low magnification: 500 μm; high magnification: 50 μm.

Figure 5: Astrocyte identity is affected in patients with AD.

A-C Multiplex cIHC of (**A**) GFAP (green) with AQP4 (purple), (**B**) GFAP (green) with ALDH1L1 (purple) and (**C**) GFAP (green) with ALDH7A1 (purple) in AD samples shows that GFAP astrocytes still co-express AQP4, ALDH1L1 and ALDH7A1 (dark purple, black arrows). AQP4+ and ALDH1L1+ astrocytes are found close to plaques while ALDH7A1+ cells are mainly observed around astrocyte tangle mesh (cases #25, #30, #31). **D** Co-staining of GFAP (green, empty arrows) with GPC5 (purple, white arrows) reveals a few single-positive GPC5+ astrocytes and many double-positive GFAP+/GPC5+ astrocytes (dark purple, full arrows) in areas of astrogliosis, around plaques and astrocyte tangle mesh (zoom-in). (cases #25, #30, #31). **E-G** In AD, GPC5 astrocytes still co-express (**E**) AQP4, (**F**) ALDH1L1 and (**G**) ALDH7A1 (black arrows). AQP4+ astrocytes are found surrounding plaques (cases #31, #26). White and black arrows indicate single and double-positive astrocytes, respectively. Scale bars: **A-C** 50 μm; D left panel 50 μm, right panel – low magnification 100 μm, high magnification 50 μm; **E-G** 50 μm.

Figure 6: GPC5 astrocytes are associated with Aβ plaques and tau tangles, but not with Lewy bodies and neurites.

A GPC5+ astrocytes (purple) form a net around Aβ plaques (green) in the hippocampus as well as the parahippocampal cortex (cases #25, #32). **B** Most of the Aβ plaques (DAB, brown) in the hippocampus are surrounded by GFAP+ astrocytes (teal), with a few GPC5+ astrocytes (purple) (case #30). **C-D** Co-staining of GPC5 (purple) with tau pathology markers (AT8 or pS396 in green) shows an association between GPC5+ astrocytes and tau tangles (cases #25, #32). **E** In PDD, multiplex cIHC of GPC5 (purple) with GFAP (green) and pSyn (DAB, brown) showed no direct interaction between GPC5 astrocytes and Lewy bodies and neurites but revealed some GFAP+ astrocytes with intracellular pSyn (right panel,

black arrows) (cases #34, #43). Scale bars: **A-B** low magnification 100 μm, high magnification 50 μm; **C** left panel – low magnification: 100 μm, high magnification: 50 μm; right panel 50 μm; **D-E** low magnification 100 μm, high magnification 50 μm.

LIST OF ABBREVIATION

Aβ: amyloid-β; AD: Alzheimer's disease; ADRC: Alzheimer's Disease Research Center; ALDH1L1: aldehyde dehydrogenase 1 family member L1; ALDH7A1: aldehyde dehydrogenase 7 family member A1; AQP4: aquaporin 4; CA: Cornu Ammonis; Cat: catalog; cIHC: chromogenic immunohistochemistry; CM: ChromoMap; CNS: central nervous system; CSF: cerebrospinal fluid, CTL: control; DAA: disease-associated astrocytes; Cx43: connexin 43; DAB: 3,3'-diaminobenzidine; DG: dentate gyrus; EAAT1/2: excitatory amino acid transporter 1/2; ECM: extracellular matrix; eGFP: enhanced Green Fluorescent Protein; ERP: Ethics Review Panel; FDR: False Discovery Rate; FFPE: formalin-fixed paraffin embedded; Fig.: Figure; GFAP: glial fibrillary acidic protein; $GFAP_{LOW}$: low-GFAP state; $GFAP_{HIGH}$: high-GFAP state; GPC5: glypican 5; H_2O_2: hydrogen peroxide; HIER: heat-induced epitope retrieval; HRP: horseradish peroxidase; IHC: immunohistochemistry; ISH: *in situ* hybridization; KEGG : Kyoto Encyclopedia of Genes and Genomes; LED: light-emitting diode; NBB: Netherlands Brain Bank; NFT: neurofibrillary tangles; NDD: neurodegenerative diseases; MAS5.0: Microarray Analysis Suite version 5.0; MGP: matrix Gla protein; Ms: mouse; PDD: Parkinson's disease with dementia; PDE: pyridoxine-dependent epilepsy; PET: positron emission tomography; PFC: prefrontal cortex; pH: potential of hydrogen; PHC: parahippocampal cortex; PMD: *post-mortem* delay; pSyn: phosphorylated α-Synuclein; QC: Quebec; Rb: rabbit; RGN: reactive glial nets; RNA-seq: RNA sequencing; RT: room temperature; S100b: S100 calcium-binding protein beta; SM: stratum moleculare; SM 1/3: inner stratum moleculare; SM 2/3: outer stratum moleculare; SO: stratum oriens; SPy: stratum pyramidale; SR: stratum radiatum; STRING: Search Tool for the Retrieval of Interacting Genes/Proteins; TGF-β: ransforming Growth Factor Beta; u133p2: Affymetrix GeneChip Human Genome U133 Plus 2.0 Array; vGAT: vesicular GABA transporter; vGLUT1: vesicular glutamate transporter.

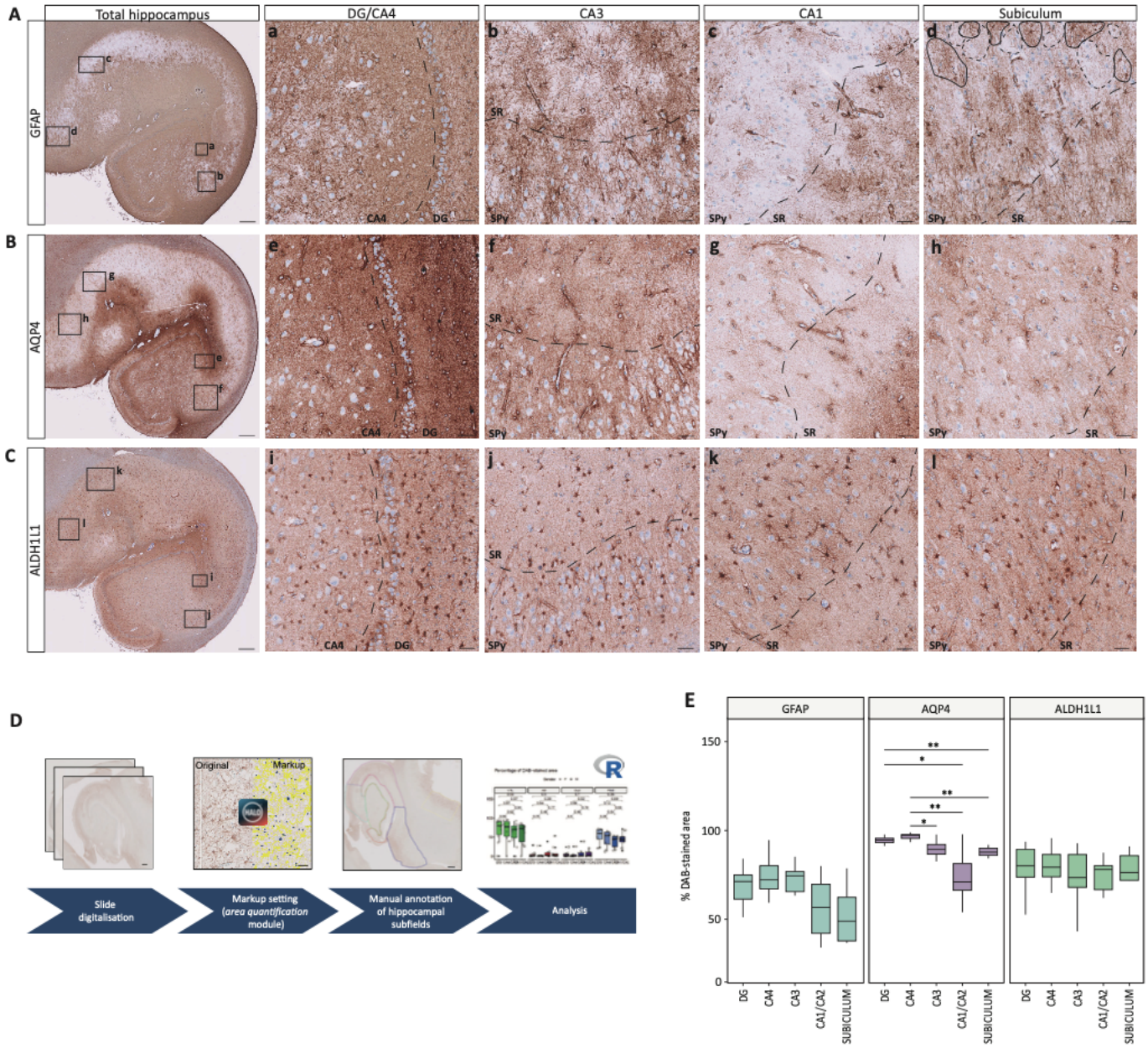
A
Total hippocampus
DG/CA4
CA3
CA1
Subiculum
GFAP
AQP4
ALDH1L1
CA4
DG
SR
SPy
B
C
D
Original
Markup
Slide digitalisation
Markup setting (area quantification module)
Manual annotation of hippocampal subfields
Analysis
E
GFAP
AQP4
ALDH1L1
% DAB-stained area
150
100
50
0
DG
CA4
CA3
CA1/CA2
SUBICULUM

Figure 1

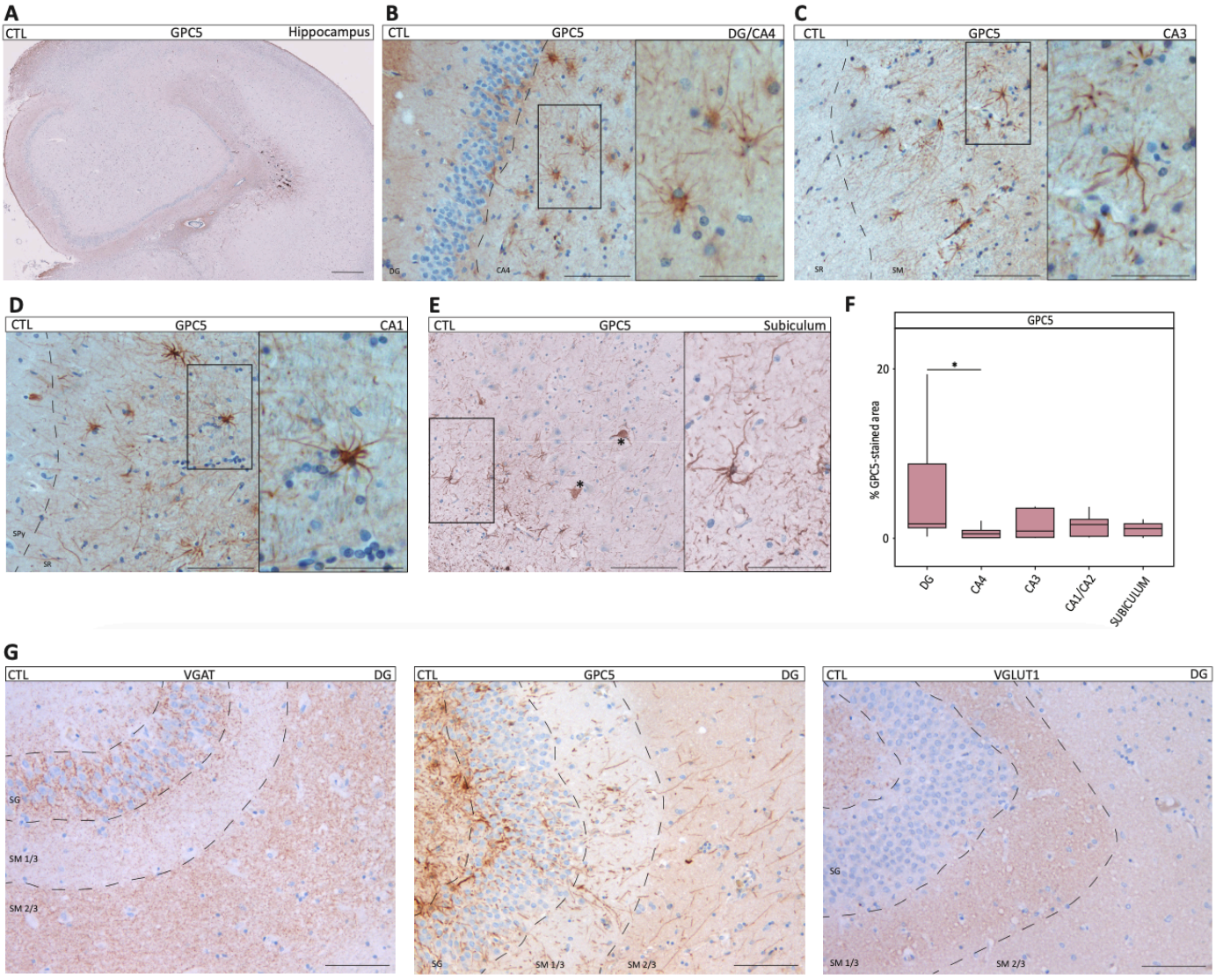
A
CTL
GPC5
Hippocampus
B
CTL
GPC5
DG/CA4
DG
CA4
C
CTL
GPC5
CA3
SR
SM
D
CTL
GPC5
CA1
SPy
SR
E
CTL
GPC5
Subiculum
F
GPC5
% GPC5-stained area
20
0
DG
CA4
CA3
CA1/CA2
SUBICULUM
G
CTL
VGAT
DG
SG
SM 1/3
SM 2/3
CTL
GPC5
DG
SG
SM 1/3
SM 2/3
CTL
VGLUT1
DG
SG
SM 1/3
SM 2/3

Figure 2

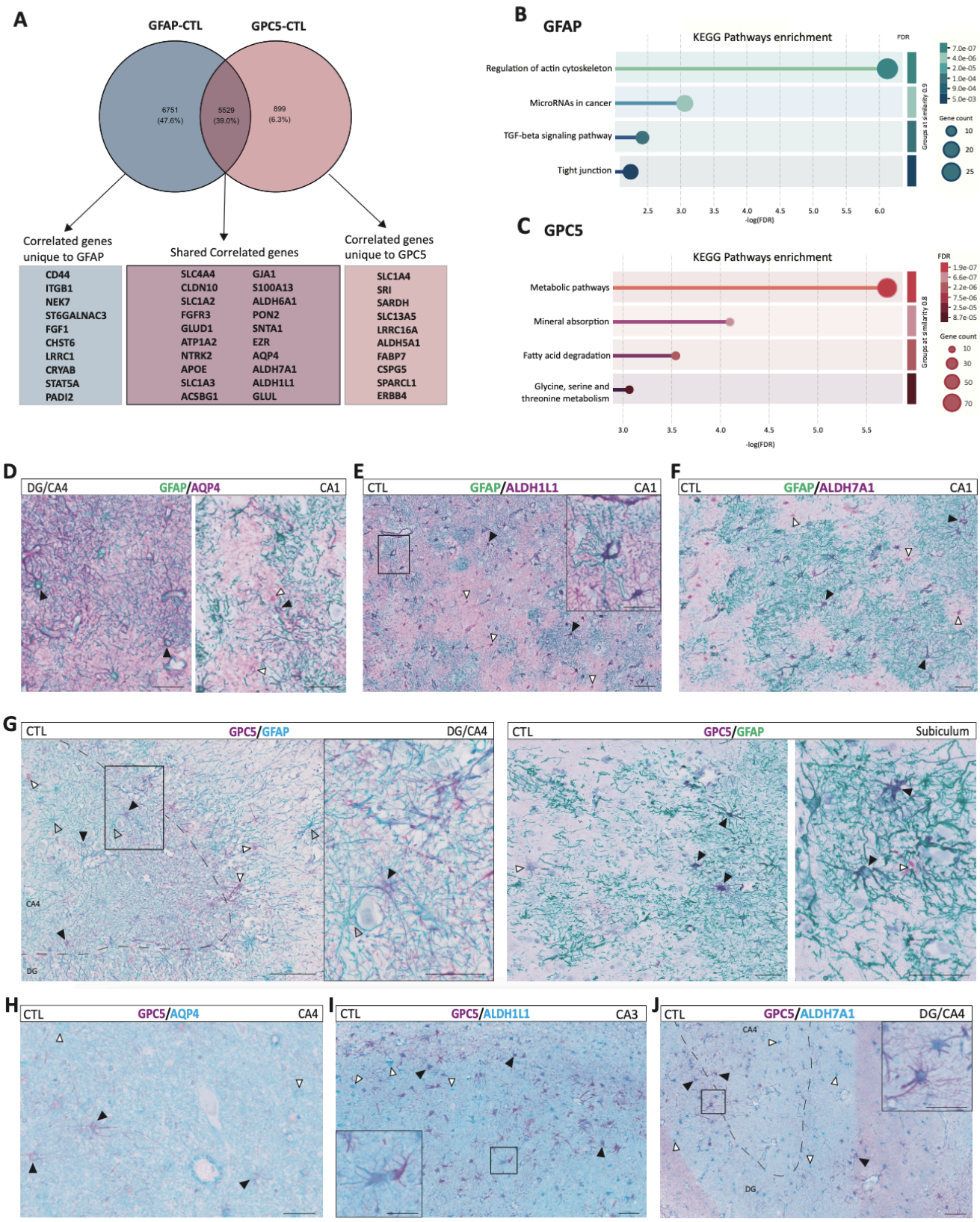
A
GFAP-CTL
GPC5-CTL
6751
(47.6%)
5529
(39.0%)
899
(6.3%)
Correlated genes unique to GFAP
CD44
ITGB1
NEK7
ST6GALNAC3
FGF1
CHST6
LRRC1
CRYAB
STAT5A
PADI2
Shared Correlated genes
SLC4A4
CLDN10
SLC1A2
FGFR3
GLUD1
ATP1A2
NTRK2
APOE
SLC1A3
ACSBG1
GJA1
S100A13
ALDH6A1
PON2
SNTA1
EZR
AQP4
ALDH7A1
ALDH1L1
GLUL
Correlated genes unique to GPC5
SLC1A4
SRI
SARDH
SLC13A5
LRRC16A
ALDH5A1
FABP7
CSPG5
SPARCL1
ERBB4
B
GFAP
KEGG Pathways enrichment
FDR
Regulation of actin cytoskeleton
MicroRNAs in cancer
TGF-beta signaling pathway
Tight junction
Groups at similarity 0.9
Gene count
-log(FDR)
C
GPC5
KEGG Pathways enrichment
Metabolic pathways
Mineral absorption
Fatty acid degradation
Glycine, serine and threonine metabolism
Groups at similarity 0.8
Gene count
-log(FDR)
D
DG/CA4
GFAP/AQP4
CA1
E
CTL
GFAP/ALDH1L1
CA1
F
CTL
GFAP/ALDH7A1
CA1
G
CTL
GPC5/GFAP
DG/CA4
CA4
DG
CTL
GPC5/GFAP
Subiculum
H
CTL
GPC5/AQP4
CA4
I
CTL
GPC5/ALDH1L1
CA3
J
CTL
GPC5/ALDH7A1
DG/CA4
CA4
DG

Figure 3

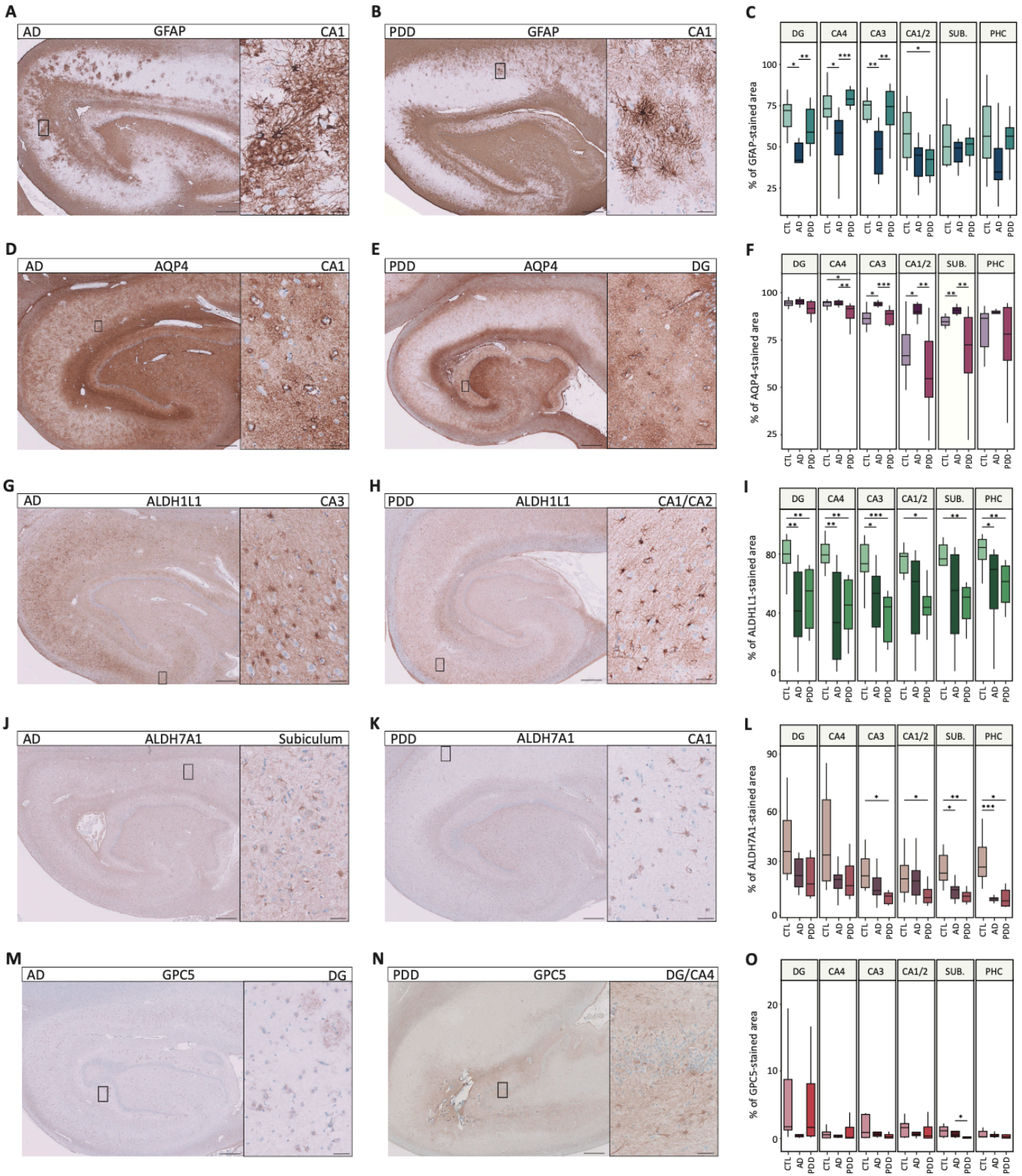
A
AD
GFAP
CA1
B
PDD
GFAP
CA1
C
DG
CA4
CA3
CA1/2
SUB.
PHC
% of GFAP-stained area
CTL
AD
PDD
D
AD
AQP4
CA1
E
PDD
AQP4
DG
F
% of AQP4-stained area
G
AD
ALDH1L1
CA3
H
PDD
ALDH1L1
CA1/CA2
I
% of ALDH1L1-stained area
J
AD
ALDH7A1
Subiculum
K
PDD
ALDH7A1
CA1
L
% of ALDH7A1-stained area
M
AD
GPC5
DG
N
PDD
GPC5
DG/CA4
O
% of GPC5-stained area

Figure 4

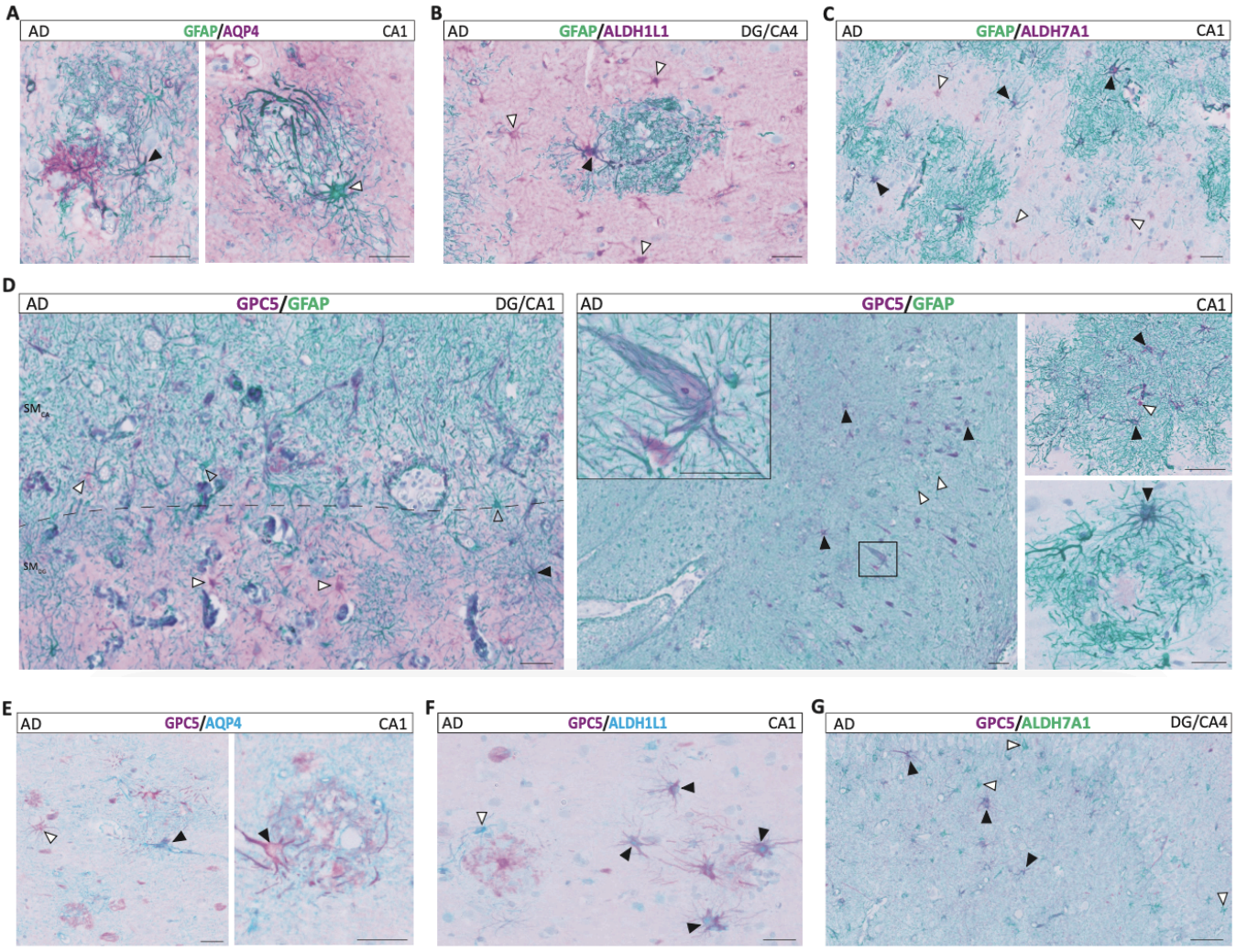
A
AD
GFAP/AQP4
CA1
B
AD
GFAP/ALDH1L1
DG/CA4
C
AD
GFAP/ALDH7A1
CA1
D
AD
GPC5/GFAP
DG/CA1
AD
GPC5/GFAP
CA1
E
AD
GPC5/AQP4
CA1
F
AD
GPC5/ALDH1L1
CA1
G
AD
GPC5/ALDH7A1
DG/CA4

Figure 5

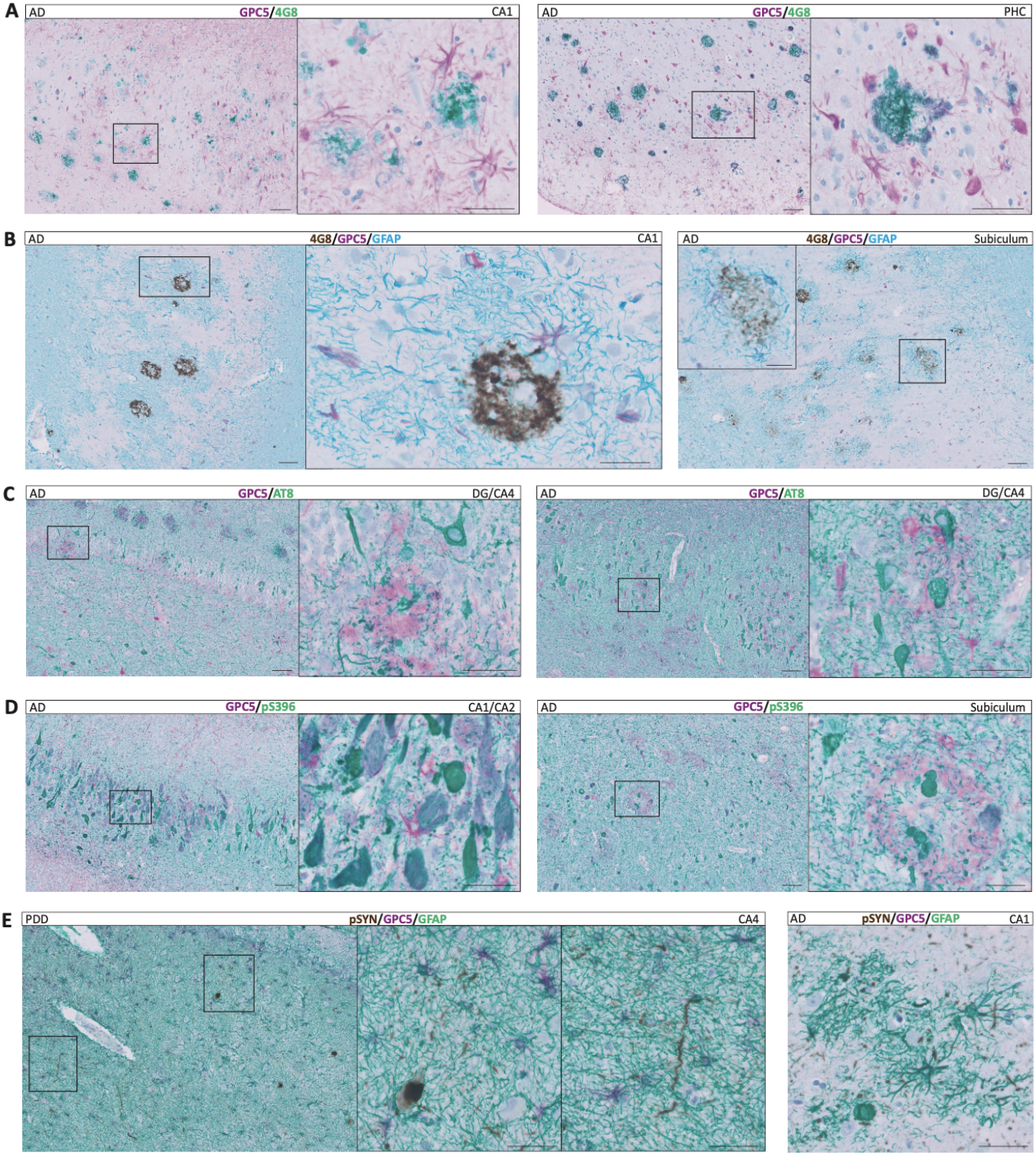
A
AD
GPC5/4G8
CA1
AD
GPC5/4G8
PHC
B
AD
4G8/GPC5/GFAP
CA1
AD
4G8/GPC5/GFAP
Subiculum
C
AD
GPC5/AT8
DG/CA4
AD
GPC5/AT8
DG/CA4
D
AD
GPC5/pS396
CA1/CA2
AD
GPC5/pS396
Subiculum
E
PDD
pSYN/GPC5/GFAP
CA4
AD
pSYN/GPC5/GFAP
CA1

Figure 6

Supplementary Fig. 1: Distribution of GPC5, GFAP, AQP4 and ALDH1L1 in the parahippocampal cortex of healthy aging brain.

A In the PHC, GPC5+ astrocytes (DAB, brown) are mainly found in the glia limitans and in the first and second cortical layers (case #6). **B** GFAP+ astrocytes (DAB, brown) are differentially distributed across the PHC layers. In the deeper layers, GFAP+ astrocytes are organised into non-overlapping domains with many expressing high levels of GFAP (GFAPHIGH, full lines) and some expressing low levels (GFAPLOW, dashed lines) (case #6). **C** AQP4 (DAB, brown) distribution shows a PHC stratification with an enrichment in the glia limitans, the second and deeper layers (case #6). **D** ALDH1L1 chromogenic staining (DAB, brown) shows that the first PHC layer is less enriched than the deeper layers (case #6). **E** GPC5 expression in the PHC is much lower than that of GFAP, AQP4 and ALDH1L1. n=8. Scale bars: **A** low magnification 100 μm, high magnification 50 μm; **B-D** low magnification 200 μm, high magnification 50 μm.

Supplementary Fig. 2: GPC5 is expressed by astrocytes of the prefrontal cortex.

In the healthy PFC, GPC5+ astrocytes (DAB, brown) are mainly observed in the three first cortical layers as well as layer V (case #2). Scale bars: left panel: 500 μm; middle and right panels: 50 μm.

Supplementary Fig. 3: Astrocytes of the parahippocampal cortex display a spectrum of identities.

A In the healthy PHC, most of GFAP+ (green) astrocytes co-express AQP4 (dark purple) (case #9). **B** They also represent a subpopulation of ALDH1L1+ astrocytes (dark purple) (case #9). **C** The glia limitans is composed of double-positive GFAP+/GPC5+ astrocytes (dark purple) that can also be observed in the first cortical layer. Deeper layers, however, are mainly populated by single GFAP+ astrocytes (green) (case #12). **D** GPC5+ astrocytes of the PHC also express (**D**) AQP4 and (**E**) ALDH1L1 (dark blue) (case #12). White and black arrows indicate single and double-positive astrocytes, respectively. Scale bars: 100 μm.

Supplementary Fig. 4: ALDH7A1 is a generic marker for hippocampal astrocytes.

A Representative IHC stainings of ALDH7A1 (DAB, brown) in the healthy hippocampus. a-d Zoom-in on the different hippocampal subfields: (**a**) DG-CA4, (**b**) CA3, (**c**) CA1 and (**d**) subiculum (case #7). **B** Multiplex cIHC of ALDH7A1 (purple) with ALDH1L1 (teal) shows that hippocampal astrocytes co- express both markers (dark blue) (case #6). SO, stratum oriens; SPy, stratum pyramidale; SR, stratum radiatum. Scale bars: **A** low magnification: 500 μm, high magnification (**a-d**) 50 μm; **B** 50 μm.

Supplementary Fig. 5: In AD patients, astrocytes of the PHC exhibit hometostatic and disease signatures.

Multiplex cIHC of GFAP (green) with (**A**) AQP4 (purple) or (**B**) ALDH1L1 (purple) or (**C**) ALDH7A1 (purple) in the PHC of AD patients highlights the mosaic pattern of expression of these markers (cases #30, #31). GPC5 staining (purple) reveals plaque-like structures surrounded by (**D**) GFAP+ astrocytes (green), GFAP+/GPC5+ double positive cells (dark purple), (**E**) AQP4+ astrocytes, (**F**) ALDH1L1+ astrocytes and (**G**) ALDH7A1+ astrocytes (cases #25, #26, #30, #31). White and black arrows indicate single and double-positive astrocytes, respectively. Scale bars: **A, D, E, F**: low magnification 100 μm, high magnification 50 μm; **B, C, G**: 50 μm.

Supplementary Fig. 6: GPC5+ astrocytes form clusters in the prefrontal cortex and accumulate around amyloid plaques.

A Immunostaining of GPC5 (DAB, brown) revealed GPC5+ astrocytes in clusters in the PFC (cases #13, #14) of AD *post-mortem* samples. **B** In the PFC, Aβ plaques (DAB, brown) are often surrounded by GPC5+ astrocytes displaying characteristics of plaque-associated astrocytes (purple, white arrows). We also found a few double-positive GFAP+/GPC5+ astrocytes (dark blue, full arrows) in the vicinity of Aβ plaques (case #13, #14). Scale bars: **A** 50 μm; B left panel – low magnification 100 μm, high magnification: 50 μm; right panel 50 μm.

Supplementary Table 1: Case information of the samples used in this study. Details regarding the samples and their corresponding neuropathological reports were obtained from brain banks.

Supplementary Table 2: Antibodies used in IHC chromogenic (Dako Omnis, Ventana Discovery Ultra).

Supplementary Table 3: Other material and resources.

Supplementary File 1 – Supplementary Excel 1: Statistical analysis from HALO® quantification (see **Part IX, 1. Supplementary data Manuscript I**).

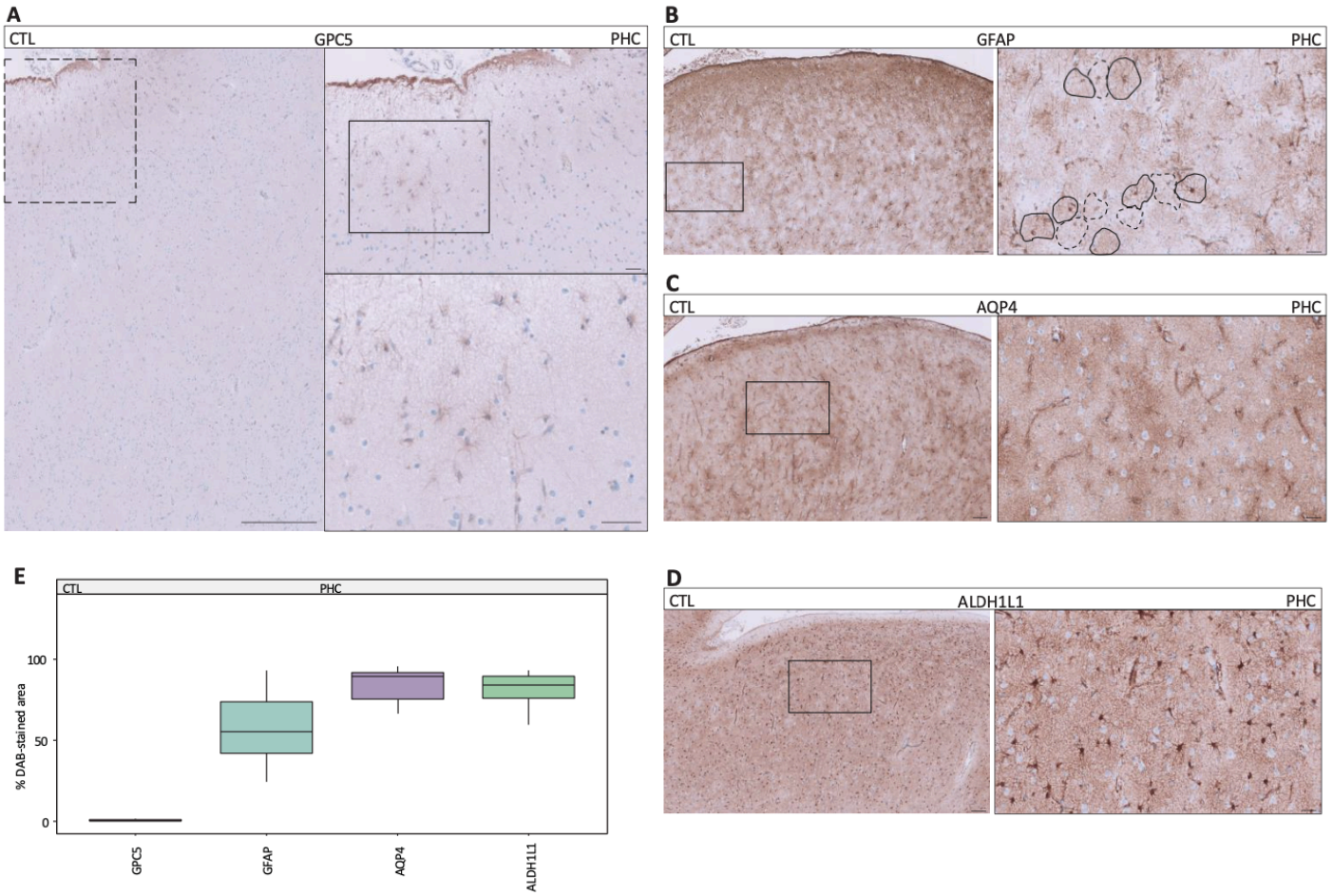

Supplementary Figure 1

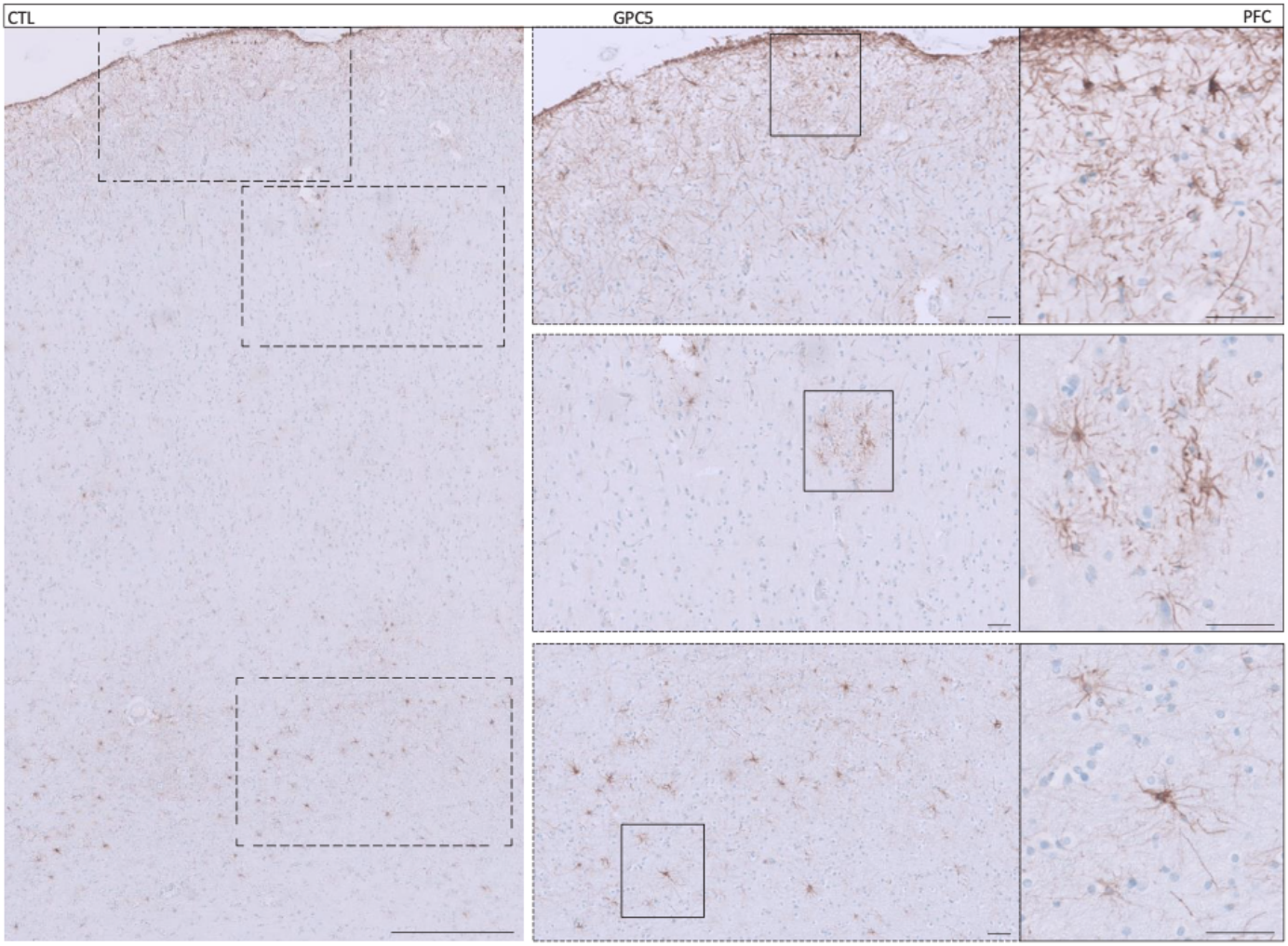

Supplementary Figure 2

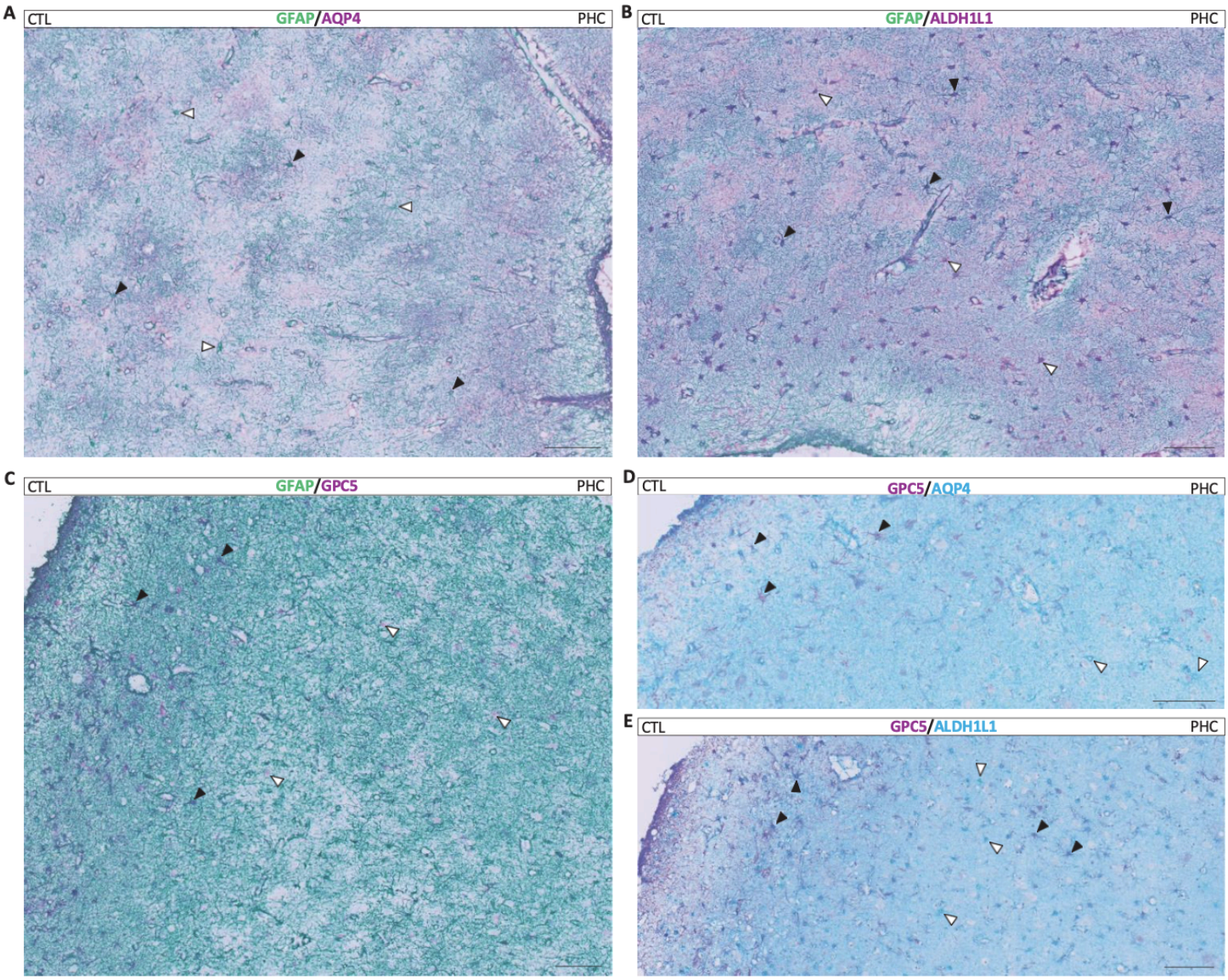

Supplementary Figure 3

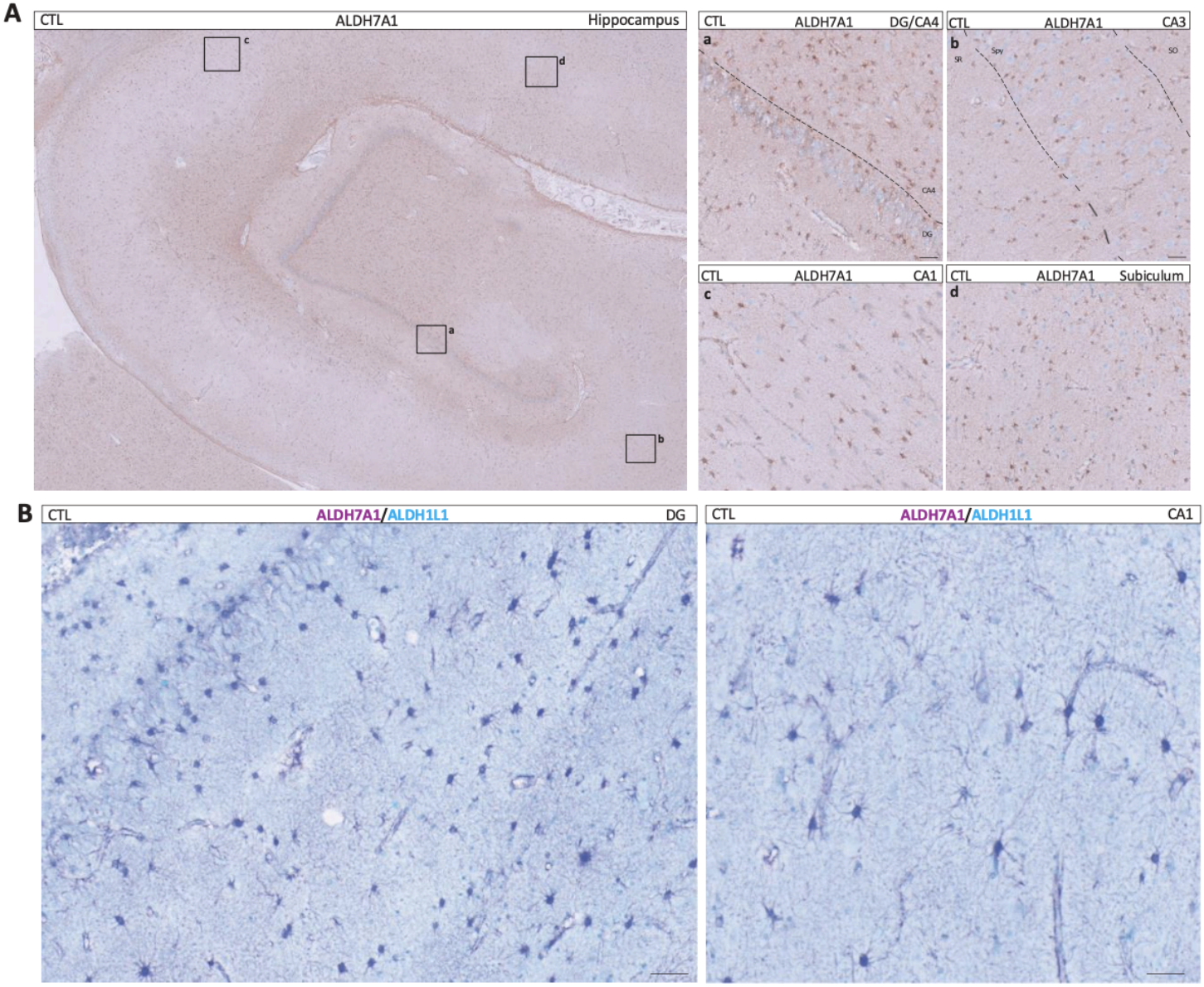

Supplementary Figure 4

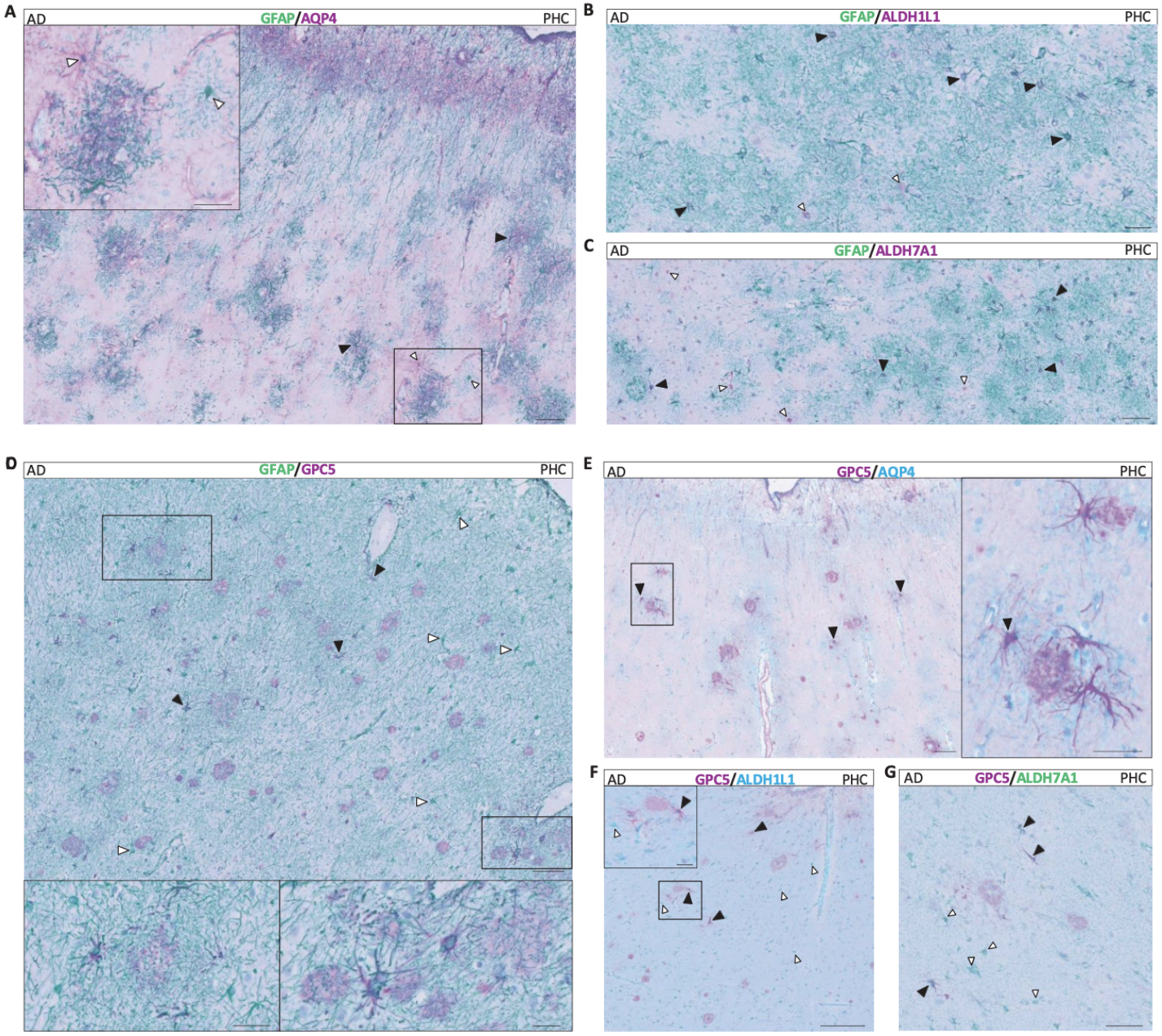

Supplementary Figure 5

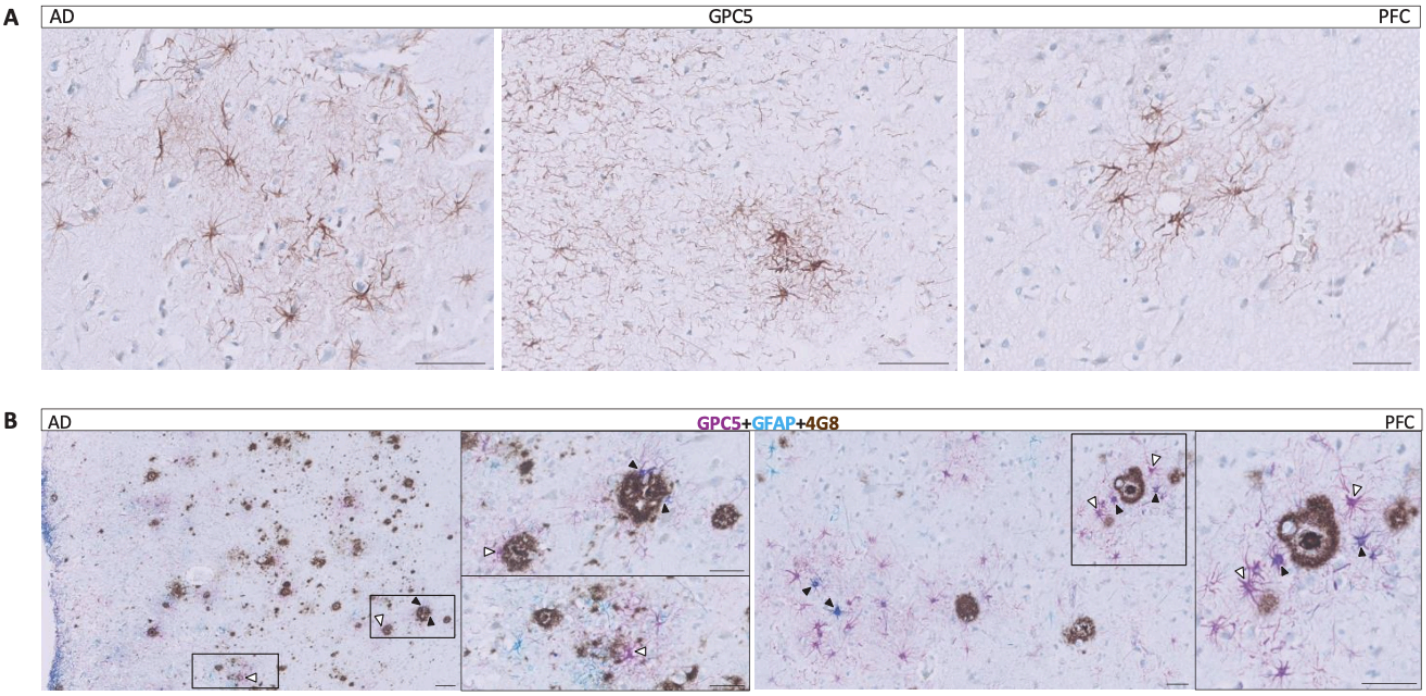

Supplementary Figure 6

Supplementary Table 1

Pathological diagnosis	Case	Sex	Age at death (years)	PMD (hh:mm)	ABC / McKeith score/ Braak Lewy Bodies	Brain Bank
CTL	1	F	83	35:45	A0B0C0	Douglas Canada Bell Brain Bank
	2	M	83	16:50	A0B0C0	
	3	M	72	07:29	A0B0C0	
	4	M	68	23:22	A0B1C0	
	5	M	87	04:50	A2B1C0	The Netherlands Brain Bank
	6	F	91	09:30	A0B2C0	
	7	M	79	06:20	A1B1C0	
	8	F	102	03:55	A1B2C0	
	9	F	79	06:00	A2B2C2	
	10	M	84	05:20	A1B1C0	
	11	F	86	06:25	A2B1C1	
	12	F	104	07:33	A2B2C1	
AD	13	F	83	25:00	A2B3C2	Douglas Canada Bell Brain Bank
	14	M	91	25:00	A2B3C2	
	15	F	96	26:30	A2B3C2	
	16	F	81	23:45	A2B3C2	
	17	M	77	19:25	A2B3C2	
	18	M	90	14:36	A2B2C2	
	19	M	90	26:07	A3B2C3	
	20	F	87	17:00	A1B2C2	
	21	M	90	31:59	A2B2C3	
	22	F	86	39:00	A3B3C2	GIE-Neuro-CEB biobank
	23	M	85	21:00	A3B1C1	
	24	F	84	24:00	A3B3C2	
	25	F	53	06:30	A3B3C3	The Netherlands Brain Bank
	26	F	70	07:25	A3B3C3	
	27	F	86	03:50	A3B3C3	
	28	M	38	05:45	A3B3C3	
	29	F	92	05:15	A3B3C3	
	30	F	98	05:45	A2B2C2	
	31	M	64	04:58	A3B3C3	
	32	M	74	05:25	A3B3C3	
	33	F	86	06:00	A3B3C3	
PDD	34	M	71	04:35	A1B1C0/LB5	The Netherlands Brain Bank
	35	M	73	05:35	A1B1C0/LB5	
	36	F	83	06:05	A0B1C0/LB5	
	37	M	72	04:00	A0B1C0/LB4	
	38	M	61	05:00	A1B1C0/LB6	
	39	F	71	09:05	A0B1C0/ LB5	
	40	M	85	05:15	A1B2C1/ LB4	
	41	F	73	06:10	A1B1C0/ LB4	
	42	F	88	06:05	A1B1C0/ LB6	
	43	F	69	07:05	A1B1C0/ LB6	

Supplementary Table 2

ANTIBODIES	SOURCE	IDENTIFIER	DILUTION IHC	DILUTION clHC
PRIMARY ANTIBODIES				
Rabbit polyclonal anti-ALDH1L1	Atlas Antibodies	Cat# HPA050139, RRID: AB_2681031	1:2000	1:2000
Rabbit polyclonal anti-ALDH7A1	Sigma-Aldrich	Cat# HPA023296, RRID: AB_1844738	-	1:1000
Mouse monoclonal anti-phospho tau (AT8) (Ser202,Thr205)	Thermo Fisher Scientific	Cat# MN1020, RRID: AB_223647	-	1:400
Rabbit polyclonal anti-phospho tau (ps396)	Thermo Fisher Scientific	Cat# 44-752G, RRID: AB_2533745	-	1:1000
Mouse monoclonal anti-AQP4	Atlas Antibodies	Cat# AMAb90537, RRID: AB_2665579	1:200	1:200
Rabbit monoclonal anti-GFAP	Ventana Medical Systems	Cat# 760-4345 (also 05269784001), RRID: N/A	-	Ready to use*
Rabbit polyclonal anti-GPC5	Atlas Antibodies	Cat# HPA040152, RRID: AB_2676863	-	1:500
Mouse monoclonal anti-phospho synuclein (clone 81A, pSYN) (Ser129)	Millipore	Cat# MABN826 RRID: AB_2904158	-	1:500
Rabbit polyclonal anti-VGAT	Sigma-Aldrich	Cat# HPA058859, RRID: AB_2683836	-	1:200
Rabbit polyclonal anti-VGLUT1	Atlas Antibodies	Cat# HPA063679, RRID: AB_2685086	-	1:200
Mouse monoclonal anti-β-Amyloid, AA17-24 (4G8)	BioLegend	Cat# 800712, RRID: AB_2734548	-	1:500
SECONDARY ANTIBODIES				

DISCOVERY OmniMap anti-Rb HRP	Roche	Cat# 760-4311, RRID: AB_2811043	-	Ready to use*
DISCOVERY OmniMap anti-Ms HRP	Roche	Cat# 760-4310, RRID: AB_2885182	-	Ready to use*
DISCOVERY CM DAB kit	Roche	Cat# 760-159, RRID: N/A	-	Ready to use*
DISCOVERY Purple Kit	Roche	Cat# 760-229, RRID: N/A	-	Ready to use*
DISCOVERY Teal HRP kit	Roche	Cat# 760-247, RRID: N/A	-	Ready to use*
Discovery Green HRP kit	Roche	Cat# 08478295001, RRID: N/A	-	Ready to use*

*Vials ready-to-use purchased from Roche Ventana Medical Systems

Supplementary Table 3

REAGENT OR RESOURCE		
Biological samples		
Human post-mortem FFPE hippocampus and prefrontal cortex	GIE-Neuro-CEB biobank	See Supplementary Table 1
	Douglas-Bell Brain Bank and GIE-Neuro-CEB biobank	
	Netherlands Institute for Neuroscience, Amsterdam, the Netherlands Brain Bank	
Software and algorithms		
Biorender	Biorender.com	RRID: SCR_018361
R studio (Version 4.5.1.)	RStudio	RRID: SCR_001905
Adobe Illustrator (Version 28.7.8.)	Adobe.com/illustrator	RRID:SCR_010279
HALO (Version 3.6.)	Indicalab.com/halo	RRID: SCR_018350
Other		
Dako Omnis Autostainers	Dako	
IntelliSite Ultra Fast Scanner	Philips	
Ventana Discovery Ultra Autostainer	Roche Diagnostics	

3.4. Conclusion

In conclusion, our results reveal the remarkable heterogeneity of human hippocampal astrocytes and highlights limitations of GFAP as a universal astrocytic marker. GFAP labels only certain subsets of astrocyte, whereas ALDH1L1 and ALDH7A1 provide broader coverage and better reflect astrocyte populations across hippocampal subregions. In advanced AD patients, we observed a general loss of astrocytic homeostatic markers, including reduced GFAP, ALDH1L1, and ALDH7A1 expression, alongside increased AQP4 levels, suggesting astrocyte dysfunction affecting metabolic, neurovascular, and glymphatic processes. Additionally, we identified a distinct GPC5+ astrocyte subtype, spatially and molecularly different from GFAP+ astrocytes, that remains relatively preserved in neurodegenerative disease but shows altered spatial organisation and polarisation toward amyloid plaques and tau pathology. Taken together, these findings emphasise the dynamic and subtype-specific nature of astrocyte responses in neurodegeneration, highlighting the importance of using a set of astrocytic markers to accurately assess astrocyte identity and changes in health and across disease progression.

4. CHAPTER II – Noradrenaline modulation of astrocytic molecular signatures is disrupted in Alzheimer's and Parkinson's dementia.

4.1. Introduction

Over the past forty years, several clinical studies have described an early degeneration of the LC in AD and PD patients. This early alteration of the NA system leads to a progressive imbalance of the NA levels in brain areas associated with memory processes, such as the hippocampus. NA is involved in core brain functions that are altered in age-associated NDDs, such as attention, alertness, memory formation and consolidation. Moreover, NA acts as a strong modulator of neuronal but also microglial and astrocytic activities. Physiologically, astrocytes and microglia are involved in neuroprotection. However, in a pathological context, these cells produce pro-inflammatory molecules associated with severe neuroinflammation that may aggravate neurodegeneration. NA is one of these neuromodulators particularly studied for its important regulatory role on astrocytes. Indeed, *in vitro* and *in vivo* studies have demonstrated that NA has potent anti-inflammatory and neuroprotective effects on astrocytes and microglia, limiting neuroinflammatory events that may occur in the brain (Heneka et al. 2010; Hinojosa et al. 2013; Ishii et al. 2015; Bharani et al. 2017). Interestingly, it has been shown that an alteration of the NA system affects glial cells in AD and PD and that NA depletion increases astrocytic oxidative stress in AD mouse models (Zorec et al. 2018; Heneka et al. 2010). However, the mechanisms underlying the modulatory effect of NA on astrocytes remain poorly understood. The aim of this study was to characterise the modulatory role of NA on astrocytes more precisely, in order to gain a deeper insight into how NA influences the molecular profile and functional roles of astrocytes. To this purpose, we have designed a translational approach using mouse primary cells in culture and human AD, PDD, and age-matched control *post-mortem* samples. *In vitro*, we analysed astrocyte phenotype and responses to NA exposure in a physiological context or under inflammatory conditions (**Manuscript II, Fig. 1A**). In parallel, we investigated NA-targeted genes in human samples as well as the interplay between astrocytes and the NA system using cIHC and digital pathology.

4.2. Personal contributions

For this article, I conducted the study under the supervision of Dr David Bouvier and with the technical support of my colleagues Mónica Miranda de la Maza, Sophie Schreiner, Dr. Gaël Hammer and Denis Charbonnier-Renaud. Below are listed my personal contributions:

- Cell culture experiments: mice take down, brain extraction, MACS isolation, routine maintenance, cell treatments;
- Sample collection: RNA/DNA/protein extraction, coverslip fixation, supernatant collection;
- Sample processing: RT-qPCR, RNAseq, Western-Blot, ELISA tests, ICF, microscopy acquisition;
- Transcriptomic data analyses and data visualisation;
- FFPE sample slicing, cIHC staining and imaging;
- HALO quantification and analysis
- Production and design of the below listed figures submitted for this manuscript:
    - Figure 1 (A-E), Figure 2 (A-D), Figure 3 (A-H), Figure 4 (A-C), Figure 5 (A-F);
    - Supplementary Figure 1, Supplementary Figure 2, Supplementary Figure 3.
- Drafting and final writing of the manuscript (with the support of Dr David Bouvier);
- Editing and reviewing of the final manuscript;
- Details of each author's individual contributions are provided in the author contribution section at the end of the manuscript.

4.3. Original manuscript II

Noradrenaline modulation of astrocytic molecular signatures is disrupted in Alzheimer's and Parkinson's dementia.

Félicia Jeannelle[1], Mónica Miranda de la Maza[2], Gaël Paul Hammer[1], Sophie Schreiner[1], Tony Heurtaux[3], Arnaud Muller[4,5], Denis Charbonnier-Renaud[6], Netherlands Brain Bank[7], Michel Mittelbronn[1,2,3,6], David S. Bouvier[1]

Author affiliations:

[1] National Center of Pathology (NCP), Laboratoire national de santé (LNS), Dudelange, Luxembourg.

[2] Department of Infection and Immunity (DII), Luxembourg Institute of Health (LIH), Belval, Luxembourg.

[3] Department of Life Science and Medicine (DLSM), University of Luxembourg, Belval, Luxembourg.

[4] Department of Microbiology, Laboratoire national de santé (LNS), Dudelange, Luxembourg.

[5] Bioinformatic Platform, Luxembourg Institute of Health (LIH), Luxembourg.

[6] Luxembourg Centre for Systems Biomedicine (LCSB), University of Luxembourg, Belval, Luxembourg.

[7] Netherlands Institute for Neuroscience, Amsterdam, the Netherlands Brain Bank.

Correspondence to: Dr. David S. Bouvier

Laboratoire national de santé (LNS)

1, Rue Louis Rech

L-3555 Dudelange

Email: david.bouvier@lns.etat.lu; david.bouvier@ext.uni.lu

Number of Figures: 5

Number of Supplementary Files: 15

Number of Pages: 36

ABSTRACT

Early alterations of the locus coeruleus (LC) have been reported in Alzheimer's disease (AD) and Parkinson's disease (PD) with particular deterioration of the noradrenergic (NA) system leading to imbalances in NA levels, especially in memory-related regions like the hippocampus. Furthermore, alterations of the NA system have been linked to glial dysfunction and increased oxidative stress in AD models, but the concrete underlying mechanisms pathologically affecting astrocytes remain unclear. In this study, we aimed to elucidate the regulatory effects of NA on astrocytic molecular signatures and functional dynamics. To achieve this, we employed a translational strategy ranging from the investigation of primary mouse astrocyte cultures to *post-mortem* brain samples from individuals with AD, PD with dementia (PDD), and age-matched healthy controls. Our *in vitro* experiments showed that NA influences core astrocytic functions by modulating the expressions of genes involved in the regulation of the cerebral blood flow (*Cbs, Ace*), circadian rhythms (*Cartpt, Bdnf*), neuroprotection (*Scg2*), inflammatory responses (*Ptgs2, Vim*) and oxidative stress (*Sod3, Nqo1*). Concurrently, we analysed the expression of NA-responsive genes and the interactions between astrocytes and the NA system in human tissues using chromogenic immunohistochemistry and digital pathology. We observed a partial decrease of VMAT2 in AD cases and severe alteration of CBS expression in both AD and PDD patients. Our results suggest that the intimate relationship between the noradrenergic system and astrocytes results in a significant phenotypic control of astrocytes by NA and may be drastically impacted in NDDs.

Our findings indicate that NA modulates key astrocytic genes and dampens inflammation-associated signatures induced by a cytokine mix. Furthermore, NA-treated astrocyte medium mitigated the pro-inflammatory response of microglia, indicating a non-cell-autonomous immunomodulatory role.

INTRODUCTION

Noradrenaline (NA), or norepinephrine (NE), is a potent neuromodulator involved in key processes such as attention, arousal, memory formation and consolidation; functions that are disrupted in neurodegenerative diseases (NDDs) (1). In the brain, NA is primarily produced by neurons located in the locus coeruleus (LC), a small brainstem nucleus of the dorsal pons. There is now accumulating evidence that LC is one of the first brain regions to deteriorate in Alzheimer's disease (AD) (2–4), but also in Parkinson's disease (PD) (5,6). These findings highlight the importance of understanding the role of the NA system in the progression of neurodegeneration (7–9). LC neurons send widespread projections to multiple brain regions, notably the hippocampus, amygdala, and prefrontal cortex. Interestingly, the loss of most rostral LC neurons, which innervate the hippocampus, is particularly pronounced in AD (10). The molecular, cellular, and pathological consequences of LC-neuron loss in LC-targeted areas involved in the memory process in AD remain to be fully characterized (9,11,12). NA transmission occurs via two mechanisms, namely conventional synaptic release and volume transmission through axonal varicosities. These varicosities release NA into the extracellular space, allowing it a paracrine-like modulation of surrounding neurons, glial cells, and the neurovascular unit (13,14). NA plays a central role in modulating astrocytic function, a highly abundant glial cell type involved in key physiological processes such as brain metabolism (15), blood flow regulation (16,17), and synaptic modulation (18–20). Astrocytes express various adrenergic receptors at their surface (21,22), and respond dynamically to NA signals by modifying their calcium activity and function (23,24). NA-driven astrocytic pathways contribute in specific memory processes during the vigilance state in awake mice (25), influence behavior (26) and regulate cortical state in rodents (27,28). Recent studies suggests that NA-mediated control of astrocyte activity is crucial for the regulation of synaptic transmission and neuronal circuitry, offering new insights into brain function across species (29–31). Studies in Drosophila have shown that NA gates astrocytic responsiveness to other neurotransmitters, such as dopamine (29). In zebrafish and mice, activating astrocytic α1A-adrenergic receptors induces ATP release, which converted to adenosine, can suppress synaptic transmission of neighboring neurons via the presynaptic adenosine A1 receptors (30,31). Lefton and colleagues showed that astrocyte activation is conditional upon the suppression of synaptic strength induced by NA in the mouse CA1 hippocampus. Moreover, NA contributes to astrocyte-mediated vasoconstriction (16) and may influence glymphatic clearance dynamics during sleep (32). Dysregulation and progressive depletion of NA, resulting from early LC degeneration, may profoundly alter astrocyte functions and their responses in NDDs. In disease conditions, astrocytes can also lose their core functions, adopt neurotoxic

phenotypes, and favour neuroinflammation and oxidative stress (33). However, how NA influences their disease responses remains poorly understood. *In vitro* studies suggest that NA has anti-inflammatory properties in astrocytes, whereas its depletion increases astrocytic oxidative stress in AD mouse models (34,35).

To better understand how NA shapes astrocyte molecular identity and functions, we compared the transcriptomic profiles of primary mouse astrocytes under homeostatic and pro-inflammatory conditions, with or without NA exposure. Using bulk RNA sequencing, RT-qPCR, and cytokine arrays, we identified differentially expressed genes (DEGs) and proteins regulated by NA, and compared these effects to those induced by dopamine (DA). To assess the relevance of these findings in human disease, we examined *post-mortem* hippocampal tissue from individuals with AD and PD with dementia (PDD), as well as age-matched non-demented individuals (CTLs). Using chromogenic immunohistochemistry (cIHC) and digital pathology, we quantified the vesicular monoamine transporter 2 (VMAT2) noradrenergic input and key NA-responsive genes *in vitro*. Altogether, our findings suggest that NA plays a critical role in modulating astrocyte reactivity and neuroinflammation, with potential relevance to NDD pathology.

MATERIAL AND METHODS

Animal experiments

Crl:CD1 mice (Charles-River, France) were bred and housed in groups of three (2 females for 1 male) in ventilated cages in a conventional animal facility at the University of Luxembourg. Mice were kept under a 12-hour light-dark cycle with *ad libitum* access to water and food. Animal experiments were approved by the Animal Experimentation Ethics Committee (AEEC) of the University of Luxembourg and the relevant government agencies. All the procedures were performed following the 2010/63/EU European Union Directive.

Primary cell cultures

Mixed glial cells were obtained from the brains of Crl:CD1 mice. Briefly, brains were removed from postnatal day 1 to 3 CD1 mouse pups. Because the number of extracted microglia or astrocytes from one newborn mouse brain is only 0.6 million or 0.8 million cells on average, respectively, we had to pool the cells from several newborn mice (both sexes included) before starting the respective experiments. The meninges and large blood vessels were removed before the brains were minced and mechanically dissociated in PBS (Life Technology Europe Cat#14040133) solution. Subsequently, the cells were seeded into 75cm^2 flasks containing culture medium, called DMEM 10%, consisting of Dulbecco's Modified Eagle Medium (DMEM, Life Technology Europe, Cat#41965039) supplemented with 10% (v/v) of fetal bovine serum (FBS, Gibco, Cat#10270-106) and 100 U/ml of penicillin and 10 mg/ml of streptomycin (Gibco, Cat#15140122). The mixed glial cell cultures were maintained at 37°C in a 5% CO_2 humidified atmosphere. Upon reaching confluency two weeks later, microglia were positively isolated using an anti-CD11b antibody (Miltenyi Biotec, Cat#130093634) and magnetic cell sorting (MACS) according to the manufacturer's instructions (Miltenyi Biotec). Microglia were plated (600,000-650,000 cells/well, 12-well plates) in a mix (1:1 v/v) of DMEM and mixed glial cell culture-conditioned medium, and treated 24h later. Astrocytes were recovered in the negative fraction and seeded in new 75cm^2 flasks. Once astrocytes reached confluency one week later, a second MACS isolation was performed as described previously to remove any remaining microglia. Astrocytes were plated (700,000-750,000 cells/well, 12-well plates) in DMEM 10% and left in culture for an additional week before cell treatments. The medium was changed with fresh DMEM 10% every 3-4 days. Both cultures were maintained at 37°C in a 5% CO_2 humidified atmosphere.

Cell treatments

Astrocyte cultures were left unstimulated (non-exposed/CTL astrocytes) or exposed to 100 μM of Noradrenaline (NA-exposed astrocytes, Sigma Aldrich Cat# A9512) or Dopamine (DA-exposed astrocytes, Sigma Aldrich Cat#H8502) for 2x24h, or to a mix of cytokines (CM, 24h) composed of recombinant mouse IFNγ, recombinant mouse IL-1β, and recombinant mouse TNFα (10 ng/ml each, Peprotech Cat# 315-05, Cat# 211-11B, Cat# 315-01A, respectively), or combined NA and CM (NA+CM-exposed astrocytes) for 72h in total (2x24h NA + 24h CM). Concentrations and exposure times were selected based on previous *in vitro* studies on primary mouse astrocytes and microglia that reported effects on glial cell responses (35–37).

To obtain astrocyte "conditioned medium" (ACM) for further *in vitro* experiments, astrocytes were treated with or without NA as described above. After initial stimulations, the conditioned medium, containing the entire astrocyte secretome, was collected and stored at -20°C. Before using it for microglia stimulation, ACM was centrifuged at 6,000 rpm and filtered through a 0.2 μm syringe filter. Microglia were left unstimulated (CTL) or exposed for 6h to 1ng/ml of lipopolysaccharide (LPS derived from *Escherichia coli* 055:B5, Sigma), or exposed to LPS combined with ACM from non-exposed or NA-exposed astrocytes, for 6h.

Immunocytofluorescence (ICF)

To verify the purity of astrocytes and microglia cultures, cells were plated (300.000 cells/well, 12-well plates) on Poly-D-Lysine (Gibco, Cat#A38904-01) coated coverslips and fixed with 4% paraformaldehyde (PFA, Sigma, Cat#818715) for 20 min at RT. Cells were then permeabilised for 10 min with 0.3% Triton-X 100 (Sigma, Cat#T8787) and washed three times in PBS 1X. After 30 min of blocking with 3% (w/v) BSA (Sigma, Cat#A3059), astrocytes and microglia were stained with primary antibodies in blocking solution for 2h at RT. Cells were then washed three times for 5 min in PBS and subsequently incubated in 3% BSA at RT for 1h with fluorophore-coupled secondary antibodies. Coverslips were finally washed three times in PBS 1X (5 min) and two times in distilled water (5 min) before mounting on glass slides with DAPI Fluoromount-G (SouthernBiotech, Cat#0100-20). Primary and secondary antibody references are listed in Supplementary Table 3.

Pictures were acquired using a Zeiss LSM 710/800 confocal microscope with a 20X objective (Zeiss Plan-APOCHROMAT 20x/0.8 420650-9902). Pictures were visualised with Imaris Viewer (9.9.0) after each channel underwent intensity normalisation and background subtraction to remove noise.

RNA extraction, reverse transcription and qPCR

Total RNA was extracted using the innuPREP RNA Mini kit (Analytikjena) following the manufacturer's instructions. The isolated RNA was stored at -80°c until they were used. For reverse transcription, the samples were processed with the ImProm-II Reverse Transcription System kit (Promega) using a Bio-Rad T100™ Thermal Cycler. For qPCR analyses, synthesized complementary DNA (cDNA) and SsoAdvanced Universal SYBR® Green Supermix (Bio-Rad) were used on a Bio-Rad Thermal Cycler (CFX Connect™ Real-Time PCR Detection System, Bio-Rad). Primer sequences are summarised in Supplementary Table 1. Gene expression was determined using the comparative threshold cycle (Ct) method employing the 2^{-ddCt} formula, with $ddCt = (C_t, \textit{target} - C_t, \textit{housekeeping})_{\text{treated sample}} - (C_t, \textit{target} - C_t, \textit{housekeeping})_{\text{control sample}}$. To standardise the expression of the target genes, *Rpl27* (coding for a ribosomal protein) served as a housekeeping gene.

RNA-seq library preparation, quality control and statistical analysis

RNA libraries for the 18 samples with 3 replicates per biological condition were prepared using the Illumina Stranded mRNA Prep Ligation Kit (polyA selection), following the manufacturer's protocol. Sequencing was performed on the Illumina NovaSeq platform® (SP200), targeting 19 million reads per sample (paired-end, 2 × 75 bp). Raw FASTQ files underwent quality assessment using FastQC, FastQ Screen, and RSeQC tools. Preliminary processing included read trimming (Cutadapt) and mapping (STAR 2.7.9a) to the mouse reference genome (GRCm39 – Mus_musculus.GRCm39.104.gtf) (38,39). Gene counting, as well as all aforementioned steps, were integrated within a local Snakemake workflow (40). Differential gene expression analysis was conducted in R (version 4.1.0) using DESeq2 (version 1.32.0) (41) on the resulting gene count tables. Multiple visual inspections were performed to assess data distribution and sample clustering. Principal component analysis (PCA) was used to verify that biological replicates clustered as expected and that no outlier sample has to be addressed. All p values were adjusted for multiple comparisons using the Benjamini–Hochberg procedure with false discovery rate (FDR) of 0.05.

Raw read counts were normalised, and genes were filtered according to the criteria: genes with at least 1 read count in at least 5 samples per comparison were considered eligible for further analysis. Significance of expression was calculated for each comparison using adjusted p value (FDR method), and results with p value < 0.01 were presented in tables and visualised with volcano plots.

To elucidate biological functions over-represented in differentially expressed gene (DEG) groups, we performed over-representation analysis (ORA) using the R package clusterProfiler (v4.5.0) for DEGs

having a log-fold change lower than – 0.5 or greater than 0.5 and adjusted p value < 0.05. We employed the following databases: Gene Ontology (GO) and Kyoto Encyclopedia of Genes and Genomes (KEGG). In this manuscript and supplementary files, * indicates P < 0.05, ** P < 0.01 and *** P < 0.001.

Measurement of cytokine and chemokine release

The measurement of secreted cytokines and chemokines by astrocytes was performed using a Mouse Cytokine Array Panel A (R&D Systems Inc., Cat#ARY006) following the manufacturer's instructions. Briefly, nitrocellulose membranes, which consist of 40 different cytokine and chemokine antibodies printed in duplicate, were incubated for 1h at RT with Array Buffer 6, a blocking buffer. Meanwhile, samples were prepared with 0.5 mL of Array Buffer 4 and Array Buffer 6 if necessary, and incubated with reconstituted Mouse Cytokine Array Panel A Detection Antibody Cocktail for 1 h at RT. This sample/antibody mixture was then applied to the membranes. After overnight incubation at 4°C, membranes were washed three times in 1X Wash Buffer, incubated with Streptavidin-HRP for 30 min at RT and finally with Chemi Reagent Mix for 1 min before being exposed to X-ray film for 1 sec to 100 sec. Membrane imaging was done with a ChemiDoc XRS+ imaging system, and chemiluminescence was quantified with ImageLab imaging and analysis software. HRP-conjugated antibody served as a positive substrate control at six spots and was additionally used to ascertain membrane orientation. Net density grey level for each spot was calculated by subtracting the background grey levels from the total raw density grey levels.

Human brain samples

All human tissues involved in this study have been pseudonymised and listed in Supplementary Table 2. All autopsy brain samples were obtained from the Netherlands Brain Bank. The use of these samples for research purposes was approved by the ethic panel of this institution and by the University of Luxembourg (ERP 16-037 and 21-009). Hippocampal samples were classified by brain bank intern neuropathologists following the established Braak (42,43), ABC (44), and McKeith staging criteria (45), which assess the presence of Aβ plaques, NFTs, and α-synuclein. The FFPE samples from the hippocampus and cortex include controls (n=8), AD patients (n=8) and PDD patients (n=13). Detailed information regarding age at death, *post-mortem* delay (PMD), sex, fixation time, reported concomitant misfolded protein pathologies ta are indicated in Supplementary Table 2.

Immunohistochemistry (IHC)

IHC experiments were carried out as previously described (46). Briefly, FFPE samples were cut into 5 μm thick sections and processed on an automated immunostainer (Dako Omnis Immunostainer, Agilent) with heat-induced epitope retrieval (HIER) (EnVision™FLEX Target Retrieval Solution high or low pH buffer, Cat#K8004 and Cat#K8005 respectively) for 30 min at 97 °C. Primary antibodies (anti-VMAT2 Cat#TA500506, anti-CBS Cat#HPA001223) were diluted in EnVision™FLEX antibody diluent (Cat#K8006) and incubated for 1h at RT, detection based on horseradish peroxidase (HRP)/ 3, 3'-diaminobenzidine (DAB) substrate system (EnVision™FLEX Detection kit, Cat#K8000) and, finally, counterstained with hematoxylin (Cat#GC808). The slides were then dehydrated through ethanol baths before being coverslipped.

Images were visualised and acquired using 5, 10, 20 and 40X objectives of a Leica bright-field DM2000 LED microscope combined with a Leica DMC2900 camera (Leica Microsystems) and scanned with a high-throughput bright-field slide scanner (IntelliSite Ultra Fast Scanner, Philips).

Multiplex chromogenic IHC

Multiplex chromogenic IHC experiments were conducted as previously described (46), using Ventana Discovery Ultra automated IHC/*in situ* hybridisation (ISH) research platform (Roche Ventana Medical Systems, Tucson, AZ, USA). The system included all reagents as advised by Roche Diagnostics, and washing was performed in between steps using Reaction buffer (Cat#950-300). Briefly, FFPE samples were cut into 5 m thick sections and mounted on Matsunami TOMO® hydrophilic adhesion glass slides (Cat#TOM-1190), dried at 60°c for 60 min minimum, stained with antibodies of interest (see Supplementary Table 3), counterstained with hematoxylin II (Cat#790-2208) and bluing reagent (Cat#760-2039), and finally washed, dehydrated and coverslipped.

For DAB single-plex IHC experiments, samples were deparaffinised using EZ Prep solution (Cat#950-102) at 69°c for 8 min over three cycles and processed with Cell Conditioning 1 reagent (standard CC1, Cat#950-224) at 95°c for 40 min for the HIER step. Sections were then treated with the inhibitor ChromoMap reagent for 8 min at 37°c to block endogenous peroxidases and proteins. Primary antibodies (anti-BACE2 Cat#HPA035416, anti-SPARC Cat#HPA003020, and anti-Vimentin V9 Cat#05278139001) were diluted in EnVision™FLEX antibody diluent (Cat#K8006), manually applied on the sections of interest and incubated for 60 min. Samples were then treated with either OmniMap anti-Rb HRP (Cat#760-4311) or OmniMap anti-Ms HRP (#Cat760-4310) for 16 min. Stainings were developed using reagents from the Discovery ChromoMap DAB kit (Cat# 760-159). This involved

sequential applications of H_2O_2 ChromoMap for 4 min, DAB ChromoMap for 8 min, and Copper ChomoMap for 4 min.

Regarding the two-plex IHC experiments (CBS/GFAP, CBS/ALDH1L1, BACE2/GFAP, BACE2/ALDH1L1, SPARC/GFAP, SPARC/ALDH1L1, VIM/GFAP and VIM/ALDH1L1), the initial steps of deparaffinisation, HIER with CC1 and blocking with inhibitor ChromoMap were performed as previously described, unless stated otherwise. A single drop of Discovery inhibitor (Cat# 760-4840) was applied for 8 minutes. Primary antibodies (anti-CBS, anti-BACE2, anti-SPARC and anti-VIM) were then incubated for 60 minutes. Detection was carried out with OmniMap anti-Rb or anti-Ms HRP (16 minutes), followed by chromogenic development using the Discovery Purple Kit (Cat# 760-229), involving 4 min substrate incubation and 32 min H_2O_2 incubation. Between staining cycles, antibody denaturation was achieved by heating at 100 °C for 24 minutes with Cell Conditioning 2 reagent (CC2, Cat# 950-223), ensuring dissociation of antibody-HRP complexes and minimizing cross-reactivity. Next, anti-GFAP (Cat# 760-4345) and anti-ALDH1L1 (Cat# HPA050139) were applied (48 minutes for anti-GFAP and 60 minutes for ALDH1L1). Signal was then amplified using OmniMap anti-Rb or anti-Ms HRP (16 minutes) and visualised with either Discovery Teal HRP chromophore (Cat# 760-247) or Discovery Green HRP chromophore (Cat# 08478295001). Chromogenic development steps included 4 minutes with HRP substrate, 32 minutes with HRP H_2O_2, and 16 minutes with HRP activator.

Brightfiel microscopy

Chromogen-stained FFPE sections were visualized using a Leica DM2000 LED microscope fitted with 5X, 10X, 20X and 40X objectives, paired with a Leica DMC2900 camera (Leica Microsystems). For comprehensive imaging, whole-slide scans were obtained with the Philips IntelliSite Ultra Fast Scanner, and images were acquired using the HALO® image analysis software (Indica Labs, version 3.6).

Digital pathology and statistical analysis

Chromogenic IHC images were analysed using HALO® image analysis platform (Indica Labs, version 3.6). To investigate the expression of the different proteins of interest in the hippocampal and para-hippocampal regions, the hippocampus was manually divided into four sub-regions (dentate gyrus (DG), CA4, CA3 and CA2/CA1) and the subiculum as well as the parahippocampal cortex (PHC) were identified, all based on the Atlas of the Human Brain (47). Sub-region areas were measured, and CBS, VMAT2, SPARC, BACE2 and VIM quantifications were assessed by measuring stain-positive areas using the area quantification module from HALO® software. With R Studio software (R version 4.5),

comparisons of stained area percentages were conducted using Wilcoxon test (Supplementary File 1–Supplementary Excel 1).

RESULTS

The stimulation of astrocytes by noradrenaline induces phenotypic and molecular changes.

To characterise the effect of NA on the regulation of astrocyte genes, we performed bulk RNA sequencing (RNA-seq) on NA-exposed and non-exposed post-natal primary mouse astrocytes (Fig. 1A). Having analysed the NA dose-response of astrocytes to three different concentrations of NA–1, 10 and 100 μM– by measuring changes in *gfap*, *s100b*, *nqo1* and *camk4*, we found that 100 μM produced the most significant modulation of gene expression (Supplementary Fig. 1), in lines with previous studies (35–37). To mimic the long-term and pulsatile modulation of NA in the brain, we stimulated the primary cells with two 24-hour sequences. We analysed the differentially expressed genes (DEGs) between astrocytes non-exposed and NA-exposed astrocytes using unpaired t test with multiple comparison adjustment (Benjamini-Hochberg with FDR of 0.1) and identified 1,037 significantly DEGs. DEGs were displayed in a volcano plot (Fig. 1B) and the top 15 up- and 15 down- DEGs were identified and sorted by *padj.overall* (most enriched and lowest *padj.overall* value) (Fig. 1C). When comparing NA-exposed astrocyte to non-exposed astrocyte transcripts, we found *Cartpt, Scg2, Sod3, Sema3g, and S1pr1* among the most enriched and statistically significant genes for NA-exposed astrocytes. In parallel, *Cxcl9, Npy, Ace, Ace2* and *Camk4* were observed among the most downregulated and statistically significant genes (Supplementary File 2– Excel 2).

We confirmed the upregulation of *Sod3, Scg2* and *Cartpt* and the downregulation of *Camk4* and *Ace2* by qPCR (Fig. 1E). We then implemented an over-representation analysis (ORA) for NA-exposed versus non-exposed astrocyte DEGs. The Gene Ontology (GO) and Kyoto Encyclopedia of Genes and Genomes (KEGG) pathways over-represented in NA-exposed astrocytes revealed inflammatory and anti-oxidative responses (e.g. *Gbp2, Ptgs2, Vim, Casp1, Mgst1, Nqo1*), cell dynamic activities (e.g. *S1pr1, Cxcl14, Scg2*), circadian rhythm (e.g. *Bdnf, Cartpt, Per1*) and muscle contraction activities (e.g. *Adra2c, Sod3, Cbs, Ptgs2*). In contrast, we observed down-regulation of pathways related to synaptogenesis (e.g. *Snta1, Dag1, EphB2, Sema6d*) and to the regulation of the blood flow (e.g. *Ace, Ace2, Adra2a, Aqp4*) (Fig. 1D, Supplementary File 3– Excel 3). Taken together, these data validated the potent modulatory role of NA on astrocyte molecular signatures and responses.

Both Noradrenaline and Dopamine are potent modulators of astrocyte molecular identity.

To investigate whether these modulatory properties are specific to NA or a shared feature by NA and Dopamine (DA), the catecholamine direct precursor of NA, we compared the transcriptome profiles of

astrocytes exposed to DA and NA. We first evaluated the DEGs between astrocytes non-exposed versus DA-exposed astrocytes (unpaired t-test and multiple comparison adjustment) and found 8,514 significantly DEGs. DEGs were presented in a volcano plot (Fig. 2A) accompanied with the top 15 up- and 15 down- DEGs sorted by *padj.overall* (most enriched and lowest *padj.overall* value) (Fig. 2B). When analysing the transcripts enriched in DA-exposed astrocytes compared to non-exposed astrocytes, we found genes previously cited for NA-exposed astrocytes, such as *Cartpt, Sod3 and Scg2*, but also *Srxn1, Hmox1* and *Nqo1* among the most up-regulated and statistically significant genes. In contrary, we found *Ctnna2, Sorcs1, C3, Adra2a, Erbb4*, and *Nrxn3* among the less enriched and statistically significant genes. We then performed an ORA analysis for DA-exposed astrocytes compared to non-exposed astrocytes (Supplementary File 4– Excel 4). According to the GO and KEGG pathway enrichment analysis, DA-exposed astrocytes up-regulated neuropeptide signaling activity, feeding behavior, circulatory system processes, ferroptosis and PD. In parallel, this analysis revealed a down-regulation of pathways associated to organelle activities, axon guidance, circadian entrainment and cAMP signaling pathway (Fig. 2C, Supplementary File 5– Excel 5).

We then compared the DEGs obtained from cells exposed with NA (vs. non-exposed) to DA-exposed astrocytes (vs. non-exposed) (Fig. 2D, Supplementary Excel 6). We found 7,733 DEGs that were only significantly differentially regulated in the DA comparison. Among these transcripts, 3,655 were significantly up-regulated (e.g *Srxn1*, *Matcap2, Pdcd2* and *Skic8*) and 4,078 were significantly down-regulated DEGs (e.g. *C3, C4a, C4b*, *Lcn2, Sparc, Sparcl1* and *Qki*). In contrast, 256 DEGs were significantly differentially regulated exclusively in the NA comparison. Among them, 179 DEGs were significantly up-regulated (e.g. *Cbs, Bdnf, Il33, Ptgs2, Vim*) and 77 were significantly down-regulated (e.g. *Cd74, Clock, Nos2, Snta1*). However, we observed that both comparisons shared 305 significantly up-regulated (e.g. *Il11, Nqo1, S1pr1, Sod3, Cartpt, Casp1*) and 448 significantly down-regulated (e.g. *Ace, Ace2, Adra2a, Aqp4, Dtna, Nrxn3, Scg3*) DEGs. Moreover, we found 28 transcripts with divergent expression between NA- and DA-comparisons: 2 (*Foxj2*, *Gsdme*) were up-regulated in DA (vs. non-exposed) but down-regulated in NA (vs. non-exposed) astrocytes, while 26 (e.g. *Slc13a4, Slc43a3, Pdcd4*) were down-regulated in DA (vs. non-exposed) and up-regulated in NA (vs. non-exposed).

These results indicated that both NA and DA played a modulatory role on primary mouse astrocytes, influencing their molecular identity. However, we observed that DA impacted a greater number of genes than NA and identified genes that were specifically regulated by one catecholamine or the other. We also found some shared and a few divergent molecular signatures. Collectively, these

findings suggest that there are some common mechanisms by which NA and DA regulate astrocytes, as well as specific regulatory processes for each of these catecholamines.

Combined stimulation of cytokines in astrocytes induces an inflammatory gene signature that is mitigated by NA.

Next, we addressed the modulatory effect of NA on astrocyte responses to inflammation. To mimic inflammatory processes, we stimulated astrocytes with a mix of cytokine (CM) composed of TNFα, IL1β and IFNγ, at 10 ng/mL each. These cytokines are commonly used to activate pro-inflammatory pathways such as NFκB and STAT1/STAT3 signaling pathways. We investigated the transcriptomic profile of these cells after either 24 hours of CM stimulation or a combined treatment with 2 x 24 h of NA followed by 24 hours of CM stimulation (NA+CM). As previously explained, we evaluated the DEGs between astrocytes non-exposed versus CM-exposed (7,385 significantly DEGs), NA+CM-exposed versus NA-exposed (6,383 significantly DEGs) and NA+CM versus CM-exposed astrocytes (986 significantly DEGs). DEGs from each comparison were presented in three distinct volcano plots (Fig. 3A-C)

Treatment with CM induced severe changes in the transcriptomic response of the astrocytes, mainly characterised by upregulation of inflammation-related genes, such as immune response (e.g. *C3, Casp1*, *C4a, C4b*, *Cd274, Irf1, Irgm1, Gbp2, Gbp6, Gbp10*), NFκB signaling pathway (e.g. *Cd40, Casp1, Nlrp3, Nod1*, *Nlrc5*) and MHC assembly and antigen presentation activities (e.g. *Calr*, *H2-Ab1, H2-DMa, Tapbp, Tap1, Tap2*) among others. This stimulation led to the downregulation of genes mainly related to cytoskeletal remodeling (e.g. *Mapt*, *Mtcl1, Ttl, Plekhb1*), as well as synapse organisation and axon guidance (e.g. *Daw1, Dnal1, Drc1*) (Supplementary Fig. 2A, Supplementary File 7– Excel 7, Supplementary File 8– Excel 8).

The comparison of DEGs between NA+CM-exposed and NA-exposed astrocytes showed the same profile of gene expression than the previous comparison with up- and downregulation of similar pathways (Supplementary Fig. 2B, Supplementary File 7– Excel 7, Supplementary File 8– Excel 8). From the comparison between NA+CM-exposed and CM-exposed astrocytes, we found some significantly differentially genes that we previously described as NA-targeted genes (e.g. *Ace*, *Cartpt, Cbs*, *Scg2, Sod3, Snta1, S1pr1*). Moreover, we observed a modulation of astrocyte responses to the inflammatory stimulation notably with downregulation of inflammation-related genes, such as antigen processing and presentation (e.g. *H2-Ab1, H2-DMa, C3*), CXCL5, CXCL12, as well as oxidative stress-related genes, including *Hmox1, Nfe2l1, Prdx1*. Interestingly, we also found *Apoe* as down-regulated DEGs. The

analysis of the upregulated DEGs mainly showed the upregulation of the mitotic activity of the cells (e.g. *Brca1, Cdc6, Clspn, Dtl, Lmnb1*) (Fig. 3C-D, Supplementary File 8– Excel 8). We validated the expression of certain genes via qPCR (Fig. 3E). These data showed that despite the strong inflammatory profile induced by CM, astrocytes pretreated with NA recovered some molecular signatures specifically induced by NA stimulation in addition to moderate their molecular responses to inflammation.

To validate these findings, we next investigated the secretome of non-exposed (CTL), NA-exposed, CM-exposed and NA+CM-exposed astrocytes by measuring released cytokines and chemokines in the cell culture medium (Fig. 3F). Because many of them were not detected or very low, we focused our analysis on 3 cytokines (TNFα, IL1β, IL6), 5 chemokines (CCL5, CXCL1, CXCL2, CXCL9, CXCL10) and CD54 (or ICAM1). We observed that the CM stimulation led to an important release of these molecules, especially TNFα, CCL5, CXCL1, CXCL2, CXCL10 and IL6, suggesting that the astrocytes actively respond to the inflammatory conditions. When astrocytes were pre-treated with NA and then stimulated with CM, we observed a global reduction of the cytokine and chemokine release, notably CXCL2 and IL6. Nevertheless, none of these differences was significant. The qualitative nature of the assays used for these experiments might explain the lack of significance in these data.

Taken together, these results showed that NA exposure modulates astrocyte responses to inflammation by changing their molecular signatures. Moreover, NA had a long-lasting effect and mitigated the secretory response of astrocytes to subsequent inflammatory challenges.

NA-exposed astrocytes exert non-cell-autonomous immunomodulatory effects on activated microglia.

To investigate whether NA influences the astrocyte-microglia crosstalk, we performed indirect co-culture experiments. We cultured primary mouse microglia that we next stimulated with LPS to create an inflammatory environment. In addition to LPS stimulation, we exposed the cells to astrocyte conditioned medium (ACM). This ACM was obtained beforehand from either non-exposed (ACM_{CTL}) or NA-exposed (ACM_{NA}) astrocytes (Fig. 3G).

To analyse microglia responses we evaluated gene expression of the cells by qPCR. We found that LPS stimulation induced a significant increase of gene expression related to inflammatory response such as *Tnfa, Cxcl10* and *Il6* (Fig. 3H). When microglia were stimulated with ACM alone (ACM_{CTL} or ACM_{NA}), very low levels of expression were observed, if any. Co-treatment with LPS and ACM_{CTL} led to increased gene expression, including *Tnfa* and *Cxcl10* whose expression was decreased when microglia were treated with LPS and ACM_{NA}, although the difference of expression was significant for *Tnfa* only.

Il6 expression was not changed, suggesting a specific response through the TNFα pathway (Fig. 3H). These results suggest that NA might modulate microglia activation through astrocyte signaling.

The noradrenergic efferences are slightly impacted in the hippocampi of AD patients.

To measure the impact of the deterioration of LC noradrenergic neurons, we assessed the distribution and density of VMAT2, which indirectly labels all NA branches accessing the hippocampus. To this purpose, we performed cIHC and quantified DAB-stained area for VMAT2 in the hippocampus of *post-mortem* samples from AD (n=8, average age at death: 71.9 years, 5 females, 3 males), and PDD patients (n=13, average age at death: 73.4 years, 7 females, 6 males), as well as age-matched non-demented individuals (n=7, average age at death: 86.9 years, 4 females, 3 males).

VMAT2 staining revealed that the hippocampus is a noradrenergic-enriched structure with heterogeneous distribution of these projections throughout the hippocampus (Fig. 4A). We observed in the DG many VMAT2+ fibers as well as a diffuse staining in the inner one-third of the molecular layer (STR. MOL 1/3) (Fig. 4Aa). The CA4, CA3 and CA2 were highly enriched with short VMAT2 fibers while CA1 mainly contained long VMAT2+ fibers, crossing the entire pyramidal layer for some of them (Fig. 4Ab-c). We also observed in the CA1 a layered distribution of the VMAT2 staining with an enrichment in the pyramidal layer, mainly due to a diffuse staining, less in the stratum radiatum and low staining in the molecular layer. We found VMAT2+ fibers in the subiculum and a few positive cells (Fig. 4Ad). The PHC showed very low density of VMAT2 staining.

Next, we performed the quantification in AD and PDD hippocampal samples. We found that VMAT2 staining was partially reduced, especially in AD patients in CA4, CA3, CA1/CA2, subiculum and PHC. In PDD, we observed a reduction of VMAT2 staining mainly in CA1/CA2, subiculum and PHC. However, these differences were not statistically significant (Fig. 4B). Interestingly, we observed significant VMAT2 staining enrichment in the inner molecular layer of the DG and the CA3 subfield of PDD patients (Fig. 4C).

CBS expression, a NA-responsive gene, is severely altered in neurodegenerative diseases.

To evaluate the significance of our *in vitro* results, we examined the expression of CBS, which is encoded by the *Cbs* gene, in human brain samples. The expression of this gene was increased in astrocytes exposed to NA and may play a direct role in responses to oxidative stress. To this purpose, we performed cIHC and quantified DAB-stained area for CBS in *post-mortem* hippocampal samples from non-demented healthy individuals (CTLs, n=7, average age at death: 89.4 years, 4 females, 3 males) and

patients with AD (n=9, average age at death: 73.4 years, 6 females, 3 males) or PDD (n=10, average age at death: 74.6 years, 5 females, 5 males), using HALO® digital pathology software.

CBS staining revealed a strong expression of this enzyme by hippocampal astrocytes although its expression was not uniform across all hippocampal subfield (Fig. 5A). CBS was highly expressed in the CA4 and the DG subregions, as well as in the pyramidal and molecular layers but less so in the radiatum and oriens layers of the CA subfields. Given its cytoplasmic location, CBS mainly labeled the soma, but also the proximal processes of astrocytes.

To further understand the identity of these astrocytes, we performed multiplex cIHC for CBS combined with GFAP (n=3) or ALDH1L1 (n=3) in CTL *post-mortem* hippocampi. Co-staining of CBS with GFAP showed many astrocytes stained only for CBS while GFAP astrocytes were mainly CBS+/GFAP+ double-positive (Fig. 5B). Multiplexing CBS together with ALDH1L1, a broader pan-astrocytic marker, showed an overlapping expression of the two markers with numerous CBS+/ALDH1L1+ double-positive cells. We also observed several astrocytes single-positive for either CBS or ALDH1L1 (Fig. 5C).

Next, we examined the expression of CBS in the hippocampi of patients with AD and PDD, as both conditions are affected by the deterioration of LC and the depletion of NA. We found a significant loss of CBS expression in AD and PDD patients across the hippocampus (Fig. 5D). CBS staining revealed a general reduction in CBS cell surface coverage and shorter positive branches, particularly in PDD cases (Fig. 5E-F).

We also investigated the expression of SPARC and BACE2, the gene expression of which was down-regulated in NA-exposed astrocytes, as well as VIM, encoded by the *Vim* gene which was up-regulated under NA exposure. We assessed the quantification of DAB-stained area in *post-mortem* hippocampal tissues from CTLs individuals (n=3, average age at death: 87.3 years, 2 females, 1 male), AD patients (n=5, average age at death: 69.4 years, 3 females, 2 males) and PDD cases (n=5, average age at death: 72.4 years, 2 females, 3 males). SPARC was found to be highly expressed by certain astrocytes, including ALDH1L1+ astrocytes (Supplementary Fig. 2A). SPARC expression was significantly decreased in the CA3, CA1/CA2, subiculum and PHC of PDD patients. In AD, we observed a slight decrease in SPARC expression in the same subregions, though these differences were not significant (Supplementary Fig. 2B-C). A few hippocampal astrocytes expressed BACE2, mainly in the oriens layer of the CA subfields. These astrocytes were also ALDH1L1+ (Supplementary Fig. 2D). No differences in BACE2 expression were observed in AD and PDD samples compared to CTLs, except in the CA4 subfield where BACE2 levels were significantly higher in patients with PDD (Supplementary Fig. 2E-F). VIM was mainly found to label blood vessels, as well as some astrocytes that were also positive for ALDH1L1

(Supplementary Fig. 2G). VIM expression was decreased in the CA3, CA1/CA2 and PHC in both AD and PDD, although these differences were only significant in the PHC of PDD cases (Supplementary Fig. 2H-I).

These data suggest that the potential disruption of the NA system in NDDs could alter the expression of key astrocytic proteins.

DISCUSSION

In this study, we provide a detailed characterisation of the effect of NA on phenotypic and molecular responses of astrocytes, integrating bulk RNA sequencing, RT-qPCR and cytokine assays on primary mouse astrocytes, in both homeostatic and inflammatory states. Our results demonstrate that NA profoundly influences the transcriptomic profile of astrocytes, controlling their molecular signature and consequently modulating core astrocytic functions. Additionally, we validated the modulatory role of NA on astrocyte responses to inflammation. By investigating the impact of the deterioration of the NA system in the human hippocampus, we revealed a moderate alteration of the NA efferences in AD patents. Furthermore, we demonstrate an association between this deterioration, which may indicate an imbalance in NA levels in the hippocampus, and a reduction in the expression of NA-stimulated proteins in astrocytes, resulting in dysregulation of their functions.

Noradrenaline and Dopamine are core modulators of astrocytic activity and identity.

Astrocytes are no longer perceived as a passive cell type with a simple structural function, but as multitasking cells deeply involved in brain functions. As neurons, astrocytes can sense and respond to various factors and neurotransmitters such as NA and DA (28–30,48,49). However, how catecholamines shape the molecular identity and functions of astrocytes is not yet fully understood. By investigating the transcriptomic identity of primary mouse astrocytes exposed to NA, we show that NA regulates the expression of certain genes involved in key astrocytic functions. Notably, we found that astrocytes exposed to NA change their transcriptomic activity related to the blood flow regulation (*Sod3, Cbs, Adra2a, Ace*). This observation aligns with previous studies that place the astrocytes as an integral part of the vascular unit (17,50). Indeed, in addition to contributing to the development and the maintenance of the blood-brain-barrier (BBB) (51), astrocytes are also involved in the neurovascular coupling, which ideally positions them to control the cerebral blood tone (50,52,53). Mulligan and MacVicar demonstrated that NA modulates the intracellular calcium concentration in the astrocytic endfeet resulting in arteriole vasomotion (16), this type of almost instantaneous modulation may depend on a chronic modulation of astrocyte molecular identity, as shown by our data.

Our results also highlight that NA could influence the astrocyte-neuron crosstalk by regulating genes involved in synaptogenesis. Indeed, we observe changes in the transcription of genes coding for proteins that mediate neuronal circuit assembly, such as *S1pr1*. The sphingosine 1 phosphatase receptor 1 (S1PR1) is expressed by perisynaptic astrocytes and has been shown to be essential for astrocyte-synapse association, regulating the expression of astrocyte-secreted synaptogenic factors

such as hevins (SPARCL1) and thrombospondins (TSP4) (54). Such data highlight the crucial role of astrocytes in synapse formation, maturation, stabilisation and transmission (55–59).

Our data also show that dopamine is a potent regulator of the astrocyte transcriptome. Dopamine signalling is also central to many functions involving the hippocampus, such as learning and memory (60). Astrocytes are also known to express dopamine receptors (61) and DA exerts a strong modulation of their activity (48). Here, we show *in vitro* an overlap of their modulation processes but also clear specificity. This might regionally influence the identity and the function of astrocytes in relation to the anatomical dopaminergic and noradrenergic innervations.

Noradrenaline mitigates astrocytes and microglia responses to neuroinflammation.

Importantly, our transcriptomic data demonstrate that NA controls astrocyte responses to inflammation and oxidative stress. When exposed to NA, astrocytes increase the expression of gene related to inflammatory (*Ptgs2, Vim*) and antioxidant (*Cbs, Sod3, Mgst1, Nqo1*) responses. This is consistent with the findings of Hinojosa and colleagues who showed that the effects of NA on astrocytes are context-dependent: in inflammatory conditions, NA reduces the production of pro-inflammatory cytokines, while under basal conditions it may contribute to maintaining their moderate expression levels (62). Indeed, by investigating the responses of NA-exposed astrocytes to inflammation, we show a moderation of their pro-inflammatory profile, notably by a down-regulation of genes associated with the MHC assembly and antigen presentation. Astrocytes have been recently reported to act as antigen-presenting cells and T cell activators in disease (63–65), suggesting astrocytes as active immune effectors in CNS immunity. Moreover, we show that NA attenuates the secretory response of astrocytes to subsequent inflammatory challenges by reducing the release of pro-inflammatory cytokines and chemokines. In addition, NA exerts non-cell-autonomous immunomodulatory effects on microglia through astrocyte-mediated signaling.

Altogether, these observations align with those of several *in vitro* studies of AD mouse models, which have shown that NA depletion leads to an increase in astrocytic and microglial inflammatory signatures and oxidative stress (34,35,66), suggesting NA as a potent anti-inflammatory agent in astrocytes and microglia responses.

Cystathionine-β-synthase, at the core of brain physiology, oxidative stress and homocysteine pathways.

CBS is the rate-limiting enzyme that catalyses the condensation of serine and homocysteine (Hcy) to cystathionine, which serves as a precursor for both glutathione (GSH) and hydrogen sulfide (H_2S). It has been reported that the expression of CBS is reduced in the ageing brain, accompanied by decreased levels of H_2S and an imbalanced GSH/GSSG ratio, resulting in increased oxidative stress, specifically in astrocytes (67). Interestingly, astrocytes have been shown to be the most active producer of H_2S that is described as a neuroprotective factor with potent anti-inflammatory and antioxidant properties (68). In our study, we first demonstrate the upregulation of the *Cbs* gene in primary mouse astrocytes exposed to NA. This suggests that CBS is an NA-sensitive target and validates NA as a neuroprotective agent via astrocyte signalling. We also confirm the expression of CBS in the human brain, particularly in hippocampal astrocytes, which strongly express the enzyme. Importantly, we show a severe reduction of CBS expression in AD and PDD patients. Both AD and PD are characterized by a progressive LC deterioration and decrease of NA levels (69–71). Here, we found that VMAT2, which we use as a marker to estimate NA projections, was moderately decreased in AD, but remained quite stable in PDD compared to CTLs. The loss of CBS is recognised to cause hyperhomocysteinemia (HHcy), resulting in metabolic, neurological and vascular disruptions. It also increases oxidative stress and the risk of cardiovascular and NDDs. HHcy has been reported to enhance neuroinflammation in ageing and CNS diseases and is associated with the risk of developing AD, vascular dementia, fronto-temporal dementia and PD (69–72). Our findings in diseased samples suggest that loss of CBS, which results in HHcy, may be caused by disruption to astrocyte identity, possibly due to dysregulation of the NA system.

Our data also show a significant decrease of SPARC expression in PDD patients. Physiologically, SPARC contributes to maintaining BBB stability and participates in processes such as tissue repair, extracellular matrix remodeling, inflammation, and immune modulation (73,74). SPARC is also crucial for synapse formation and maturation (75). In the human brain, elevated SPARC levels have been reported in reactive astrocytes located near brain tumors, as well as in individuals with neurological conditions such as epilepsy, stroke, and AD (75–77). To date, however, there is no clear evidence linking SPARC directly to the pathogenesis of PDD. Given its key physiological functions, reduced SPARC expression may compromise astrocyte-mediated roles, particularly vascular regulation and BBB maintenance.

Conclusion

In conclusion, our study highlights the strong phenotypic control exerted by NA and DA on astrocyte physiology and responses. Each catecholamine exhibits specific modulatory properties, although there is also overlap in the regulatory processes. We demonstrate profound transcriptomic changes, as well as modulation of the astrocyte secretome, in response to an inflammatory microenvironment. Our investigation of the human hippocampus revealed a partial reduction in NA efferences in AD patients, which may indicate an imbalance in NA levels within the hippocampus. Associated with this, we demonstrated severe loss of CBS expression in astrocytes, which may increase oxidative stress, decrease neuroprotection, and cause deregulation of homocysteine metabolism. Taken together, these findings emphasise the importance of understanding the role of glial cells in the NA system to gain new insights into the physiopathology of NDDs as well as in therapeutic effort against dementia progression.

DECLARATIONS

Ethics approval

Use of human brain *post-mortem* samples for research was approved by the Ethic Panel of the Netherlands Brain Bank (Netherlands Institute for Neuroscience, Amsterdam) as well as of the University of Luxembourg (ERP 16-037 and 21-009).

Data availability

Raw data is available on request.

Consent for publication

All authors have consented for the publication of manuscript.

Declaration of interests

The authors report no competing interests.

Funding

This work was supported by the Espoir-en-tête Rotary-International awards (to DSB) and the Luxembourg National Research Fund (FNR: PEARL P16/BM/11192868 and NCER13/BM/11264123 (to MM)). FJ and SSc were supported by the AFR program of the Luxembourg National Research Found through the grants AFR15735457 and AFR17129900. MMM was supported by the PRIDE program of the Luxembourg National Research Found through the grant PRIDE21/16749720/NEXTIMMUNE2.

Acknowledgments

We thank the brain donors and their family for their support of the project. We thank the LuxGen core facility for their support for the RNA sequencing.

Author contributions

DSB conceived and supervised the study. FJ, MMM and SSc performed the experiments. FJ, MMM, SSc, DCR and GH produced and analyzed the statistical data. FJ and DSB prepared the figures. NBB provided cohort of human brain samples and neuropathological reports. FJ and DSB drafted the manuscript. AM and GH wrote the RNAseq methodology. MM analysed neuropathological data and co-supervised the study.All authors contributed to the final version of the manuscript.

FIGURES

Figure 1: Noradrenaline induces distinct phenotypic and molecular changes in primary mouse astrocytes

A Cell culture workflow used to obtain primary mouse astrocytes. After four weeks in culture, including isolation steps, the cells were treated with 100 μM for 2 x 24 h. Biological material was then recovered to perform different analysis. **B** Volcano plot representing the differentially expressed genes (DEGs) in NA-exposed astrocytes compared to non-exposed cells (n=3). Thresholds of Log2FC=0.5, *P* value=0.05 and FDR=0.1 are indicated in the graph. **C** Representation of the top 15 up- and top 15 down-regulated DEGs in astrocytes exposed to NA compared non-exposed cells, sorted by *padj.overall* value. **D** Over-representation analysis (ORA) dotplot representing the significance of selected up- and down-regulated pathways, based on Kyoto Encyclopedia of Genes and Genomes (KEGG) database, comparing NA-exposed vs non-exposed astrocytes, sorted by *padjust* value and gene counts (see full list in Supplementary File 3- Excel 3). **E** Via qPCR, we validated the difference of expression of certain genes between NA-exposed (NA) and non-exposed astrocytes (CTL). Expression normalised to *Rpl27*. n=3 per condition, statistical analysis: t test, * $p<0.05$, *** $p<0.005$, *** $p<0.0005$, **** $p<0.00005$.

Figure 2: In primary mouse astrocytes, dopamine induces certain molecular changes that are similar to those induced by noradrenaline.

A-C RNA-seq analysis from primary mouse astrocytes exposed to DA or non-exposed (n=3). **A** Volcano plot representing the DEGs in DA-exposed astrocytes compared to non-exposed (n=3). Thresholds of Log2FC=0.5, *P* value=0.05 and FDR=0.1 are indicated in the graph. **B** Representation of the top 15 up- and top 15 down-regulated DEGs in astrocytes exposed to DA compared with non-exposed cells, sorted by *padj.overall* value. **C** ORA KEGG of up- and down-regulated DEGs in DA-exposed astrocytes shows that DA is another strong modulator of astrocyte physiology and responses (see full list in Supplementary File 5- Excel 5). **D** Comparing the DEGs induced by NA exposure with those induced by DA stimulation reveals several shared transcripts, as well as numerous DEGs that are specific to either NA or DA. The Venn diagram represents the overlap (total number and percentage) of all significantly DEGs in either comparisons (NA-exposed vs. Non-exposed and DA-exposed vs. Non-exposed astrocytes). Red and blue transcript names correspond to up- and down-regulated DEGs, respectively (see full list in Supplementary File 6- Excel 6).

Figure 3: NA modulates astrocytes responses under inflammatory conditions.

Volcano plots representing the DEGs in (**A**) CM-exposed versus non-exposed, in (**B**) NA+CM exposed versus NA-exposed and in (**C**) NA+CM-exposed versus CM-exposed astrocytes (n=3 per condition). Thresholds of Log2FC=0.5, *P* value=0.05 and FDR=0.1 are indicated in the graph. Each volcano plot is accompanied with the list of the top 15 up- and top 15 down-regulated DEGs, sorted by *padj.overall* value. **D** ORA KEGG of up- and down-regulated DEGs in NA+CM-exposed astrocytes shows that NA reduces astrocyte responses to oxidative stress and inflammation (see full list in Supplementary File 8-Excel 8). **E** qPCR validation of gene expression between all conditions (CTL = non-exposed astrocytes). Expression normalised to *Rpl27*. n=3 per condition, statistical analysis: one-way ANOVA, Tukey's multiple comparisons test, * p<0.05, *** p<0.005, *** p<0.0005, **** p<0.00005*. **F** Cytokine assays (n=3) show an increase of cytokine and chemokine release when astrocytes are stimulated with CM. NA tends to modulate this response (NA+CM), slightly reducing the release of chemokines. **G** Experimental design representing the indirect co-culture between microglia and astrocytes. Microglia were non-stimulated (CTL) or stimulated with LPS and/or with astrocyte conditioned media (ACM) from NA-exposed (ACM_{NA}) or non-exposed (ACM_{CTL}) astrocytes. **H** Under inflammation, microglia exposed to ACM_{NA} showed a significant reduction of *Tnfa* gene expression and a slight decrease of *Cxcl10*, but no change in *Il6* gene expression. Expression normalised to *Rpl27*. n=4 per condition, statistical analysis: one-way ANOVA, Tukey's multiple comparisons test, * p<0.05, *** p<0.005, *** p<0.0005, **** p<0.00005*.

Figure 4: Noradrenergic efferences are slightly affected by neurodegeneration in AD hippocampi.

A Representative cIHC stainings of VMAT2 (DAB, brown) in the healthy hippocampus reveal VMAT2+ projections across all hippocampal subfields: (**a**) DG/CA4, (**b**) CA3, (**c**) CA1 and (**d**) subiculum (case #7). **B** The quantitative analysis of VMAT2 (surface coverage area of the DAB staining) shows a partial decrease of VMAT2 expression in AD patients, although these differences are not statistical. n=7 CTL, n=8 AD, n=13 PDD; statistical analysis: Wilcoxon test, ** p<0.05*, *** p<0.005, *** p<0.0005*. **C** VMAT2 staining (DAB, brown) remains stable in the CA3 of AD patients and is enriched in the inner molecular layer of the DG of PDD cases (AD case #11, PDD case #19). **SG**, stratum granulosum; **$SM_{1/3}$**, inner stratum moleuclar 1/3; **$SM_{2/3}$**, outer stratum moleculare 2/3; **SPy**, stratum pyramidale; **SR**, stratum radiatum. Scale bars: **A** low magnification: 500 μm, high magnification (a-d) 50 μm; **C** low magnification: 500 μm, high magnification 50 μm.

Figure 5: CBS expression is severely reduced in AD and PDD brains.

A Representative IHC staining of CBS (DAB, brown) in the healthy hippocampus. **a-d** Zoom-in on different hippocampal subfields: (**a**) CA4, (**b**) CA3, (**c**) CA1 and (**d**) subiculum (case #5). **B** Multiplex cIHC of CBS with GFAP shows that all GFAP+ astrocytes express CBS (dark blue, black arrows) while CBS (purple, white arrows) is expressed by astrocytes to a greater extent than GFAP (teal) (case #5). **C** Duplex staining of CBS with ALDH1L1 reveals that numerous CBS+ astrocytes are also ALDH1L1+ (dark blue, black arrows) although several astrocytes are single-positive (white arrows) for either CBS (purple) or ALDH1L1 (teal) (case #5). **D** CBS expression is drastically decreased in AD and PDD. n=7 CTL, n=9 AD, n=10 PDD; statistical analysis: Wilcoxon test, ** $p<0.05$, ** $p<0.005$, *** $p<0.0005$*. **E** Representative IHC staining of CBS (DAB, brown) in AD and PDD hippocampi. In both AD and PDD, the intensity of CBS staining appears decreased in astrocyte processes (AD case #9, PDD case #22). **SPy**, stratum pyramidale; **SR**, stratum radiatum. Scale bars: **A** low magnification: 500 μm, high magnification (a-d) 50 μm; **B** 50 μm; **E** low magnification: 500 μm, high magnification 50 μm.

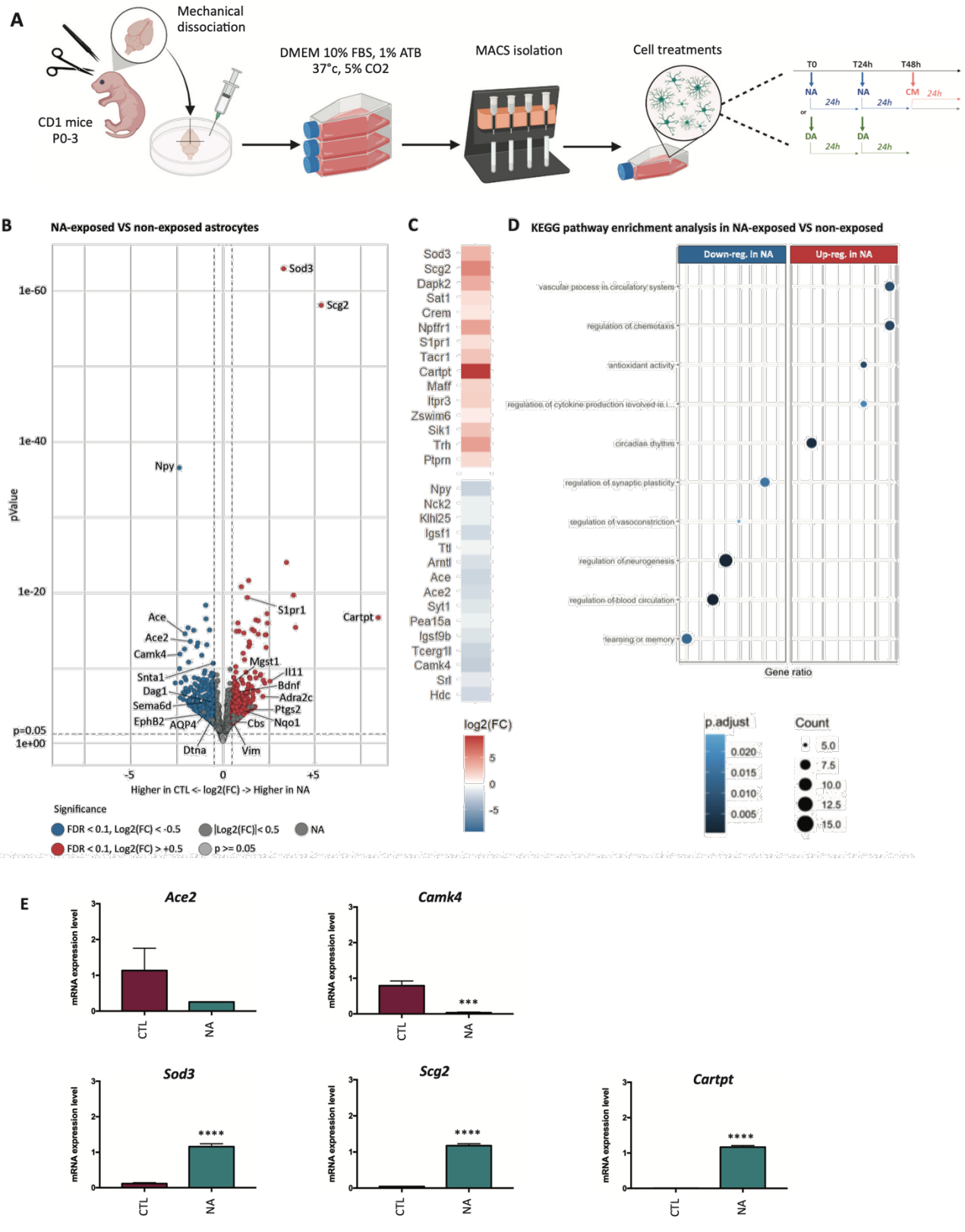
A
Mechanical dissociation
CD1 mice P0-3
DMEM 10% FBS, 1% ATB 37°c, 5% CO2
MACS isolation
Cell treatments
T0
T24h
T48h
NA
CM
DA
24h
B
NA-exposed VS non-exposed astrocytes
pValue
1e-60
1e-40
1e-20
p=0.05
1e+00
Sod3
Scg2
Npy
S1pr1
Cartpt
Ace
Ace2
Camk4
Mgst1
Il11
Bdnf
Adra2c
Ptgs2
Nqo1
Snta1
Dag1
Sema6d
EphB2
AQP4
Cbs
Dtna
Vim
-5
0
+5
Higher in CTL <- log2(FC) -> Higher in NA
Significance
FDR < 0.1, Log2(FC) < -0.5
|Log2(FC)|< 0.5
NA
FDR < 0.1, Log2(FC) > +0.5
p >= 0.05
C
Sod3
Scg2
Dapk2
Sat1
Crem
Npffr1
S1pr1
Tacr1
Cartpt
Maff
Itpr3
Zswim6
Sik1
Trh
Ptprn
Npy
Nck2
Klhl25
Igsf1
Ttl
Arntl
Ace
Ace2
Syt1
Pea15a
Igsf9b
Tcerg1l
Camk4
Srl
Hdc
log2(FC)
5
0
-5
D
KEGG pathway enrichment analysis in NA-exposed VS non-exposed
Down-reg. in NA
Up-reg. in NA
vascular process in circulatory system
regulation of chemotaxis
antioxidant activity
regulation of cytokine production involved in i...
circadian rhythm
regulation of synaptic plasticity
regulation of vasoconstriction
regulation of neurogenesis
regulation of blood circulation
learning or memory
Gene ratio
p.adjust
0.020
0.015
0.010
0.005
Count
5.0
7.5
10.0
12.5
15.0
E
Ace2
Camk4
Sod3
Scg2
Cartpt
mRNA expression level
CTL
NA
***
****

Figure 1

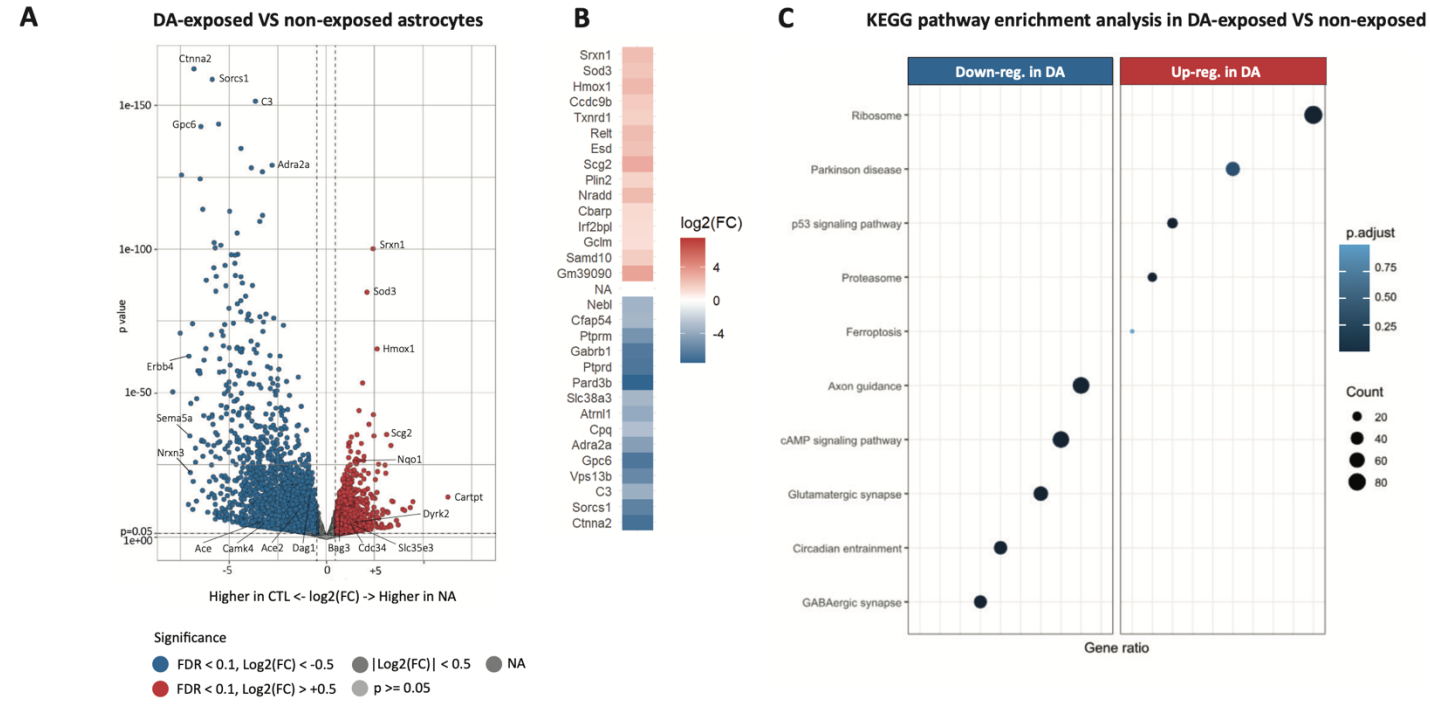

D

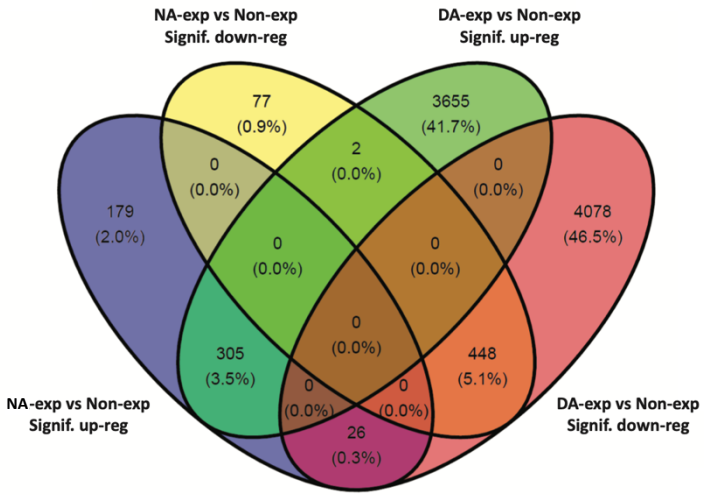

Shared genes in both comparisons:

Il11 *Cartpt* *Ace* *Dtna*
Nqo1 *Casp1* *Ace2* *Nrxn3*
S1pr1 ... *Adra2a* *Scg3*
Sod3 *Aqp4* ....

Genes specific to NA:

Cbs *Vim* *Snta1* ...
Bdnf ... *Nos2*
Il33 *Clock*
Ptgs2 *Cd74*

Genes specific to DA:

Srxn1 ... *C3* *Lcn2*
Matcap2 *C4a/C4b* ...
Pdcd2 *Sparcl1*
Skic8 *Sparc*

Genes with divergent expression:

Foxj2 Slc13a4
Gsdme Slc43a3
Pdcd4
...

Figure 2

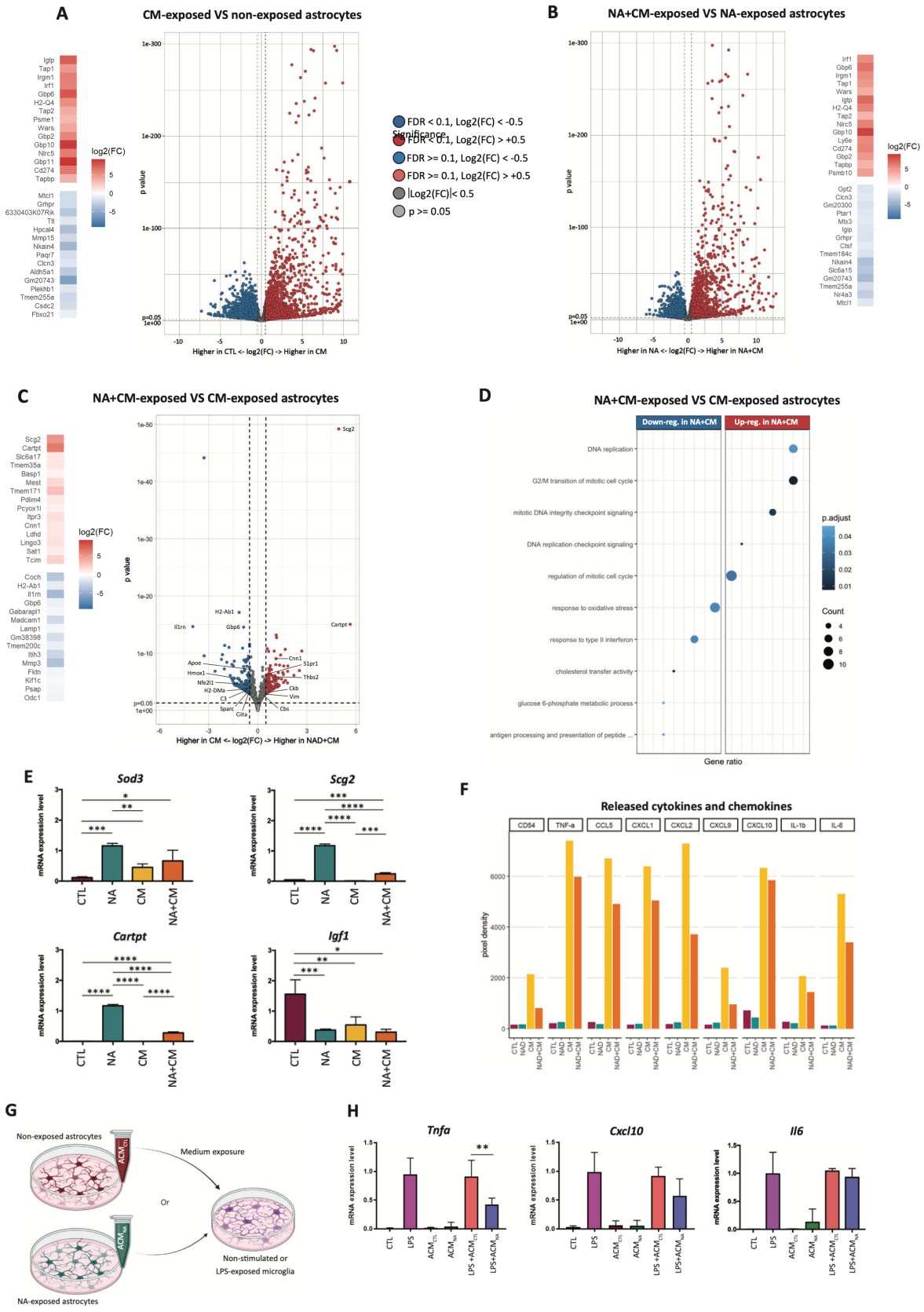
A
CM-exposed VS non-exposed astrocytes
log2(FC)
p value
Higher in CTL <- log2(FC) -> Higher in CM
FDR < 0.1, Log2(FC) < -0.5
FDR < 0.1, Log2(FC) > +0.5
FDR >= 0.1, Log2(FC) < -0.5
FDR >= 0.1, Log2(FC) > +0.5
|Log2(FC)|< 0.5
p >= 0.05
B
NA+CM-exposed VS NA-exposed astrocytes
Higher in NA <- log2(FC) -> Higher in NA+CM
C
NA+CM-exposed VS CM-exposed astrocytes
Higher in CM <- log2(FC) -> Higher in NAD+CM
D
NA+CM-exposed VS CM-exposed astrocytes
Down-reg. in NA+CM
Up-reg. in NA+CM
DNA replication
G2/M transition of mitotic cell cycle
mitotic DNA integrity checkpoint signaling
DNA replication checkpoint signaling
regulation of mitotic cell cycle
response to oxidative stress
response to type II interferon
cholesterol transfer activity
glucose 6-phosphate metabolic process
antigen processing and presentation of peptide ...
p.adjust
Count
Gene ratio
E
Sod3
Scg2
Cartpt
Igf1
mRNA expression level
CTL
NA
CM
NA+CM
F
Released cytokines and chemokines
CD54
TNF-a
CCL5
CXCL1
CXCL2
CXCL9
CXCL10
IL-1b
IL-6
pixel density
G
Non-exposed astrocytes
Medium exposure
Or
Non-stimulated or
LPS-exposed microglia
NA-exposed astrocytes
H
Tnfa
Cxcl10
Il6
CTL
LPS
ACM
LPS +ACM
LPS+ACM

Figure 3

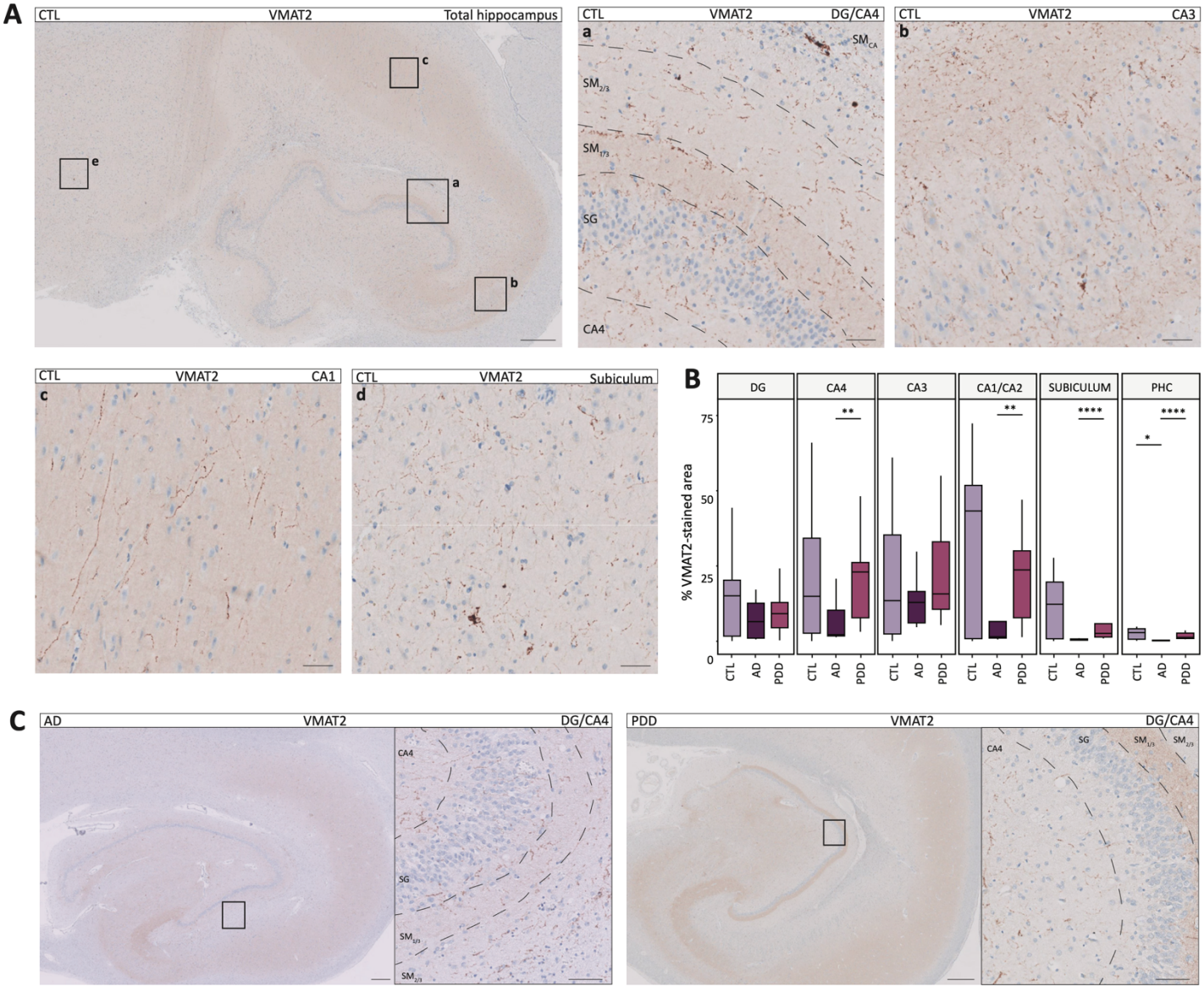
A
CTL
VMAT2
Total hippocampus
c
e
a
b
CTL
VMAT2
DG/CA4
a
SM_CA
SM_2/3
SM_1/3
SG
CA4
CTL
VMAT2
CA3
b
CTL
VMAT2
CA1
c
CTL
VMAT2
Subiculum
d
B
DG
CA4
CA3
CA1/CA2
SUBICULUM
PHC
% VMAT2-stained area
75
50
25
0
**
**
****
*
****
CTL
AD
PDD
C
AD
VMAT2
DG/CA4
CA4
SG
SM_1/3
SM_2/3
PDD
VMAT2
DG/CA4
CA4
SG
SM_1/3
SM_2/3

Figure 4

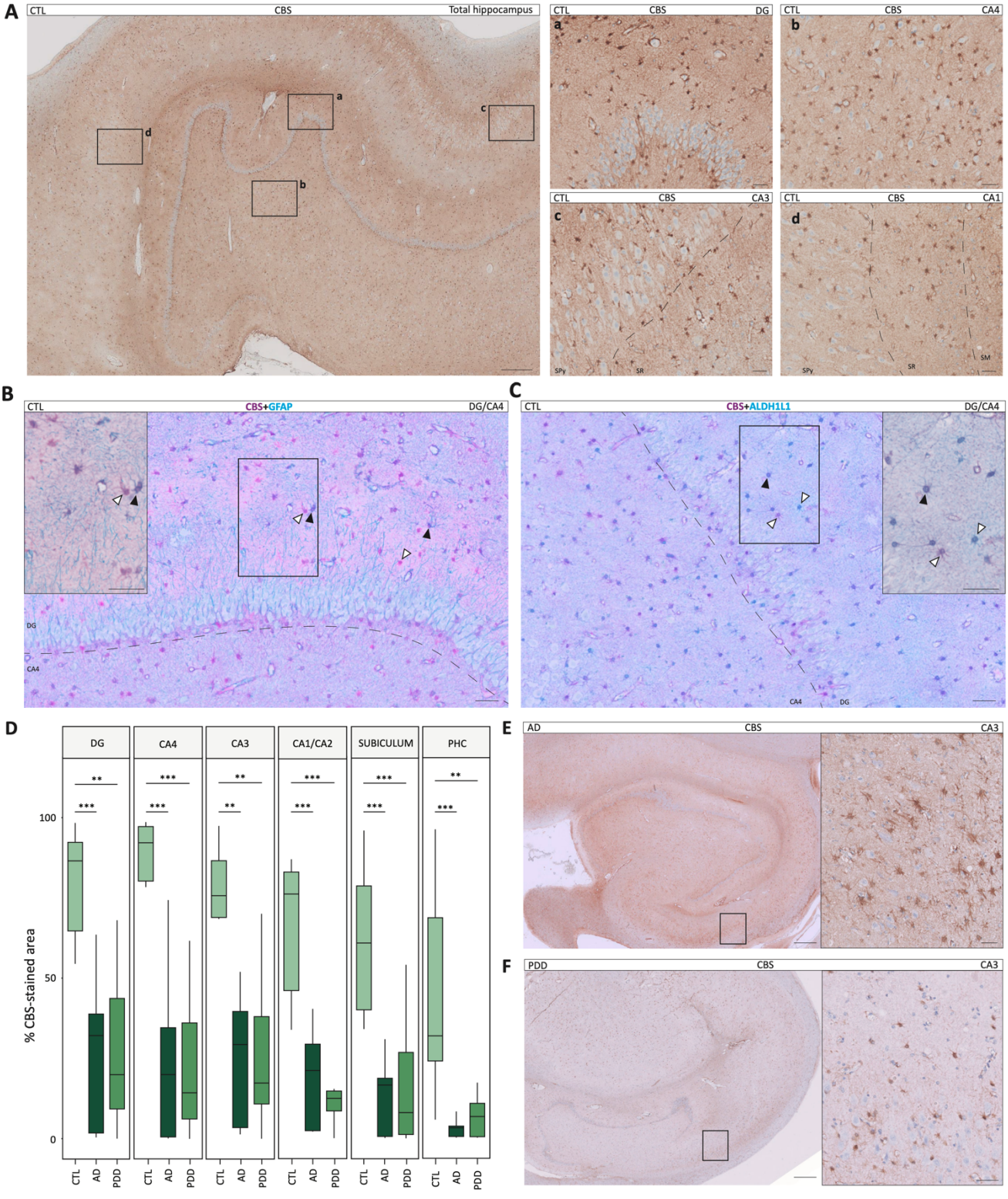
A
CTL
CBS
Total hippocampus
DG
CA4
CA3
CA1
B
CBS+GFAP
DG/CA4
C
CBS+ALDH1L1
D
DG
CA4
CA3
CA1/CA2
SUBICULUM
PHC
% CBS-stained area
CTL
AD
PDD
E
AD
F
PDD

Figure 5

Supplementary Figure 1: Astrocyte responses to noradrenaline.

To determine the optimal concentration of NA to which astrocytes respond most strongly, we evaluated three different concentrations (1 μM, 10 μM, 100 μM) by measuring the gene expression of *Gfap*, *S100b*, *Nqo1* and *Camk4* via qPCR. (CTL = non-exposed astrocytes). Expression normalised to *Rpl27*. n=3 per condition, statistical analysis: t test, * $p<0.05$, ** $p<0.005$, *** $p<0.0005$.

Supplementary Figure 2: Astrocytes are highly responsive to inflammatory stimuli.

ORA dotplot representing the significance of selected up- and down-regulated pathways, based on KEGG database, comparing (**A**) CM-exposed vs. non-exposed astrocytes and (**B**) NA+CM-exposed vs. NA-exposed astrocytes, sorted by *padjust* value and gene counts (see full list in Supplementary File 8-Excel 8).

Supplementary Figure 3: Sets of human astrocytes express proteins that are modulated in diseased hippocampi.

A SPARC (DAB, brown) is expressed by hippocampal astrocytes (case #5). Some ALDH1L1+ astrocytes (green) are also SPARC+ (purple) (case #6). **B-C** SPARC expression is slightly decreased in AD hippocampi and severely altered in PDD patients (AD case #10, PDD case #18). **D** BACE2 (DAB, brown) labels some astrocytes mainly localised in the stratum oriens of healthy hippocampi (case #3). Multiplex staining reveals that BACE2 (purple) is expressed by ALDH1L1+ astrocytes (green) (case #3). **E-F** The expression of BACE2 is significantly increased in the CA4 of PDD patients (AD case #8, PDD case #18). **G** VIM (DAB, brown) is expressed by astrocytes and labels blood vessels in the healthy hippocampus (case #5). A few ALDH1L1+ astrocytes (green) also express VIM (purple) (case #6). **H-I** VIM expression is significantly decreased in the PHC of PDD cases (AD case #10, PDD case #29). Black arrows indicate double-positive astrocytes. n=3 CTL, n=5 AD and n=5 PDD; statistical analysis: Wilcoxon test, * $p<0.05$. Scale bars: low magnification: 500 μm, high magnification 50 μm.

Supplementary Table 1: Primer sequences used for real-time qPCR.

Supplementary Table 2: Case information of the human samples used in this study. Details regarding the 29 samples and their corresponding neuropathological reports were obtained from The Netherlands Brain Bank.

Supplementary Table 3: List of antibodies used in IHC chromogenic (Dako Omnis and Ventana Discovery Ultra).

Supplementary File 1– Supplementary Excel 1*: Statistical analysis from HALO® quantification.

Supplementary File 2– Supplementary Excel 2:** DESeq2 analysis from NA-exposed astrocytes.

Supplementary File 3– Supplementary Excel 3:** ORA analysis from NA-exposed astrocytes.

Supplementary File 4– Supplementary Excel 4:** DESeq2 analysis from DA-exposed astrocytes.

Supplementary File 5– Supplementary Excel 5:** ORA analysis from DA-exposed astrocytes.

Supplementary File 6– Supplementary Excel 6:** Comparison analysis from NA- versus DA-exposed astrocytes.

Supplementary File 7– Supplementary Excel 7:** DESeq2 analysis from CM- and NA+CM-exposed astrocytes.

Supplementary File 8– Supplementary Excel 8:** ORA analysis from CM- and NA+CM-exposed astrocytes.

* see supplementary data in **Part IX, 2. Supplementary data Manuscript II, 2.1 to 2.5**

** see summary of supplementary files (1 to 8) in **Part IX, 2. Supplementary data Manuscript II, 2.6** to **2.7.** The original files can be found through the following link: https://uniluxembourg-my.sharepoint.com/:f:/g/personal/0211640329_uni_lu/IgC2xRz8nc6hSYLVC_IVP1oYAchJdQ20qKHE9ccOT6dY5ls

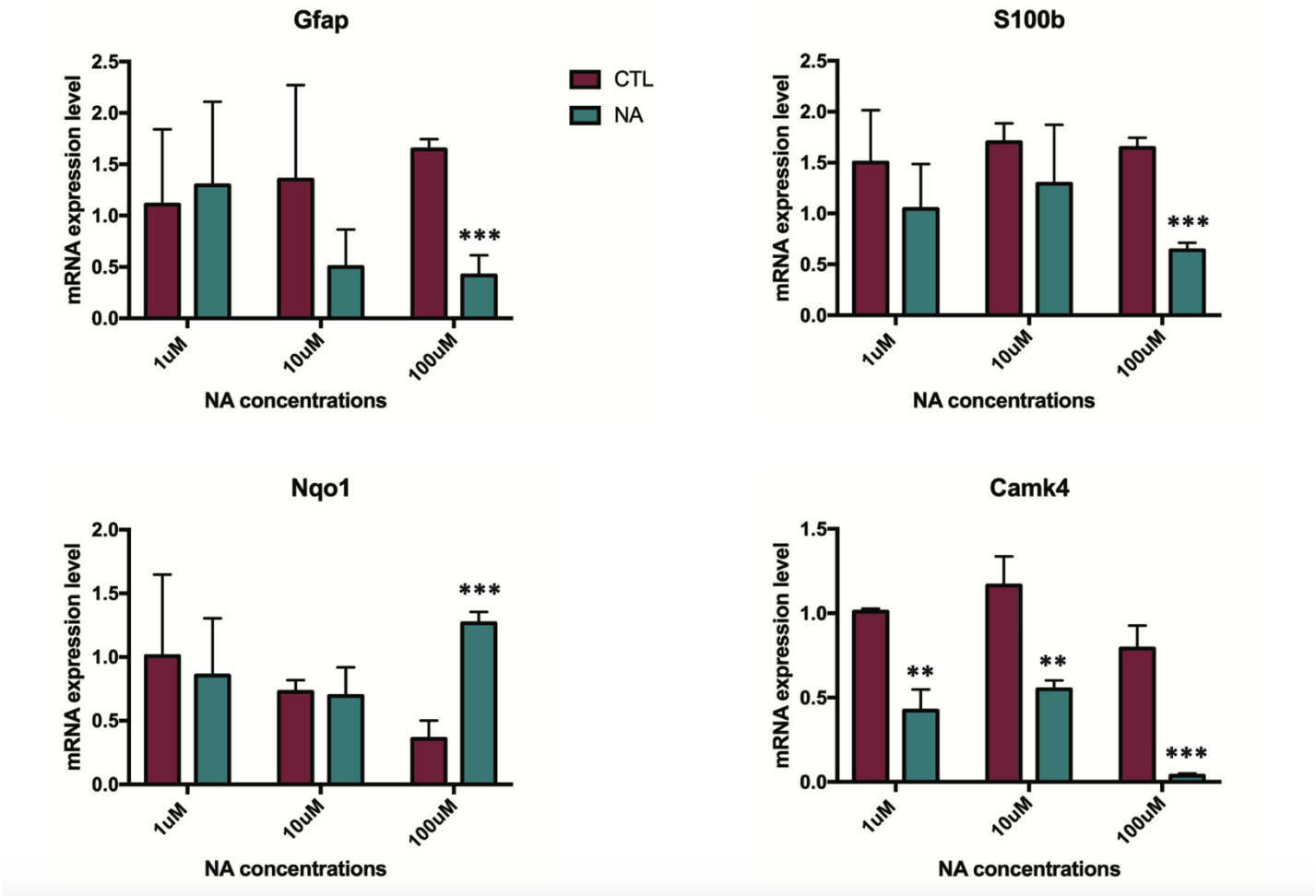

Supplementary Figure 1

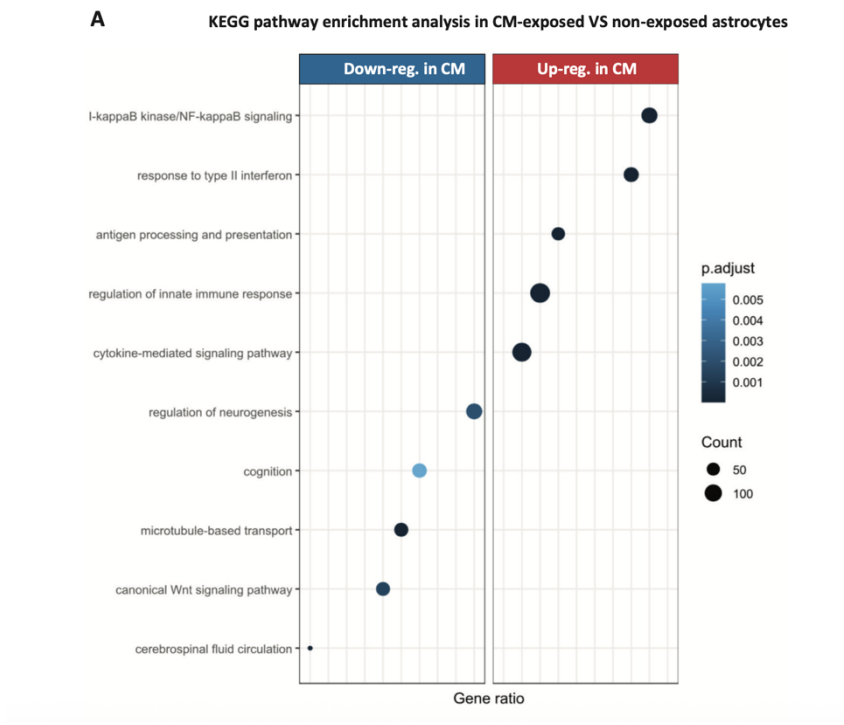

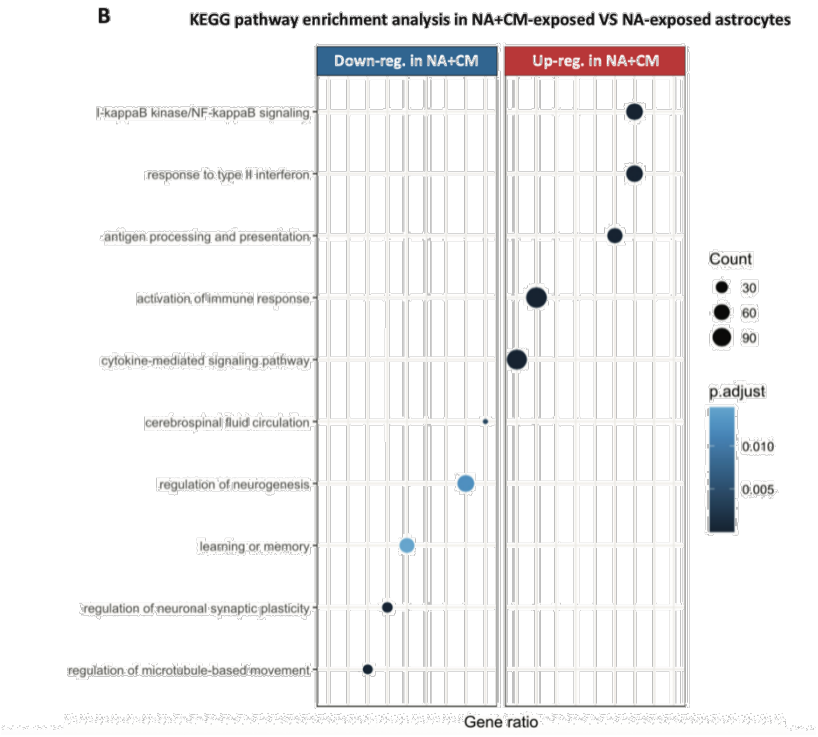

Supplementary Figure 2

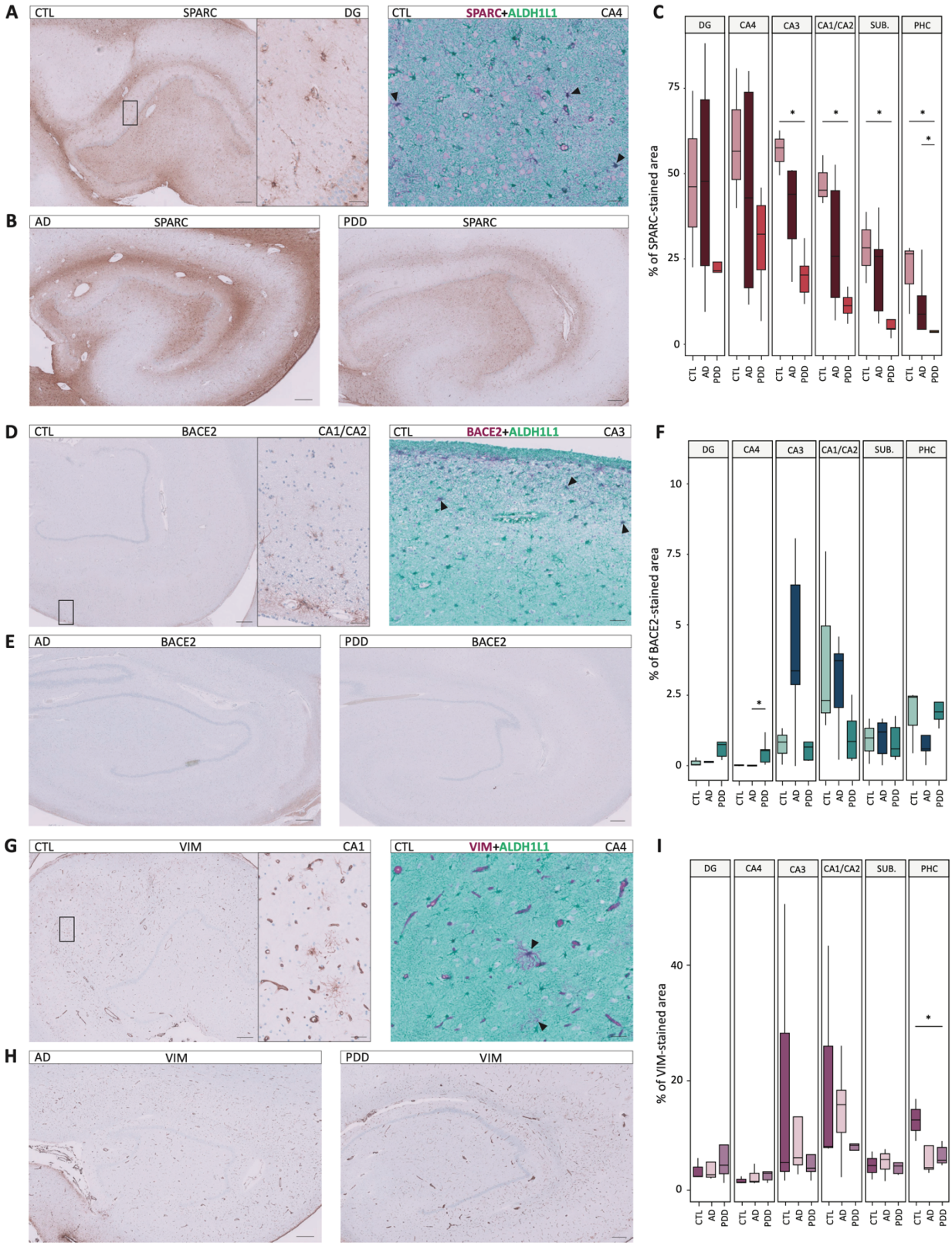

Supplementary Figure 3

Supplementary Table 1

PRIMERS (Accession number)	SEQUENCES	SOURCE
Ace2 primers (NM_ 001130513)	F: 5'-GAC-AAC-TTC-TTG-ACA-GCC-CA-3' R: 5'-CAA-CAG-CTT-CAT-GGA-ACC-CT-3'	Eurogentec
Camk4 primers (NM_ 009793)	F: 5'-ATG-CAA-ACA-GAA-GGG-GAC-C-3' R: 5'-ATG-TTC-GGG-TGT-GAG-AGA-CG-3'	Eurogentec
Cartpt primers (NM_ 013732)	F: 5'-ACA-TCT-ACT-CTG-CCG-TGG-AT-3' R: 5'-GCT-TCG-ATC-TGC-AAC-ATA-GCG-3'	Eurogentec
Cxcl10 primers (NM_ 021274.2)	F: 5'-TGCTGCCGTCATTTTCTGCCTC-3' R: 5'-AGCTTCCCTATGGCCCTCATTCTC-3'	Eurogentec
Igf1 primers (NM_010512)	F: 5'- CTC TGC TTG CTC ACC TTC-3' R: 5'- CAA CAC TCA TCC ACA ATG C-3'	Eurogentec
Rpl27 primers (NM_011289.3)	F: 5'-TGGGCAAGAAGAAGATCGCCAAG-3' R: 5'-TTCAAAGCTGGGTCCCTGAACAC-3'	Eurogentec
Scg2 primers (NM_009129.3)	F: 5'-AGA-TGA-AAC-GTT-CAG-GGC-AG-3' R: 5'-CCC-ACA-GCA-TTC-ACT-AAC-CT-3'	Eurogentec
Sod3 primers (NM_011435.3)	F: 5'-GCC-TTC-TTG-TTC-TAC-GGC-TTG-CTA-C-3' R: 5'-GCG-TGT-CGC-CTA-TCT-TCT-CAA-CC-3'	Eurogentec
Tnfa primers (NM_013693.3)	F: 5'-GCA-CAG-AAA-GCA-TGA-TCC-GCG-AC-3' R: 5'-TGA-GAA-GAG-GCT-GAG-ACA-TAG-GCA-C-3'	Eurogentec

Supplementary Table 2

Pathological Diagnosis	Case	Sex	Age at death (years)	PMD (hh:mm)	ABC / McKeith score/ Braak Lewy Bodies
CTL	1	M	87	04:50	A2B1C0
	2	F	91	09:30	A0B2C0
	3	M	79	06:20	A1B1C0
	4	F	102	03:55	A1B2C0
	5	F	79	06:00	A2B2C2
	6	M	84	05:20	A1B1C0
	7	F	86	06:25	A2B1C1
	8	F	104	07:33	A2B2C1
AD	9	F	53	06:30	A3B3C3
	10	F	70	07:25	A3B3C3
	11	F	86	03:50	A3B3C3
	12	M	38	05:45	A3B3C3
	13	F	92	05:15	A3B3C3
	14	F	98	05:45	A2B2C2
	15	M	64	04:58	A3B3C3
	16	M	74	05:25	A3B3C3
PDD	17	F	75	06:10	A1B1C0/ LB5-6
	18	M	71	04:35	A1B1C0/LB5
	19	M	73	05:35	A1B1C0/LB5
	20	M	67	06:30	A1B1C0/LB6
	21	F	83	06:05	A0B1C0/LB4
	22	M	72	04:00	A1B1C0/LB6
	23	M	61	05:00	A0B1C0/LB5
	24	F	71	09:05	A0B1C0/ LB5
	25	M	85	05:15	A1B2C1/ LB4
	26	F	73	06:10	A1B1C0/ LB4
	27	F	88	06:05	A1B1C0/ LB6
	28	F	66	05:50	A2B0C0/ LB6
	29	F	69	07:05	A1B1C0/ LB6

Supplementary Table 3

ANTIBODIES	SOURCE	IDENTIFIER	DILUTION IHC fluorescent	DILUTION IHC chromogenic	DILUTION Ventana Discovery Ultra
PRIMARY ANTIBODIES					
Rabbit polyclonal anti-ALDH1L1	Atlas Antibodies	Cat# HPA050139, RRID: AB_2681031	-	1:2000	1:2000
Rabbit polyclonal BACE2	Sigma-Aldrich	Cat# HPA035416, RRID: AB_2732467	-	-	1:100
Rabbit polyclonal anti-CBS	Sigma-Aldrich	Cat#HPA001223 , RRID: AB_1846112	-	1:500	1:200
Guinea-pig anti-GFAP	SynapticSystem	Cat#173004, RRID: AB_10641162	1:500	-	-
Rabbit monoclonal anti-GFAP	Ventana Medical Systems	Cat# 760-4345 (also 05269784001), RRID: N/A	-	-	Ready to use*
Rat monoclonal anti-F4/80	BioRad	Cat# MCA497, RRID: AB_2098196	1:300	-	-
Rat monoclonal anti-MBP	Abcam	Cat# ab7349, RRID: AB_305869	1:50	-	-
Rabbit polyclonal SPARC	Sigma-Aldrich	Cat# HPA003020, RRID: AB_1079531	-	-	1:200
Mouse monoclonal Vimentin	Ventana Medical Systems	Cat# 05278139001, RRID: AB_2687607	-	-	Ready to use*
Mouse monoclonal anti-VMAT2	OriGene	Cat# TA500506, RRID: AB_2188120	-	1:500	-

SECONDARY ANTIBODIES				
DISCOVERY OmniMap anti-Rb HRP	Roche	Cat# 760-4311, RRID: AB_2811043	-	Ready to use*
DISCOVERY OmniMap anti-Ms HRP	Roche	Cat# 760-4310, RRID: AB_2885182	-	Ready to use*
DISCOVERY CM DAB kit	Roche	Cat# 760-159, RRID: N/A	-	Ready to use*
DISCOVERY Purple Kit	Roche	Cat# 760-229, RRID: N/A	-	Ready to use*
DISCOVERY Teal HRP kit	Roche	Cat# 760-247, RRID: N/A	-	Ready to use*
Discovery Green HRP kit	Roche	Cat# 08478295001, RRID: N/A	-	Ready to use*
Donkey anti-guinea pig Alexa Fluor 647	Jackson ImmunoResearch Labs	Cat# 706-605-148, RRID: AB_2340476	1:300	-
Donkey anti-rabbit Alexa Fluor 555	Invitrogen	Cat# A-31572, RRID: AB_ 162543	1:500	-
Donkey anti-rat Alexa Fluor 488	Life Technologies	Cat# A21208, RRID: AB_2535794	1:500	-

*Vials ready-to-use purchased from Roche Ventana Medical Systems

4.4. Conclusion

In conclusion, our findings demonstrate that catecholamines, and NA in particular, are potent modulators of astrocyte molecular identity and responses. Under homeostatic conditions, NA and DA regulate overlapping yet distinct astrocytic transcriptional signatures involved in vascular regulation, synaptic support, oxidative stress responses, and immune surveillance, highlighting complementary roles in maintaining brain homeostasis. NA further attenuates astrocyte inflammatory responses and exerts non–cell-autonomous immunomodulatory effects on microglia, indicating a broader role in regulating neuroinflammation. Importantly, analysis of human *post-mortem* samples revealed that disruption of NA signalling in AD and PDD is associated with reduced expression of key astrocytic proteins, including CBS and SPARC, implicating impaired antioxidant response, metabolic regulation, vascular support, and blood–brain barrier integrity. Taken together, our results highlight the profound transcriptomic changes induced by NA in astrocytes, under both homeostatic and inflammatory states. Our findings suggest that progressive depletion of NA may affect the expression of key astrocytic proteins, disrupting some core astrocyte functions and contributing to increased oxidative stress, decreased neuroprotection, and metabolism deregulation, among other detrimental effects.

5. CHAPTER III – The multifaceted neurotoxicity of the astrocytes in ageing and age-related neurodegenerative diseases: a translational perspective.

5.1. Introduction

In the broader context of NDD research, the intricate role of glial cells, particularly astrocytes, has emerged as a key area of focus for understanding the pathophysiological mechanisms underlying the onset and/or progression of neurodegeneration. In this review, we aimed at providing comprehensive and critical synthesis of current insights into astrocyte-mediated neurotoxicity across experimental models and human pathology. We reviewed the diverse and context-dependent neurotoxic roles of astrocytes in ageing and age-related NDDs, including AD and PD as well as primary tauopathies (e.g. progressive supranuclear palsy, globular glial tauopathy, corticobasal degeneration), synucleinopathies (e.g. PDD, DLB, multiple system atrophy), and TDP-43 associated proteinopathies (e.g. fronto-temporal dementia, amyotrophic lateral sclerosis). We described how reactive astrocytes can lose supportive functions and adopt neurotoxic roles, often driven by inflammatory cytokines from microglia or by exposure to disease-specific protein aggregates such as Aβ, tau, α-synuclein, or TDP-43. We discussed about diverse molecular "neurotoxic" signatures that astrocyte can adopt (e.g., A1 astrocytes, disease-associated astrocytes, and UPR-reactive astrocytes), with emphasis on their heterogeneity and limited consensus across models. We reported on the various factors that could influence the transformation of neuroprotective astrocytes into neurotoxic cells (e.g., ageing, neuroinflammation, oxidative stress, neurotransmitter depletion). Finally, bringing cellular and molecular observations from *in vitro* systems, rodent models and human studies, we highlighted both the similarities and significant differences between human and rodent astrocytes.

5.2. Personal contributions

Below are listed my personal contributions to this publication:

- Conducting literature research and selecting relevant references concerning the effects of the alteration of the noradrenergic and dopaminergic systems on astrocytes;
- Writing of the part entitled “Depletion of Noradrenaline and Dopamine, Vectors for Neurotoxic Astrocytes”;
- Editing and reviewing of the final manuscript;
- Details of each author’s individual contributions are provided in the author contribution section at the end of the manuscript.

frontiers in Physiology

REVIEW
published: 17 March 2022
doi: 10.3389/fphys.2022.814889

The Multifaceted Neurotoxicity of Astrocytes in Ageing and Age-Related Neurodegenerative Diseases: A Translational Perspective

David S. Bouvier[1,2,3], Sonja Fixemer[2,3], Tony Heurtaux[3,4], Félicia Jeannelle[1,3], Katrin B. M. Frauenknecht[1,3,5] and Michel Mittelbronn[1,2,3,6,7,8]**

[1]National Center of Pathology (NCP), Laboratoire National de Santé (LNS), Dudelange, Luxembourg, [2]Luxembourg Center of Systems Biomedicine (LCSB), University of Luxembourg (UL), Belvaux, Luxembourg, [3]Luxembourg Center of Neuropathology (LCNP), Dudelange, Luxembourg, [4]Systems Biology Group, Department of Life Sciences and Medicine (DLSM), University of Luxembourg, Belvaux, Luxembourg, [5]Institute of Neuropathology, Medical Center of the Johannes Gutenberg University Mainz, Mainz, Germany, [6]Department of Cancer Research (DOCR), Luxembourg Institute of Health (LIH), Luxembourg, Luxembourg, [7]Faculty of Science, Technology, and Medicine (FSTM), University of Luxembourg, Esch-sur-Alzette, Luxembourg, [8]Department of Life Sciences and Medicine (DLSM), University of Luxembourg, Esch-sur-Alzette, Luxembourg

In a healthy physiological context, astrocytes are multitasking cells contributing to central nervous system (CNS) homeostasis, defense, and immunity. In cell culture or rodent models of age-related neurodegenerative diseases (NDDs), such as Alzheimer's disease (AD) and Parkinson's disease (PD), numerous studies have shown that astrocytes can adopt neurotoxic phenotypes that could enhance disease progression. Chronic inflammatory responses, oxidative stress, unbalanced phagocytosis, or alteration of their core physiological roles are the main manifestations of their detrimental states. However, if astrocytes are directly involved in brain deterioration by exerting neurotoxic functions in patients with NDDs is still controversial. The large spectrum of NDDs, with often overlapping pathologies, and the technical challenges associated with the study of human brain samples complexify the analysis of astrocyte involvement in specific neurodegenerative cascades. With this review, we aim to provide a translational overview about the multi-facets of astrocyte neurotoxicity ranging from *in vitro* findings over mouse and human cell-based studies to rodent NDDs research and finally evidence from patient-related research. We also discuss the role of ageing in astrocytes encompassing changes in physiology and response to pathologic stimuli and how this may prime detrimental responses in NDDs. To conclude, we discuss how potentially therapeutic strategies could be adopted to alleviate or reverse astrocytic toxicity and their potential to impact neurodegeneration and dementia progression in patients.

Keywords: astrocyte, neurotoxicity, reactive astrogliosis, heterogeneity, neurodegeneration, ageing

OPEN ACCESS

Edited by:
Lin-Hua Jiang,
University of Leeds, United Kingdom

Reviewed by:
Eberhard Weihe,
University of Marburg, Germany
Yaling Yin,
Xinxiang Medical University, China
Maria Giuliana Vannucchi,
University of Florence, Italy
Paul Roy Heath,
The University of Sheffield, United Kingdom

****Correspondence:***
David S. Bouvier
david.bouvier@lns.etat.lu
Michel Mittelbronn
michel.mittelbronn@lns.etat.lu

Specialty section:
This article was submitted to Integrative Physiology, a section of the journal Frontiers in Physiology

Received: *14 November 2021*
Accepted: *23 February 2022*
Published: *17 March 2022*

Citation:
Bouvier DS, Fixemer S, Heurtaux T, Jeannelle F, Frauenknecht KBM, and Mittelbronn M (2022) The Multifaceted Neurotoxicity of Astrocytes in Ageing and Age-Related Neurodegenerative Diseases: A Translational Perspective. Front. Physiol. 13:814889. doi: 10.3389/fphys.2022.814889

INTRODUCTION

Designed to Protect, Maintain, Support, and Regulate Brain Function

The paradigm on glial cells has considerably shifted over the last 20 years. Glial cells are now recognized to be at the center of many primordial processes for brain homeostasis maintenance but also involved in protective as well as, paradoxically, detrimental responses. Astrocytes represent the most abundant glial cell type of the CNS. They form a heterogeneous group of cells, comprising distinct subtypes characterized by a specific morphology, physiology, or spatial distribution (Pestana et al., 2020). The general classification distinguishes mainly white matter fibrous astrocytes from grey matter protoplasmic astrocytes. However, numerous specialized subtypes have been described in distinct brain areas such as the Bergman glia in the cerebellum (De Zeeuw and Hoogland, 2015), the Müller glia in the retina, or the interlaminar astrocytes in the neo-cortex (Colombo, 2018) or in specific localization such as the perivascular astrocytes or the subpial astrocytes. The morphology, density, overlap, and diversity of astrocytes can vary depending on brain areas and species (Oberheim et al., 2009; Batiuk et al., 2020; Muñoz et al., 2021). The classic description of the astrocyte, representing mainly protoplasmic ones, is the following:

- A complex morphology made by long processes and protrusions (Bushong et al., 2004), sculpted around a "star-shaped" cytoskeleton frequently highlighted by the staining of the intermediate filament, the glial fibrillar acidic protein (GFAP).
- An exclusive parenchyma territory with peripheral overlapping cellular contacts to neighboring astrocytes by gap-junctions such as connexins 30 and 43 (Bushong et al., 2002; Huang et al., 2021).
- Specialized compartments, the endfeet, which enwrap blood vessels and take-up nutrients from the circulation.
- Microcompartments enveloping pre- and post-synapses, forming together a tripartite synapse, with an estimation of 10^5–10^6 synapses contacted/enwrapped per astrocyte (Volterra et al., 2014; Allen and Eroglu, 2017).

Many of these features considerably differ between the astrocyte subtypes. The interlaminar astrocytes, located in the first layer of some of the neocortical areas, project long processes with varicosities in deeper layers. Twin astrocytes are joined by their soma, and perivascular astrocytes have their cell bodies sitting on blood vessels (Verkhratsky and Nedergaard, 2018). Still, astrocytes are multitasking cells being responsible for the metabolic support of neurons by taking up glucose by their privileged connection to the blood flow, delivering it to the surrounding cells and storing glycogen in the CNS. They also serve as extracellular milieu buffering cells (K^+, Cl^-, Ca^{2+}, and water). Many reviews have extensively discussed the key roles of astrocytes in brain metabolism (Deitmer et al., 2019; Rose et al., 2020). At the synapse, astrocytes act as sensors and modulators of synaptic activity. They express the glutamate transporters EAAT1 (GLAST) and EAAT2 (GLT1) enriched in perisynaptic processes. It allows them to pump the excess of neurotransmitters at the synaptic cleft and recycle them. However, astrocytes can also directly release neurotransmitters, such as glutamate, D-serine, and/or ATP and modulate synaptic activity (Araque et al., 2014; Volterra et al., 2014). The neuron-astrocyte communication is bilateral and fundamental for brain function. Astrocytes are intimately associated with the establishment and maintenance of neuronal circuits. During development, they remodel the extracellular matrix by secreting some matricellular proteins, such as secreted protein acidic and rich in cysteine (SPARC), Tenascin C, or/and Thrombospondins (Jones and Bouvier, 2014). Astrocytes also eliminate unnecessary excitatory synapses through MEGF10 and MERKT phagocytosis receptors (Chung et al., 2013). Their multiple functions at the cellular level are commonly accepted, however, there are still pending questions about their role as a collective entity in higher brain functions. Indeed, they form a widespread and dynamic network of non-excitable cells, communicate *via* calcium transient waves, and provide an active cell layer for information and modulation of CNS homeostasis (Guerra-Gomes et al., 2018).

Being Reactive Is Not Being Toxic?

Astrocytes are also directly involved in CNS protection from pathogens and pathologies. They are highly adaptive to their micro-environment, and in adverse conditions, they can change their molecular program and morphology to counteract insults and protect surrounding tissue. This phenomenon is called reactive astrogliosis (see consensus statement in Escartin et al., 2021). Reactive astrocytes are commonly observed in virtually all brain disorders. The shift of morphology toward large and dysmorphic processes, and the increase of the expression of proteins forming the intermediate filaments, GFAP and vimentin, are often considered as the main characteristics to characterize reactive astrogliosis. But the reactivity of astrocytes is neither an "all or none" nor a unidirectional mechanism. It is now described as a gradient of severity from mild to severe with a contextual time course (Sofroniew and Vinters, 2010). Their reactivity is also heterogeneous, conditioned by their intrinsic nature (species, localization, age, gender, genetics background, and epigenetics), their macro-environment (stage of a disease, brain region vulnerability) and the immediate pathological micro-environment. By becoming reactive, an astrocyte can gain or lose some functions, alter its physiology in the short- or long-term, modify its interplay with surrounding cells, or even engage detrimental responses. Reactive astrocytes can produce growth factors and neurotrophins, thereby promoting neuronal survival and synaptic function (Sofroniew and Vinters, 2010; Escartin et al., 2021). They can mimic immune responses and secrete a large variety of anti- and pro-inflammatory molecules, such as interferon gamma (IFN-γ), tumor necrosis factor alpha (TNF-α), interleukin (IL)-6 and IL-1β or act as antigen-presenting cells. Although many of those inflammation-related factors are mainly expressed by cells of the myeloid lineage, we here focused on the potential capacity of astrocytes to also secrete those molecules under pathological conditions.

Depending on the context, they work in synergy or interfere with microglia or with infiltrating immune cells. However, in numerous models, they can also alter the surrounding cells by secreting toxic factors and drive the progression of neurodegeneration. The questions about where and when astrocytes lose their protective functions and become toxic for surrounding cells are fundamental to solve the complex puzzle of brain disorders and age-related neurodegenerative diseases (NDDs), such as Alzheimer's disease (AD), Parkinson's disease (PD), Lewy body dementias (LBDs), primary tauopathies, primary synucleinopathies, fronto-temporal dementia (FTD), and amyotrophic lateral sclerosis (ALS).

This review is composed of two main parts. The first chapter is about how, when and why astrocytes turn neurotoxic: from the attempts to define a prototypical neurotoxic molecular signature across various disease models, to the characterization of stressors associated with NDDs that have been shown to induce astrocyte neurotoxicity and subsequent damages or death of neurons in culture and rodent models. We then compile reports about the identification of neurotoxic astrocytic markers in autopsy brain samples from NDDs patients. In the second chapter, we discuss the impact of ageing on astrocytes, on their senescence and epigenetics and if the ageing process could prime them to execute maladaptive/toxic responses in NDDs. Finally, we discuss the challenges targeting reactive/neurotoxic/aged/senescent astrocytes to alleviate NDDs progression.

BREAKING BAD: WHEN DO ASTROCYTES BECOME TOXIC TO SURROUNDING CELLS IN NDDs?

The Neurotoxic Astrocyte Signatures: Identity and Context of Harmful Astrocytes

Because astrocytes are at the core of brain homeostasis and function, their turnover into neurotoxic cells could trigger or exacerbate NDDs. Thus, it is essential to precisely characterize their changes in NDDs. Astrocytes are often found to be atrophic or dysmorphic in AD and associated dementias (see the chapter "Pieces of Evidence of Astrocyte Neurotoxicity in NDD Patient Samples"). However, to ponder on the dual faces of astrocytes, it is important to distinguish between reactivity and toxicity, between chronic changes and acute responses. The reactivity state engages various molecular and morphological changes (Viejo et al., 2021), and is a direct consequence of alterations of their macro- and/or microenvironment (Sofroniew and Vinters, 2010; Haim et al., 2015; Escartin et al., 2021). Chun et al. (2020) designed a new mouse model to modulate stages of astrocyte reactivity, from mild to severe, by crossing inducible diphtheria toxin receptor (iDTR) mice with GFAP-CreERT2 mice (GiD). The severity of the reactivity in GiD mice has been scaled by the level of GFAP expression, the dystrophy and branching of processes, by some proliferation and astrocytic production of monoamine oxidase B (MAO-B), GABA, and inducible nitric oxide synthase (iNOS). The activation of severe reactive profiles led to pronounced atrophy, particularly in the CA1 subregion of the hippocampus, but also in the cortex, striatum, and amygdala, and an increase in cleaved caspase-3 expression as well as tauopathy in neurons. Behavioral tests on severe GiD mice also showed memory impairments. Thus, severe astrocyte reactivity is neurotoxic and can trigger, if induced systematically, some NDDs features and symptoms. The authors also observed a gradient of severity across the brain.

Using single-cell RNA sequencing (scRNAseq) and spatial transcriptomics, Hasel and colleagues characterized ten astrocytic clusters with specific molecular signatures across the mouse brain in responses to systemic lipopolysaccharide (LPS) treatment (Hasel et al., 2021). Among these clusters, that also changed over time post-injection, none of them was characterized as fully neurotoxic. Inflammatory genes increased in some clusters and were found along with potentially neuroprotective genes in others, highlighting the complexity of astrocyte responses. Numerous studies have attempted to define a prototypical molecular signature for neurotoxic astrocytes. *In vitro*, with isolated astrocytes from young adult (P30-P35) transgenic Aldh1l1-eGFP mice, Zamanian et al. (2012) observed various astrocytic reactive responses dependent on the type of perturbation. The authors described that reactive astrocytes isolated from the cortex, corpus callosum, hippocampus, and striatum of mice with ischemic stroke showed a particular "protective" profile with induced neurotrophic cytokines LIF and CLCF1, IL-6, and some other genes related to metabolic activity, cell-cycle genes, and transcription factors. On the other hand, the reactive astrocytes isolated from the cortex and corpus callosum from mice that underwent systemic LPS treatment presented what was described as a "detrimental" profile with an increased expression of genes related to the induced antigen presentation pathway, complement pathway, interferon response, class I major histocompatibility complex (MHC) molecules (H2-D1, H2-K1, and H2-T10), and complement cascade (initiating: C1r, C1s, C3, and C4B; inhibiting: Serping 1). Both types of astrocytes share a set of upregulated genes, including proteins involved in extracellular matrix modification and cytokine signaling. Liddelow and colleagues gave a more detailed description of the reactive signatures obtained in these models (Liddelow et al., 2017). They defined two signature groups of reactive astrocytes. The neurotoxic one is now named A1, the neuroprotective A2, both sharing a pan-reactive astrocyte set of increased genes. In their co-culture model, A1 astrocytes decreased synaptogenesis and even induced neuronal death at high concentrations. Furthermore, the authors demonstrated that the A1 neurotoxic signature was dependent on the microglia-released pro-inflammatory cytokines (see the section "Interplay Between Astrocytes and Immune Cells: the Control of Neurotoxicity?"). The authors choose C3 as a marker for A1 astrocytes and identified C3-positive astrocytes in human post-mortem brain tissue from AD, PD, ALS, multiple sclerosis (MS), and Huntington disease (HD). Since then, many studies using NDDs models have reported at least a partial A1 neurotoxic signature in their results (see the section "Maladaptive Responses to Stressors in Cell Culture and Transgenic Rodents Modeling NDDs"), but there is no consensus that this signature is generally

found in NDDs. Other reports have added some insights in distinct astrocytic neurotoxic molecular signatures in NDDs.

Smith et al. (2020) have investigated the role of the unfolded protein response (UPR), a pathway dysregulated in NDDs, in the response of astrocytes. Using the endoplasmic reticulum (ER) stressors thapsigargin or tunicamycin, they have chronically activated the UPR through protein kinase R-like ER kinase (PERK) pathways in cortical primary astrocytes (Smith et al., 2020). The authors observed an upregulation of the pan-reactive markers Cxcl10, Lipocalin 2 (Lcn2), and Vimentin (Vim) upon thapsigargin treatment. C3 was the only gene increased of the A1 signature, but Ggta1 and Serping1 were significantly reduced. The A2 markers Cd109, Emp1 were also significantly decreased. Blocking PERK activation through a knockdown let to deceased expression of C3, Cxcl10, Lcn2, and Vim. The authors reproduced these data in a prion-diseased mouse and demonstrated *in vitro* that the UPR-reactive astrocytes presented an altered secretome, were unable to support synapses and harmful to neurons.

Wheeler et al. (2020) performed scRNAseq on brain and spinal cord from experimental autoimmune encephalomyelitis (EAE) mice and fresh autopsy brain samples from MS patients. In EAE mice, the largest subgroup of astrocytes was enriched for UPR, showing high level of NF-κB and iNOS pathways activation, as well as granulocyte-macrophage colony-stimulating factor (GM-CSF) signaling. In the same cluster, the authors also identified transcriptional regulators including Kdm5a, Hif1a, Fos, and Jun and to a lower extent Nfe2l2. Nfe2l2 encodes the transcription factor NRF2 (nuclear factor erythroid 2-related factor 2), a limiter for oxidative stress and inflammation. The authors further confirmed with *in vitro* experiments that NRF2 is a negative regulator of pro-inflammatory and neurotoxic pathways. Some markers of the A1 signature were found throughout the different clusters isolated (Cluster 0: H2-T23, cluster 1: H2-D1, Psmb8, cluster 2: Srgn, and cluster 4: C3ar1). To identify astrocyte regulators, the authors have isolated astrocytes from Ribotag^{Gfap} mice during EAE. They have observed increased levels of the small MAF protein musculoaponeurotic fibrosarcoma homolog G (MAFG), concomitant with a decreased expression of NRF2. After analysis of their scRNAseq data from fresh autopsy MS brain tissue and previous published MS data (Lake et al., 2018; Jäkel et al., 2019; Schirmer et al., 2019), they have recovered an astrocyte population with the same molecular signature. At the tissue level, the authors observed MAFG-positive astrocytes in active lesions of white matter from MS patients. They have concluded that MAFG-positive astrocytes are harmful and promote CNS inflammation in EAE and MS.

Habib et al. (2020) performed single-nucleus RNAseq (snRNAseq) analysis on hippocampi from 5xFAD mice. Compared to WT, the AD mice displayed an enriched astrocytic cluster expressing high levels of Gfap, Serpina3n, Ctsb, Apoe, and Clu17, which they termed disease-associated astrocytes (DAAs). The authors found an overlap of some A1 genes in the DAAs. A2 signature was not seen. Interestingly, an increase of A1/DAAs astrocytes was associated with ageing in WT mice. The authors were also able to retrace DAA-like cells in another snRNAseq database from the post-mortem human AD prefrontal cortex (Mathys et al., 2019). Zhou et al. (2020b) also performed snRNAseq on 5xFAD mice and dorsolateral pre-frontal cortex from AD patients with R62H variant of TREM2. In 5XFAD mice, astrocytes displayed an upregulation of Gfap and C4b. Interestingly they observed an upregulation of Serpina3n, previously linked to DAAs, mainly in oligodendrocytes. They also detected little colocalization of Serpina3n with astrocytes and amyloid-β plaques. In human AD samples, they observed a downregulation of a cluster that was highly enriched in genes controlling free-fatty acid transport (FABP5), storage in lipid droplets (HILPDA), as well as oxidation and detoxification of the resulting reactive oxygen species (ROS; SOD2). On the other hand, AD astrocytes presented an increase in the expression of genes encoding the proteoglycan NCAN and collagen COL5A3. The authors speculated that these extracellular matrix molecules may contribute to glial scarring and could prevent axonal regeneration. The authors could not identify A1 signatures.

The neurotoxic astrocytic signatures collected across models share few markers, but all play a role in the disease progression in their respective models. Some of these signatures were at least partially found in the brain tissue of patients (see the section "Pieces of Evidence of Astrocyte Neurotoxicity in NDD Patient Samples" for additional insights). However, these studies accentuate the idea of subgroups of astrocytes that become harmful, with a specific distribution or linked to a condition (resumed in **Figure 1**). In the following chapters, we will navigate between *in vitro* and mouse models to identify stressors that could alter astrocyte responses toward a detrimental role and thus recapitulate if astrocyte neurotoxicity has been detected and measured in brains from NDDs patients.

Maladaptive Responses to Stressors in Cell Culture and Transgenic Rodents Modeling NDDs

In age-related NDDs, astrocytes, among other brain cells, are exposed to a variety of stressors. AD, PD, LBD, primary tauopathies, primary synucleinopathies, FTD, and ALS are often grouped under the umbrella appellation "proteinopathies" because they are characterized by abnormal accumulations of peptides or proteins in the extracellular milieu or inside brain cells. These accumulations are often thought to be the cause of NDDs and responsible for a complex chain of degenerative events. Proteinopathies are defined by one type or overlap of pathological misfolded protein inclusions (Golde et al., 2013). Overproduction and release in the extracellular space of the amyloid-β (Aβ) peptide 1–42 results in the formation of senile plaques in the parenchyma. The hyperphosphorylated form of tau, a microtubule-associated protein, is prone to cluster into paired helical filaments (PHF) and neurofibrillary tangles (NFTs), which are most often found inside neurons. Intracellular inclusions of phosphorylated α-synuclein (α-Syn) form Lewy neurites and Lewy bodies (LBs) in the soma of neurons. The accumulation of TAR DNA-binding protein 43 (TDP-43), a protein involved in DNA transcription and RNA modulation, is found in numerous cell types but primarily in neurons. The concomitance of these misfolded protein accumulations is common across NDDs. However, Aβ and tau pathologies *in*

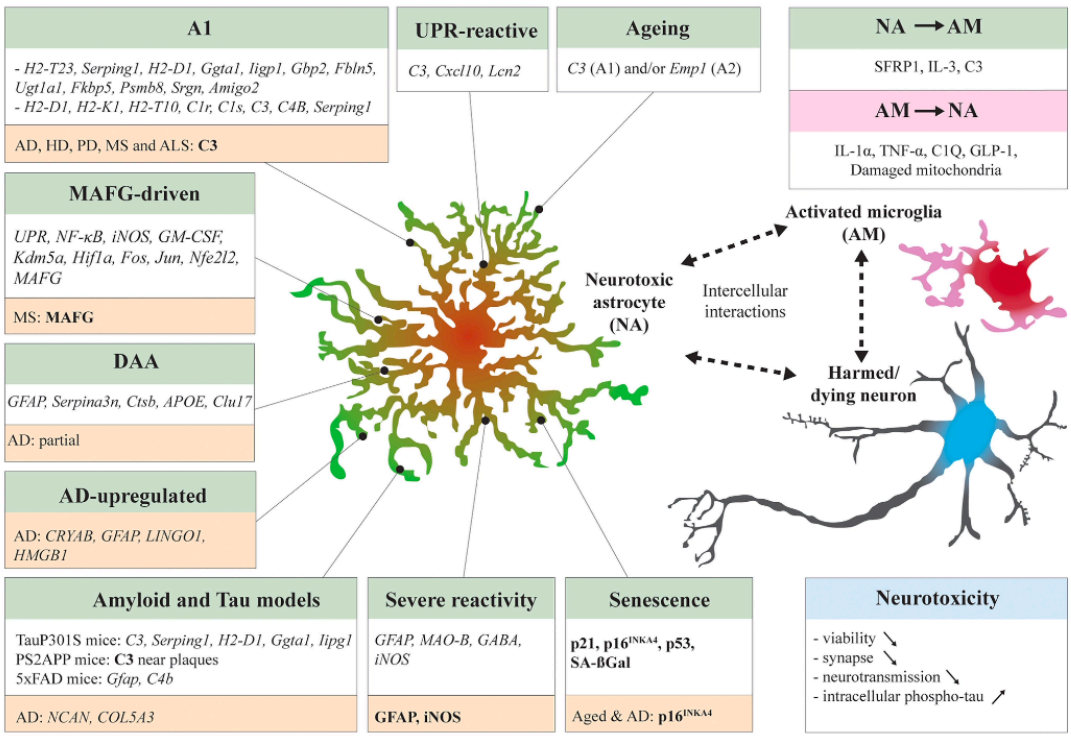

FIGURE 1 | Neurotoxic astrocytic signatures and interaction with neighboring cells. Many studies have identified neurotoxic astrocytic molecular signatures (italic) and markers (bold) across specific experimental conditions: A1 in systemic LPS treated mice (Zamanian et al., 2012; Liddelow et al., 2017), unfolded protein response (UPR)-reactive astrocytes in UPR-activated mice and prion-diseased mice (Smith et al., 2020), musculoaponeurotic fibrosarcoma homolog G (MAFG)-driven astrocytes in experimental autoimmune encephalomyelitis (EAE) mice (Wheeler et al., 2020), Disease associated astrocytes (DAAs) in 5xFAD mice (Habib et al., 2020), Alzheimer's disease (AD)-upregulated astrocytes in AD patients (Lau et al., 2020), Aged mouse astrocytes (Clarke et al., 2018), senescent mouse astrocytes (Bussian et al., 2018; Gaikwad et al., 2021), and severe reactive mouse astrocytes (Chun et al., 2020). Other studies have compared neurotoxic astrocyte signatures in distinct disease mouse models such as TauP301S mice and PS2APP mice (Wu et al., 2019) and 5xFAD mice (Zhou et al., 2020b). Some signatures overlapped between models. In NDDs patient samples, neurotoxic astrocyte markers have been identified by transcriptomics or IHC (highlighted in orange). The neurotoxic astrocytes are in close bilateral communication with surrounding cells. Activated microglia can induce astrocytes to adapt a neurotoxic profile (Liddelow et al., 2017; Joshi et al., 2019; Park et al., 2021), vice versa neurotoxic astrocytes secrete microglia-activating factors (McAlpine et al., 2021; Rueda-Carrasco et al., 2021). Finally, the induced neurotoxicity can decrease neuron viability, exacerbate synaptic loss, neurotransmission impairment, and tau pathology. Reciprocally, harmed or dying neurons can stimulate activation of microglia and reactivity of astrocytes (not detailed here).

vitro and mouse models are usually considered to recapitulate AD, alpha-synuclein pathology, PD and TDP-43, and ALS.

The effect of the monomers, oligomers, or filaments of these proteins/peptides can be mimicked *in vitro*, and the parenchymal protein inclusions found in patients *in vivo* with transgenic mouse models expressing mutated forms of human genes. Astrocytes responses to such exposures have been well documented. Astrocytes have been involved in clearance, spreading, and propagation of Aβ, tau, and α-Syn pathologies (Batarseh et al., 2016; De Strooper and Karran, 2016; Frost and Li, 2017; Sorrentino et al., 2019). This literature is quite extended; therefore, we emphasize studies that found a direct association between pathological protein exposure and astrocytic neurotoxicity. We further highlight the "context" of the experimental procedures *in vitro*, characteristics of the model, age, brain regions, and nature of the transgene. All these aspects must be carefully examined before extrapolating it to the human situation, even more, when contradictive results have been published across these models.

Amyloid Pathology

Amyloid-ß pathology is central to AD progression. Many reports have shown a direct effect of Aβ exposure on the phenotype of astrocytes toward neurotoxic profiles in culture. Exposure to aggregated Aβ-42 peptides or oligomers induced, in a dose-dependent manner, the production of reactive oxygen species (ROS) and iNOS by cortical rat astrocytes through the activation of NF-κB pathways (Akama et al., 1998) and by human primary

astrocytes (Singh et al., 2020). It was shown that even picomolar concentrations of Aβ-40 and Aβ-42 oligomers destabilized calcium activity in rat hippocampal astrocytes in co-culture with neurons, increase their ROS production and caspase-3 activation in both astrocytes and neurons (Narayan et al., 2014). *In vitro*, astrocytes seem to mediate Aβ-induced toxicity on neurons. Indeed, Garwood et al. (2011) have shown that the viability of cortical neurons was not perturbed by oligomeric Aβ at their working concentration but was impacted by altered astrocytes in mixed cultures. In this model, Aβ-exposed astrocytes increased cleaved-caspase 3 induction, tau truncation, and phosphorylation in neurons. This deleterious effect was rescued by minocycline, which dampens the secretion of inflammatory factors, such as IL-6, IL-1β, and IFN-γ of Aβ-exposed astrocytes. Numerous markers of astrocytic toxicity have also been found in transgenic rodent modeling the amyloid pathology, where the intensity of astrocytic reactivity usually correlates with pathology (Spanos and Liddelow, 2020). Amyloid transgenic rodents express a mutated form of the human amyloid precursor protein (APP) or/and presenilin, thus mimicking the early onset familial form of AD, and the formation of Aβ plaques in the parenchyma. These models recapitulate numerous features of AD such as synaptic loss or cognitive defect but no to only poor neuronal loss. Thus, the active role of neurotoxic astrocytes in the atrophy processes cannot be considered in this context. However, the astrocytes surrounding the plaques, that form the reactive glial net (RGN) together with microglia, have been particularly studied (Bouvier et al., 2016; Walker, 2020). RGN astrocytes can express inflammatory factors, such as IL-6 or IL-1β in CRND8Tg (Bouvier et al., 2016), iNOS in APP (V717I; Heneka et al., 2005), and C3 in 3xTg, Tg2576, and PS2APP mice (Fonseca et al., 2011; Wu et al., 2019) and TgF344-AD rats (Balu et al., 2019).

Interestingly, the control or ablation of astrocyte reactivity in amyloid models had different outcomes depending on the experimental strategy and the model used. Kraft et al. (2013) designed an APP/PS1 $Gfap^{-/-}Vim^{-/-}$ model to dampen astrocyte hypertrophy and reactivity in amyloidosis conditions. It resulted in a large increase in plaque load, of the number of microglia associated with plaques and of the neurites dystrophia at 8 and 12 months of age, arguing for a beneficial impact of astrocyte reactivity in AD. The inducible ablation of proliferative reactive astrocytes in APP/GFAP-TK mice, treated with ganciclovir at 9 months of age, significantly increased the levels of monomeric Aβ-42 and exacerbated synaptic loss, neuroinflammation, and memory deficits (Katsouri et al., 2020). The selective pharmacological ablation of astrocytes with the toxin L-alpha-aminoadipate in organotypic brain culture slices (OBCSs) from 7 days old 5xFAD animals, grown over 2 weeks, led to an increase of Aβ levels in medium, of IL-6 production, and decrease in spine size (Davis et al., 2020). All these results favor a protective role of reactive astrocytes in disease progression, however, other studies have reported opposite conclusions. Furman and collaborators used a different methodological approach that consists of injecting a viral construct into APP/PS1 mice hippocampi to selectively express a synthetic peptide named VIVIT in astrocytes, which will inhibit their inflammatory response (Furman et al., 2012). The authors found that treated 7–8-month-old mice had significantly lower soluble and insoluble amyloid levels, reduced microglia activation, and improved cognitive performance at 16–17 months of age, compared to the non-treated transgenic mice. Other studies highlighted the pathological and detrimental roles of astrocytes in amyloid models of AD. Two different strategies to inhibit the Janus kinases (JAK)/signal transducer and activator of transcription 3 (STAT3) pathway, which is deeply involved in the induction of the reactivity of astrocytes, led to similar conclusions. Ceyzériat et al. (2018) used viral construction to overexpress an inhibitor of JAK, the suppressor of cytokine signaling 3 (SOCS3) in the CA1 hippocampal astrocytes of 3–4-month-old APP/PS1dE9 mice. Six months after injection, they reported a downregulation of the pro-inflammatory responses in transfected astrocytes, a reduction of plaque loads, and improved spatial learning compared to non-transfected transgenic. After SOCS3 transfection in astrocytes of 3xTg, the authors described a complete restoration of long-term potentiation (LTP) deficits. Reichenbach et al. (2019) have further investigated the impact of astrocytic Stat3 induced pathway in an inducible Stat3 deficient APP/PS1 mouse model. When the Stat3 knock-out in astrocytes was initiated at 6 weeks of age, effects were beneficial showing a decrease of amyloid loads, neuronal dystrophy, cytokines levels, and rescue of memory decline at 8–10 months of age. The A1 transcripts Amigo2 and C3 were significantly decreased compared to age-matched APP/PS1.

In conclusion, in most models *in vitro* and *in vivo*, astrocytes engage neurotoxic responses that could exacerbate disease progression. However, there is no consensus and neither a prototypical neurotoxic signature.

Tau Pathology

The tau pathology is often described in neurons, which are mainly bearing PHF and NFT in the AD patient brain. However, tau positive astrocytes are also found in primary tauopathies and less often in AD (see the section "Pieces of Evidence of Astrocyte Neurotoxicity in NDD Patient Samples"). The relationship between tau and the neurotoxicity of astrocytes is still not clearly defined. However, the exposure of monomeric tau or tau fibrils on primary astrocytes led to their internalization and subsequent integrin- and NF-κB-dependent production of neurotoxic factors, among them typical cytokines, such as IL-6, IL-1β, TNF-α, and CCL10, and a consecutive decrease of neuronal viability in culture (Wang and Ye, 2021). In this study, the molecular profiling of phosphorylated-tau-exposed astrocytes revealed many similarities with the A1 signature, Gibp2, and Ligp1 being the most abundant mRNAs, and with the pan-reactive signature, with an increase of Lcn2 transcripts also involved in neurotoxicity. Wu et al. (2019) obtained similar results with astrocytes sorted from the hippocampus of TauP301S mice at 6-month-old of age. TauP301S astrocytes shared an induction of A1 and pan-reactive astrocyte genes, such as C3, Serping 1, H2-D1, Ggta1, and Ligp1. This induction was stronger than in forebrain astrocytes from PS2APP mice (7–13 months of age). The authors described a strong increase of C3-positive astrocytes in both models but with a more robust one in the

TauP301S hippocampus. Sidoryk and colleagues have shown that primary astrocytes extracted from 7 day-old newborn TauP301S pups already exhibit defects in neuroprotective features, such as a reduction of thrombospondin-1 (TSP-1) expression (Sidoryk-Wegrzynowicz et al., 2017; Wu et al., 2019), that negatively impact synapses formation and cell survival (Christopherson et al., 2005).

The specific expression of T34 human tau isoform selectively in astrocytes in a transgenic mouse model led to astrocytic morphological alterations resembling those found in corticobasal degeneration (CBD) or other primary tauopathies (see the section "Pieces of Evidence of Astrocyte Neurotoxicity in NDD Patient Samples") called tufted astrocytes, astrocytic plaques, or threads (Forman et al., 2005). However, no neuronal loss was observed in this model but focal neuronal injury and mild blood–brain barrier disruption. Richetin et al. (2020) showed that the overexpression of 3RTau in the hilus of mice *via* viral transduction led 4 months later to an impaired inhibitory circuitry and synchronous activity with a decrease of parvalbumin-positive neurons and vesicular GABA transporter (VGAT) positive synapses. The stimulation of parvalbumin-positive interneurons with neuregulin-1 peptide rescued the spatial memory impairments. In this model, the general neuritic density was not affected. However, the number of immature doublecortin-newborn neurons was reduced indicating a selective detrimental impact of tau-expressing astrocytes on neurogenesis.

To conclude, astrocytes are found detrimental in most models *in vitro* and *in vivo* when they react to oligomers, fibrils, and inclusions or carry Tau aggregates or Tau isoforms.

Synuclein Pathology

Exposure to monomers and preformed fibrils (PFFs) of α-Synuclein can also change astrocyte molecular profiles towards neurotoxic states. Chou et al. (2021) found that the treatment of human midbrain primary astrocytes by synuclein PFFs induced an nuclear factor kappa B (NF-κB)- and RIPK1-dependent inflammatory factor release; an A1 partial signature (SERPING1, HLA-E, SRGN, and PSMB8) impacted MEGF10 and MERTK activity. Chavarría et al. (2018) described concordant results after incubation of primary rat cortical astrocytes with monomers, oligomers, and PFF of α-Syn. Pre-treated astrocytes were found to engage neurotoxic features by drastically decreasing the survival of primary hippocampal neurons after 72 h, with a gradual effect from monomers to PFFs. The astrocyte-induced neurotoxicity was defined by a mitochondrial dysfunction, subsequent oxidative stress, and by an overproduction of typical pro-inflammatory cytokines TNF-α and IL-1β. However, Russ et al. (2021) showed that human iPSC-derived healthy astrocytes treated with α-Syn monomers and fibrillar polymorphs react differently than the ones treated with TNF-α and do not engage a pro-inflammatory response. In their experimental procedure, α-Syn fibrils-treated astrocytes showed dysfunctional mitochondria respiration and adopt an antigen-presenting phenotype, with an increase of expression of the human leukocyte antigen (HLA) genes encoding MHC I and II. Characterizing the response of astrocytes to α-Syn in rodent models is not straightforward as only a few models overexpressing α-Syn have been reported to mimic some PD pathological features. We think that 1-methyl-4-phenyl-1,2,3,6-tetrahydropyridine (MPTP), 6-hydroxydopamine (6-OHDA), paraquat, and rotenone are irrelevant for this discussion because neurotoxin-induced models can alter directly the glial cells and neurons bypassing a sequential pathological cascade linked to α-Syn. The selective expression of A53T α-Syn in astrocytes has surprisingly led to a more severe phenotype than the expression of A53T α-Syn by a neuronal promoter in transgenic mice (Gu et al., 2010). These animals showed general astrocyte reactivity with a dysmorphic appearance, even in the pre-symptomatic phase, concomitant with a high neuronal loss in the midbrain and spinal cord, where microglia were also found activated and agglomerated. Mice became paralytic after 7 weeks and quickly died afterwards. In conclusion, based on models *in vitro* and mouse models experiments *in vivo*, α-Syn could trigger either neurotoxic phenotypes or antigen-presenting phenotypes. An aggregation of α-Syn in astrocytes could severely negatively impact the pathological progression of the disease.

TDP-43 Pathology and ALS Models

Similar experimental approaches were undertaken to expose astrocytes to TDP-43 pathology. In Smethurst et al. (2020) insoluble material from the spinal cord of ALS patients was used to seed TDP-43 aggregation in transfected human IPSC-derived astrocytes. Phosphorylated TDP-43 inclusions were found but in lesser quantity than in human motor neurons after the same treatment. In co-culture experiments, healthy astrocytes exerted a protective function alleviating TPD-43 spreading and pathology. Transfecting rat primary astrocytes with a vector expressing the C-terminal fragment of TDP-43 led to the formation of TDP-43 typical inclusions. TDP-43 positives astrocytes showed increased lipid droplets and a differential response to noradrenaline (NA) revealing calcium and metabolic dysfunction (Velebit et al., 2020). When Lee et al. have transfected primary cortical mouse astrocytes with the human form of TDP-43, they found an increase of inflammatory factors (IL-6, IL-1β, LCN2, iNOS, or NF-κB) dependent on the Protein tyrosine phosphatase 1B (PTP1B; Lee et al., 2020). The neurons in culture treated with TDP-43 transfected astrocyte culture medium had lower survival rates partially corrected by PTP1B inhibition.

The selective expression of the mutated form of TDP-43 (M337V substitution) in astrocytes in transgenic rat led to a severe degenerative phenotype with a progressive loss of motor neurons and concomitant atrophy of skeletal muscles leading to paralysis (Tong et al., 2013). Along with the disease progression, authors reported a decline of GLAST and GLT1, and the upregulation of Lipocalin 2 (Lcn2) and Chi3L1, two neurotoxic factors in a dose-dependent manner on cortical neuronal culture cells (Bi et al., 2013; Huang et al., 2014). When the same mutated form of TDP-43 (M337V) was expressed in neurons, LCN2 was progressively up-regulated in astrocytes and found in CSF.

Several studies using hiPSC-derived astrocytes from ALS patients have reported cell-autonomous astrocytic dysfunction and proposed a consecutive loss of the astrocytic protective/

homeostatic function and/or increased toxicity. The release of TNF-α, the reduction of astrocytic glutamate uptake or the decrease of antioxidants may then result in non-cell-autonomous damage and consecutive death of motor neurons (MNs; Haidet-Phillips et al., 2011; Madill et al., 2017; Kia et al., 2018; Birger et al., 2019). Intranuclear RNA foci have been observed not only in neurons but also in a small proportion of astrocytes in postmortem CNS tissue from C9-ALS patients (Lagier-Tourenne et al., 2013) as well as in iPSC-derived C9-mut astrocytes (Zhao et al., 2020). Mutations in C9orf72 are the most common cause of ALS. Subsequent transcriptomic analysis revealed almost 700 dysregulated genes in C9-mut astrocytes with increased expression of genes involved in ionotropic glutamate receptor signaling (GRIA1, GRIA4), complement activation, ribosomal subunit assembly (large and small), and nuclear RNA export. Reduced gene expression was observed in genes involved in cell adhesion (L1CAM, TSP1, and NTN1), synapse assembly (BDNF, NRG1, and THBS2), cell-to-cell signaling (GPC6), regulation of sodium ion transport (SLC8A1, ATP1B2, and NKAIN4), and potassium ion import (DLG1, ATP1B2; Zhao et al., 2020). Another transcriptome analysis of C9-mut astrocytes further revealed a senescent phenotype with 899 differently expressed genes compared to controls, including upregulation of TNFRSF10D, SERPINE1, SA β-gal, p21, CDKN1A, and PTDGS, as well as downregulation of CDKN2C, STMN1, and E2F1.

Thus, there are many mechanistic roads to impact astrocyte phenotypes and induce molecular and structural changes that will affect surrounding cells. There is a huge variability between models but clear proof of principle that astrocytes could lead to disease progression and turn toxic to neurons. This turn to detrimental features is also hypothesized to be directly associated with the activation of the microglia.

Interplay Between Astrocytes and Immune Cells: The Control of Neurotoxicity?

Astrocytes have an intimate relationship with immune cells, especially with microglia with who they collaborate to respond and clean the insult of the CNS (Bouvier and Murai, 2015; Matejuk and Ransohoff, 2020). Microglia appear central to disease progression in AD and other NDDs (Heneka, 2019). When microglia get activated in pathological contexts, they engage phagocytic functions, activate anti-inflammatory or pro-inflammatory responses to fulfil their immune function, and protect the tissue (Salter and Stevens, 2017). Microglia influence astrocytes directly. Indeed, astrocytes express key cytokine/chemokine receptors at their surface (IFN-R, TNF-R, IL-R, and TLR) that sense inflammatory factors released by immune cells. They also respond to such stimuli by adapting their molecular profile and turning reactive. Interestingly, the A1 signature is fully dependent on microglia activation and on their release of pro-inflammatory cytokines, such as IL-1α, TNF-α, and C1Q as seen after LPS stimulation. In microglia depleted mice ($Csf1r^{-/-}$) astrocytes did not adopt the A1 signature after LPS injection. To further investigate microglia-astrocyte crosstalk *in vitro*, Guttikonda and colleagues developed human pluripotent stem cells (hPSC)-derived tri-culture system containing pure populations of hPSC-derived microglia, astrocytes, and neurons (harboring the $APPSWE^{+/+}$ mutation or isogenic controls; Guttikonda et al., 2021). They found that C3 is increased in control tri-culture compared to astrocyte/neuron or neuron only cultures. In the $APPSWE^{+/+}$ tri-cultures, C3 was further increased, but only in the presence of microglia. They identified microglial TNF-α as the main inducer of C3 expression in astrocytes but found that microglia were also releasing C3. Joshi et al. (2019) focused on the role of mitochondria damage in the induction of astrocytes neurotoxicity. They found a simultaneous reduction of microglia and astrocyte activation in mouse models of AD (5xFAD), HD (R6/2), and ALS (SOD1-G93A) by decreasing mitochondria fragmentation through the inhibition of the binding of the dynamin-related protein 1 (Drp1) to the mitochondria receptor Fis1 with the compound P110. They further reported that applying conditioned media of Q73 or mutant G93A SOD1 microglia (ALS model) showing excessive mitochondria damage, induced a similar mitochondria fragmentation in astrocytes and a concomitant A1 signature. Park et al. (2021) found that the astrocytic reactivity dependent of the microglia was associated with microglial Glucagon-like peptide-1 (GLP-1) receptor signaling. They showed that the GLP-1R was upregulated in 5xFAD mice. They have injected these mice with NLY01, an engineered agonist of GLP-1R, and observed suppression of Aβ-induced microglial activation and astrocytic reactivity as well as neuronal cell death, and partial rescue of cognitive decline. But microglia-astrocyte interplay is dynamic and astrocytes do influence microglia states as well. Rueda-Carrasco et al. (2021) showed that the astrocyte secreted frizzled-related protein 1 (SFRP1) is necessary for inducing microglia activation after LPS injections. McAlpine and colleagues found that IL-3 release by astrocytes is a regulator of microglia activation favoring their protective role against amyloid pathology in 5xFAD mice (McAlpine et al., 2021). They confirmed colocalization of IL-3 with astrocytes and IL-3R alpha with microglia in frontal cortex autopsy samples from AD patients. Neurotoxic astrocytes could also drastically alter microglia phenotypes. Indeed, C3 was found specifically expressed by astrocytes and C3aR by microglia in WT and APP/PS1 mice (Lian et al., 2016). The inhibition of the C3aR with an antagonist was sufficient to reduce amyloid pathology in APP/PS1 mice.

The relationship of astrocytes with the infiltration of peripheral immune cells, such as CD8 cells, in AD, and other NDDs, is still under scrutiny and would need to be further explored.

Gate and colleagues discovered that the presence of a subgroup of peripheral immune cells called the $CD8^+$ T effector memory $CD45RA^+$ or T_{EMRA} in individuals, after an analysis of AD patients, MCI individuals, and healthy controls, is predictive for cognitive decline (Gate et al., 2019). The T_{EMRA} were often found in the vicinity of Aβ blood vessels and astrocytes are good candidates to serve as chemoattractants for peripheral immune cells infiltration. Some cytokines and chemokines associated with neurotoxic signatures, such as IL-6, IL-1β, or CXCL10 have been involved in the blood brain barrier (BBB) disruption and the attraction of B and T cells (Rothhammer and Quintana, 2015).

The states of the astrocytes, beneficial or detrimental, are intermingled in a more global reaction of brain cells (**Figure 1**) and their bilateral interaction with the brain and peripheral immune cells is at the center of numerous short-term and long-term responses that could shape the progression of NDDs.

Depletion of Noradrenaline and Dopamine, Vectors for Neurotoxic Astrocytes?

In the most common NDDs, astrocytes, among other brain cells, are confronted with numerous global brain alterations. Apart from pathological protein inclusions, the brain is affected by a progressive alteration of its neurochemistry as well as an imbalance of numerous neurotransmitters that disturb the activity of neurons and glial cells. The progressive depletion of NA and dopamine (DA) is associated with ageing (Manaye et al., 1995; Volkow et al., 1998; Beardmore et al., 2021) and the onset of NDDs such as AD and PD (Weinshenker, 2018; Biondetti et al., 2021). A local change of availability of NA or DA could strongly alter the responses of astrocytes in NDDs and favor their neurotoxicity.

The degeneration of the locus coeruleus (LC), the primary source of NA, is a hallmark shared by multiple neurodegenerative disorders (Holland et al., 2021). The LC is a small brainstem nucleus mainly composed of NA producing neurons (Hansen, 2017) innervating multiple brain regions, such as the hippocampus, the amygdala, and the prefrontal cortex. NA is essential for hippocampus-based declarative memory formation, and for the regulation of cellular responses such as neuroinflammation and neuronal survival (Matchett et al., 2021). Its unbalance or progressive depletion in NDDs could impact the responses and fate of astrocytes. Indeed, astrocytes express numerous noradrenergic receptors at their surface (α and β), and NA modulates their metabolic activity, glutamate uptake, glycogen production, and glucose metabolism (O'Donnell et al., 2012), but also their calcium activity (Ding et al., 2013; Oe et al., 2020). NA has been also directly involved in astrocyte mediated memory consolidation (Gao et al., 2016; Wahis and Holt, 2021). NA can downregulate transcription of pro-inflammatory genes (such as TNF-α, IL-1β, and iNOS), and upregulate anti-inflammatory molecules (such as HSP-70 and MCP-1) in astrocytes and microglia (Heneka et al., 2010; Chalermpalanupap et al., 2013). The DSP4 (N-(2-chloroethyl)-N-ethyl-bromo-benzylamine) model is based on a systemic administration of the selective neurotoxin DSP4 that causes a huge NA depletion through a terminal retrograde degeneration of the majority of LC-noradrenergic neurons (Carnevale et al., 2007). In this model, astrocytes increased their IL-1β expression in response to NA depletion (Heneka et al., 2002). Heneka and colleagues showed with a DSP4-APP23 transgenic mouse model that astrocytes develop a reactive phenotype and express a plethora of pro-inflammatory molecules (Heneka et al., 2006). In this study, NA deficiency increased neuronal loss in CA1 hippocampus and frontal cortex, plaque loads, $CD11^+$ microglia, GFAP, and iNOS expressions, and induced the formation of NO-mediated peroxynitrite, a free radical with high cell toxicity (Vodovotz et al., 1996; Smith et al., 1997). High-GFAP astrocytes were also shown highly abundant in the hippocampus after DSP4 treatment of an APP mouse model (9-month-old male mice) in concomitance with higher plaque loads (Kalinin et al., 2007).

Dopamine (DA) is an essential catecholamine and neurotransmitter (Meiser et al., 2013). Dopaminergic neurons are distributed in nine cell groups from the midbrain to the olfactory bulb. In adult brain, dopaminergic pathways project from the substantia nigra pars compacta (SNpc) to the striatum, and from the ventral tegmental (VTA) area to the cortex (Björklund and Dunnett, 2007). It forms three mains dopaminergic pathways: the nigrostriatal pathway, the mesolimbic pathway, and the corticolimbic pathway. In PD patients, the nigrostriatal pathway is severely affected because of the specific degeneration of dopaminergic neurons located in SNpc (Arias-Carrián et al., 2010). A decrease in the DA levels was also shown to be significant in dementia of Alzheimer type (Adolfsson et al., 1979). DA deprivation in PD and other NDDs could also impact the phenotypes of astrocytes in DA targeted areas. Indeed, astrocytes from various brain regions can express DA receptors at their surface, D1–D5 (Khan et al., 2001; Miyazaki et al., 2004; Xin et al., 2019). DA can directly affect their Ca2+ signaling. Nucleus accumbens astrocytes respond to DA through D1 receptors and seem to mediate DA-evoked depression at the synaptic level (Corkrum et al., 2020). Galloway et al. (2018) demonstrated an interesting role of DA in the epigenetic remodeling of primary astrocytes in culture. Both NA and DA deprivation could have a profound effect on astrocytes and prime them to maladaptive responses.

Pieces of Evidence of Astrocyte Neurotoxicity in NDD Patient Samples

Neurotoxic states of astrocytes can be triggered by numerous stressors *in vitro*, in mouse and human cells as well as in rodent models. Direct exposure or internalization of NDD typical pathological protein inclusions, and/or unbalance of neurotransmitters/neuromodulators, activation of microglia are all factors involved in the triggering of astrocyte neurotoxicity. There is no consensus around a prototypical signature. However, some overlap was found in different models. Some studies also gave contradictory conclusions on the role of astrocytes in disease progression. As the experimental set-ups impact the responses of astrocytes, translational research is mandatory to further understand their roles in the neurodegenerative cascades. The rise of new technologies such as snRNAseq allows for investigating frozen human post-mortem tissue with a precision never obtained before. The published data already reflect the heterogeneity of their states across brain regions, stage of the disease, and condition. It is now essential to associate the state of an astrocyte to its macro- (type and stage of the disease, brain region) and micro-environment (pathological protein inclusion proximity, inflammation associated to microglia and peripheral immune cells) to further understand its involvement in disease progression. Few points to consider before extrapolating *in vitro* and rodent model data to the human brain:

- For each NDD, the concomitance of typical pathological inclusions is more the rule than the exception (Golde et al., 2013; Robinson et al., 2018).
- The ageing process is poorly mimicked in cell culture and transgenic rodents.
- Human astrocytes are distinct from rodent ones in many aspects and their heterogeneity is greater.

Indeed, human astrocytes are different from mouse ones in size, morphology, proportion per neuron, and responses (Oberheim et al., 2006, 2009; Li et al., 2021). The Li et al. (2021) study confirmed the differential responses of immunoisolated mouse (P1-P3) and human astrocytes (gestational week 17–20) under oxidative stress, hypoxia, inflammatory conditions, and viral infections. Murine and human astrocytes showed already significant differences in gene expression in serum-free conditions. These differences persisted through development even when human astrocytes were grafted in a mouse brain, attesting to an intrinsic differential program. Facing stress and pathological conditions, human astrocytes differed in their mitochondria-energy metabolism and immune responses showing more vulnerability to oxidative stress and capacity to engage the antigen presentation pathway. The same authors have identified a core astrocyte signature in human NDDs by comparing transcriptomic analysis of AD and MS cases to poly I: C-, and TNF-α-induced changes of cultured human astrocytes. Some commonly upregulated genes were associated with inflammation such as C3, IFITM3, NFkBIA, CCL2, and CXCL10 and have been associated with neurotoxic signatures.

In this chapter, we attempt to map out molecular signatures, markers, and pieces of evidence of astrocyte neurotoxic responses in NDD patient brains.

Alzheimer's Disease

A high level of GFAP is commonly detected by positron emission tomography (PET; Carter et al., 2012, 2019; Verberk et al., 2020; Calsolaro et al., 2021; Chatterjee et al., 2021), in the blood (Goetzl et al., 2018; Cicognola et al., 2021) or CSF (Sathe et al., 2019) of MCI and AD patients. This GFAP level increase has been associated with the level of Aβ (Pereira et al., 2021) and negatively correlated with Mini-Mental State Examination score (Oeckl et al., 2019). The analysis of isolated astrocyte-derived exosomes (ADE) GLAST positive from plasma of AD patients and controls showed significantly higher levels of the cytokines IL-6, TNF-α, and IL-1β and of numerous complement proteins (Goetzl et al., 2018). Surprisingly, GFAP is also described as a potential biomarker for early AD in the saliva of MCI and AD patients where its levels are correlated with $A\beta_{42}$, IL-1β, and caspase-8 (Katsipis et al., 2021). An increase of GFAP staining is commonly observed in the parenchyma of AD cases (Serrano-Pozo et al., 2013). Kobayashi and colleagues classified their cohort of samples into three groups, the control group, AD with and without dementia (Kobayashi et al., 2018). They found an increase of GFAP in the entorhinal cortex of both AD groups, however; the non-demented AD group was characterized by an increase in the expression of GLT-1. A recent analysis of astrocytes markers across IHC and RNAseq data collections in human samples have highlighted the complexity of astrocyte responses in AD and delimited a core reactive signature of AD astrocyte (ADRA) that points towards dysfunctions and neurotoxicity (Viejo et al., 2021). The authors build an online resource where each ADRA marker confirmation by IHC or RNAseq is mapped.

Numerous studies characterized astrocyte neurotoxic markers in post-mortem AD samples. C3-positive astrocytes were detected in numerous NDDs (Liddelow et al., 2017), in the entorhinal cortex layers I-III and CA1 hippocampus with a co-expression of serine racemase, an enzyme that produces D-Serine (Balu et al., 2019), and in the frontal upper cortex (King et al., 2020). Chun et al. (2020) found an increase of Nos2 in the AD temporal cortex. Subpial and RGN astrocytes expressed Nos2, Nos3, and nitrotyrosine in AD hippocampus, frontal, temporal, and entorhinal cortices (Heneka et al., 2001; Lüth et al., 2002). IL-6-positive astrocytes were detected in the lateral hypothalamus, cingulate cortex (Lyra e Silva et al., 2021), and prefrontal and temporal cortices (Bouvier et al., 2016). Recent snRNAseq data also gave new insights on astrocyte molecular status in AD. Grubman et al. (2019) found two AD specific astrocyte clusters from the entorhinal cortex of AD patients. One was defined by an increase of genes related to ribosomal, mitochondrial, neuron differentiation, and heat shock responses and the other cluster by enrichment for transcripts related to transforming growth factor (TGF)-β signaling and immune responses. Neither of them overlapped significantly with the A1 or A2 profiles but the second cluster showed an upregulation of C3. Lau et al. (2020) performed snRNAseq on AD prefrontal cortex and control samples. They have identified two "AD-upregulated" astrocytic subpopulations expressing CRYAB, GFAP, LINGO1, and HMGB1 and one "AD-downregulated" subpopulation. The authors concluded for dysregulation of neurotransmitter recycling and an exaggerated alarming response of astrocytes. Gerrits et al. (2021) proceeded to single-cell RNA-seq of the entorhinal cortex of AD patients, but they did not find any AD-associated changes in astrocytes.

Overall, there are no prototypical neurotoxic signatures such as the A1 or DAA ones found in AD yet. However, some subgroups of astrocytes showed some overlapping trends of transcripts or increase of markers associated with severe reactivity and/or neurotoxic responses.

Primary Tauopathies

Primary tauopathies are defined by a tau-driven pathology, the absence of Aβ plaques and are associated with presenile dementia. They are grouped according to their ratio in the predominant isoform, either the 3-repeat tau (3R) or the 4-repeat tau (4R) in 3R, 4R predominant, or mixed. They comprise 3R Pick disease, and 4R CBD, progressive supranuclear palsy (PSP), globular glial tauopathy (GGT), and argyrophilic grain disease (AGD; Chung et al., 2021). All these NDDs are characterized by the presence of tau-positive astrocytes reviewed in (Kovacs et al., 2016). The expression of tau by astrocytes, mostly 4R, directly impacts their morphologies. They are called tufted astrocytes, astrocytic plaques, ramified astrocytes, globular astroglial inclusions (GAIs), Thorn-shaped astrocytes (TSA),

and granular/fuzzy astrocytes (GFA). The post-mortem stratification of patients in the "ageing-related tau astrogliopathy" (ARTAG) group is now based on the high frequency of TSA and GFA in specific anatomical regions (Kovacs et al., 2016, 2018; McCann et al., 2021). However, the relationship of tau positive astrocytes with neurodegeneration in human post-mortem NDD samples is still under scrutiny. Briel et al. (2021) analyzed the relationship between astrocyte plaques and tufted astrocytes and the peripheral synaptic density in cortical and striatal areas from PSP and CBD patient samples. General lower excitatory and inhibitory synapse densities were found significant in PSP Frontal Cortex. Local synaptic density was negatively correlated with astrocytic plaques only in CBD cases. Using image analysis, the authors also demonstrated a local loss of synapses in the territory of tau-positive astrocytes, especially exacerbated in astrocyte plaques. Interestingly tufted astrocytes were also found in Lewy body disease (Hishikawa et al., 2005) and were not associated with pathological inclusions but with age.

Parkinson's Disease and Synucleinopathies

Synucleinopathies are characterized by the pathological accumulation of α-Syn mainly in neurons but also in glia, in the form of granular intra-cellular accumulations, Lewy neurites and Lewy bodies. The synucleinopathies are classified into three major entities: PD, LBDs which comprise Parkinson's disease dementia (PDD) and dementia with Lewy bodies (DLB), and multiple system atrophy (MSA). DLB is the second most common cause of dementia and often share amyloid and tau pathologies with AD. In most of the synucleinopathies, astrocyte reactivity is considered as low or inexistent in the human brain, which rather contradicts previous conclusions made *in vitro* and mouse model studies. Mirza et al. (1999) did not observe differences in GFAP density, distribution or morphology of astrocytes in the substantia nigra (SN), or putamen in post-mortem samples from PD patients compared to age-matched controls. Tong and colleagues confirmed these results at the protein level by reporting similar levels of GFAP, Vimentin, and heat shock protein-27 (Hsp27) by quantitative immunoblotting in the SN from PD patients compared to controls (Tong et al., 2015). However, all these markers were increased in SN and putamen of MSA patients. Looking across LBD cohort samples, Van Den Berge et al. (2012) did not find any increase of astrocyte reactivity using GFAP and vimentin IHC or Western blot in the frontal cortex of PD, PDD, and DLB patients. Few reports found a change in the astrocyte signatures in PD and DLB. Rostami et al. (2020) reported the expression of MHC2 markers colocalized with GFAP staining nearby $CD4^+$ cells in PD brains. Few "neurotoxic" markers were found in astrocytes in PD brains: C3 in SN and frontal cortex (Liddelow et al., 2017) and an increase of LCN2 in the SN of PD patients by Western blot analyses. Some TNF-α and iNOS positive astrocytes were detected in the hippocampus of DLB patients (Katsuse et al., 2003). Agarwal and collaborators performed snRNAseq on SN from PD and control subjects and found two PD astrocyte clusters, one with upregulated neuroinflammatory genes (Olr1), and one expressing gene associated with growth and reparative functions (Gins3; Agarwal et al., 2020). The authors do not report any A1, A2, pan-reactive, or other previously described reactive astrocyte signatures. However, astrocytic reactivity is found in the proximity of alpha-synuclein inclusions in the white matter of visual and frontal cortices and the grey matter of the putamen in MSA brain samples (Radford et al., 2015). Inoue et al. (2021) described a positive correlation of GFAP with the expression of the stimulator of interferon genes (STING) in the putamen and SN of MSA cases. STING, a cytosolic DNA sensor can trigger type 1 interferons and is involved in defensive immune mechanisms against pathogens but also in autoimmunity. Astrocytic toxicity across synucleinopathies remains uncertain but could be more prominent in MSA than in PD or LDB progression.

TDP-43 Associated Proteinopathies

Although ALS and FTD are clinically distinct NDDs they genetically and pathologically overlap and share central features (Gerovska et al., 2020). Around 30% of ALS patients and up to 15% of FTD patients will develop an overlap of clinical features (for review, see Lomen-Hoerth, 2011). Intraneuronal accumulation of misfolded, ubiquitinated/phosphorylated proteins, such as TDP-43, C9orf72 (C9), superoxide dismutase 1 (SOD1), and fused in sarcoma (FUS), is a major key factor in sporadic and familial ALS (sALS, fALS; for review, see Peters et al., 2015; Volk et al., 2018) but are not exclusive to ALS. Accumulation of TDP-43 can be found in the majority of cases of frontotemporal lobar degeneration (FTLD), so-called FTLD-TDP (Arai et al., 2006; Neumann et al., 2006) as well as in limbic-predominant age-related TDP-43 encephalopathy (LATE; Nelson et al., 2019). Astrocytes are hypothesized as significant actors in ALS and FTD progression mainly due to results from *in vitro* and *in vivo* rodent models (Izrael et al., 2020). Analyses of human post-mortem spinal cord tissue revealed enrichment of astrocyte-specific genes and enlarged perivascular spaces with separation of astrocyte and mural basement membranes in sALS (Månberg et al., 2021). RNA-seq datasets implicated enrichment of upregulated DEGs related to astrocyte functions in ALS compared to control spinal cord samples (Wang et al., 2021). Blood-spinal cord-barrier (BSCB) disruption and leakage has been described in ALS patients and detachment of astrocytic end feet from vessels (Miyazaki et al., 2011) or regional differences in astrogliosis or GFAP expression (Schiffer et al., 1996; Oberheim et al., 2009; Sofroniew, 2015) are proposed to be responsible for a reduction of GFAP in the perivascular space (Waters et al., 2021). Further research on post-mortem human brain and/or spinal cord tissue indicated astrocyte-related neurotoxicity and/or MN loss mediated. This is reflected by an increase of astrocytic cystine/glutamate antiporter (xCT) as a response to oxidative stress, a decrease of astrocytic glutamate transporter GLT-1 (Rothstein et al., 1995) further leading to increased extracellular glutamate accumulation (Kazama et al., 2020), an increase of astrocytic connexin 43 (Cx43; Almad et al., 2016), and an increase of astrocytic chitinase-3-like protein 1 (CHI3L1) and 2 (CHI3L2; Sanfilippo et al., 2017; Vu et al., 2020), the latter negatively correlated with the survival time of ALS patients. Gorter et al.

(2019) reported the expression of small heat shock proteins (HSPBs) in reactive lateral column astrocytes in ALS patients with short disease duration (SDD; HSPB5, HSPB8) as well as with moderate disease duration (MDD: HSP16.2). HSPBs are required for protein quality control and are relevant for stabilization of intermediately folded proteins to prevent misfolding and/or aggregation and subsequent cytotoxicity (Sharma et al., 1997; Van Montfort et al., 2001; Jaya et al., 2009; Haslbeck et al., 2015) and HSPB8 facilitates autophagy *via* BAG3 interaction (Fuchs et al., 2010, 2015). Thus, the upregulation of HSPBs could be a direct response to altered protein homeostasis. The pathogenic protein aggregates may subsequently trigger the glial inflammasome. Microglial NLR family pyrin domain containing 3 (NLRP3) inflammasome activation is an emerging key factor of neuroinflammation and contributor to disease progression in an ALS mouse model (Deora et al., 2020) and may further contribute to disease progression during neurodegeneration. Inflammasome components, such as NLRP1, NLRP3, adaptor protein apoptosis-associated speck-like protein containing a CARD (ASC), and interferon-inducible protein AIM2 (AIM2) colocalize with GFAP positive astrocytes in spinal cords of sALS patients (Johann et al., 2015; Hummel et al., 2021). Taken together, astrocyte-associated toxicity and neuroinflammation could be significant factors in the progression of ALS-related neurodegeneration.

THE IMPACT OF AGEING ON THE RESPONSES AND PHENOTYPES OF ASTROCYTES IN NDDs

It is interesting to note that in most of the experimental models, the highest risk factor for NDDs which is ageing is strongly neglected. However, enough studies have demonstrated the change of states of astrocytes across ageing and their tendency to mimic certain reactive and even neurotoxic features. The cellular senescence is also an important factor to consider as senescent astrocytes would be detrimental for their surroundings.

Ageing Signatures: Does the Progressive Loss of Homeostatic Astrocytic Phenotypes Prime Neurotoxicity?

In the ageing CNS, cells that are in mitosis or proliferating represent a small minority. Pools of new neurons, and sometimes astrocytes, are born from the neural stem cells of the subgranular zone (SGZ) in the dentate gyrus (DG) of the hippocampus and subventricular zone (SVG) but decrease in ageing mice (Baptista and Andrade, 2018). In humans, neurogenesis in the adult and ageing brain is still difficult to assess and results in the literature are often contradictory (Sorrells et al., 2018). However, Boldrini et al. (2018) showed that neurogenesis is relatively stable during ageing in DG and at least persists in humans until their 80s. Astrocytes seem to have a long lifespan with a low proliferation rate limited to severe astrogliosis in acute injuries or advanced stages of NDDs (Colodner et al., 2005; Sofroniew and Vinters, 2010). New astrocytes can be occasionally produced by the stem cells of SGZ (Bonzano et al., 2018) but the absence of data collected from the human brain does not allow further discussion. The general agreement is that astrocytes also show stereotypical phenotypic changes in ageing.

Numerous analyses based on GFAP and vimentin staining quantification in brain sections showed their increase in ageing in frontal, temporal, and entorhinal cortices, in the hippocampus of rats (Nichols et al., 1993; Amenta et al., 1998; Bernal and Peterson, 2011) and humans (David et al., 1997; Porchet et al., 2003). No change was observed in the chimpanzee brain (Munger et al., 2019). Cerbai et al. (2012) reported smaller astrocytes with simplified arborization in CA1 Stratum radiatum of aged rats compared to adults. Bronzuoli et al. (2019) showed by Western blot and immunofluorescence a reduction of GFAP, S100B, and connexin-43 expression but an increase of aquaporin-4 in hippocampal astrocytes from 12-month compared to 6-month-old mice. Thus, the homeostatic functions of astrocytes could be progressively altered during ageing. By using the Ribo-Tag technique, Boisvert et al. (2018) isolated specifically the ribosomal RNA of mouse astrocytes at specific ages from the visual (VC), the motor cortex (MC), hypothalamus (HTH), and cerebellum (CB). By comparing 2-year-old mice transcriptomes to 4 months old, they found that seven genes are commonly upregulated in all regions isolated, which are the serine protease inhibitor A3N and M (Serpina3n and Serpina3m), Gfap, some proto-cadherins-b 6 and 11, and C4b a component of the complement cascade. Some transcripts increased were specific to astrocytes of certain regions, such as Bmp6 and Sparc in VC astrocytes and pro-inflammatory factors such as Cxcl5, caspase-1 and 12 along Tlr-2 and 4 in CB. Overall, astrocytes seem to engage an ageing functional decline that could disrupt their interplay with surrounding neurons and alter their response to stress and pathology in older individuals. In line with these observations, Clarke and colleagues described a prevalence of the A1 or neurotoxic signature in astrocytes of older mice (Clarke et al., 2018). With a similar strategy to the Boisvert study, a translating ribosome affinity purification (TRAP) technique was used to isolate RNA astrocytes from the hippocampus, cortex, and striatum, later analyzed by RNAseq, across the lifespan of a mouse (Boisvert et al., 2018). They showed that aged astrocytes upregulate a high number of the A1 genes, especially in the hippocampus and striatum. Serpina3n, complement (C3 and C4B), and cytokine pathway (Cxcl10), but also antigen presentation (H2-D1 and H2-K1) were some of the most prominent. In parallel, the downregulation of genes involved in metabolic functions, such as mitochondria energy production and antioxidant defense, pointed out a general decline of astrocyte homeostasis. Upregulation of genes involved in synaptic elimination and extracellular matrix degradation was confirmed in mouse aged isolated- astrocytes by another study (Pan et al., 2020). Interestingly, Habib et al. (2020) found a strong association between the DAA signature and aged astrocytes in mouse wild-type and healthy humans. Soreq et al. (2017) have highlighted the severe impact of ageing on glial cells and more specifically on astrocytes and oligodendrocytes through

an extensive analysis of gene expression datasets of numerous brain regions coming from postmortem tissue of 480 individuals between 16 and 106 years old. They were able to report a shift of identity of hippocampal astrocytes, more related to cortical ones in young humans, toward intralobular white matter and putamen astrocytes in the aged brain. Natural and healthy ageing is then a significant factor in the ability of astrocytes to maintain their homeostatic functions and respond to insults. The overlap of signatures between human astrocytes of aged individuals and A1 or DAA neurotoxic ones is intriguing and could contribute to their maladaptive or detrimental responses in the early phases of NDDs.

Cellular Senescence in Astrocytes: The Ultimate Fate?

Cellular senescence is a hallmark of ageing. It is characterized by the irreversible loss of the ability of the cell to divide. It is a direct consequence of telomeres shortening and comes as a protective mechanism to avoid genome instability and cancer cell production (Di Micco et al., 2021). Senescent cells are not restricted to aged CNS, but their proportion is likely to increase during the ageing course and could affect or trigger some pathological cascades associated with NDDs (Rueda-Carrasco et al., 2021). Senescent cells can be identified by measuring the increased expression of cell cycle inhibitory proteins such the cyclin-dependent kinase inhibitors p21 and $p16^{INKA4}$, the tumor suppressor protein p53, and by the ectopic expression of the senescence-associated beta-galactosidase (SA-β-Gal). Cellular senescence also induces a general change of the molecular state of the cell that provokes morphological alteration, metabolic stress, and chromatin remodeling. Cells under the senescent-associated secretory phenotype (SASP) secrete proinflammatory molecules, metalloproteinases, and growth-stimulating factors (Swenson et al., 2019). Senescent cells are resilient to cell death and are often called "zombie" cells. They can create local chronic inflammations in the CNS parenchyma and destabilize the micro-environment. Baker and collaborators demonstrated the impact of senescent cells *in vivo*, in healthy and aged cells (Baker et al., 2016). The authors have shown the ablation of senescent cells promotes normal tissue function and delays the onset of age-related pathologies. The same effects have been observed in mice (Zhu et al., 2016). Cellular senescence features partially overlap with neurotoxic astrocytes ones, which challenges their identification in the astrocytic population. *In vitro*, multiple conditions and stressors can activate a senescence program in astrocytes. Ageing can be mimicked in a dish by multiplying the number of passages of cells, by cultivating them over a longer period or by using primary cells extracted from aged animals. All these conditions trigger senescence in cultivated microglia and astrocytes (Bitto et al., 2010; Caldeira et al., 2014; Stojiljkovic et al., 2019). Many chemicals or active molecules have been used *in vitro* as stressors to induce senescent-like states in mouse or human astrocytes (Bitto et al., 2010; Stojiljkovic et al., 2019). Hydrogen peroxide (Bitto et al., 2010) inflammatory challenges, such as repeated LPS exposure (Yu et al., 2012), irradiation (Limbad et al., 2020), transient oxidative stress (Crowe et al., 2016), Aβ (Bhat et al., 2012; Zhang et al., 2019), or even the herbicide paraquat (Chinta et al., 2018) can trigger senescence in astrocytes. Transcriptome analysis of oxidative stress-induced senescence in human fetal astrocytes in culture (Crowe et al., 2016) revealed an upregulation of genes associated with inflammation and extracellular remodeling and a downregulation of genes involved in cell cycle and of GFAP and S100B. The senescence accelerated mouse (SAM) strain induces a shortened life span, loss of normal behavior, senile amyloidosis, and mitochondrial dysfunction, deficits in learning and memory, and brain atrophy (Takeda et al., 1997). Interestingly, SAM isolated astrocytes are more sensitive to artificial oxidative stress mimicked by an H_2O_2 exposure (Lü et al., 2008). Additionally, senescence has been shown to modify astrocytic ROS detoxification responses (Lü et al., 2008) and to compromise glutamate and potassium transport by decreasing the expression of EAAT1, EAAT2, and Kir4.1 (Limbad et al., 2020). Thus, *in vitro* experiments have demonstrated that numerous stressors, usually associated with ageing or disease context, can activate senescence in astrocytes. However, if glial senescence occurs *in situ* still needs to be further investigated.

Astrocytes are stable cells with a low turnover and are theoretically more prone to senescence. However, the measurement of telomere shortening in astrocytes *in vitro* contradicts this idea (Flanary and Streit, 2004; Szebeni et al., 2014). In female mice, the proportion of hypothalamic senescent astrocytes increased with age and appeared to be mainly modulated by the ovarian estradiol, which would associate astrocyte senescence with an early reproductive decline (Dai et al., 2020). Bussian and colleagues measured an increase of the expression of SA-βGal in cells identified as microglia and astrocytes by transmission electron microscopy in MAPTP301SPS19 mice (Bussian et al., 2018). In this model, senescence in glia was not linked to ageing (6-month-old animals) but mainly to the tau neuropathology. Interestingly, treating astrocyte senescence had major outcomes in mouse models. The clearance of glia senescent cells using INK-ATTAC transgenic mice had multiple beneficial effects. It prevented gliosis, decreased NFTs deposition and degeneration of neurons, and helped to preserve cognitive functions. Xu et al. (2021) reported downregulation of the Yes-associated protein (YAP) paralleled with a decrease of lamin B1 in hippocampal astrocytes during normal ageing and in APP/PS1 mice. The downregulation of YAP was also shown in D-galactose and paraquat-induced senescent astrocytes. YAP is involved in cell proliferation, differentiation, and tissue regeneration. Its activation delays senescence *in vitro* and reduces cognitive defects in old AD-like mice. Gaikwad et al. (2021) described a high proportion of $p16^{INK4A}$ astrocytes that were also positive for pathological tau oligomers (TauO) in the frontal cortex of AD and FTD patients. They found that TauO exposure induced the nuclear translocation and release of high mobility group box 1 (HMGB1) in primary astrocytes and consequent paracrine induction of senescent profile in culture. Preventing HMGB1 release using inhibitors over 8 weeks showed a significant decrease of $p16^{INK4A}$ astrocytes in 12-month-old hTau mice, a reduction of tau pathology and

neuronal loss, and partial rescue of cognitive defects. A high proportion of $p16^{INK4A}$-positive astrocytes were found in FFPE post-mortem brain samples of 78–90-year-old healthy humans (Bhat et al., 2012). Their number was even increased in AD patients, with a respective average of 35 and 50%. This staining was correlated with an increase of metalloproteinase MMP-1 expression. If these numbers stand true across NDDs, senescent astrocytes may represent the main neurotoxic astrocyte population, drive the most transformative alterations in ageing, and exacerbate disease progression in NDD. Paradoxically, treating them may be more straightforward. However, senescent astrocytes will need to be carefully quantified with multiple markers across NDD to define if senolytic targeted treatment may become a serious curative opportunity.

Epigenetic of Ageing and Ageing Astrocytes

Epigenetics is an emerging field in both diagnostics and research. It encompasses several distinct modifications of the DNA that impact transcriptional activity while leaving the nucleotide sequence unchanged (Gibney and Nolan, 2010). It includes methylation, histone modification, or non-coding RNAs (ncRNA). In general, a hypermethylated phenotype is associated with ageing processes in mammals. However, data about cell-type-specific epigenetic alterations were lacking for a long time (Maegawa et al., 2010). For brain tissue, differentially methylated sites (DMS) significantly associated with ageing were mainly localized within CpG islands and displayed a frequent hypomethylated status. Furthermore, age-associated DMS in brain tissue were enriched in H3K27me3 and frequently found within laminar-associated domains (LADs). H3K27me3 constitutes a repressive post-translational histone mark and LADs show general low transcription levels indicating a reduced gene activity in line with the ageing processes (Lochs et al., 2019). NDDs studies have shown significant differences in epigenetic marks, such as increased DNA methylation and hydroxymethylation in AD, features that correlated with pathological Aβ, tau, and ubiquitin load (Coppieters et al., 2014). A recent meta-analysis study about brain methylation revealed a very high correlation between age-related DNA methylation patterns in normal ageing and AD brain tissue, for both usually hypo- but with some hypermethylated CpGs (Pellegrini et al., 2021). It might indicate that NDDs may also be the result of abnormal, accelerated ageing processes. However, those epigenetic marks were differentially regulated between neuronal and glial cells, thereby indicating a rather cell type-specific epigenetic regulation in age-related CNS pathologies (Coppieters et al., 2014). Of note, mainly astrocytes and pyramidal neurons displayed an altered methylation profile while cell types that seem to be less affected in AD such as calretinin-positive interneurons remained relatively unaffected (Phipps et al., 2016). To better understand the implication of epigenetic regulation in the ageing process of astrocytes, it is important to understand the impact of epigenetics on the normal development of astrocytic cells. A pioneering study in the field showed that genes, that are generally considered as being astrocytic-specific, become rather de- or hypomethylated once neural precursor cells (NPC) start to differentiate into astrocytes (Hatada et al., 2008). This process allows key signal transducers in astrocytes such as SMAD or STAT3 to finally bind to their respective binding sites within astrocyte-specific genes such as GFAP, showing increased expression levels in both brain ageing and neurodegenerative disorders (Nichols et al., 1993; Porchet et al., 2003).

Epigenetic changes of the ageing astrocyte are still poorly understood. A murine stroke study revealed that aged astrocytes displayed less active chromatin, represented by weaker trimethylation of histone 3 lysine 4 (H3K4me3) acting as an enhancer while displaying stronger trimethylation of the repressive lysine residue at histone 3 lysine 9 (H3K9me3; Chisholm et al., 2015). This age-dependent impairment of active astrocytic gene transcription was associated with an increased stroke size. It indicates that aged astrocytes may be less capable of counteracting pathological conditions. Furthermore, it was demonstrated that inhibition of histone deacetylases (HDAC) increased the release of neurotrophic factors in astrocytes (Chen et al., 2006). It was shown in cell culture models that the administration of HDAC inhibitors led to increased clusterin levels, a molecular chaperone that may prevent disease progression in AD (Nuutinen et al., 2010). Although the first therapeutic strategies using HDAC inhibitors have been successful in AD-like mouse models (Francis et al., 2009) its translation into a clinical trial for NDDs seems to be much more challenging, as HDAC inhibitors may also have neurotoxic side effects (see review Shukla and Tekwani, 2020). In summary, epigenetic modifications play a central role in ageing processes, but it becomes more and more evident that these age-dependent changes or neurodegenerative alterations considerably differ between cell types. However, to date, it is still unclear if an epigenetically regulated cellular "age clock" can be selectively reverted to restore neuroprotective properties in a complex system such as the human brain, or if any interference with such fine-tuned, age-dependent epigenetic processes rather aggravates neurotoxic features in general or more specifically in astrocytes. Understanding the epigenetic regulation of astrocytes will be an asset to control their phenotypes in ageing and NDDs and may be important for the future development of novel treatment.

CONCLUSION

Many roads are leading to astrocytic neurotoxicity (**Figure 2**). There is a consensus about the potential of such an astrocytic phenotype to alter its micro-environment and exacerbate NDD pathologies and in the last few years, many researchers attempted to define a prototypical signature of a neurotoxic astrocyte (**Figure 1**). But what emerged from this translational review is a complex patchwork of heterogeneous neurotoxic signatures that vary across experimental models and conditions and are still controversial in human NDDs. Because cell culture or mouse models fail to fully recapitulate human NDDs and microscopy as well as even scRNAseq experiments from human samples provide only snapshots on the states of astrocytes, there is a

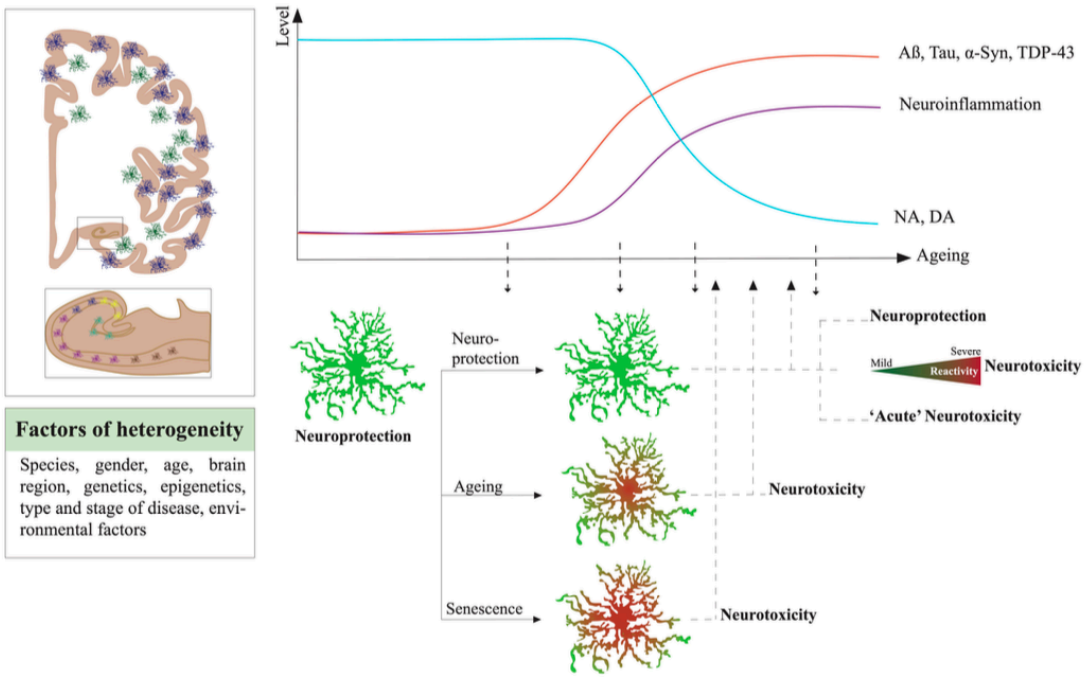

FIGURE 2 | Hypothetical roads to astrocyte neurotoxicity in the context of neurodegenerative diseases (NDDs) and ageing. The heterogeneity of astrocyte response and change depends on numerous factors, such as the species, gender, age, anatomic localization, genetics and epigenetics, their micro-environment, and the type and stage of the disease. In NDDs, one or several subgroups of astrocytes could lose their neuroprotective function and become neurotoxic. Many factors could impact their transformation into toxic cells. The effect of ageing could prime them to maladaptive responses, cellular senescence would turn them detrimental to their surroundings, pathological protein inclusions [Aβ, tau, α-synuclein (α-Syn), and TAR DNA-binding protein 43 (TDP-43)], neuroinflammation and neurotransmitter concentration, and activation of immune cells would condition their shift to toxic thereby enhancing their detrimental features. Neurotoxic astrocytes would then contribute disease progression.

need for more translational and multi-disciplinary approaches to solve the mystery of the roles of astrocytes in NDD progression. To advance in our understanding, astrocytic signatures in NDDs will have to be carefully associated with neuropathological diagnostics, especially focusing on distinct brain regions and composition of their surrounding microenvironment. There is still a lot to investigate before defining astrocytes as a therapeutic target in patients. Translational AD research points toward a strong evidence of direct implications of neurotoxic or detrimental astrocytes in the disease progression. However, their roles in other NDDs such as PD and ALS are still speculative and mainly based on *in vitro* and rodent model studies.

Furthermore, if we succeed in proving that neurotoxic astrocytes are leading neurodegenerative cascades, how could we treat them? Who to treat first, microglia or astrocytes? Both together? Should we target the ageing and senescence process or be more specific to the condition?

Non-targeted anti-inflammatory treatments (e.g., dexamethasone, minocycline, ibuprofen, and IL-10) have been efficient in animal models and have the benefit to target both microglia and astrocytes. But the search for an effective anti-inflammatory molecule for AD and NDD patients is still ongoing (Kwon and Koh, 2020). Non-steroidal anti-inflammatory drugs, such as ibuprofen, celecoxib, rofecoxib, or tarenflurbil have all failed to reduce cognitive decline in clinical trials in AD patients (Zanetti et al., 2009; Rivers-Auty et al., 2020).

The Nrf2 signaling pathway represents a potential target for the treatment of NDDs. Indeed, Nrf2 is a key endogenous regulator of oxidative stress and neuroinflammation (Johnson et al., 2008; Buendia et al., 2016; Sivandzade et al., 2019). Its overexpression prevented neurotoxicity in murine microglia and astrocytes (Sigfridsson et al., 2018; Heurtaux et al., 2021) but also protected neurons from potentially toxic insults (Shih et al., 2003; Bell and Robinson, 2011; Cui et al., 2016). Furthermore, pharmacological activators of Nrf2 are already in clinical development for treating traumatic brain injury, stroke, and cancer and could also be tested in NDDs (Robledinos-Antón et al., 2019; Zhou et al., 2020a).

Targeting senescence is also a promising avenue. Senotherapies target senescent cells to kill them or block their detrimental effects, e.g., growth arrest and the onset of a SASP (von Kobbe, 2019; Birch and Gil, 2020). Some senolytic cocktails relieved age-related

brain inflammation and improved brain function in mouse models of NDDs (Ogrodnik et al., 2021). Finally, epigenetic manipulation is a promising approach to modulate the state of brain cells and reverse ageing and senescence. Over the last years, potential epigenetic inhibitors have emerged (Verma and Kumar, 2018). DNA methylation inhibitors (Decitabine, Zebularine, and 5'Aza) but also histone deacetylase inhibitors (Trichostatin A, Vorinostat) have shown promising results in experimental models of NDDs (Narayan and Dragunow, 2010; Konsoula and Barile, 2012; Coppedè, 2014; Kim and Hong, 2014). The use of genome-engineering tools, e.g., the CRISPR/Cas9 system, could also emerge as potential epigenetic regulators to treat patients (Yao et al., 2015; Vojta et al., 2016).

Overall, maintaining protective astrocyte function or alleviating astrocyte neurotoxicity seems a promising avenue for AD and NDDs. However, before crystallizing such a strategy, it is crucial to map with more precision the detrimental phenotypes of astrocytes across ageing and age-associated NDDs.

AUTHOR CONTRIBUTIONS

DB, SF, TH, FJ, KF, and MM performed literature searches and wrote the manuscript. DB build the structure of the manuscript and made the figures with SF. All authors contributed to the article and approved the submitted version.

FUNDING

DB was supported by the Luxembourg Espoir-en-Tête Rotary Club award, the Auguste et Simone Prévot foundation, and the Agaajani family donation. SF was supported by the PRIDE program of the Luxembourg National Research Found through the grant PRIDE17/12244779/PARK-QC, and FJ was supported by the AFR FNR program. MM would like to thank the Luxembourg National Research Fond (FNR) for the support (FNR PEARL P16/BM/11192868 grant).

5.4. Conclusion

In summary, we highlighted the heterogeneity and context-dependent nature of astrocyte responses in NDDs. By integrating evidence from diverse methodologies and disease contexts, we shed light on the complex interplay between astrocyte reactivity, ageing, and disease progression, and discuss translational strategies aimed at mitigating astrocyte-driven neurotoxicity. This review underscores the importance of a system-level understanding of glial biology in neurodegeneration. Importantly, it reflects the evolving view that targeting non-neuronal cell types may hold key therapeutic promise in slowing or halting the progression of neurodegeneration.

Part V: Discussion

1. Hippocampal astrocytes exhibit complex heterogeneity and disease signatures.

1.1 GFAP labels a substantial subset of astrocytes and is severely reduced in AD patients.

By evaluating the expression of GFAP, AQP4 ALDH1L1, and ALDH7A1 in the hippocampus of CTLs individuals, we showed that GFAP is actually labelling only certain subsets of astrocytes that are specifically distributed in the hippocampus and within the hippocampal subregions. Indeed, we observed a patchy distribution in the pyramidal layers of the CA subfields as well as in the subiculum and the PHC, while the molecular, radiatum and oriens layers display an intense GFAP expression. Nonetheless, regions lacking GFAP expression are not devoid of astrocytes; they contain astrocytes expressing ALDH1L1, ALDH7A1, and to a lesser degree AQP4, all these markers showing a broader coverage of the astrocytic populations in the human hippocampus (**Manuscript I, Fig. 1, Supplementary Fig. 1B-E, Supplementary Fig. 3A-B, Supplementary Fig. 4**). These findings suggest ALDH1L1 and ALDH7A1 as more generic markers for hippocampal astrocytes.

Interestingly, our quantification data revealed a severe decrease of the expression of GFAP in AD patients across the hippocampus, although strong GFAP expression was observed in some focal areas where clusters of GFAP+ astrocytes and hypertrophic GFAP+ cells are evident (**Manuscript I, Fig. 4A-C, Fig. 5A-C, Supplementary Fig. 5A-C**). These findings contrast previous studies showing notably an upregulation of GFAP in both animal models (Kamphuis et al. 2012; Olsen et al. 2018) and AD brain patients (Simpson et al. 2010; Phillips et al. 2024). We explained our results by the fact that the brain samples we used reflect advanced stages of the disease during which astrocyte reactivity may decline or shifting to a neurotoxic phenotype (Ding et al. 2021; Livingston et al. 2022). ALDH1L1 expression is significantly reduced in both AD and PDD, while expression of ALDH7A1 is significantly decreased mainly in PDD patients (**Manuscript I, Fig. 4G-L**). Both proteins are widely involved in basic astrocytic functions; ALDH1L1 being associated to metabolic functions and ALDH7A1 to learning and memory processes, known to be affected in NDDs (Coughlin and Gospe 2023; Bou Ghanem et al. 2024; Salih et al. 2024; Yan et al. 2024; Doddaballapur et al. 2025). Interestingly, our quantification data show an increase of AQP4 expression in AD cases (**Manuscript I, Fig. 4D-F**). AQP4 is very well known for its crucial roles in ensuring and maintaining water and glymphatic homeostasis (Nagelhus and Ottersen 2013). Importantly, studies on AD models (Xu et al. 2015; Ishida et al. 2022; Pedersen et al. 2023) and patients (Zeppenfeld et al. 2017) have reported alterations in AQP4 expression and of its perivascular

localisation. Such alterations result in impaired clearance of Aβ and tau (MohanaSundaram et al. 2024), contributing to cognitive decline (Xu et al. 2015) and supporting astrocyte dysfunction associated with the neurovascular and glymphatic system.

Overall, our findings argue for a loss of astrocyte homeostatic signatures, suggesting astrocyte dysfunction (e.g. neurovascular, glymphatic, metabolic dysfunctions) in advanced stages of AD.

1.2 Glypican 5 identifies a subtype of astrocytes with a distinct disease signature.

Glypican 5 (GPC5) is a member of the glypican family of GPI-anchored heparan sulphate proteoglycans, expressed by astrocytes (among other cells). GPC5 has been shown to be associated with GFAP-low astrocyte population in previous single cell transcriptomic analysis (Habib et al. 2020). Our study showed that GPC5 labels a specific subtype of astrocytes that is distinct from GFAP+ astrocytes in terms of spatial distribution in the human hippocampus. Although both subtypes share a common core identity, we identified marker-specific molecular signatures (**Manuscript I, Fig. 2, Fig. 3, Supplementary Fig. 1, Supplementary Fig. 3C-E**) that may indicate marker-specific biological functions. While GFAP+ astrocytes would support a variety of functions, such as buffering the extracellular milieu or providing metabolic and physical support to neurons (see **Part II, 2.1 "The core roles of the astrocytes in the healthy brain."**), GPC5+ cells may specialise in synaptic maturation and stabilisation, given their synaptogenic properties (Bosworth et al. 2023; Salas et al. 2024b). Moreover, our quantification data showed that GPC5+ and GFAP+ subtypes were differently affected in NDDs with GPC5 expression remaining comparable in AD and PDD to CTLs (**Manuscript I, Fig. 4M-O**). However, the spatial distribution of GPC5+ astrocytes in AD appeared sparser with GPC5+ cells tending to form small clusters. Interestingly, we observed in AD hippocampi GPC5+ astrocytes polarised towards Aβ plaques, together with GFAP+ and AQP4+ astrocytes. We also found several GPC5+ astrocytes surrounding pS396+ tau tangles (**Manuscript I, Fig. 5, Fig. 6, Supplementary Fig. 5, Supplementary Fig. 6**), suggesting GPC5 astrocytes to be associated with amyloid deposition and potentially with advanced stages of tau pathology.

Nevertheless, further research may help clarify the relationship between these astrocyte subtypes and amyloid or tau pathology. One possible avenue of investigation would be to determine whether the GFAP+ and GPC5+ astrocytes that we found to be polarised towards Aβ plaques constitute distinct subpopulations within the broader population of Aβ-containing astrocytes. Indeed, previous neuropathological studies have described morphologically distinct astrocyte populations associated with different amyloid structures. These include astrocytes associated with fleecy amyloid and

containing N-terminal-truncated Aβ (Thal et al. 2000; Lasagna-Reeves and Kayed 2011; Funato et al. 1998; Nagele et al. 2003). As fleecy amyloid deposits have been reported in the entorhinal cortex and are associated with early stages of Alzheimer's disease (Thal et al. 2000), it implies to extend the study beyond the hippocampus and include cases representing earlier disease stages.

Overall, our study suggests ALDH1L1 and ALDH7A1 as broader canonical markers than GFAP, and the use of a set of astrocytic markers (including AQP4) to better evaluate astrocyte changes in healthy and diseased conditions. We identified two astrocytic subpopulations that exhibit distinct profiles and responses to diseased states, reinforcing the idea that astrocyte identity changes across both spatial and temporal axes of neurodegeneration.

2. Noradrenaline shapes astrocyte identity and responses

2.1. Catecholamines induce distinct phenotypic and molecular changes in primary mouse astrocytes.

By analysing the transcriptomic profile of astrocytes exposed to NA versus non-exposed astrocytes, we showed that NA strongly influences astrocyte physiology and responses (**Manuscript II, Fig. 1**). In physiological conditions, NA modulates core functions of the astrocytes by influencing the expression of genes that are involved in blood flow regulation (*Cbs, Snta1, Aqp4*), responses to inflammation (*Ptgs2, Vim*) and oxidative stress (*Sod3, Nqo1, Hmox1*), neuroprotection (*Scg2*), regulation of the synaptogenesis (*Snta1, EphB2, Sparc*), but also genes related to the circadian clock (*Cartpt, Bdnf*).
To investigate whether these modulatory properties are specific to NA or a shared feature by the catecholamines in general, we decided to analyse the transcriptome profile of astrocytes exposed to DA (**Manuscript II, Fig. 2**). Our results revealed DA as another strong modulator of astrocyte molecular identity. We showed that astrocyte signatures and responses to NA and DA are partially overlapping, most of the DEGs being shared in both conditions (**Manuscript II, Fig. 2D**). However, we found some genes that were specific for either NA or DA. For example, *Cbs* was found significantly up-regulated upon NA exposure only. *Cbs* codes for the hydrolase enzyme cystathionine-β-synthase (CBS) that is a key enzyme for the homocysteine (Hcy) metabolism (Jhee and Kruger 2005). Importantly, CBS catalyses the production of cysteine, which is a precursor of both glutathione (GSH) and hydrogen sulfide (H_2S), two potent antioxidant molecules (Lee et al. 2009; Dey et al. 2023). In parallel, DA exposure induces significant up-regulation of *Srxn1*, coding for the sulfiredoxin-1 protein, another powerful antioxidant factor protecting from oxidative stress and apoptosis induced by H_2O_2 exposure (Zhou et al. 2015).

These results emphasise the potent antioxidant properties of catecholamine-sensitive astrocytes. Interestingly, DA exposure results in a significant down-regulation of genes associated to the complement pathways, such as *C3*, *C4a* and *C4b*, whereas NA induces significant up-regulation of certain genes that can be associated to a pro-inflammatory response (e.g. *Vim, Il33, Ptsg2*). This suggests that, under homeostatic conditions, NA and DA may play complementary roles in astrocyte surveillance: NA could support basal, low-level expression of some pro-inflammatory mediators, while DA could counterbalance by reducing the expression and/or secretion of others.

2.2. Noradrenaline mitigates the response of astrocytes to inflammation.

To understand whether NA influences astrocyte responses to inflammation, we exposed astrocytes to a mix of cytokines mimicking inflammatory conditions. Transcriptomic analyses (RNAseq) confirmed strong molecular changes of the astrocytes in response to inflammation with up-regulation of many genes involved in inflammatory pathways such as type II interferon (*Gbp2, Irf1, Stat1*) and NFκB signalling pathways (*Nfkb1, Ikbkb, Tnf*) (**Manuscript II, Fig. 3A-B**). When exposed to NA (**Manuscript II, Fig. 3C-D**), we observed that astrocytes mitigate their responses to inflammation by down-regulating certain genes that are notably implicated in antigen processing and presentation (*Ciita, H2-DMa, H2-Ab1*), as well as in complement (*C3*), NFκB (*Tollip, Ikbkb, Ikbkg*) and interferon (*Gbp6, Gbp10, Gbp11, Ifi27*) pathways. We confirmed these observations by analysing the secretome of these cells that indicated a reduced release of certain cytokines (IL6) and chemokines (CXCL2, CXCL9) (**Manuscript II, Fig. 3F**). However, these data were obtained from qualitative tests (cytokine assays) and need to be further validated with quantitative experiments (e.g., ELISA tests).

We also showed that NA exerts a non-cell-autonomous immunomodulatory effect. Indeed, by exposing reactive microglia (LPS stimulation) to the medium of NA-exposed astrocytes (**Manuscript II, Fig. 3G-H**), we observed a modulation of microglia inflammatory responses, notably with a decrease of *Tnfa* gene expression. Nevertheless, these results should be validated regarding the effect of NA exposure on microglia molecular signatures. To this purpose, we performed RNAseq on NA-exposed microglia compared to non-exposed microglia. The resulting data is currently being analysed.

Together, these results suggest that a depletion of NA levels, as observed in disease conditions, might affect several core roles of the astrocytes leading to dysfunction of fundamental functions such as synaptic plasticity, vascular tone and glymphatic drainage. To assess this assumption, we investigated certain NA-targeted genes identified in our RNA-seq data in *post-mortem* samples from AD and PDD patients, as well as from age-matched individuals.

2.3. Dysregulation of the noradrenergic system affects key astrocytic proteins in AD and PDD.

Using cIHC and digital pathology, we mapped and quantified the expression of VMAT2, CBS, SPARC, VIM and BACE2. To address whether hippocampal NA efferences are affected in our collection of samples, we stained for and quantified VMAT2 that indirectly reveals NA projections (**Manuscript II, Fig. 4**). Our results showed a partial alteration of the NA efferences in the hippocampus of patients with AD, although no significance was obtained. Such alteration might affect NA levels in the hippocampus, thus altering the phenotype and/or responses of NA-sensitive cells of the hippocampal areas. However, to characterise the NA efferences in the hippocampus more precisely, this analysis should be supplemented with a quantification of DBH expression. Indeed, DBH (dopamine β-hydroxylase) is responsible for the conversion of DA into NA, making it more specific to NA projections.

To determine whether a potential reduction in NA efferences could impact astrocytic signatures, we analysed the expression of CBS, SPARC, VIM and BACE2, proteins encoded by genes previously identified *in vitro* as NA-sensitive. CBS staining revealed a strong labelling of hippocampal astrocytes throughout the hippocampus, with an enrichment in the CA4 subfield as well as in the pyramidal layer of the CA (**Manuscript II, Fig. 5A**). Multiplex staining showed that all GFAP+ astrocytes also expressed CBS, whereas many CBS+ astrocytes were single-positive (**Manuscript II, Fig. 5B**). The latter were mainly double-positive CBS+/ALDH1L1+, although we found single-positive astrocytes for either CBS+ or ALDH1L1+ (**Manuscript II, Fig. 5C**). The quantitative analysis of CBS expression in AD and PDD hippocampi revealed a severe decrease of CBS in both diseases compare to CTLs (**Manuscript II, Fig. 5D**). These results are in line with the literature that reports predominant expression of CBS in astrocytes as well as a decrease of its expression in aging brain (Dey et al. 2023). Dey and colleagues showed that the loss of CBS expression in astrocytes leads to mitochondrial dysfunction and increased levels of ROS. This was accompanied by a decrease of H_2S production that has been shown to be severely decreased in AD patients (Eto et al. 2002), resulting in increased oxidative damages (Tabassum et al. 2020). Furthermore, it is reported that a loss of CBS activity leads to hyperhomocysteinemia (HHcy), which is characterised by elevated plasma Hcy levels (Kamath et al. 2006). Such elevated Hcy levels have been shown to affect brain microvessels and compromise BBB integrity in mice. This establishes HHcy as a risk factor for ischemic stroke (Kamath et al. 2006) and cerebral small vessel disease (Hassan 2004), which is one of the most common causes of vascular contributions to cognitive impairment and dementia (Hainsworth et al. 2016). Previous research has also demonstrated an association between HHcy and hippocampal atrophy in patients with AD (Clarke et al. 1998). All these studies highlight the role of homocysteine metabolism in AD development and suggest that CBS plays

a central role in the pathophysiology of NDDs. Hence, our findings support disruption of the CBS/H_2S/homocysteine pathway in AD but also in PDD patients and reinforce the hypothesis of disrupted astrocytic functions in NDDs.

SPARC staining was enriched in hippocampal astrocytes across the hippocampus (**Manuscript II, Supplementary Fig. 3A**). Interestingly, our quantitative analysis revealed a strong decrease of SPARC expression in patients with PDD (**Manuscript II, Supplementary Fig. 3B-C**). Physiologically, SPARC is essential for BBB homeostasis and is involved in tissue repair and remodeling as well as in inflammation and immune regulation (McGovern et al. 2021; Yang et al. 2024). SPARC also plays a fundamental role in synapse development (Jones and Bouvier 2014). In the human brain, SPARC has been shown to be upregulated in reactive astrocytes close to brain tumours but also in patients suffering of CNS disorders, including epilepsy, stroke and AD (Jones and Bouvier 2014; Strunz et al. 2019; Yang et al. 2025). However, to our knowledge, there is no evidence of a direct involvement of SPARC in PD(D) pathogenesis. Due to its fundamental roles described above, a loss of SPARC expression could impair certain astrocytic functions, including vascular support and BBB integrity.

VIM immunostaining predominantly labeled blood vessels, with additional labelling of a subset of hippocampal astrocytes, whereas BACE2 marked only a small number of astrocytes (**Manuscript II, Supplementary Fig. 3D,G**). Quantitative analyses indicated largely unchanged expression of both markers across hippocampal subregions and disease conditions, except from a significant increase in BACE2 expression in the CA4 of PDD patients compared to AD cases and a significant decrease in VIM expression in the PHC of PDD patients compared to CTLs (**Manuscript II, Supplementary Fig. 3E-F, H-I**). However, these results require further validation by increasing the number of replicates for each condition.

VIM, together with GFAP, is a type III intermediate filament and component of the astrocytic cytoskeleton. The upregulation of both markers is usually indicative of reactive astrogliosis, notably observed surrounding Ab plaques in AD (Calvo et al. 1991; Pixley and De Vellis 1984; O'Leary et al. 2020). Importantly, *in vivo* studies have reported that VIM deletion ($Vim^{-/-}$ mouse model) affects synaptic plasticity and hippocampal neurogenesis, thereby resulting in deficits in learning and memory processes, and notably accelerated forgetting (Zhang et al. 2025; Wilhelmsson et al. 2019). In this context, the reduced VIM expression observed in PDD may reflect compromised astrocytic and cytoskeletal responses to ongoing neurodegeneration, thereby limiting neuronal support mechanisms and contributing to the progression of cognitive decline.

BACE2 is a close homologue of BACE1, which is recognised as the main β-secretase involved in the amyloidogenic pathway. BACE2, however, is involved in both the amyloidogenic and non-amyloidogenic pathways of AβAPP processing (Yeap et al. 2023). Notably, increased BACE2 expression has been reported in patients with MCI and preclinical AD, while an inverse correlation with Braak stages has been observed in advanced AD. This supports the idea that BACE2 upregulation may be an early event in neurodegenerative processes (Yeap et al. 2023). Thus, given the early NA depletion observed in NDDs, it is plausible that reduced NA signalling contributes to the dysregulation of BACE2 expression in astrocytes. Such alterations could shift APP processing towards increased amyloidogenic activity, thereby promoting Aβ accumulation and plaque formation. Furthermore, these data further support the concept of shared molecular pathways between AD and PDD (Compta et al. 2011; McKeith et al. 2017b; Wakasugi and Hanakawa 2021; Zhou et al. 2025; Canal-Garcia et al. 2025).

Taken together, these results suggest that progressive loss of NA efferences contributes to astrocyte dysfunction and may exacerbate neurodegenerative processes by compromising homeostatic, metabolic, and neuroprotective astrocyte functions.

Finally, it should be noted that, for both studies, we did control for age and sex in our statistical analyses of the human *post-mortem* samples. However, neither parameter had a significant effect on the measured outcomes, nor modified the observed group differences. For this reason, age and sex were not represented in the quantification plots, as their inclusion did not provide additional interpretative value and would have reduced figure readability. Nevertheless, we acknowledge that including these variables in the visual representation could enhance transparency further. We are therefore currently exploring alternative chart designs that would allow age and sex to be included without compromising clarity.

Part VI: Conclusions & Perspectives

In recent decades, evidence has emerged indicating that astrocytes play an active role on the onset and progression of neurodegeneration. On the other hand, continuous research efforts on the LC-noradrenergic system over the past forty years have demonstrated its early vulnerability to neurodegeneration, progressively disrupting NA levels within the CNS. The main aims of this PhD project were to (**i**) understand the multifaceted responses of astrocytes in NDDs; (**ii**) better characterise the heterogeneity of hippocampal astrocytes in both healthy and diseased conditions; and (**iii**) identify the modulatory role of NA on astrocyte physiology and understand whether their responses might be affected by NA progressive depletion in neurodegeneration. To address these objectives, we first reviewed the evidence collected on astrocyte neurotoxic signatures in ageing and NDDs. Then, using human *post-mortem* samples from healthy individuals, AD and PDD patients, we highlighted the considerable heterogeneity of hippocampal astrocytes and identified two distinct astrocytic subtypes with divergent identity and responses to neurodegeneration. Finally, we addressed astrocytic transcriptional and functional changes upon NA exposure and/or inflammatory conditions using murine primary cells. Using a translational approach, we investigated whether NA-targeted genes are affected by neurodegeneration in human AD and PDD *post-mortem* samples.

The main findings of this thesis can be summarised as follows: (**i**) Hippocampal astrocytes exhibit significant heterogeneity across the entire hippocampus, including between and within subfields and subfield layers. This diversity is reflected in their molecular profiles, spatial distribution and morphological features. (**ii**) GFAP labels only a subpopulation of astrocytes, while ALDH1L1 and ALDH7A1 are broader astrocytic markers. Therefore, the astrocyte identity should be determined using a combination of multiple astrocytic markers rather than relying on a single marker. (**iii**) Astrocyte heterogeneity is affected in NDDs, notably with decreased expression of GFAP in AD and of ALDH1L1 and ALDH7A1 in both AD and PDD. In contrast, AQP4 expression is increased in AD patients. Certain markers, such as GPC5 that identifies a distinct subgroup of astrocytes with specific disease signatures, remain stable throughout ageing and NDDs. Thus, distinct subtypes of astrocytes might promote selective vulnerability, evolving along the spatial and temporal trajectory of NDDs. (**iv**) NA and DA exert a strong phenotypic control on astrocyte physiology and responses, notably by regulating core astrocytic functions. (**v**) NA mitigates astrocytes and microglia responses to inflammation by modulating their pro-inflammatory profile. (**vi**) In AD patients, NA efferences in the hippocampus might

be altered, leading to an imbalance in NA levels. (**vii**) In the human hippocampus, certain genes that we identified to be NA-sensitive targets in primary mouse astrocytes, such as *Cbs* and *Sparc,* are strongly expressed by hippocampal astrocytes, but also severely affected in NDDs. Therefore, disruption of the NA system might lead to imbalanced NA levels in the hippocampus and progressively affect the expression of key astrocytic proteins, thus impacting core functions of the astrocytes and, *in fine,* pathology progression.

Overall, this PhD thesis highlights the central role of the astrocytes in brain function and the intimate relationship between this glial cell type and the NA system. Our results support the hypothesis of direct and indirect effects of NA on astrocyte signatures and their responses to physiological and pathological stimuli. They also suggest that astrocyte identity and heterogeneity are partly influenced by NA and certainly by catecholamines in general. Our work strengthens the idea that, alongside microglia, astrocytes are crucial for neuroprotection and play an active role in the brain's immune response (Fisher and Liddelow 2024b). This makes astrocytes as promising targets for new therapeutic approaches, notably those aimed at enhancing resilience against neurodegeneration (De La Fuente et al. 2023; Wareham et al. 2022).

Nevertheless, this pioneer work on the human hippocampus needs further refinement, notably by integrating new astrocytic markers (e.g. AQP1, ITPKA) but also new analytic tools to improve the mapping and quantification of these markers. Moreover, additional studies exploring other key brain regions implicated in NDDs (e.g. LC, substantia nigra, amygdala, PFC) are essential to refine the characterisation of astrocyte identity in the human brain. This would help to further elucidate whether neurodegeneration impacts astrocytic identity and heterogeneity and clarify the critical role of astrocytes in the onset and/or progression of neurodegeneration. This also implies to develop a correlation tool in order to understand the potential association of certain astrocytic markers with pathological ones, such as 4G8, AT8 and pS396. *In vitro* and *in vivo* studies using induced pluripotent stem cells, brain organoids and conditioned knockout models are necessary to investigate the markers we studied, including GPC5 and CBS, and better understand their physiological functions and their implication in disease progression. Indeed, the neuroprotective properties of both markers, GPC5 and CBS, make them as potential interesting targets for therapeutic approaches. Furthermore, it is crucial to precisely define the distribution of the NA receptors and understand whether certain astrocyte populations might be more sensitive to NA signalling and finally more vulnerable to neurodegeneration when NA levels are disrupted. Such investigations require cutting-edge technologies such as single cell

RNA sequencing and/or spatial transcriptomic and proteomic. Moreover, there is a real need to develop antibodies that can specifically target different NA receptor subtypes. This would help refine the mapping of NA receptor expression. It would be also interesting to analyse the potential correlations between the NA system (e.g. VMAT2 and NA receptors) and concomitant misfolded pathology markers (e.g. 4G8, AT8, pS396, pSyn), in order to determine whether proteinopathy affect the disruption of the NA system. Furthermore, by demonstrating the potent modulatory effect of DA on the transcriptomic signatures of astrocytes, we have opened up new avenues of research into the global effects of catecholamines on glial cell identity and activity, and on the ability of the cells to integrate simultaneous catecholaminergic signalling. Ultimately, expanding these investigations beyond astrocytes to include microglia, oligodendrocytes, as well as infiltrating immune cells, will be essential for achieving a more comprehensive understanding of the cellular mechanisms underlying NDDs. Furthermore, accumulating evidence highlights the involvement of glial cells, including astrocytes, in psychiatric disorders (e.g. schizophrenia, anxiety disorders, and ADHD) which are also shaped by dysfunction of the catecholaminergic systems, particularly NA and DA systems (Yamamoto et al. 2014; Brisch et al. 2014; Bacchi 2025; Mäki-Marttunen et al. 2020). Thus, an in-depth exploration of the glial–noradrenergic/dopaminergic interplay would not only advance our understanding of neurodegenerative processes, but also open up promising avenues into broader fields such as psychiatric disorders.

Part VII: Thesis References

Abdelhak, Ahmed, Matteo Foschi, Samir Abu-Rumeileh, et al. 2022. 'Blood GFAP as an Emerging Biomarker in Brain and Spinal Cord Disorders'. *Nature Reviews Neurology* 18 (3): 158–72. https://doi.org/10.1038/s41582-021-00616-3.

Af Bjerkén, Sara, Rasmus Stenmark Persson, Anna Barkander, et al. 2019. 'Noradrenaline Is Crucial for the Substantia Nigra Dopaminergic Cell Maintenance'. *Neurochemistry International* 131 (December): 104551. https://doi.org/10.1016/j.neuint.2019.104551.

Ağaç, Didem, Leonardo D. Estrada, Robert Maples, Lora V. Hooper, and J. David Farrar. 2018. 'The B2-Adrenergic Receptor Controls Inflammation by Driving Rapid IL-10 Secretion'. *Brain, Behavior, and Immunity* 74 (November): 176–85. https://doi.org/10.1016/j.bbi.2018.09.004.

Alafuzoff, Irina, Paul G. Ince, Thomas Arzberger, et al. 2009. 'Staging/Typing of Lewy Body Related α-Synuclein Pathology: A Study of the BrainNet Europe Consortium'. *Acta Neuropathologica* 117 (6): 635–52. https://doi.org/10.1007/s00401-009-0523-2.

Almeida, Zaida L., Daniela C. Vaz, and Rui M. M. Brito. 2025. 'Morphological and Molecular Profiling of Amyloid-β Species in Alzheimer's Pathogenesis'. *Molecular Neurobiology* 62 (4): 4391–419. https://doi.org/10.1007/s12035-024-04543-4.

Andrews, Shea J., Alan E. Renton, Brian Fulton-Howard, Anna Podlesny-Drabiniok, Edoardo Marcora, and Alison M. Goate. 2023. 'The Complex Genetic Architecture of Alzheimer's Disease: Novel Insights and Future Directions'. *eBioMedicine* 90 (April): 104511. https://doi.org/10.1016/j.ebiom.2023.104511.

Ardestani, Pooneh Memar, Andrew K. Evans, Bitna Yi, Tiffany Nguyen, Laurence Coutellier, and Mehrdad Shamloo. 2017. 'Modulation of Neuroinflammation and Pathology in the 5XFAD Mouse Model of Alzheimer's Disease Using a Biased and Selective Beta-1 Adrenergic Receptor Partial Agonist'. *Neuropharmacology* 116 (April): 371–86. https://doi.org/10.1016/j.neuropharm.2017.01.010.

Arias-Carrión, Oscar, Magdalena Guerra-Crespo, Francisco J. Padilla-Godínez, Luis O. Soto-Rojas, and Elías Manjarrez. 2025. 'α-Synuclein Pathology in Synucleinopathies: Mechanisms, Biomarkers, and Therapeutic Challenges'. *International Journal of Molecular Sciences* 26 (11): 5405. https://doi.org/10.3390/ijms26115405.

Aston-Jones, Gary, and Jonathan D. Cohen. 2005. 'AN INTEGRATIVE THEORY OF LOCUS COERULEUS-NOREPINEPHRINE FUNCTION: Adaptive Gain and Optimal Performance'. *Annual Review of Neuroscience* 28 (1): 403–50. https://doi.org/10.1146/annurev.neuro.28.061604.135709.

Augustinack, Jean C., Anja Schneider, Eva-Maria Mandelkow, and Bradley T. Hyman. 2002. 'Specific Tau Phosphorylation Sites Correlate with Severity of Neuronal Cytopathology in Alzheimer's Disease'. *Acta Neuropathologica* 103 (1): 26–35. https://doi.org/10.1007/s004010100423.

Bacchi, André Demambre. 2025. 'Beyond the Neuron: The Integrated Role of Glia in Psychiatric Disorders'. *Neuroglia* 6 (2): 15. https://doi.org/10.3390/neuroglia6020015.

Bae, Jonghyun, Zhaoyuan Gong, Caio Mazucanti, et al. 2025. 'Age-Related Differences in Rostral-Middle Locus Coeruleus Microstructure: A Critical Role in Cognitive Decline Revealed by Magnetic Resonance Relaxometry'. *Alzheimer's Research & Therapy* 17 (1): 161. https://doi.org/10.1186/s13195-025-01809-4.

Baldwin, Katherine T., Keith K. Murai, and Baljit S. Khakh. 2024. 'Astrocyte Morphology'. *Trends in Cell Biology* 34 (7): 547–65. https://doi.org/10.1016/j.tcb.2023.09.006.

Bancher, C., C. Brunner, H. Lassmann, et al. 1989. 'Accumulation of Abnormally Phosphorylated τ Precedes the Formation of Neurofibrillary Tangles in Alzheimer's Disease'. *Brain Research* 477 (1–2): 90–99. https://doi.org/10.1016/0006-8993(89)91396-6.

Batiuk, Mykhailo Y., Araks Martirosyan, Jérôme Wahis, et al. 2020. 'Identification of Region-Specific Astrocyte Subtypes at Single Cell Resolution'. *Nature Communications* 11 (1): 1220. https://doi.org/10.1038/s41467-019-14198-8.

Beach, Thomas G., Charles H. Adler, LihFen Lue, et al. 2009. 'Unified Staging System for Lewy Body Disorders: Correlation with Nigrostriatal Degeneration, Cognitive Impairment and Motor Dysfunction'. *Acta Neuropathologica* 117 (6): 613–34. https://doi.org/10.1007/s00401-009-0538-8.

Bekar, Lane K., Wei He, and Maiken Nedergaard. 2008. 'Locus Coeruleus α-Adrenergic–Mediated Activation of Cortical Astrocytes In Vivo'. *Cerebral Cortex* 18 (12): 2789–95. https://doi.org/10.1093/cercor/bhn040.

Bélanger, Mireille, Igor Allaman, and Pierre J. Magistretti. 2011. 'Brain Energy Metabolism: Focus on Astrocyte-Neuron Metabolic Cooperation'. *Cell Metabolism* 14 (6): 724–38. https://doi.org/10.1016/j.cmet.2011.08.016.

Bellier, Félix, Augustin Walter, Laure Lecoin, Fréderic Chauveau, Nathalie Rouach, and Armelle Rancillac. 2025. 'Astrocytes at the Heart of Sleep: From Genes to Network Dynamics'. *Cellular and Molecular Life Sciences* 82 (1): 207. https://doi.org/10.1007/s00018-025-05671-3.

Benedet, Andréa L., Marta Milà-Alomà, Agathe Vrillon, et al. 2021. 'Differences Between Plasma and Cerebrospinal Fluid Glial Fibrillary Acidic Protein Levels Across the Alzheimer Disease Continuum'. *JAMA Neurology* 78 (12): 1471. https://doi.org/10.1001/jamaneurol.2021.3671.

Beretta, Chiara, Abdulkhalek Dakhel, Khalid Eltom, et al. 2025. 'Astrocytic Lipid Droplets Contain MHCII and May Act as Cogs in the Antigen Presentation Machinery'. *Journal of Neuroinflammation* 22 (1): 117. https://doi.org/10.1186/s12974-025-03452-0.

Berge, Simone A. van den, Josta T. Kevenaar, Jacqueline A. Sluijs, and Elly M. Hol. 2012. 'Dementia in Parkinson's Disease Correlates with α-Synuclein Pathology but Not with Cortical Astrogliosis'. *Parkinson's Disease* 2012: 420957. https://doi.org/10.1155/2012/420957.

Berridge, Craig W, and Barry D Waterhouse. 2003. 'The Locus Coeruleus–Noradrenergic System: Modulation of Behavioral State and State-Dependent Cognitive Processes'. *Brain Research Reviews* 42 (1): 33–84. https://doi.org/10.1016/S0165-0173(03)00143-7.

Bertrand, E., W. Lechowicz, G. M. Szpak, and J. Dymecki. 1997. 'Qualitative and Quantitative Analysis of Locus Coeruleus Neurons in Parkinson's Disease'. *Folia Neuropathologica* 35 (2): 80–86.

Bharani, Krishna L., Rebecca Derex, Ann-Charlotte Granholm, and Aurélie Ledreux. 2017. 'A Noradrenergic Lesion Aggravates the Effects of Systemic Inflammation on the Hippocampus of Aged Rats'. *PLOS ONE* 12 (12): e0189821. https://doi.org/10.1371/journal.pone.0189821.

Bocchi, Riccardo, Manja Thorwirth, Tatiana Simon-Ebert, et al. 2025. 'Astrocyte Heterogeneity Reveals Region-Specific Astrogenesis in the White Matter'. *Nature Neuroscience* 28 (3): 457–69. https://doi.org/10.1038/s41593-025-01878-6.

Bogdanović Pristov, Jelena, Danijela Bataveljić, Dunja Bijelić, Katarina Milićević, Jelena Korać Jačić, and Ljiljana Nikolić. 2025. 'Norepinephrine-Induced Intracellular Ca^{2+} Increase Is Coupled with Astrocytic BK Channel Activation and Capillary Response'. *American Journal of Physiology-Cell Physiology* 329 (4): C1061–74. https://doi.org/10.1152/ajpcell.00538.2025.

Bork, Peter A. R., Antonio Ladrón-de-Guevara, Anneline H. Christensen, Kaare H. Jensen, Maiken Nedergaard, and Tomas Bohr. 2023. 'Astrocyte Endfeet May Theoretically Act as Valves to Convert Pressure Oscillations to Glymphatic Flow'. *Journal of The Royal Society Interface* 20 (204). https://doi.org/10.1098/rsif.2023.0050.

Bosworth, Ap, M Contreras, S Weiser Novak, et al. 2023. 'Astrocyte Glypican 5 Regulates Synapse Maturation and Stabilization'. Preprint, Neuroscience, March 2. https://doi.org/10.1101/2023.03.02.529949.

Bou Ghanem, Ayman, Yaman Hussayni, Raghid Kadbey, et al. 2024. 'Exploring the Complexities of 1C Metabolism: Implications in Aging and Neurodegenerative Diseases'. *Frontiers in Aging Neuroscience* 15 (January): 1322419. https://doi.org/10.3389/fnagi.2023.1322419.

Bouvier, David S., Sonja Fixemer, Tony Heurtaux, Félicia Jeannelle, Katrin B. M. Frauenknecht, and Michel Mittelbronn. 2022. 'The Multifaceted Neurotoxicity of Astrocytes in Ageing and Age-Related Neurodegenerative Diseases: A Translational Perspective'. *Frontiers in Physiology* 13. https://www.frontiersin.org/articles/10.3389/fphys.2022.814889.

Bouvier, David S., Emma V. Jones, Gaël Quesseveur, et al. 2016. 'High Resolution Dissection of Reactive Glial Nets in Alzheimer's Disease'. *Scientific Reports* 6 (April): 24544. https://doi.org/10.1038/srep24544.

Bouvier, David S., and Keith K. Murai. 2015. 'Synergistic Actions of Microglia and Astrocytes in the Progression of Alzheimer's Disease'. *Journal of Alzheimer's Disease* 45 (4): 1001–14. https://doi.org/10.3233/JAD-143156.

Braak, H., and E. Braak. 1988. 'Neuropil Threads Occur in Dendrites of Tangle—Bearing Nerve Cells'. *Neuropathology and Applied Neurobiology* 14 (1): 39–44. https://doi.org/10.1111/j.1365-2990.1988.tb00864.x.

Braak, H., and E. Braak. 1991. 'Neuropathological Stageing of Alzheimer-Related Changes'. *Acta Neuropathologica* 82 (4): 239–59. https://doi.org/10.1007/BF00308809.

Braak, Heiko, and Kelly Del Tredici. 2011. 'The Pathological Process Underlying Alzheimer's Disease in Individuals under Thirty'. *Acta Neuropathologica* 121 (2): 171–81. https://doi.org/10.1007/s00401-010-0789-4.

Braak, Heiko, Dietmar R. Thal, Estifanos Ghebremedhin, and Kelly Del Tredici. 2011. 'Stages of the Pathologic Process in Alzheimer Disease: Age Categories From 1 to 100 Years'. *Journal of Neuropathology & Experimental Neurology* 70 (11): 960–69. https://doi.org/10.1097/nen.0b013e318232a379.

Braak, Heiko, Kelly Del Tredici, Udo Rüb, Rob A.I De Vos, Ernst N.H Jansen Steur, and Eva Braak. 2003. 'Staging of Brain Pathology Related to Sporadic Parkinson's Disease'. *Neurobiology of Aging* 24 (2): 197–211. https://doi.org/10.1016/S0197-4580(02)00065-9.

Brancaccio, Marco, Mathew D. Edwards, Andrew P. Patton, et al. 2019. 'Cell-Autonomous Clock of Astrocytes Drives Circadian Behavior in Mammals'. *Science* 363 (6423): 187–92. https://doi.org/10.1126/science.aat4104.

Braun, David, Jose Madrigal, and Douglas Feinstein. 2014. 'Noradrenergic Regulation of Glial Activation: Molecular Mechanisms and Therapeutic Implications'. *Current Neuropharmacology* 12 (4): 342–52. https://doi.org/10.2174/1570159X12666140828220938.

Bringmann, Andreas, Thomas Pannicke, Bernd Biedermann, et al. 2009. 'Role of Retinal Glial Cells in Neurotransmitter Uptake and Metabolism'. *Neurochemistry International* 54 (3–4): 143–60. https://doi.org/10.1016/j.neuint.2008.10.014.

Brisch, Ralf, Arthur Saniotis, Rainer Wolf, et al. 2014. 'The Role of Dopamine in Schizophrenia from a Neurobiological and Evolutionary Perspective: Old Fashioned, but Still in Vogue'. *Frontiers in Psychiatry* 5 (May). https://doi.org/10.3389/fpsyt.2014.00047.

Bueichekú, Elisenda, Ibai Diez, Chan-Mi Kim, et al. 2024. 'Spatiotemporal Patterns of Locus Coeruleus Integrity Predict Cortical Tau and Cognition'. *Nature Aging* 4 (5): 625–37. https://doi.org/10.1038/s43587-024-00626-y.

Bussière, Thierry, Frédérique Bard, Robin Barbour, et al. 2004. 'Morphological Characterization of Thioflavin-S-Positive Amyloid Plaques in Transgenic Alzheimer Mice and Effect of Passive Aβ Immunotherapy on Their Clearance'. *The American Journal of Pathology* 165 (3): 987–95. https://doi.org/10.1016/S0002-9440(10)63360-3.

Cahoy, John D., Ben Emery, Amit Kaushal, et al. 2008. 'A Transcriptome Database for Astrocytes, Neurons, and Oligodendrocytes: A New Resource for Understanding Brain Development and Function'. *The Journal of Neuroscience* 28 (1): 264–78. https://doi.org/10.1523/JNEUROSCI.4178-07.2008.

Cajal, Santiago Ramón y. 1913. *Un Nuevo Proceder Para La Impregnación de La Neuroglía*.

Calvo, J.L., A.L. Carbonell, and J. Boya. 1991. 'Co-Expression of Glial Fabrillary Acidic Protein and Vimentin in Reactive Astrocytes Following Brain Injury in Rats'. *Brain Research* 566 (1–2): 333–36. https://doi.org/10.1016/0006-8993(91)91720-L.

Canal-Garcia, Anna, Rui M. Branca, Paul T. Francis, et al. 2025. 'Proteomic Signatures of Alzheimer's Disease and Lewy Body Dementias: A Comparative Analysis'. *Alzheimer's & Dementia* 21 (1): e14375. https://doi.org/10.1002/alz.14375.

Carotenuto, Antonio, Laura Cacciaguerra, Elisabetta Pagani, Paolo Preziosa, Massimo Filippi, and Maria A Rocca. 2022. 'Glymphatic System Impairment in Multiple Sclerosis: Relation with Brain Damage and Disability'. *Brain* 145 (8): 2785–95. https://doi.org/10.1093/brain/awab454.

Chai, Hua, Blanca Diaz-Castro, Eiji Shigetomi, et al. 2017. 'Neural Circuit-Specialized Astrocytes: Transcriptomic, Proteomic, Morphological, and Functional Evidence'. *Neuron* 95 (3): 531-549.e9. https://doi.org/10.1016/j.neuron.2017.06.029.

Chen, Alex B., Marc Duque, Altyn Rymbek, et al. 2025. 'Norepinephrine Changes Behavioral State through Astroglial Purinergic Signaling'. *Science* 388 (6748): 769–75. https://doi.org/10.1126/science.adq5233.

Chen, Wenchao, Chuntian Liang, Shasha Peng, et al. 2025. 'Aquaporin-4 Activation Facilitates Glymphatic System Function and Hematoma Clearance Post-intracerebral Hemorrhage'. *Glia* 73 (2): 368–80. https://doi.org/10.1002/glia.24639.

Chen, Yaxing, Chen Qin, Jianhan Huang, et al. 2020. 'The Role of Astrocytes in Oxidative Stress of Central Nervous System: A Mixed Blessing'. *Cell Proliferation* 53 (3): e12781. https://doi.org/10.1111/cpr.12781.

Chiotis, Konstantinos, Charlotte Johansson, Elena Rodriguez-Vieitez, et al. 2023. 'Tracking Reactive Astrogliosis in Autosomal Dominant and Sporadic Alzheimer's Disease with Multi-Modal PET and Plasma GFAP'. *Molecular Neurodegeneration* 18 (1): 60. https://doi.org/10.1186/s13024-023-00647-y.

Christopherson, Karen S., Erik M. Ullian, Caleb C.A. Stokes, et al. 2005. 'Thrombospondins Are Astrocyte-Secreted Proteins That Promote CNS Synaptogenesis'. *Cell* 120 (3): 421–33. https://doi.org/10.1016/j.cell.2004.12.020.

Ciani, Caterina, and Carmen Falcone. 2024. 'Interlaminar and Varicose-Projection Astrocytes: Toward a New Understanding of the Primate Brain'. *Frontiers in Cellular Neuroscience* 18 (November): 1477753. https://doi.org/10.3389/fncel.2024.1477753.

Ciani, Caterina, Giulio Pistorio, Simona Giancola, et al. 2025. 'Varicose-Projection Astrocytes: A Reactive Phenotype Associated with Neuropathology'. Preprint, Neuroscience, March 18. https://doi.org/10.1101/2025.03.17.643488.

Clarke, Laura E., and Ben A. Barres. 2013. 'Emerging Roles of Astrocytes in Neural Circuit Development'. *Nature Reviews Neuroscience* 14 (5): 311–21. https://doi.org/10.1038/nrn3484.

Clarke, Robert, A. David Smith, Kim A. Jobst, Helga Refsum, Lesley Sutton, and Per M. Ueland. 1998. 'Folate, Vitamin B12, and Serum Total Homocysteine Levels in Confirmed Alzheimer Disease'. *Archives of Neurology* 55 (11): 1449. https://doi.org/10.1001/archneur.55.11.1449.

Clewett, David V., Tae-Ho Lee, Steven Greening, Allison Ponzio, Eshed Margalit, and Mara Mather. 2016. 'Neuromelanin Marks the Spot: Identifying a Locus Coeruleus Biomarker of Cognitive Reserve in Healthy Aging'. *Neurobiology of Aging* 37 (January): 117–26. https://doi.org/10.1016/j.neurobiolaging.2015.09.019.

Colombo, Jorge A., Silvina Gayol, Alberto Y□□ez, and Pilar Marco. 1997. 'Immunocytochemical and Electron Microscope Observations on Astroglial Interlaminar Processes in the Primate Neocortex'. *Journal of Neuroscience Research* 48 (4): 352–57. https://doi.org/10.1002/(SICI)1097-4547(19970515)48:4%253C352::AID-JNR7%253E3.0.CO;2-A.

Colombo, Jorge A., and Hernán D. Reisin. 2004. 'Interlaminar Astroglia of the Cerebral Cortex: A Marker of the Primate Brain'. *Brain Research* 1006 (1): 126–31. https://doi.org/10.1016/j.brainres.2004.02.003.

Colombo, Jorge A., A. Yáñez, V. Puissant, and S. Lipina. 1995. 'Long, Interlaminar Astroglial Cell Processes in the Cortex of Adult Monkeys'. *Journal of Neuroscience Research* 40 (4): 551–56. https://doi.org/10.1002/jnr.490400414.

Compta, Y., L. Parkkinen, S. S. O'Sullivan, et al. 2011. 'Lewy- and Alzheimer-Type Pathologies in Parkinson's Disease Dementia: Which Is More Important?' *Brain* 134 (5): 1493–505. https://doi.org/10.1093/brain/awr031.

Coughlin, Curtis R., and Sidney M. Gospe. 2023. 'Pyridoxine-dependent Epilepsy: Current Perspectives and Questions for Future Research'. *Annals of the Child Neurology Society* 1 (1): 24–37. https://doi.org/10.1002/cns3.20016.

Dai, David L., Mingyao Li, and Edward B. Lee. 2023. 'Human Alzheimer's Disease Reactive Astrocytes Exhibit a Loss of Homeostastic Gene Expression'. *Acta Neuropathologica Communications* 11 (1): 127. https://doi.org/10.1186/s40478-023-01624-8.

Dam, Tien, Gennaro Pagano, Michael C. Brumm, et al. 2024. 'Neuronal Alpha-Synuclein Disease Integrated Staging System Performance in PPMI, PASADENA, and SPARK Baseline Cohorts'. *Npj Parkinson's Disease* 10 (1): 178. https://doi.org/10.1038/s41531-024-00789-w.

D'Andrea, Mr, and Rg Nagele. 2010. 'Morphologically Distinct Types of Amyloid Plaques Point the Way to a Better Understanding of Alzheimer's Disease Pathogenesis'. *Biotechnic & Histochemistry* 85 (2): 133–47. https://doi.org/10.3109/10520290903389445.

Das, Nikita, Ravi Dhamija, and Sumit Sarkar. 2023. 'The Role of Astrocytes in the Glymphatic Network: A Narrative Review'. *Metabolic Brain Disease* 39 (3): 453–65. https://doi.org/10.1007/s11011-023-01327-y.

De La Fuente, Alerie G., Silvia Pelucchi, Jerome Mertens, Monica Di Luca, Daniela Mauceri, and Elena Marcello. 2023. 'Novel Therapeutic Approaches to Target Neurodegeneration'. *British Journal of Pharmacology* 180 (13): 1651–73. https://doi.org/10.1111/bph.16078.

De Zeeuw, Chris I., and Tycho M. Hoogland. 2015. 'Reappraisal of Bergmann Glial Cells as Modulators of Cerebellar Circuit Function'. *Frontiers in Cellular Neuroscience* 9 (July). https://doi.org/10.3389/fncel.2015.00246.

Dello Russo, Cinzia, Anne I Boullerne, Vitaliy Gavrilyuk, and Douglas L Feinstein. 2004. 'Inhibition of Microglial Inflammatory Responses by Norepinephrine: Effects on Nitric Oxide and Interleukin-1β Production.' *Journal of Neuroinflammation* 1 (1): 9. https://doi.org/10.1186/1742-2094-1-9.

Derevyanko, Aksinya, Tao Tao, and Nicola J. Allen. 2025. 'Common Alterations to Astrocytes across Neurodegenerative Disorders'. *Current Opinion in Neurobiology* 90 (February): 102970. https://doi.org/10.1016/j.conb.2025.102970.

Dey, Anindya, Pijush Kanti Pramanik, Shailendra Kumar Dhar Dwivedi, et al. 2023. 'A Role for the Cystathionine-β-Synthase /H2S Axis in Astrocyte Dysfunction in the Aging Brain'. *Redox Biology* 68 (December): 102958. https://doi.org/10.1016/j.redox.2023.102958.

Díaz-Castro, Blanca, Stefanie Robel, and Anusha Mishra. 2023. 'Astrocyte Endfeet in Brain Function and Pathology: Open Questions'. *Annual Review of Neuroscience* 46 (1): 101–21. https://doi.org/10.1146/annurev-neuro-091922-031205.

Dickson, T.C, and J.C Vickers. 2001. 'The Morphological Phenotype of β-Amyloid Plaques and Associated Neuritic Changes in Alzheimer's Disease'. *Neuroscience* 105 (1): 99–107. https://doi.org/10.1016/S0306-4522(01)00169-5.

Ding, Fengfei, John O'Donnell, Alexander S. Thrane, et al. 2013. 'A1-Adrenergic Receptors Mediate Coordinated Ca2+ Signaling of Cortical Astrocytes in Awake, Behaving Mice'. *Cell Calcium* 54 (6): 387–94. https://doi.org/10.1016/j.ceca.2013.09.001.

Ding, Zhi-Bin, Li-Juan Song, Qing Wang, Gajendra Kumar, Yu-Qing Yan, and Cun-Gen Ma. 2021. 'Astrocytes: A Double-Edged Sword in Neurodegenerative Diseases'. *Neural Regeneration Research* 16 (9): 1702. https://doi.org/10.4103/1673-5374.306064.

Doddaballapur, Dhruti Balakrishna, Derren J. Heyes, and Jaleel A. Miyan. 2025. 'Multiple Hits on Cerebral Folate, Tetrahydrobiopterin and Dopamine Metabolism in the Pathophysiology of Parkinson's Disorder: A Limited Study of Post-Mortem Human Brain Tissues'. *Metabolites* 15 (5): 307. https://doi.org/10.3390/metabo15050307.

Dringen, Ralf, and Christian Arend. 2025. 'Glutathione Metabolism of the Brain—The Role of Astrocytes'. *Journal of Neurochemistry* 169 (5): e70073. https://doi.org/10.1111/jnc.70073.

Duff, Melissa C., Natalie V. Covington, Caitlin Hilverman, and Neal J. Cohen. 2020. 'Semantic Memory and the Hippocampus: Revisiting, Reaffirming, and Extending the Reach of Their Critical Relationship'. *Frontiers in Human Neuroscience* 13 (January): 471. https://doi.org/10.3389/fnhum.2019.00471.

Duffy, S, and Ba MacVicar. 1995. 'Adrenergic Calcium Signaling in Astrocyte Networks within the Hippocampal Slice'. *The Journal of Neuroscience* 15 (8): 5535–50. https://doi.org/10.1523/JNEUROSCI.15-08-05535.1995.

Durcan, Robert, Claire O'Callaghan, and James B Rowe. 2025. 'Noradrenergic Therapies in Neurodegenerative Disease: From Symptomatic to Disease Modifying Therapy?' *Brain Communications* 7 (5): fcaf310. https://doi.org/10.1093/braincomms/fcaf310.

Duvernoy, Henri M., ed. 2005. *The Human Hippocampus: Functional Anatomy, Vascularization and Serial Sections with MRI*. Third Edition. SpringerLink Bücher. Springer-Verlag Berlin Heidelberg. https://doi.org/10.1007/b138576.

Edison, Paul. 2024. 'Astroglial Activation: Current Concepts and Future Directions'. *Alzheimer's & Dementia* 20 (4): 3034–53. https://doi.org/10.1002/alz.13678.

Ehrenberg, Alexander J., Cathrine Sant, Felipe L. Pereira, et al. 2025. 'Pathways Underlying Selective Neuronal Vulnerability in Alzheimer's Disease: Contrasting the Vulnerable Locus Coeruleus to the Resilient Substantia Nigra'. *Alzheimer's & Dementia* 21 (3). https://doi.org/10.1002/alz.70087.

Eichenbaum, Howard. 2017. 'Prefrontal–Hippocampal Interactions in Episodic Memory'. *Nature Reviews Neuroscience* 18 (9): 547–58. https://doi.org/10.1038/nrn.2017.74.

Ekstrom, Arne D., and Paul F. Hill. 2023. 'Spatial Navigation and Memory: A Review of the Similarities and Differences Relevant to Brain Models and Age'. *Neuron* 111 (7): 1037–49. https://doi.org/10.1016/j.neuron.2023.03.001.

Eroglu, Cagla, and Ben A. Barres. 2010. 'Regulation of Synaptic Connectivity by Glia'. *Nature* 468 (7321): 223–31. https://doi.org/10.1038/nature09612.

Escalada, Paula, Amaia Ezkurdia, María Javier Ramírez, and Maite Solas. 2024. 'Essential Role of Astrocytes in Learning and Memory'. *International Journal of Molecular Sciences* 25 (3): 1899. https://doi.org/10.3390/ijms25031899.

Escartin, Carole, Elena Galea, András Lakatos, et al. 2021. 'Reactive Astrocyte Nomenclature, Definitions, and Future Directions'. *Nature Neuroscience* 24 (3): 312–25. https://doi.org/10.1038/s41593-020-00783-4.

Eto, Ko, Takashi Asada, Kunimasa Arima, Takao Makifuchi, and Hideo Kimura. 2002. 'Brain Hydrogen Sulfide Is Severely Decreased in Alzheimer's Disease'. *Biochemical and Biophysical Research Communications* 293 (5): 1485–88. https://doi.org/10.1016/S0006-291X(02)00422-9.

Euler, U. S. V. 1946. 'A Specific Sympathomimetic Ergone in Adrenergic Nerve Fibres (Sympathin) and Its Relations to Adrenaline and Nor-Adrenaline'. *Acta Physiologica Scandinavica* 12 (1): 73–97. https://doi.org/10.1111/j.1748-1716.1946.tb00368.x.

Evans, Andrew K., Pooneh M. Ardestani, Bitna Yi, Heui Hye Park, Rachel K. Lam, and Mehrdad Shamloo. 2020. 'Beta-Adrenergic Receptor Antagonism Is Proinflammatory and Exacerbates

Neuroinflammation in a Mouse Model of Alzheimer's Disease'. *Neurobiology of Disease* 146 (December): 105089. https://doi.org/10.1016/j.nbd.2020.105089.

Evans, Andrew K., Heui Hye Park, Claire E. Woods, et al. 2024a. 'Impact of Noradrenergic Inhibition on Neuroinflammation and Pathophysiology in Mouse Models of Alzheimer's Disease'. *Journal of Neuroinflammation* 21 (1): 322. https://doi.org/10.1186/s12974-024-03306-1.

Evans, Andrew K., Heui Hye Park, Claire E. Woods, et al. 2024b. 'Impact of Noradrenergic Inhibition on Neuroinflammation and Pathophysiology in Mouse Models of Alzheimer's Disease'. *Journal of Neuroinflammation* 21 (1): 322. https://doi.org/10.1186/s12974-024-03306-1.

Falcone, Carmen, Elisa Penna, Tiffany Hong, et al. 2021. 'Cortical Interlaminar Astrocytes Are Generated Prenatally, Mature Postnatally, and Express Unique Markers in Human and Nonhuman Primates'. *Cerebral Cortex* 31 (1): 379–95. https://doi.org/10.1093/cercor/bhaa231.

Fang, Congcong, Longqin Lv, Shanping Mao, Huimin Dong, and Baohui Liu. 2020. 'Cognition Deficits in Parkinson's Disease: Mechanisms and Treatment'. *Parkinson's Disease* 2020 (March): 1–11. https://doi.org/10.1155/2020/2076942.

Farmer, W. Todd, and Keith Murai. 2017. 'Resolving Astrocyte Heterogeneity in the CNS'. *Frontiers in Cellular Neuroscience* 11 (September): 300. https://doi.org/10.3389/fncel.2017.00300.

Feinstein, Douglas L, Michael T Heneka, Vitaliy Gavrilyuk, Cinzia Dello Russo, Guy Weinberg, and Elena Galea. 2002. 'Noradrenergic Regulation of Inflammatory Gene Expression in Brain'. *Neurochemistry International* 41 (5): 357–65. https://doi.org/10.1016/s0197-0186(02)00049-9.

Feinstein, Douglas L., Sergey Kalinin, and David Braun. 2016. 'Causes, Consequences, and Cures for Neuroinflammation Mediated via the Locus Coeruleus: Noradrenergic Signaling System'. *Journal of Neurochemistry* 139 (S2): 154–78. https://doi.org/10.1111/jnc.13447.

Filmus, Jorge, Mariana Capurro, and Jonathan Rast. 2008. 'Glypicans'. *Genome Biology* 9 (5): 224. https://doi.org/10.1186/gb-2008-9-5-224.

Fink, Katja, Jelena Velebit, Nina Vardjan, Robert Zorec, and Marko Kreft. 2021. 'Noradrenaline-induced L -lactate Production Requires D -glucose Entry and Transit through the Glycogen Shunt in Single-cultured Rat Astrocytes'. *Journal of Neuroscience Research* 99 (4): 1084–98. https://doi.org/10.1002/jnr.24783.

Fiore, Frederic, Khaleel Alhalaseh, Ram R. Dereddi, et al. 2023. 'Norepinephrine Regulates Calcium Signals and Fate of Oligodendrocyte Precursor Cells in the Mouse Cerebral Cortex'. *Nature Communications* 14 (1): 8122. https://doi.org/10.1038/s41467-023-43920-w.

Fisher, Theodore M., and Shane A. Liddelow. 2024a. 'Emerging Roles of Astrocytes as Immune Effectors in the Central Nervous System'. *Trends in Immunology* 45 (10): 824–36. https://doi.org/10.1016/j.it.2024.08.008.

Fisher, Theodore M., and Shane A. Liddelow. 2024b. 'Emerging Roles of Astrocytes as Immune Effectors in the Central Nervous System'. *Trends in Immunology* 45 (10): 824–36. https://doi.org/10.1016/j.it.2024.08.008.

Fixemer, Sonja, Mónica Miranda De La Maza, Gaël Paul Hammer, et al. 2025. 'Microglia Aggregates Define Distinct Immune and Neurodegenerative Niches in Alzheimer's Disease Hippocampus'. *Acta Neuropathologica* 149 (1): 19. https://doi.org/10.1007/s00401-025-02857-8.

Foote, S. L., F. E. Bloom, and G. Aston-Jones. 1983. 'Nucleus Locus Ceruleus: New Evidence of Anatomical and Physiological Specificity'. *Physiological Reviews* 63 (3): 844–914. https://doi.org/10.1152/physrev.1983.63.3.844.

Fornai, Francesco, Filippo S. Giorgi, Maria G. Alessandrì, Mario Giusiani, and Giovanni U. Corsini. 1999. 'Effects of Pretreatment with *N* -(2-Chloroethyl)- *N* -Ethyl-2-Bromobenzylamine (DSP-4) on Methamphetamine Pharmacokinetics and Striatal Dopamine Losses'. *Journal of Neurochemistry* 72 (2): 777–84. https://doi.org/10.1046/j.1471-4159.1999.0720777.x.

Funato, H., M. Yoshimura, T. Yamazaki, et al. 1998. 'Astrocytes Containing Amyloid Beta-Protein (Abeta)-Positive Granules Are Associated with Abeta40-Positive Diffuse Plaques in the Aged Human Brain'. *The American Journal of Pathology* 152 (4): 983–92.

Funayama, Manabu, Kenya Nishioka, Yuanzhe Li, and Nobutaka Hattori. 2023. 'Molecular Genetics of Parkinson's Disease: Contributions and Global Trends'. *Journal of Human Genetics* 68 (3): 125–30. https://doi.org/10.1038/s10038-022-01058-5.

Gan, Yiming, Stephanie Holstein-Rønsbo, Maiken Nedergaard, Kimberly A. S. Boster, John H. Thomas, and Douglas H. Kelley. 2023. 'Perivascular Pumping of Cerebrospinal Fluid in the Brain with a Valve Mechanism'. *Journal of The Royal Society Interface* 20 (206). https://doi.org/10.1098/rsif.2023.0288.

German, Dwight C., Kebreten F. Manaye, Charles L White, et al. 1992. 'Disease-specific Patterns of Locus Coeruleus Cell Loss'. *Annals of Neurology* 32 (5): 667–76. https://doi.org/10.1002/ana.410320510.

Gilvesy, Abris, Evelina Husen, Zsofia Magloczky, et al. 2022. 'Spatiotemporal Characterization of Cellular Tau Pathology in the Human Locus Coeruleus–Pericoerulear Complex by Three-Dimensional Imaging'. *Acta Neuropathologica* 144 (4): 651–76. https://doi.org/10.1007/s00401-022-02477-6.

Gogishvili, Dea, Madison I. J. Honey, Inge M. W. Verberk, et al. 2025. 'The GFAP Proteoform Puzzle: How to Advance GFAP as a Fluid Biomarker in Neurological Diseases'. *Journal of Neurochemistry* 169 (1): e16226. https://doi.org/10.1111/jnc.16226.

Gordon, Grant R. J., Hyun B. Choi, Ravi L. Rungta, Graham C. R. Ellis-Davies, and Brian A. MacVicar. 2008. 'Brain Metabolism Dictates the Polarity of Astrocyte Control over Arterioles'. *Nature* 456 (7223): 745–49. https://doi.org/10.1038/nature07525.

Green, Gilad Sahar, Masashi Fujita, Hyun-Sik Yang, et al. 2024. 'Cellular Communities Reveal Trajectories of Brain Ageing and Alzheimer's Disease'. *Nature* 633 (8030): 634–45. https://doi.org/10.1038/s41586-024-07871-6.

Guo, Qinxi, Zilai Wang, Hongmei Li, Mary Wiese, and Hui Zheng. 2012. 'APP Physiological and Pathophysiological Functions: Insights from Animal Models'. *Cell Research* 22 (1): 78–89. https://doi.org/10.1038/cr.2011.116.

Guo, Tong, Wendy Noble, and Diane P. Hanger. 2017. 'Roles of Tau Protein in Health and Disease'. *Acta Neuropathologica* 133 (5): 665–704. https://doi.org/10.1007/s00401-017-1707-9.

Gutiérrez, Irene L., Cinzia Dello Russo, Fabiana Novellino, et al. 2022. 'Noradrenaline in Alzheimer's Disease: A New Potential Therapeutic Target'. *International Journal of Molecular Sciences* 23 (11): 6143. https://doi.org/10.3390/ijms23116143.

Guttenplan, Kevin A., Isa Maxwell, Erin Santos, et al. 2025. 'GPCR Signaling Gates Astrocyte Responsiveness to Neurotransmitters and Control of Neuronal Activity'. *Science* 388 (6748): 763–68. https://doi.org/10.1126/science.adq5729.

Gyoneva, Stefka, and Stephen F. Traynelis. 2013. 'Norepinephrine Modulates the Motility of Resting and Activated Microglia via Different Adrenergic Receptors'. *Journal of Biological Chemistry* 288 (21): 15291–302. https://doi.org/10.1074/jbc.M113.458901.

Habib, Naomi, Cristin McCabe, Sedi Medina, et al. 2020. 'Disease-Associated Astrocytes in Alzheimer's Disease and Aging'. *Nature Neuroscience* 23 (6): 701–6. https://doi.org/10.1038/s41593-020-0624-8.

Hahn, Junghyun, Xianhong Wang, and Marta Margeta. 2015. 'Astrocytes Increase the Activity of Synaptic GluN2B NMDA Receptors'. *Frontiers in Cellular Neuroscience* 9 (April). https://doi.org/10.3389/fncel.2015.00117.

Hainsworth, Atticus H., Natalie E. Yeo, Erica M. Weekman, and Donna M. Wilcock. 2016. 'Homocysteine, Hyperhomocysteinemia and Vascular Contributions to Cognitive Impairment and Dementia (VCID)'. *Biochimica et Biophysica Acta (BBA) - Molecular Basis of Disease* 1862 (5): 1008–17. https://doi.org/10.1016/j.bbadis.2015.11.015.

Hampel, Harald, John Hardy, Kaj Blennow, et al. 2021. 'The Amyloid-β Pathway in Alzheimer's Disease'. *Molecular Psychiatry* 26 (10): 5481–503. https://doi.org/10.1038/s41380-021-01249-0.

Hary, Alexander T., Smriti Chadha, Nathaniel Mercaldo, et al. 2025. 'Locus Coeruleus Tau Validates and Informs High-Resolution MRI in Aging and at Earliest Alzheimer's Pathology Stages'. *Acta Neuropathologica Communications* 13 (1): 44. https://doi.org/10.1186/s40478-025-01957-6.

Hasel, Philip, Melissa L. Cooper, Anne E. Marchildon, et al. 2025. 'Defining the Molecular Identity and Morphology of Glia Limitans Superficialis Astrocytes in Vertebrates'. *Cell Reports* 44 (3): 115344. https://doi.org/10.1016/j.celrep.2025.115344.

Hasel, Philip, Indigo V. L. Rose, Jessica S. Sadick, Rachel D. Kim, and Shane A. Liddelow. 2021. 'Neuroinflammatory Astrocyte Subtypes in the Mouse Brain'. *Nature Neuroscience* 24 (10): 1475–87. https://doi.org/10.1038/s41593-021-00905-6.

Hassan, A. 2004. 'Homocysteine Is a Risk Factor for Cerebral Small Vessel Disease, Acting via Endothelial Dysfunction'. *Brain* 127 (1): 212–19. https://doi.org/10.1093/brain/awh023.

Hastings, Michael H., Marco Brancaccio, Maria F. Gonzalez-Aponte, and Erik D. Herzog. 2023. 'Circadian Rhythms and Astrocytes: The Good, the Bad, and the Ugly'. *Annual Review of Neuroscience* 46 (1): 123–43. https://doi.org/10.1146/annurev-neuro-100322-112249.

Hauglund, Natalie L., Mie Andersen, Klaudia Tokarska, et al. 2025. 'Norepinephrine-Mediated Slow Vasomotion Drives Glymphatic Clearance during Sleep'. *Cell* 188 (3): 606-622.e17. https://doi.org/10.1016/j.cell.2024.11.027.

Heneka, Michael T., Fabian Nadrigny, Tommy Regen, et al. 2010. 'Locus Ceruleus Controls Alzheimer's Disease Pathology by Modulating Microglial Functions through Norepinephrine'. *Proceedings of the National Academy of Sciences of the United States of America* 107 (13): 6058–63. https://doi.org/10.1073/pnas.0909586107.

Heneka, Michael T., Mutiah Ramanathan, Andreas H. Jacobs, et al. 2006. 'Locus Ceruleus Degeneration Promotes Alzheimer Pathogenesis in Amyloid Precursor Protein 23 Transgenic Mice'. *The Journal of Neuroscience* 26 (5): 1343–54. https://doi.org/10.1523/JNEUROSCI.4236-05.2006.

Henneberger, Christian, Lucie Bard, Aude Panatier, et al. 2020. 'LTP Induction Boosts Glutamate Spillover by Driving Withdrawal of Perisynaptic Astroglia'. *Neuron* 108 (5): 919-936.e11. https://doi.org/10.1016/j.neuron.2020.08.030.

Hertz, L., Y. Chen, M. Gibbs, P. Zang, and L. Peng. 2004. 'Astrocytic Adrenoceptors: A Major Drug Target in Neurological and Psychiatric Disorders?' *Current Drug Target -CNS & Neurological Disorders* 3 (3): 239–68. https://doi.org/10.2174/1568007043337535.

Hertz, Leif, Ditte Lovatt, Steven A. Goldman, and Maiken Nedergaard. 2010. 'Adrenoceptors in Brain: Cellular Gene Expression and Effects on Astrocytic Metabolism and [Ca2+]i'. *Neurochemistry International* 57 (4): 411–20. https://doi.org/10.1016/j.neuint.2010.03.019.

Heurtaux, Tony, David S. Bouvier, Alexandre Benani, et al. 2022. 'Normal and Pathological NRF2 Signalling in the Central Nervous System'. *Antioxidants* 11 (8): 1426. https://doi.org/10.3390/antiox11081426.

Hinojosa, Ara E, Javier R Caso, Borja García-Bueno, Juan C Leza, and José Lm Madrigal. 2013. 'Dual Effects of Noradrenaline on Astroglial Production of Chemokines and Pro-Inflammatory Mediators'. *Journal of Neuroinflammation* 10 (1): 852. https://doi.org/10.1186/1742-2094-10-81.

Holt, Matthew G. 2023. 'Astrocyte Heterogeneity and Interactions with Local Neural Circuits'. *Essays in Biochemistry* 67 (1): 93–106. https://doi.org/10.1042/EBC20220136.

Hou, Liyan, Fuqiang Sun, Wei Sun, Lin Zhang, and Qingshan Wang. 2019. 'Lesion of the Locus Coeruleus Damages Learning and Memory Performance in Paraquat and Maneb-Induced Mouse Parkinson's Disease Model'. *Neuroscience* 419 (November): 129–40. https://doi.org/10.1016/j.neuroscience.2019.09.006.

Hsiao, Wen-Chiu, Hsin-I Chang, Shih-Wei Hsu, et al. 2023. 'Association of Cognition and Brain Reserve in Aging and Glymphatic Function Using Diffusion Tensor Image-along the Perivascular Space (DTI-ALPS)'. *Neuroscience* 524 (August): 11–20. https://doi.org/10.1016/j.neuroscience.2023.04.004.

Huang, Yong, Minghui Wang, Haofei Ni, et al. 2024. 'Regulation of Cell Distancing in Peri-Plaque Glial Nets by Plexin-B1 Affects Glial Activation and Amyloid Compaction in Alzheimer's Disease'. *Nature Neuroscience* 27 (8): 1489–504. https://doi.org/10.1038/s41593-024-01664-w.

Hussain, Laila S., Vamsi Reddy, and Christopher V. Maani. 2025. 'Physiology, Noradrenergic Synapse'. In *StatPearls*. StatPearls Publishing. http://www.ncbi.nlm.nih.gov/books/NBK540977/.

Iadecola, Costantino, and Rebecca F. Gottesman. 2018. 'Cerebrovascular Alterations in Alzheimer Disease: Incidental or Pathogenic?' *Circulation Research* 123 (4): 406–8. https://doi.org/10.1161/CIRCRESAHA.118.313400.

Iba, Michiyo, Jennifer D. McBride, Jing L. Guo, Bin Zhang, John Q. Trojanowski, and Virginia M.-Y. Lee. 2015. 'Tau Pathology Spread in PS19 Tau Transgenic Mice Following Locus Coeruleus (LC) Injections of Synthetic Tau Fibrils Is Determined by the LC's Afferent and Efferent Connections'. *Acta Neuropathologica* 130 (3): 349–62. https://doi.org/10.1007/s00401-015-1458-4.

Iliff, Jeffrey J., Minghuan Wang, Yonghong Liao, et al. 2012. 'A Paravascular Pathway Facilitates CSF Flow Through the Brain Parenchyma and the Clearance of Interstitial Solutes, Including Amyloid β'. *Science Translational Medicine* 4 (147). https://doi.org/10.1126/scitranslmed.3003748.

Iqbal, Khalid, Fei Liu, Cheng-Xin Gong, Alejandra Del C. Alonso, and Inge Grundke-Iqbal. 2009. 'Mechanisms of Tau-Induced Neurodegeneration'. *Acta Neuropathologica* 118 (1): 53–69. https://doi.org/10.1007/s00401-009-0486-3.

Ishida, Kazuhisa, Kaoru Yamada, Risa Nishiyama, et al. 2022. 'Glymphatic System Clears Extracellular Tau and Protects from Tau Aggregation and Neurodegeneration'. *Journal of Experimental Medicine* 219 (3): e20211275. https://doi.org/10.1084/jem.20211275.

Ishii, Yurika, Ayaka Yamaizumi, Ayu Kawakami, et al. 2015. 'Anti-Inflammatory Effects of Noradrenaline on LPS-Treated Microglial Cells: Suppression of NFκB Nuclear Translocation and Subsequent STAT1 Phosphorylation'. *Neurochemistry International* 90 (November): 56–66. https://doi.org/10.1016/j.neuint.2015.07.010.

Jacobs, Heidi Il, Nikos Priovoulos, Benedikt A Poser, et al. 2020. 'Dynamic Behavior of the Locus Coeruleus during Arousal-Related Memory Processing in a Multi-Modal 7T fMRI Paradigm'. *eLife* 9 (June): e52059. https://doi.org/10.7554/eLife.52059.

Jacobson, Kathryn R., and Hailong Song. 2024. 'Changes in the Extracellular Matrix with Aging: A Larger Role in Alzheimer's Disease'. *The Journal of Neuroscience* 44 (22): e0081242024. https://doi.org/10.1523/JNEUROSCI.0081-24.2024.

Jahn, Holger. 2013. 'Memory Loss in Alzheimer's Disease'. *Dialogues in Clinical Neuroscience* 15 (4): 445–54. https://doi.org/10.31887/DCNS.2013.15.4/hjahn.

Jansen, Laura A., Robert F. Hevner, William H. Roden, Si Houn Hahn, Sunhee Jung, and Sidney M. Gospe. 2014. 'Glial Localization of Antiquitin: Implications for Pyridoxine-dependent Epilepsy'. *Annals of Neurology* 75 (1): 22–32. https://doi.org/10.1002/ana.24027.

Jellinger, Kurt A. 2020. 'Neuropathology of the Alzheimer's Continuum: An Update'. *Free Neuropathology*, November 11, 32 Seiten. 32 Seiten. https://doi.org/10.17879/FREENEUROPATHOLOGY-2020-3050.

Jellinger, Kurt A. 2021. 'Significance of Cerebral Amyloid Angiopathy and Other Co-Morbidities in Lewy Body Diseases'. *Journal of Neural Transmission* 128 (5): 687–99. https://doi.org/10.1007/s00702-021-02345-9.

Jellinger, Kurt A., and Johannes Attems. 2005. 'Prevalence and Pathogenic Role of Cerebrovascular Lesions in Alzheimer Disease'. *Journal of the Neurological Sciences* 229–230 (March): 37–41. https://doi.org/10.1016/j.jns.2004.11.018.

Jellinger, Kurt A., and Johannes Attems. 2015. 'Challenges of Multimorbidity of the Aging Brain: A Critical Update'. *Journal of Neural Transmission* 122 (4): 505–21. https://doi.org/10.1007/s00702-014-1288-x.

Jhee, Kwang-Hwan, and Warren D. Kruger. 2005. 'The Role of Cystathionine β-Synthase in Homocysteine Metabolism'. *Antioxidants & Redox Signaling* 7 (5–6): 813–22. https://doi.org/10.1089/ars.2005.7.813.

Jones, Emma V., and David S. Bouvier. 2014. 'Astrocyte-Secreted Matricellular Proteins in CNS Remodelling during Development and Disease'. *Neural Plasticity* 2014: 1–12. https://doi.org/10.1155/2014/321209.

Jurga, Agnieszka M., Martyna Paleczna, Justyna Kadluczka, and Katarzyna Z. Kuter. 2021. 'Beyond the GFAP-Astrocyte Protein Markers in the Brain'. *Biomolecules* 11 (9): 1361. https://doi.org/10.3390/biom11091361.

Kamath, Atul F., Anil K. Chauhan, Janka Kisucka, et al. 2006. 'Elevated Levels of Homocysteine Compromise Blood-Brain Barrier Integrity in Mice'. *Blood* 107 (2): 591–93. https://doi.org/10.1182/blood-2005-06-2506.

Kamphuis, Willem, Carlyn Mamber, Martina Moeton, et al. 2012. 'GFAP Isoforms in Adult Mouse Brain with a Focus on Neurogenic Astrocytes and Reactive Astrogliosis in Mouse Models of Alzheimer Disease'. *PLoS ONE* 7 (8): e42823. https://doi.org/10.1371/journal.pone.0042823.

Kang, Seokjo, V. Alexandra Moser, Clive N. Svendsen, and Helen S. Goodridge. 2020. 'Rejuvenating the Blood and Bone Marrow to Slow Aging-Associated Cognitive Decline and Alzheimer's Disease'. *Communications Biology* 3 (1): 1. https://doi.org/10.1038/s42003-020-0797-4.

Kautzky, Alexander, Rene Seiger, Andreas Hahn, et al. 2018. 'Prediction of Autopsy Verified Neuropathological Change of Alzheimer's Disease Using Machine Learning and MRI'. *Frontiers in Aging Neuroscience* 10 (December): 406. https://doi.org/10.3389/fnagi.2018.00406.

Kettenmann, Helmut, and Alexei Verkhratsky. 2008. 'Neuroglia: The 150 Years After'. *Trends in Neurosciences* 31 (12): 653–59. https://doi.org/10.1016/j.tins.2008.09.003.

Khakh, Baljit S, and Michael V Sofroniew. 2015. 'Diversity of Astrocyte Functions and Phenotypes in Neural Circuits'. *Nature Neuroscience* 18 (7): 942–52. https://doi.org/10.1038/nn.4043.

Kim, Junhyung, Ik Dong Yoo, Jaejoon Lim, and Jong-Seok Moon. 2024. 'Pathological Phenotypes of Astrocytes in Alzheimer's Disease'. *Experimental & Molecular Medicine* 56 (1): 95–99. https://doi.org/10.1038/s12276-023-01148-0.

Kofuji, Paulo, and Alfonso Araque. 2021. 'Astrocytes and Behavior'. *Annual Review of Neuroscience* 44 (1): 49–67. https://doi.org/10.1146/annurev-neuro-101920-112225.

Kress, Benjamin T., Jeffrey J. Iliff, Maosheng Xia, et al. 2014. 'Impairment of Paravascular Clearance Pathways in the Aging Brain'. *Annals of Neurology* 76 (6): 845–61. https://doi.org/10.1002/ana.24271.

Kucukdereli, Hakan, Nicola J. Allen, Anthony T. Lee, et al. 2011. 'Control of Excitatory CNS Synaptogenesis by Astrocyte-Secreted Proteins Hevin and SPARC'. *Proceedings of the National Academy of Sciences* 108 (32). https://doi.org/10.1073/pnas.1104977108.

Lasagna-Reeves, Cristian A., and Rakez Kayed. 2011. 'Astrocytes Contain Amyloid-β Annular Protofibrils in Alzheimer's Disease Brains'. *FEBS Letters* 585 (19): 3052–57. https://doi.org/10.1016/j.febslet.2011.08.027.

Lau, Shun-Fat, Han Cao, Amy K. Y. Fu, and Nancy Y. Ip. 2020. 'Single-Nucleus Transcriptome Analysis Reveals Dysregulation of Angiogenic Endothelial Cells and Neuroprotective Glia in Alzheimer's Disease'. *Proceedings of the National Academy of Sciences* 117 (41): 25800–25809. https://doi.org/10.1073/pnas.2008762117.

Laureys, Guy, Sarah Gerlo, Anneleen Spooren, Frauke Demol, Jacques De Keyser, and Joeri L Aerts. 2014. 'B2-Adrenergic Agonists Modulate TNF-α Induced Astrocytic Inflammatory Gene Expression and Brain Inflammatory Cell Populations'. *Journal of Neuroinflammation* 11 (1): 21. https://doi.org/10.1186/1742-2094-11-21.

Lawrence, Jill M., Kayla Schardien, Brian Wigdahl, and Michael R. Nonnemacher. 2023. 'Roles of Neuropathology-Associated Reactive Astrocytes: A Systematic Review'. *Acta Neuropathologica Communications* 11 (1): 42. https://doi.org/10.1186/s40478-023-01526-9.

Lee, Moonhee, Claudia Schwab, Sheng Yu, Edith McGeer, and Patrick L. McGeer. 2009. 'Astrocytes Produce the Antiinflammatory and Neuroprotective Agent Hydrogen Sulfide'. *Neurobiology of Aging* 30 (10): 1523–34. https://doi.org/10.1016/j.neurobiolaging.2009.06.001.

Lefton, Katheryn B., Yifan Wu, Yanchao Dai, et al. 2025. 'Norepinephrine Signals through Astrocytes to Modulate Synapses'. *Science* 388 (6748): 776–83. https://doi.org/10.1126/science.adq5480.

Lenhossék, M. von, and W. Mills. 1895. *Der Feinere Bau Des Nervensystems Im Lichte Neuester Forschungen*. Fischer. https://books.google.fr/books?id=oP5FAQAAMAAJ.

Leverenz, James B., Ronald Hamilton, Debby W. Tsuang, et al. 2008. 'RESEARCH ARTICLE: Empiric Refinement of the Pathologic Assessment of Lewy-Related Pathology in the Dementia Patient'. *Brain Pathology* 18 (2): 220–24. https://doi.org/10.1111/j.1750-3639.2007.00117.x.

Levites, Yona, Eric B. Dammer, Yong Ran, et al. 2024. 'Integrative Proteomics Identifies a Conserved Aβ Amyloid Responsome, Novel Plaque Proteins, and Pathology Modifiers in Alzheimer's Disease'. *Cell Reports Medicine* 5 (8): 101669. https://doi.org/10.1016/j.xcrm.2024.101669.

Liddelow, Shane A., and Ben A. Barres. 2017. 'Reactive Astrocytes: Production, Function, and Therapeutic Potential'. *Immunity* 46 (6): 957–67. https://doi.org/10.1016/j.immuni.2017.06.006.

Liddelow, Shane A., Kevin A. Guttenplan, Laura E. Clarke, et al. 2017. 'Neurotoxic Reactive Astrocytes Are Induced by Activated Microglia'. *Nature* 541 (7638): 481–87. https://doi.org/10.1038/nature21029.

Lin, Junyu, Ruwei Ou, Chunyu Li, et al. 2023. 'Plasma Glial Fibrillary Acidic Protein as a Biomarker of Disease Progression in Parkinson's Disease: A Prospective Cohort Study'. *BMC Medicine* 21 (1): 420. https://doi.org/10.1186/s12916-023-03120-1.

Liu, Shuangwu, Xiaohan Sun, Qingguo Ren, et al. 2024. 'Glymphatic Dysfunction in Patients with Early-Stage Amyotrophic Lateral Sclerosis'. *Brain* 147 (1): 100–108. https://doi.org/10.1093/brain/awad274.

Liu, Tingting, Hongzhou Zuo, Di Ma, Dan Song, Yuying Zhao, and Oumei Cheng. 2023. 'Cerebrospinal Fluid GFAP Is a Predictive Biomarker for Conversion to Dementia and Alzheimer's Disease-Associated Biomarkers Alterations among de Novo Parkinson's Disease Patients: A Prospective Cohort Study'. *Journal of Neuroinflammation* 20 (1): 167. https://doi.org/10.1186/s12974-023-02843-5.

Liu, Yong U., Yanlu Ying, Yujiao Li, et al. 2019. 'Neuronal Network Activity Controls Microglial Process Surveillance in Awake Mice via Norepinephrine Signaling'. *Nature Neuroscience* 22 (11): 1771–81. https://doi.org/10.1038/s41593-019-0511-3.

Livingston, Nicholas R., Valeria Calsolaro, Rainer Hinz, et al. 2022. 'Relationship between Astrocyte Reactivity, Using Novel 11C-BU99008 PET, and Glucose Metabolism, Grey Matter Volume and Amyloid Load in Cognitively Impaired Individuals'. *Molecular Psychiatry* 27 (4): 2019–29. https://doi.org/10.1038/s41380-021-01429-y.

Loughlin, A. J., M. N. Woodroofe, and M. L. Cuzner. 1993. 'Modulation of Interferon-Gamma-Induced Major Histocompatibility Complex Class II and Fc Receptor Expression on Isolated Microglia by Transforming Growth Factor-Beta 1, Interleukin-4, Noradrenaline and Glucocorticoids'. *Immunology* 79 (1): 125–30.

Lu, Tsai-Yi, Priyanka Hanumaihgari, Eric T. Hsu, et al. 2023. 'Norepinephrine Modulates Calcium Dynamics in Cortical Oligodendrocyte Precursor Cells Promoting Proliferation during Arousal in Mice'. *Nature Neuroscience* 26 (10): 1739–50. https://doi.org/10.1038/s41593-023-01426-0.

Luijerink, Lauren, Michael Rodriguez, and Rita Machaalani. 2024. 'Quantifying GFAP Immunohistochemistry in the Brain – Introduction of the Reactivity Score (R-Score) and How It Compares to Other Methodologies'. *Journal of Neuroscience Methods* 402 (February): 110025. https://doi.org/10.1016/j.jneumeth.2023.110025.

MacVicar, Brian A., and Eric A. Newman. 2015. 'Astrocyte Regulation of Blood Flow in the Brain'. *Cold Spring Harbor Perspectives in Biology* 7 (5): a020388. https://doi.org/10.1101/cshperspect.a020388.

Madrigal, Jose L. M., Juan C. Leza, Paul Polak, Sergey Kalinin, and Douglas L. Feinstein. 2009. 'Astrocyte-Derived MCP-1 Mediates Neuroprotective Effects of Noradrenaline'. *The Journal of Neuroscience* 29 (1): 263–67. https://doi.org/10.1523/JNEUROSCI.4926-08.2009.

Mäki-Marttunen, Verónica, Ole A. Andreassen, and Thomas Espeseth. 2020. 'The Role of Norepinephrine in the Pathophysiology of Schizophrenia'. *Neuroscience & Biobehavioral Reviews* 118 (November): 298–314. https://doi.org/10.1016/j.neubiorev.2020.07.038.

Mallach, Anna, Magdalena Zielonka, Veerle Van Lieshout, et al. 2024. 'Microglia-Astrocyte Crosstalk in the Amyloid Plaque Niche of an Alzheimer's Disease Mouse Model, as Revealed by Spatial Transcriptomics'. *Cell Reports* 43 (6): 114216. https://doi.org/10.1016/j.celrep.2024.114216.

Marien, Marc R, Francis C Colpaert, and Alan C Rosenquist. 2004. 'Noradrenergic Mechanisms in Neurodegenerative Diseases: A Theory'. *Brain Research Reviews* 45 (1): 38–78. https://doi.org/10.1016/j.brainresrev.2004.02.002.

Marsan, Elise, Dmitry Velmeshev, Arren Ramsey, et al. 2023. 'Astroglial Toxicity Promotes Synaptic Degeneration in the Thalamocortical Circuit in Frontotemporal Dementia with GRN Mutations'. *Journal of Clinical Investigation* 133 (6): e164919. https://doi.org/10.1172/JCI164919.

Masters, C L, G Simms, N A Weinman, G Multhaup, B L McDonald, and K Beyreuther. 1985. 'Amyloid Plaque Core Protein in Alzheimer Disease and Down Syndrome.' *Proceedings of the National Academy of Sciences* 82 (12): 4245–49. https://doi.org/10.1073/pnas.82.12.4245.

Matchett, Billie J., Lea T. Grinberg, Panos Theofilas, and Melissa E. Murray. 2021. 'The Mechanistic Link between Selective Vulnerability of the Locus Coeruleus and Neurodegeneration in Alzheimer's Disease'. *Acta Neuropathologica*, ahead of print, January 11. https://doi.org/10.1007/s00401-020-02248-1.

Mather, Mara, and Carolyn W. Harley. 2016. 'The Locus Coeruleus: Essential for Maintaining Cognitive Function and the Aging Brain'. *Trends in Cognitive Sciences* 20 (3): 214–26. https://doi.org/10.1016/j.tics.2016.01.001.

Mathys, Hansruedi, Jose Davila-Velderrain, Zhuyu Peng, et al. 2019. 'Single-Cell Transcriptomic Analysis of Alzheimer's Disease'. *Nature* 570 (7761): 332–37. https://doi.org/10.1038/s41586-019-1195-2.

McAlpine, Cameron S., Joseph Park, Ana Griciuc, et al. 2021. 'Astrocytic Interleukin-3 Programs Microglia and Limits Alzheimer's Disease'. *Nature* 595 (7869): 701–6. https://doi.org/10.1038/s41586-021-03734-6.

McGovern, Kathryn E., J. Philip Nance, Clément N. David, et al. 2021. 'SPARC Coordinates Extracellular Matrix Remodeling and Efficient Recruitment to and Migration of Antigen-Specific T Cells in the Brain Following Infection'. *Scientific Reports* 11 (1): 4549. https://doi.org/10.1038/s41598-021-83952-0.

McKeith, Ian G. 2006. 'Consensus Guidelines for the Clinical and Pathologic Diagnosis of Dementia with Lewy Bodies (DLB): Report of the Consortium on DLB International Workshop'. *Journal of Alzheimer's Disease* 9 (s3): 417–23. https://doi.org/10.3233/JAD-2006-9S347.

McKeith, Ian G., Bradley F. Boeve, Dennis W. Dickson, et al. 2017a. 'Diagnosis and Management of Dementia with Lewy Bodies: Fourth Consensus Report of the DLB Consortium'. *Neurology* 89 (1): 88–100. https://doi.org/10.1212/WNL.0000000000004058.

McKeith, Ian G., Bradley F. Boeve, Dennis W. Dickson, et al. 2017b. 'Diagnosis and Management of Dementia with Lewy Bodies: Fourth Consensus Report of the DLB Consortium'. *Neurology* 89 (1): 88–100. https://doi.org/10.1212/WNL.0000000000004058.

McKnight, Colin D., Paula Trujillo, Alexander M. Lopez, et al. 2021. 'Diffusion along Perivascular Spaces Reveals Evidence Supportive of Glymphatic Function Impairment in Parkinson Disease'. *Parkinsonism & Related Disorders* 89 (August): 98–104. https://doi.org/10.1016/j.parkreldis.2021.06.004.

McNeill, Jessica, Christopher Rudyk, Michael E. Hildebrand, and Natalina Salmaso. 2021. 'Ion Channels and Electrophysiological Properties of Astrocytes: Implications for Emergent Stimulation Technologies'. *Frontiers in Cellular Neuroscience* 15 (May): 644126. https://doi.org/10.3389/fncel.2021.644126.

Mellergaard, Clara, Gunhild Waldemar, Asmus Vogel, and Kristian Steen Frederiksen. 2023. 'Characterising the Prodromal Phase in Dementia with Lewy Bodies'. *Parkinsonism & Related Disorders* 107 (February): 105279. https://doi.org/10.1016/j.parkreldis.2023.105279.

Meneses, Axel, Shunsuke Koga, Justin O'Leary, Dennis W. Dickson, Guojun Bu, and Na Zhao. 2021. 'TDP-43 Pathology in Alzheimer's Disease'. *Molecular Neurodegeneration* 16 (1): 84. https://doi.org/10.1186/s13024-021-00503-x.

Mercan, Dilek, and Michael T. Heneka. 2019. 'Norepinephrine as a Modulator of Microglial Dynamics'. *Nature Neuroscience* 22 (11): 1745–46. https://doi.org/10.1038/s41593-019-0526-9.

Mercan, Dilek, and Michael Thomas Heneka. 2022. 'The Contribution of the Locus Coeruleus–Noradrenaline System Degeneration during the Progression of Alzheimer's Disease'. *Biology* 11 (12): 1822. https://doi.org/10.3390/biology11121822.

Metea, Monica R., and Eric A. Newman. 2006. 'Glial Cells Dilate and Constrict Blood Vessels: A Mechanism of Neurovascular Coupling'. *The Journal of Neuroscience* 26 (11): 2862–70. https://doi.org/10.1523/JNEUROSCI.4048-05.2006.

Mohamed, Amany, and Elena Posse De Chaves. 2011. 'A *β* Internalization by Neurons and Glia'. *International Journal of Alzheimer's Disease* 2011 (1): 127984. https://doi.org/10.4061/2011/127984.

Mohamed, Mohamed A, Zhou Zeng, Marta Gennaro, et al. 2022. 'Astrogliosis in Aging and Parkinson's Disease Dementia: A New Clinical Study with 11C-BU99008 PET'. *Brain Communications* 4 (5): fcac199. https://doi.org/10.1093/braincomms/fcac199.

MohanaSundaram, ArunSundar, Mohammad Mofatteh, Ghulam Md Ashraf, and Domenico Praticò. 2024. 'Glymphotherapeutics for Alzheimer's Disease: Time to Move the Needle'. *Ageing Research Reviews* 101 (November): 102478. https://doi.org/10.1016/j.arr.2024.102478.

Montine, Thomas J., Creighton H. Phelps, Thomas G. Beach, et al. 2012. 'National Institute on Aging–Alzheimer's Association Guidelines for the Neuropathologic Assessment of Alzheimer's Disease: A Practical Approach'. *Acta Neuropathologica* 123 (1): 1–11. https://doi.org/10.1007/s00401-011-0910-3.

Mulder, Sandra D., Robert Veerhuis, Marinus A. Blankenstein, and Henrietta M. Nielsen. 2012. 'The Effect of Amyloid Associated Proteins on the Expression of Genes Involved in Amyloid-β Clearance by Adult Human Astrocytes'. *Experimental Neurology* 233 (1): 373–79. https://doi.org/10.1016/j.expneurol.2011.11.001.

Mulligan, Sean J., and Brian A. MacVicar. 2004. 'Calcium Transients in Astrocyte Endfeet Cause Cerebrovascular Constrictions'. *Nature* 431 (7005): 195–99. https://doi.org/10.1038/nature02827.

Nagele, Robert G., Michael R. D'Andrea, H. Lee, Venkateswar Venkataraman, and Hoau-Yan Wang. 2003. 'Astrocytes Accumulate Aβ42 and Give Rise to Astrocytic Amyloid Plaques in Alzheimer Disease Brains'. *Brain Research* 971 (2): 197–209. https://doi.org/10.1016/S0006-8993(03)02361-8.

Nagelhus, Erlend A., and Ole P. Ottersen. 2013. 'Physiological Roles of Aquaporin-4 in Brain'. *Physiological Reviews* 93 (4): 1543–62. https://doi.org/10.1152/physrev.00011.2013.

Nolte, Christiane, Marina Matyash, Tatjyana Pivneva, et al. 2001. 'GFAP Promoter-Controlled EGFP-Expressing Transgenic Mice: A Tool to Visualize Astrocytes and Astrogliosis in Living Brain Tissue'. *Glia* 33 (1): 72–86. https://doi.org/10.1002/1098-1136(20010101)33:1%253C72::AID-GLIA1007%253E3.0.CO;2-A.

Oberheim, Nancy Ann, Steven A. Goldman, and Maiken Nedergaard. 2012. 'Heterogeneity of Astrocytic Form and Function'. In *Astrocytes*, edited by Richard Milner, vol. 814. Methods in Molecular Biology. Humana Press. https://doi.org/10.1007/978-1-61779-452-0_3.

Oberheim, Nancy Ann, Takahiro Takano, Xiaoning Han, et al. 2009. 'Uniquely Hominid Features of Adult Human Astrocytes'. *The Journal of Neuroscience* 29 (10): 3276–87. https://doi.org/10.1523/JNEUROSCI.4707-08.2009.

O'Donnell, John, Douglas Zeppenfeld, Evan McConnell, Salvador Pena, and Maiken Nedergaard. 2012. 'Norepinephrine: A Neuromodulator That Boosts the Function of Multiple Cell Types to Optimize CNS Performance'. *Neurochemical Research* 37 (11): 2496–512. https://doi.org/10.1007/s11064-012-0818-x.

Oe, Yuki, Xiaowen Wang, Tommaso Patriarchi, et al. 2020. 'Distinct Temporal Integration of Noradrenaline Signaling by Astrocytic Second Messengers during Vigilance'. *Nature Communications* 11 (1): 471. https://doi.org/10.1038/s41467-020-14378-x.

O'Leary, Liam Anuj, Maria Antonietta Davoli, Claudia Belliveau, et al. 2020. 'Characterization of Vimentin-Immunoreactive Astrocytes in the Human Brain'. *Frontiers in Neuroanatomy* 14 (July): 31. https://doi.org/10.3389/fnana.2020.00031.

Olsen, Malin, Ximena Aguilar, Dag Sehlin, et al. 2018. 'Astroglial Responses to Amyloid-Beta Progression in a Mouse Model of Alzheimer's Disease'. *Molecular Imaging and Biology* 20 (4): 605–14. https://doi.org/10.1007/s11307-017-1153-z.

Ono, Daisuke, Hiroaki Sekiya, Alexia R. Maier, Melissa E. Murray, Shunsuke Koga, and Dennis W. Dickson. 2025. 'Parkinsonism in Alzheimer's Disease without Lewy Bodies in Association with Nigral Neuron Loss: A Data-driven Clinicopathologic Study'. *Alzheimer's & Dementia* 21 (3): e14628. https://doi.org/10.1002/alz.14628.

Ordway, Gregory A., Michael A. Schwartz, and Alan Frazer, eds. 2007. *Brain Norepinephrine: Neurobiology and Therapeutics*. Cambridge University Press.

Ota, Yusuke, Alexander T. Zanetti, and Robert M. Hallock. 2013. 'The Role of Astrocytes in the Regulation of Synaptic Plasticity and Memory Formation'. *Neural Plasticity* 2013: 1–11. https://doi.org/10.1155/2013/185463.

Outeiro, Tiago Fleming, David J. Koss, Daniel Erskine, et al. 2019. 'Dementia with Lewy Bodies: An Update and Outlook'. *Molecular Neurodegeneration* 14 (1): 5. https://doi.org/10.1186/s13024-019-0306-8.

Pan, Zixin, Zhaoxing Jia, Tianxiang Jiang, et al. 2025. 'Modulation of the Neurovascular Unit by the Locus Coeruleus–Norepinephrine System: From Physiological Mechanisms to Therapeutic Applications'. *The FASEB Journal* 39 (20): e71127. https://doi.org/10.1096/fj.202502069R.

Park, Kyung Won, Hyun Sook Kim, Sang-Myung Cheon, Jae-Kwan Cha, Sang-Ho Kim, and Jae Woo Kim. 2011. 'Dementia with Lewy Bodies versus Alzheimer's Disease and Parkinson's Disease Dementia: A Comparison of Cognitive Profiles'. *Journal of Clinical Neurology* 7 (1): 19. https://doi.org/10.3988/jcn.2011.7.1.19.

Parkinson, James. 2002. ‘An Essay on the Shaking Palsy’. *Neuropsychiatry Classics*, 14.

Paukert, Martin, Amit Agarwal, Jaepyeong Cha, Van A. Doze, Jin U. Kang, and Dwight E. Bergles. 2014. ‘Norepinephrine Controls Astroglial Responsiveness to Local Circuit Activity’. *Neuron* 82 (6): 1263–70. https://doi.org/10.1016/j.neuron.2014.04.038.

Pedersen, Taylor J., Samantha A. Keil, Warren Han, Marie X. Wang, and Jeffrey J. Iliff. 2023. ‘The Effect of Aquaporin-4 Mis-Localization on Aβ Deposition in Mice’. *Neurobiology of Disease* 181 (June): 106100. https://doi.org/10.1016/j.nbd.2023.106100.

Pelkmans, Wiesje, Mahnaz Shekari, Anna Brugulat-Serrat, et al. 2024. ‘Astrocyte Biomarkers GFAP and YKL-40 Mediate Early Alzheimer’s Disease Progression’. *Alzheimer’s & Dementia* 20 (1): 483–93. https://doi.org/10.1002/alz.13450.

Pellerin, L, and P J Magistretti. 1994. ‘Glutamate Uptake into Astrocytes Stimulates Aerobic Glycolysis: A Mechanism Coupling Neuronal Activity to Glucose Utilization.’ *Proceedings of the National Academy of Sciences of the United States of America* 91 (22): 10625–29.

Perea, Gertrudis, Marta Navarrete, and Alfonso Araque. 2009. ‘Tripartite Synapses: Astrocytes Process and Control Synaptic Information’. *Trends in Neurosciences* 32 (8): 421–31. https://doi.org/10.1016/j.tins.2009.05.001.

Pérez-Sala, Dolores, and María A. Pajares. 2023. ‘Appraising the Role of Astrocytes as Suppliers of Neuronal Glutathione Precursors’. *International Journal of Molecular Sciences* 24 (9): 8059. https://doi.org/10.3390/ijms24098059.

Perry, Robert H., Dorothy Irving, Garry Blessed, Andrew Fairbairn, and Elaine K. Perry. 1990. ‘Senile Dementia of Lewy Body Type’. *Journal of the Neurological Sciences* 95 (2): 119–39. https://doi.org/10.1016/0022-510X(90)90236-G.

Pham, Cuong, Yuji Komaki, Anna Deàs-Just, et al. 2024. ‘Astrocyte Aquaporin Mediates a Tonic Water Efflux Maintaining Brain Homeostasis’. *eLife* 13 (November): RP95873. https://doi.org/10.7554/eLife.95873.3.

Phillips, Jared M., Rebecca L. Winfree, Mabel Seto, et al. 2024. ‘Pathologic and Clinical Correlates of Region-Specific Brain GFAP in Alzheimer’s Disease’. *Acta Neuropathologica* 148 (1): 69. https://doi.org/10.1007/s00401-024-02828-5.

Pixley, Sarah K.R., and Jean De Vellis. 1984. ‘Transition between Immature Radial Glia and Mature Astrocytes Studied with a Monoclonal Antibody to Vimentin’. *Developmental Brain Research* 15 (2): 201–9. https://doi.org/10.1016/0165-3806(84)90097-X.

Qin, Hongwei, Lianna Zhou, Faris T. Haque, et al. 2023. ‘Diverse Signaling Mechanisms and Heterogeneity of Astrocyte Reactivity in Alzheimer’s Disease’. *Journal of Neurochemistry*, November 6, jnc.16002. https://doi.org/10.1111/jnc.16002.

Rahimi, Jasmin, and Gabor G Kovacs. 2014. ‘Prevalence of Mixed Pathologies in the Aging Brain’. *Alzheimer’s Research & Therapy* 6 (9): 82. https://doi.org/10.1186/s13195-014-0082-1.

Reichenbach, Andreas, and Andreas Bringmann. 2013. 'New Functions of Müller Cells'. *Glia* 61 (5): 651–78. https://doi.org/10.1002/glia.22477.

Reid, Matthew J., Melissa Leija Salazar, Claire Troakes, et al. 2025. 'Alzheimer's Disease Brain-Derived Tau Extracts Show Differential Processing and Transcriptional Effects in Human Astrocytes'. *iScience* 28 (7): 112793. https://doi.org/10.1016/j.isci.2025.112793.

Riedel, Oliver, Jens Klotsche, Annika Spottke, et al. 2010. 'Frequency of Dementia, Depression, and Other Neuropsychiatric Symptoms in 1,449 Outpatients with Parkinson's Disease'. *Journal of Neurology* 257 (7): 1073–82. https://doi.org/10.1007/s00415-010-5465-z.

Roos, Dareia S., Martin Klein, Dorly J.H. Deeg, Richard L. Doty, and Henk W. Berendse. 2022. 'Prevalence of Prodromal Symptoms of Parkinson's Disease in the Late Middle-Aged Population'. *Journal of Parkinson's Disease* 12 (3): 967–74. https://doi.org/10.3233/JPD-213007.

Roozendaal, Benno. 2007. 'Norepinephrine and Long-Term Memory Function'. In *Brain Norepinephrine*, 1st edn, edited by Gregory A. Ordway, Michael A. Schwartz, and Alan Frazer. Cambridge University Press. https://doi.org/10.1017/CBO9780511544156.009.

Rostami, Jinar, Grammatiki Fotaki, Julien Sirois, et al. 2020. 'Astrocytes Have the Capacity to Act as Antigen-Presenting Cells in the Parkinson's Disease Brain'. *Journal of Neuroinflammation* 17 (1): 119. https://doi.org/10.1186/s12974-020-01776-7.

Rothhammer, Veit, and Francisco J. Quintana. 2015. 'Control of Autoimmune CNS Inflammation by Astrocytes'. *Seminars in Immunopathology* 37 (6): 625–38. https://doi.org/10.1007/s00281-015-0515-3.

Rothstein, Jeffrey D, Margaret Dykes-Hoberg, Carlos A Pardo, et al. 1996. 'Knockout of Glutamate Transporters Reveals a Major Role for Astroglial Transport in Excitotoxicity and Clearance of Glutamate'. *Neuron* 16 (3): 675–86. https://doi.org/10.1016/S0896-6273(00)80086-0.

Roumes, Hélène, Luc Pellerin, and Anne-Karine Bouzier-Sore. 2023. 'Astrocytes as Metabolic Suppliers to Support Neuronal Activity and Brain Functions'. *Essays in Biochemistry* 67 (1): 27–37. https://doi.org/10.1042/EBC20220080.

Salas, Isabel H., Adrien Paumier, Tao Tao, et al. 2024a. 'Astrocyte Transcriptomic Analysis Identifies Glypican 5 Downregulation as a Contributor to Synaptic Dysfunction in Alzheimer's Disease Models'. Preprint, Neuroscience, October 31. https://doi.org/10.1101/2024.10.30.621182.

Salas, Isabel H., Adrien Paumier, Tao Tao, et al. 2024b. 'Astrocyte Transcriptomic Analysis Identifies Glypican 5 Downregulation as a Contributor to Synaptic Dysfunction in Alzheimer's Disease Models'. Preprint, Neuroscience, October 31. https://doi.org/10.1101/2024.10.30.621182.

Salih, Mustafa A., Albandary AlBakheet, Rawan Almass, Ahlam A. A. Hamed, Ali AlOdaib, and Namik Kaya. 2024. 'Case Report: Clinical and Genetic Characterization of a Novel ALDH7A1 Variant Causing Pyridoxine-Dependent Epilepsy, Developmental Delay, and Intellectual Disability in Two Siblings'. *Frontiers in Psychiatry* 15 (December): 1501238. https://doi.org/10.3389/fpsyt.2024.1501238.

Saliu, Ibrahim Olabayode, and Guoyan Zhao. 2024. 'New Insights into Astrocyte Diversity from the Lens of Transcriptional Regulation and Their Implications for Neurodegenerative Disease Treatments'. *Neural Regeneration Research* 19 (11): 2335–36. https://doi.org/10.4103/NRR.NRR-D-23-01790.

Sanchez-Padilla, Javier, Jaime N Guzman, Ema Ilijic, et al. 2014. 'Mitochondrial Oxidant Stress in Locus Coeruleus Is Regulated by Activity and Nitric Oxide Synthase'. *Nature Neuroscience* 17 (6): 832–40. https://doi.org/10.1038/nn.3717.

Sancho, Laura, Minerva Contreras, and Nicola J. Allen. 2021. 'Glia as Sculptors of Synaptic Plasticity'. *Neuroscience Research* 167 (June): 17–29. https://doi.org/10.1016/j.neures.2020.11.005.

Sara, Susan J. 2009. 'The Locus Coeruleus and Noradrenergic Modulation of Cognition'. *Nature Reviews Neuroscience* 10 (3): 211–23. https://doi.org/10.1038/nrn2573.

Sarro, Lidia, Nirubol Tosakulwong, Christopher G. Schwarz, et al. 2017. 'An Investigation of Cerebrovascular Lesions in Dementia with Lewy Bodies Compared to Alzheimer's Disease'. *Alzheimer's & Dementia* 13 (3): 257–66. https://doi.org/10.1016/j.jalz.2016.07.003.

Schirmer, Lucas, Dmitry Velmeshev, Staffan Holmqvist, et al. 2019. 'Neuronal Vulnerability and Multilineage Diversity in Multiple Sclerosis'. *Nature* 573 (7772): 75–82. https://doi.org/10.1038/s41586-019-1404-z.

Schlachetzki, Johannes Cm, Bernd L Fiebich, Elisabeth Haake, et al. 2010. 'Norepinephrine Enhances the LPS-Induced Expression of COX-2 and Secretion of PGE2 in Primary Rat Microglia'. *Journal of Neuroinflammation* 7 (1): 2. https://doi.org/10.1186/1742-2094-7-2.

Serrano-Pozo, Alberto, Huan Li, Zhaozhi Li, et al. 2024. 'Astrocyte Transcriptomic Changes along the Spatiotemporal Progression of Alzheimer's Disease'. *Nature Neuroscience* 27 (12): 2384–400. https://doi.org/10.1038/s41593-024-01791-4.

Sezgin, Mine, Basar Bilgic, Sule Tinaz, and Murat Emre. 2019. 'Parkinson's Disease Dementia and Lewy Body Disease'. *Seminars in Neurology* 39 (2): 274–82. https://doi.org/10.1055/s-0039-1678579.

Sherpa, Ang Doma, Fanrong Xiao, Neethu Joseph, Chiye Aoki, and Sabina Hrabetova. 2016. 'Activation of B-adrenergic Receptors in Rat Visual Cortex Expands Astrocytic Processes and Reduces Extracellular Space Volume'. *Synapse* 70 (8): 307–16. https://doi.org/10.1002/syn.21908.

Silva, Inês, Jéssica Silva, Rita Ferreira, and Diogo Trigo. 2021. 'Glymphatic System, AQP4, and Their Implications in Alzheimer's Disease'. *Neurological Research and Practice* 3 (1): 5. https://doi.org/10.1186/s42466-021-00102-7.

Simpson, J.E., P.G. Ince, G. Lace, et al. 2010. 'Astrocyte Phenotype in Relation to Alzheimer-Type Pathology in the Ageing Brain'. *Neurobiology of Aging* 31 (4): 578–90. https://doi.org/10.1016/j.neurobiolaging.2008.05.015.

Simuni, Tanya, Lana M Chahine, Kathleen Poston, et al. 2024a. 'A Biological Definition of Neuronal α-Synuclein Disease: Towards an Integrated Staging System for Research'. *The Lancet Neurology* 23 (2): 178–90. https://doi.org/10.1016/S1474-4422(23)00405-2.

Simuni, Tanya, Lana M Chahine, Kathleen Poston, et al. 2024b. 'A Biological Definition of Neuronal α-Synuclein Disease: Towards an Integrated Staging System for Research'. *The Lancet Neurology* 23 (2): 178–90. https://doi.org/10.1016/S1474-4422(23)00405-2.

Sofroniew, Michael V., and Harry V. Vinters. 2010. 'Astrocytes: Biology and Pathology'. *Acta Neuropathologica* 119 (1): 7–35. https://doi.org/10.1007/s00401-009-0619-8.

Song, Sheng, Lulu Jiang, Esteban A. Oyarzabal, et al. 2019. 'Loss of Brain Norepinephrine Elicits Neuroinflammation-Mediated Oxidative Injury and Selective Caudo-Rostral Neurodegeneration'. *Molecular Neurobiology* 56 (4): 2653–69. https://doi.org/10.1007/s12035-018-1235-1.

Song, Yun Ju C., Glenda M. Halliday, Janice L. Holton, et al. 2009. 'Degeneration in Different Parkinsonian Syndromes Relates to Astrocyte Type and Astrocyte Protein Expression'. *Journal of Neuropathology & Experimental Neurology* 68 (10): 1073–83. https://doi.org/10.1097/NEN.0b013e3181b66f1b.

Sorg, O, and Pj Magistretti. 1992. 'Vasoactive Intestinal Peptide and Noradrenaline Exert Long-Term Control on Glycogen Levels in Astrocytes: Blockade by Protein Synthesis Inhibition'. *The Journal of Neuroscience* 12 (12): 4923–31. https://doi.org/10.1523/JNEUROSCI.12-12-04923.1992.

Sosunov, Alexander A., Xiaoping Wu, Nadejda M. Tsankova, Eileen Guilfoyle, Guy M. McKhann, and James E. Goldman. 2014. 'Phenotypic Heterogeneity and Plasticity of Isocortical and Hippocampal Astrocytes in the Human Brain'. *The Journal of Neuroscience* 34 (6): 2285–98. https://doi.org/10.1523/JNEUROSCI.4037-13.2014.

Srinivasan, Rahul, Tsai-Yi Lu, Hua Chai, et al. 2016. 'New Transgenic Mouse Lines for Selectively Targeting Astrocytes and Studying Calcium Signals in Astrocyte Processes In Situ and In Vivo'. *Neuron* 92 (6): 1181–95. https://doi.org/10.1016/j.neuron.2016.11.030.

Stelzmann, Rainulf A., H. Norman Schnitzlein, and F. Reed Murtagh. 1995. 'An English Translation of Alzheimer's 1907 Paper, "Über Eine Eigenartige Erkankung Der Hirnrinde"'. *Clinical Anatomy* 8 (6): 429–31. https://doi.org/10.1002/ca.980080612.

Stone, Eric A., and Marjorie A. Ariano. 1989. 'Are Glial Cells Targets of the Central Noradrenergic System? A Review of the Evidence'. *Brain Research Reviews* 14 (4): 297–309. https://doi.org/10.1016/0165-0173(89)90015-5.

Stowell, Rianne D., Grayson O. Sipe, Ryan P. Dawes, et al. 2019. 'Noradrenergic Signaling in the Wakeful State Inhibits Microglial Surveillance and Synaptic Plasticity in the Mouse Visual Cortex'. *Nature Neuroscience* 22 (11): 1782–92. https://doi.org/10.1038/s41593-019-0514-0.

Strunz, Maximilian, Juliet T. Jarrell, David S. Cohen, Eric R. Rosin, Charles R. Vanderburg, and Xudong Huang. 2019. 'Modulation of SPARC/Hevin Proteins in Alzheimer's Disease Brain Injury'. *Journal of Alzheimer's Disease* 68 (2): 695–710. https://doi.org/10.3233/JAD-181032.

Sun, Junyan, Jinghong Ma, Linlin Gao, et al. 2023. 'Disruption of Locus Coeruleus-Related Functional Networks in Parkinson's Disease'. *Npj Parkinson's Disease* 9 (1): 81. https://doi.org/10.1038/s41531-023-00532-x.

Szot, Patricia, Sylvia S. White, J. Lynne Greenup, James B. Leverenz, Elaine R. Peskind, and Murray A. Raskind. 2006. 'Compensatory Changes in the Noradrenergic Nervous System in the Locus Ceruleus and Hippocampus of Postmortem Subjects with Alzheimer's Disease and Dementia with Lewy Bodies'. *The Journal of Neuroscience* 26 (2): 467–78. https://doi.org/10.1523/JNEUROSCI.4265-05.2006.

Tabassum, Rubaiya, NaYoung Jeong, and Junyang Jung. 2020. 'Protective Effect of Hydrogen Sulfide on Oxidative Stress-Induced Neurodegenerative Diseases'. *Neural Regeneration Research* 15 (2): 232. https://doi.org/10.4103/1673-5374.265543.

Tabata, Hidenori. 2015. 'Diverse Subtypes of Astrocytes and Their Development during Corticogenesis'. *Frontiers in Neuroscience* 9 (April). https://doi.org/10.3389/fnins.2015.00114.

Tang, F., S. Lane, A. Korsak, et al. 2014. 'Lactate-Mediated Glia-Neuronal Signalling in the Mammalian Brain'. *Nature Communications* 5 (1). https://doi.org/10.1038/ncomms4284.

Tao-Cheng, Jh, Z Nagy, and Mw Brightman. 1987. 'Tight Junctions of Brain Endothelium in Vitro Are Enhanced by Astroglia'. *The Journal of Neuroscience* 7 (10): 3293–99. https://doi.org/10.1523/JNEUROSCI.07-10-03293.1987.

Thal, D. R., Christian Schultz, Faramarz Dehghani, Haruyasu Yamaguchi, Heiko Braak, and Eva Braak. 2000. 'Amyloid β-Protein (Aβ)-Containing Astrocytes Are Located Preferentially near N-Terminal-Truncated Aβ Deposits in the Human Entorhinal Cortex'. *Acta Neuropathologica* 100 (6): 608–17. https://doi.org/10.1007/s004010000242.

Thal, Dietmar R., Udo Rüb, Mario Orantes, and Heiko Braak. 2002. 'Phases of Aβ-Deposition in the Human Brain and Its Relevance for the Development of AD'. *Neurology* 58 (12): 1791–800. https://doi.org/10.1212/WNL.58.12.1791.

Thal, Dietmar Rudolf, Koen Poesen, Rik Vandenberghe, and Steffi De Meyer. 2025. 'Alzheimer's Disease Neuropathology and Its Estimation with Fluid and Imaging Biomarkers'. *Molecular Neurodegeneration* 20 (1): 33. https://doi.org/10.1186/s13024-025-00819-y.

Theofilas, Panos, Alexander J. Ehrenberg, Sara Dunlop, et al. 2017. 'Locus Coeruleus Volume and Cell Population Changes during Alzheimer's Disease Progression: A Stereological Study in Human Postmortem Brains with Potential Implication for Early-stage Biomarker Discovery'. *Alzheimer's & Dementia* 13 (3): 236–46. https://doi.org/10.1016/j.jalz.2016.06.2362.

Tontsch, Ulrike, and Hans-Christian Bauer. 1991. 'Glial Cells and Neurons Induce Blood-Brain Barrier Related Enzymes in Cultured Cerebral Endothelial Cells'. *Brain Research* 539 (2): 247–53. https://doi.org/10.1016/0006-8993(91)91628-E.

Troadec, Jean-Denis, Marc Marien, Frédéric Darios, et al. 2001. 'Noradrenaline Provides Long-term Protection to Dopaminergic Neurons by Reducing Oxidative Stress'. *Journal of Neurochemistry* 79 (1): 200–210. https://doi.org/10.1046/j.1471-4159.2001.00556.x.

Tso, Chak Foon, Tatiana Simon, Alison C. Greenlaw, Tanvi Puri, Michihiro Mieda, and Erik D. Herzog. 2017. 'Astrocytes Regulate Daily Rhythms in the Suprachiasmatic Nucleus and Behavior'. *Current Biology* 27 (7): 1055–61. https://doi.org/10.1016/j.cub.2017.02.037.

Uchikado, Hirotake, Wen-Lang Lin, Michael W. DeLucia, and Dennis W. Dickson. 2006. 'Alzheimer Disease With Amygdala Lewy Bodies: A Distinct Form of α-Synucleinopathy'. *Journal of Neuropathology and Experimental Neurology* 65 (7): 685–97. https://doi.org/10.1097/01.jnen.0000225908.90052.07.

Van Horssen, Jack, Johanneke Kleinnijenhuis, Cathy N. Maass, et al. 2002. 'Accumulation of Heparan Sulfate Proteoglycans in Cerebellar Senile Plaques'. *Neurobiology of Aging* 23 (4): 537–45. https://doi.org/10.1016/S0197-4580(02)00010-6.

Vardjan, Nina, Helena H. Chowdhury, Anemari Horvat, et al. 2018. 'Enhancement of Astroglial Aerobic Glycolysis by Extracellular Lactate-Mediated Increase in cAMP'. *Frontiers in Molecular Neuroscience* 11 (May). https://doi.org/10.3389/fnmol.2018.00148.

Vardjan, Nina, Marko Kreft, and Robert Zorec. 2014. 'Dynamics of B-adrenergic/cAMP Signaling and Morphological Changes in Cultured Astrocytes'. *Glia* 62 (4): 566–79. https://doi.org/10.1002/glia.22626.

Vasile, Flora, Elena Dossi, and Nathalie Rouach. 2017. 'Human Astrocytes: Structure and Functions in the Healthy Brain'. *Brain Structure and Function* 222 (5): 2017–29. https://doi.org/10.1007/s00429-017-1383-5.

Vemuri, Prashanthi, and Clifford R Jack. 2010. 'Role of Structural MRI in Alzheimer's Disease'. *Alzheimer's Research & Therapy* 2 (4): 23. https://doi.org/10.1186/alzrt47.

Verkhratsky, Alexei, and Vladimir Parpura. 2010a. 'Recent Advances in (Patho)Physiology of Astroglia'. *Acta Pharmacologica Sinica* 31 (9): 1044–54. https://doi.org/10.1038/aps.2010.108.

Verkhratsky, Alexei, and Vladimir Parpura. 2010b. 'Recent Advances in (Patho)Physiology of Astroglia'. *Acta Pharmacologica Sinica* 31 (9): 1044–54. https://doi.org/10.1038/aps.2010.108.

Viana, João Filipe, João Luís Machado, Daniela Sofia Abreu, et al. 2023. 'Astrocyte Structural Heterogeneity in the Mouse Hippocampus'. *Glia* 71 (7): 1667–82. https://doi.org/10.1002/glia.24362.

Vizi, Es, A Fekete, R Karoly, and A Mike. 2010. 'Non-synaptic Receptors and Transporters Involved in Brain Functions and Targets of Drug Treatment'. *British Journal of Pharmacology* 160 (4): 785–809. https://doi.org/10.1111/j.1476-5381.2009.00624.x.

Vogt, Marthe. 1954. 'The Concentration of Sympathin in Different Parts of the Central Nervous System under Normal Conditions and after the Administration of Drugs'. *The Journal of Physiology* 123 (3): 451–81. https://doi.org/10.1113/jphysiol.1954.sp005064.

Wahis, Jérôme, and Matthew G. Holt. 2021. 'Astrocytes, Noradrenaline, A1-Adrenoreceptors, and Neuromodulation: Evidence and Unanswered Questions'. *Frontiers in Cellular Neuroscience* 15 (February): 645691. https://doi.org/10.3389/fncel.2021.645691.

Wakasugi, Noritaka, and Takashi Hanakawa. 2021. 'It Is Time to Study Overlapping Molecular and Circuit Pathophysiologies in Alzheimer's and Lewy Body Disease Spectra'. *Frontiers in Systems Neuroscience* 15 (November): 777706. https://doi.org/10.3389/fnsys.2021.777706.

Walker, Lary C. 2020. 'Aβ Plaques'. *Free Neuropathology*, October 30, 31 Pages. 31 Pages. https://doi.org/10.17879/FREENEUROPATHOLOGY-2020-3025.

Walker, Lauren, Leonidas Stefanis, and Johannes Attems. 2019. 'Clinical and Neuropathological Differences between Parkinson's Disease, Parkinson's Disease Dementia and Dementia with Lewy Bodies – Current Issues and Future Directions'. *Journal of Neurochemistry* 150 (5): 467–74. https://doi.org/10.1111/jnc.14698.

Walz, Wolfgang, and Melody K Lang. 1998. 'Immunocytochemical Evidence for a Distinct GFAP-Negative Subpopulation of Astrocytes in the Adult Rat Hippocampus'. *Neuroscience Letters* 257 (3): 127–30. https://doi.org/10.1016/S0304-3940(98)00813-1.

Wang, Jun, Jie Tu, Bing Cao, et al. 2017. 'Astrocytic l -Lactate Signaling Facilitates Amygdala-Anterior Cingulate Cortex Synchrony and Decision Making in Rats'. *Cell Reports* 21 (9): 2407–18. https://doi.org/10.1016/j.celrep.2017.11.012.

Wang, Qingshan, Esteban A. Oyarzabal, Sheng Song, Belinda Wilson, Janine H. Santos, and Jau-Shyong Hong. 2020. 'Locus Coeruleus Neurons Are Most Sensitive to Chronic Neuroinflammation-Induced Neurodegeneration'. *Brain, Behavior, and Immunity* 87 (July): 359–68. https://doi.org/10.1016/j.bbi.2020.01.003.

Wareham, Lauren K., Shane A. Liddelow, Sally Temple, et al. 2022. 'Solving Neurodegeneration: Common Mechanisms and Strategies for New Treatments'. *Molecular Neurodegeneration* 17 (1): 23. https://doi.org/10.1186/s13024-022-00524-0.

Weinshenker, David. 2008. 'Functional Consequences of Locus Coeruleus Degeneration in Alzheimers Disease'. *Current Alzheimer Research* 5 (3): 342–45. https://doi.org/10.2174/156720508784533286.

Weinshenker, David. 2018. 'Long Road to Ruin: Noradrenergic Dysfunction in Neurodegenerative Disease'. *Trends in Neurosciences* 41 (4): 211–23. https://doi.org/10.1016/j.tins.2018.01.010.

Wilhelmsson, Ulrika, Andrea Pozo-Rodrigalvarez, Marie Kalm, et al. 2019. 'The Role of GFAP and Vimentin in Learning and Memory'. *Biological Chemistry* 400 (9): 1147–56. https://doi.org/10.1515/hsz-2019-0199.

Williams, Susan Schneider. 2016. 'The Terrorist inside My Husband's Brain'. *Neurology* 87 (13): 1308–11. https://doi.org/10.1212/WNL.0000000000003162.

Williamson, Timothy G., Su San Mok, Anna Henry, et al. 1996. 'Secreted Glypican Binds to the Amyloid Precursor Protein of Alzheimer's Disease (APP) and Inhibits APP-Induced Neurite Outgrowth'. *Journal of Biological Chemistry* 271 (49): 31215–21. https://doi.org/10.1074/jbc.271.49.31215.

Willis, M.A., and D.E. Haines. 2018. 'The Limbic System'. In *Fundamental Neuroscience for Basic and Clinical Applications*. Elsevier. https://doi.org/10.1016/B978-0-323-39632-5.00031-1.

Wilson, David M., Mark R. Cookson, Ludo Van Den Bosch, Henrik Zetterberg, David M. Holtzman, and Ilse Dewachter. 2023. 'Hallmarks of Neurodegenerative Diseases'. *Cell* 186 (4): 693–714. https://doi.org/10.1016/j.cell.2022.12.032.

Wilson, Robert S., David A. Bennett, David W. Gilley, Laurel A. Beckett, Julie A. Schneider, and Denis A. Evans. 2000. 'Progression of Parkinsonism and Loss of Cognitive Function in Alzheimer Disease'. *Archives of Neurology* 57 (6): 855. https://doi.org/10.1001/archneur.57.6.855.

Wu, Junjie, Dezhe Qin, Ziqi Liang, et al. 2025. 'Dysregulation of Astrocyte-Derived Matrix Gla Protein Impairs Dendritic Spine Development in Pyridoxine-Dependent Epilepsy'. *Molecular Therapy* 33 (4): 1785–802. https://doi.org/10.1016/j.ymthe.2025.02.027.

Xu, Zhiqiang, Na Xiao, Yali Chen, et al. 2015. 'Deletion of Aquaporin-4 in APP/PS1 Mice Exacerbates Brain Aβ Accumulation and Memory Deficits'. *Molecular Neurodegeneration* 10 (1): 58. https://doi.org/10.1186/s13024-015-0056-1.

Yamamoto, Ken-ichi, Toshikazu Shinba, and Mitsunobu Yoshii. 2014. 'Psychiatric Symptoms of Noradrenergic Dysfunction: A Pathophysiological View'. *Psychiatry and Clinical Neurosciences* 68 (1): 1–20. https://doi.org/10.1111/pcn.12126.

Yan, Jianfei, Junjie Wu, Mingyue Xu, Min Wang, and Weixiang Guo. 2024. 'Disrupted de Novo Pyrimidine Biosynthesis Impairs Adult Hippocampal Neurogenesis and Cognition in Pyridoxine-Dependent Epilepsy'. *Science Advances* 10 (14): eadl2764. https://doi.org/10.1126/sciadv.adl2764.

Yang, Hui, Yuanyuan Xiang, Jiaxuan Wang, et al. 2025. 'Modulating the Blood-Brain Barrier in CNS Disorders: A Review of the Therapeutic Implications of Secreted Protein Acidic and Rich in Cysteine (SPARC)'. *International Journal of Biological Macromolecules* 288 (February): 138747. https://doi.org/10.1016/j.ijbiomac.2024.138747.

Yang, Qinghu, Chengxiang Yan, Yahan Sun, et al. 2024. 'Extracellular Matrix Remodeling Alleviates Memory Deficits in Alzheimer's Disease by Enhancing the Astrocytic Autophagy-Lysosome Pathway'. *Advanced Science* 11 (31): 2400480. https://doi.org/10.1002/advs.202400480.

Yang, Yongjie, Svetlana Vidensky, Lin Jin, et al. 2011. 'Molecular Comparison of $GLT1^+$ and $ALDH1L1^+$ Astrocytes *in Vivo* in Astroglial Reporter Mice'. *Glia* 59 (2): 200–207. https://doi.org/10.1002/glia.21089.

Yao, Ning, Yanhong Wu, Yan Zhou, et al. 2015. 'Lesion of the Locus Coeruleus Aggravates Dopaminergic Neuron Degeneration by Modulating Microglial Function in Mouse Models of Parkinson's Disease'. *Brain Research* 1625 (November): 255–74. https://doi.org/10.1016/j.brainres.2015.08.032.

Yeap, Yee Jie, Nagaendran Kandiah, Dean Nizetic, and Kah-Leong Lim. 2023. 'BACE2: A Promising Neuroprotective Candidate for Alzheimer's Disease'. *Journal of Alzheimer's Disease* 94 (s1): S159–71. https://doi.org/10.3233/JAD-220867.

Yoshioka, Yasuhiro, Hisatsugu Kadoi, Akiko Yamamuro, Yuki Ishimaru, and Sadaaki Maeda. 2016. 'Noradrenaline Increases Intracellular Glutathione in Human Astrocytoma U-251 MG Cells by

Inducing Glutamate-Cysteine Ligase Protein via B3-Adrenoceptor Stimulation'. *European Journal of Pharmacology* 772 (February): 51–61. https://doi.org/10.1016/j.ejphar.2015.12.041.

Yoshioka, Yasuhiro, Ryosuke Negoro, Hisatsugu Kadoi, et al. 2021. 'Noradrenaline Protects Neurons against $H_2 O_2$ -induced Death by Increasing the Supply of Glutathione from Astrocytes via β_3 -adrenoceptor Stimulation'. *Journal of Neuroscience Research* 99 (2): 621–37. https://doi.org/10.1002/jnr.24733.

Youn, Wongu, Mijin Yun, C. Justin Lee, and Michael Schöll. 2025. 'Cautions on Utilizing Plasma GFAP Level as a Biomarker for Reactive Astrocytes in Neurodegenerative Diseases'. *Molecular Neurodegeneration* 20 (1): 54. https://doi.org/10.1186/s13024-025-00846-9.

Zamanian, Jennifer L., Lijun Xu, Lynette C. Foo, et al. 2012. 'Genomic Analysis of Reactive Astrogliosis'. *The Journal of Neuroscience* 32 (18): 6391–410. https://doi.org/10.1523/JNEUROSCI.6221-11.2012.

Zarow, Chris, Scott A. Lyness, James A. Mortimer, and Helena C. Chui. 2003. 'Neuronal Loss Is Greater in the Locus Coeruleus Than Nucleus Basalis and Substantia Nigra in Alzheimer and Parkinson Diseases'. *Archives of Neurology* 60 (3): 337. https://doi.org/10.1001/archneur.60.3.337.

Železníková, Žaneta, L'ubomíra Nováková, Lubomír Vojtíšek, et al. 2025. 'Early Changes in the Locus Coeruleus in Mild Cognitive Impairment with Lewy Bodies'. *Movement Disorders* 40 (2): 276–84. https://doi.org/10.1002/mds.30058.

Zeppenfeld, Douglas M., Matthew Simon, J. Douglas Haswell, et al. 2017. 'Association of Perivascular Localization of Aquaporin-4 With Cognition and Alzheimer Disease in Aging Brains'. *JAMA Neurology* 74 (1): 91. https://doi.org/10.1001/jamaneurol.2016.4370.

Zhang, Lan, Ji Wang, Yalong Yan, et al. 2025. 'Vimentin Fragmentation and Its Role in Amyloid-Beta Plaque Deposition in Alzheimer's Disease'. *International Journal of Molecular Sciences* 26 (7): 2857. https://doi.org/10.3390/ijms26072857.

Zhou, Kaige, Jingxing Zhang, Junhui Su, et al. 2025. 'Exploration and Validation of the Immune-Related Genes Signatures and Potential Molecular Mechanisms Shared between Alzheimer's Disease (AD) and Parkinson's Disease (PD)'. *BMC Medical Genomics* 18 (1): 141. https://doi.org/10.1186/s12920-025-02219-z.

Zhou, Yunchuan, Yang Zhou, Shanshan Yu, Jingxian Wu, Yanlin Chen, and Yong Zhao. 2015. 'Sulfiredoxin-1 Exerts Anti-Apoptotic and Neuroprotective Effects against Oxidative Stress-Induced Injury in Rat Cortical Astrocytes Following Exposure to Oxygen-Glucose Deprivation and Hydrogen Peroxide'. *International Journal of Molecular Medicine* 36 (1): 43–52. https://doi.org/10.3892/ijmm.2015.2205.

Zimmer, Till S., Adam L. Orr, and Anna G. Orr. 2024. 'Astrocytes in Selective Vulnerability to Neurodegenerative Disease'. *Trends in Neurosciences* 47 (4): 289–302. https://doi.org/10.1016/j.tins.2024.02.008.

Zorec, Robert. 2025. ‘Noradrenergic System in the Pathogenesis of Age-Dependent Neurodegeneration’. *Ageing & Longevity*, no. 1.2025 (January): 28–34. https://doi.org/10.47855/jal9020-2025-1-4.

Zorec, Robert, Vladimir Parpura, and Alexei Verkhratsky. 2018. ‘Preventing Neurodegeneration by Adrenergic Astroglial Excitation’. *The FEBS Journal* 285 (19): 3645–56. https://doi.org/10.1111/febs.14456.

Zou, He-Lin, Juan Li, Jun-Li Zhou, Xi Yi, and Song Cao. 2021. ‘Effects of Norepinephrine on Microglial Neuroinflammation and Neuropathic Pain’. *Ibrain* 7 (4): 309–17. https://doi.org/10.1002/ibra.12001.

Zucca, F. A., C. Bellei, S. Giannelli, et al. 2006. ‘Neuromelanin and Iron in Human Locus Coeruleus and Substantia Nigra during Aging: Consequences for Neuronal Vulnerability’. *Journal of Neural Transmission* 113 (6): 757–67. https://doi.org/10.1007/s00702-006-0453-2.

Part VIII: Manuscript references

1. Manuscript I

1. Khakh BS, Sofroniew MV. Diversity of astrocyte functions and phenotypes in neural circuits. Nat Neurosci. juill 2015;18(7):942-52.

2. Perea G, Navarrete M, Araque A. Tripartite synapses: astrocytes process and control synaptic information. Trends Neurosci. août 2009;32(8):421-31.

3. Eroglu C, Barres BA. Regulation of synaptic connectivity by glia. Nature. nov 2010;468(7321):223-31.

4. Sancho L, Contreras M, Allen NJ. Glia as sculptors of synaptic plasticity. Neurosci Res. juin 2021;167:17-29.

5. Bouvier DS, Fixemer S, Heurtaux T, Jeannelle F, Frauenknecht KBM, Mittelbronn M. The Multifaceted Neurotoxicity of Astrocytes in Ageing and Age-Related Neurodegenerative Diseases: A Translational Perspective. Front Physiol [Internet]. 2022;13. Disponible sur: https://www.frontiersin.org/articles/10.3389/fphys.2022.814889

6. Díaz-Castro B, Robel S, Mishra A. Astrocyte Endfeet in Brain Function and Pathology: Open Questions. Annu Rev Neurosci. 10 juill 2023;46(1):101-21.

7. MacVicar BA, Newman EA. Astrocyte Regulation of Blood Flow in the Brain. Cold Spring Harb Perspect Biol. mai 2015;7(5):a020388.

8. Bélanger M, Allaman I, Magistretti PJ. Brain Energy Metabolism: Focus on Astrocyte-Neuron Metabolic Cooperation. Cell Metab. déc 2011;14(6):724-38.

9. Mulligan SJ, MacVicar BA. Calcium transients in astrocyte endfeet cause cerebrovascular constrictions. Nature. sept 2004;431(7005):195-9.

10. Silva I, Silva J, Ferreira R, Trigo D. Glymphatic system, AQP4, and their implications in Alzheimer's disease. Neurol Res Pract. déc 2021;3(1):5.

11. Das N, Dhamija R, Sarkar S. The role of astrocytes in the glymphatic network: a narrative review. Metab Brain Dis. 27 nov 2023;39(3):453-65.

12. Fisher TM, Liddelow SA. Emerging roles of astrocytes as immune effectors in the central nervous system. Trends Immunol. oct 2024;45(10):824-36.

13. Chen Y, Qin C, Huang J, Tang X, Liu C, Huang K, et al. The role of astrocytes in oxidative stress of central nervous system: A mixed blessing. Cell Prolif. mars 2020;53(3):e12781.

14. Hastings MH, Brancaccio M, Gonzalez-Aponte MF, Herzog ED. Circadian Rhythms and Astrocytes: The Good, the Bad, and the Ugly. Annu Rev Neurosci. 10 juill 2023;46(1):123-43.
15. Wang J, Tu J, Cao B, Mu L, Yang X, Cong M, et al. Astrocytic l -Lactate Signaling Facilitates Amygdala-Anterior Cingulate Cortex Synchrony and Decision Making in Rats. Cell Rep. nov 2017;21(9):2407-18.
16. Kofuji P, Araque A. Astrocytes and Behavior. Annu Rev Neurosci. 8 juill 2021;44(1):49-67.
17. Escalada P, Ezkurdia A, Ramírez MJ, Solas M. Essential Role of Astrocytes in Learning and Memory. Int J Mol Sci. 5 févr 2024;25(3):1899.
18. Rothhammer V, Quintana FJ. Control of autoimmune CNS inflammation by astrocytes. Semin Immunopathol. nov 2015;37(6):625-38.
19. Liddelow SA, Barres BA. Reactive Astrocytes: Production, Function, and Therapeutic Potential. Immunity. juin 2017;46(6):957-67.
20. Escartin C, Galea E, Lakatos A, O'Callaghan JP, Petzold GC, Serrano-Pozo A, et al. Reactive astrocyte nomenclature, definitions, and future directions. Nat Neurosci. mars 2021;24(3):312-25.
21. Lawrence JM, Schardien K, Wigdahl B, Nonnemacher MR. Roles of neuropathology-associated reactive astrocytes: a systematic review. Acta Neuropathol Commun. 13 mars 2023;11(1):42.
22. Luijerink L, Rodriguez M, Machaalani R. Quantifying GFAP immunohistochemistry in the brain – Introduction of the Reactivity score (R-score) and how it compares to other methodologies. J Neurosci Methods. févr 2024;402:110025.
23. Jurga AM, Paleczna M, Kadluczka J, Kuter KZ. Beyond the GFAP-Astrocyte Protein Markers in the Brain. Biomolecules. 14 sept 2021;11(9):1361.
24. Benedet AL, Milà-Alomà M, Vrillon A, Ashton NJ, Pascoal TA, Lussier F, et al. Differences Between Plasma and Cerebrospinal Fluid Glial Fibrillary Acidic Protein Levels Across the Alzheimer Disease Continuum. JAMA Neurol. 1 déc 2021;78(12):1471.
25. Abdelhak A, Foschi M, Abu-Rumeileh S, Yue JK, D'Anna L, Huss A, et al. Blood GFAP as an emerging biomarker in brain and spinal cord disorders. Nat Rev Neurol. mars 2022;18(3):158-72.
26. Lin J, Ou R, Li C, Hou Y, Zhang L, Wei Q, et al. Plasma glial fibrillary acidic protein as a biomarker of disease progression in Parkinson's disease: a prospective cohort study. BMC Med. 6 nov 2023;21(1):420.
27. Liu T, Zuo H, Ma D, Song D, Zhao Y, Cheng O. Cerebrospinal fluid GFAP is a predictive biomarker for conversion to dementia and Alzheimer's disease-associated biomarkers alterations among de novo Parkinson's disease patients: a prospective cohort study. J Neuroinflammation. 20 juill 2023;20(1):167.

28. Gogishvili D, Honey MIJ, Verberk IMW, Vermunt L, Hol EM, Teunissen CE, et al. The GFAP proteoform puzzle: How to advance GFAP as a fluid biomarker in neurological diseases. J Neurochem. janv 2025;169(1):e16226.
29. Chiotis K, Johansson C, Rodriguez-Vieitez E, Ashton NJ, Blennow K, Zetterberg H, et al. Tracking reactive astrogliosis in autosomal dominant and sporadic Alzheimer's disease with multi-modal PET and plasma GFAP. Mol Neurodegener. 12 sept 2023;18(1):60.
30. Youn W, Yun M, Lee CJ, Schöll M. Cautions on utilizing plasma GFAP level as a biomarker for reactive astrocytes in neurodegenerative diseases. Mol Neurodegener. 9 mai 2025;20(1):54.
31. Edison P. Astroglial activation: Current concepts and future directions. Alzheimers Dement. avr 2024;20(4):3034-53.
32. Oberheim NA, Takano T, Han X, He W, Lin JHC, Wang F, et al. Uniquely Hominid Features of Adult Human Astrocytes. J Neurosci. 11 mars 2009;29(10):3276-87.
33. Vasile F, Dossi E, Rouach N. Human astrocytes: structure and functions in the healthy brain. Brain Struct Funct. juill 2017;222(5):2017-29.
34. Verkhratsky A, Parpura V. Recent advances in (patho)physiology of astroglia. Acta Pharmacol Sin. sept 2010;31(9):1044-54.
35. Farmer WT, Murai K. Resolving Astrocyte Heterogeneity in the CNS. Front Cell Neurosci. 27 sept 2017;11:300.
36. Baldwin KT, Murai KK, Khakh BS. Astrocyte morphology. Trends Cell Biol. juill 2024;34(7):547-65.
37. Oberheim NA, Goldman SA, Nedergaard M. Heterogeneity of Astrocytic Form and Function. In: Milner R, éditeur. Astrocytes [Internet]. Totowa, NJ: Humana Press; 2012 [cité 9 juin 2025]. p. 23-45. (Methods in Molecular Biology; vol. 814). Disponible sur: https://link.springer.com/10.1007/978-1-61779-452-0_3
38. Falcone C, Penna E, Hong T, Tarantal AF, Hof PR, Hopkins WD, et al. Cortical Interlaminar Astrocytes Are Generated Prenatally, Mature Postnatally, and Express Unique Markers in Human and Nonhuman Primates. Cereb Cortex. 1 janv 2021;31(1):379-95.
39. Ciani C, Falcone C. Interlaminar and varicose-projection astrocytes: toward a new understanding of the primate brain. Front Cell Neurosci. 25 nov 2024;18:1477753.
40. Hasel P, Cooper ML, Marchildon AE, Rufen-Blanchette U, Kim RD, Ma TC, et al. Defining the molecular identity and morphology of glia limitans superficialis astrocytes in vertebrates. Cell Rep. mars 2025;44(3):115344.

41. Mathys H, Davila-Velderrain J, Peng Z, Gao F, Mohammadi S, Young JZ, et al. Single-cell transcriptomic analysis of Alzheimer's disease. Nature. 20 juin 2019;570(7761):332-7.
42. Green GS, Fujita M, Yang HS, Taga M, Cain A, McCabe C, et al. Cellular communities reveal trajectories of brain ageing and Alzheimer's disease. Nature. 19 sept 2024;633(8030):634-45.
43. Habib N, McCabe C, Medina S, Varshavsky M, Kitsberg D, Dvir-Szternfeld R, et al. Disease-associated astrocytes in Alzheimer's disease and aging. Nat Neurosci. juin 2020;23(6):701-6.
44. Braak H, Braak E. Neuropathological stageing of Alzheimer-related changes. Acta Neuropathol (Berl). sept 1991;82(4):239-59.
45. Braak H, Tredici KD, Rüb U, De Vos RAI, Jansen Steur ENH, Braak E. Staging of brain pathology related to sporadic Parkinson's disease. Neurobiol Aging. mars 2003;24(2):197-211.
46. Montine TJ, Phelps CH, Beach TG, Bigio EH, Cairns NJ, Dickson DW, et al. National Institute on Aging–Alzheimer's Association guidelines for the neuropathologic assessment of Alzheimer's disease: a practical approach. Acta Neuropathol (Berl). janv 2012;123(1):1-11.
47. McKeith IG. Consensus guidelines for the clinical and pathologic diagnosis of dementia with Lewy bodies (DLB): Report of the Consortium on DLB International Workshop. J Alzheimers Dis. 27 juill 2006;9(s3):417-23.
48. Bosworth A, Contreras M, Weiser Novak S, Sancho L, Salas I, Manor U, et al. Astrocyte glypican 5 regulates synapse maturation and stabilization [Internet]. Neuroscience; 2023 [cité 3 févr 2025]. Disponible sur: http://biorxiv.org/lookup/doi/10.1101/2023.03.02.529949
49. Salas IH, Paumier A, Tao T, Derevyanko A, Switzler C, Burgado J, et al. Astrocyte transcriptomic analysis identifies glypican 5 downregulation as a contributor to synaptic dysfunction in Alzheimer's disease models [Internet]. Neuroscience; 2024 [cité 14 juin 2025]. Disponible sur: http://biorxiv.org/lookup/doi/10.1101/2024.10.30.621182
50. Salas IH, Paumier A, Tao T, Derevyanko A, Switzler C, Burgado J, et al. Astrocyte transcriptomic analysis identifies glypican 5 downregulation as a contributor to synaptic dysfunction in Alzheimer's disease models [Internet]. Neuroscience; 2024 [cité 21 janv 2025]. Disponible sur: http://biorxiv.org/lookup/doi/10.1101/2024.10.30.621182
51. Thal DR, Rüb U, Orantes M, Braak H. Phases of Aβ-deposition in the human brain and its relevance for the development of AD. Neurology. 25 juin 2002;58(12):1791-800.
52. Almeida ZL, Vaz DC, Brito RMM. Morphological and Molecular Profiling of Amyloid-β Species in Alzheimer's Pathogenesis. Mol Neurobiol. avr 2025;62(4):4391-419.

53. Augustinack JC, Schneider A, Mandelkow EM, Hyman BT. Specific tau phosphorylation sites correlate with severity of neuronal cytopathology in Alzheimer's disease. Acta Neuropathol (Berl). janv 2002;103(1):26-35.

54. Fixemer S, Miranda De La Maza M, Hammer GP, Jeannelle F, Schreiner S, Gérardy JJ, et al. Microglia aggregates define distinct immune and neurodegenerative niches in Alzheimer's disease hippocampus. Acta Neuropathol (Berl). 15 févr 2025;149(1):19.

55. Chai H, Diaz-Castro B, Shigetomi E, Monte E, Octeau JC, Yu X, et al. Neural Circuit-Specialized Astrocytes: Transcriptomic, Proteomic, Morphological, and Functional Evidence. Neuron. août 2017;95(3):531-549.e9.

56. Batiuk MY, Martirosyan A, Wahis J, De Vin F, Marneffe C, Kusserow C, et al. Identification of region-specific astrocyte subtypes at single cell resolution. Nat Commun. 5 mars 2020;11(1):1220.

57. Viana JF, Machado JL, Abreu DS, Veiga A, Barsanti S, Tavares G, et al. Astrocyte structural heterogeneity in the mouse hippocampus. Glia. juill 2023;71(7):1667-82.

58. Bocchi R, Thorwirth M, Simon-Ebert T, Koupourtidou C, Clavreul S, Kolf K, et al. Astrocyte heterogeneity reveals region-specific astrogenesis in the white matter. Nat Neurosci. mars 2025;28(3):457-69.

59. Zimmer TS, Orr AL, Orr AG. Astrocytes in selective vulnerability to neurodegenerative disease. Trends Neurosci. avr 2024;47(4):289-302.

60. Sofroniew MV, Vinters HV. Astrocytes: biology and pathology. Acta Neuropathol (Berl). janv 2010;119(1):7-35.

61. Walz W, Lang MK. Immunocytochemical evidence for a distinct GFAP-negative subpopulation of astrocytes in the adult rat hippocampus. Neurosci Lett. déc 1998;257(3):127-30.

62. Nolte C, Matyash M, Pivneva T, Schipke CG, Ohlemeyer C, Hanisch UK, et al. GFAP promoter-controlled EGFP-expressing transgenic mice: A tool to visualize astrocytes and astrogliosis in living brain tissue. Glia. 1 janv 2001;33(1):72-86.

63. Cahoy JD, Emery B, Kaushal A, Foo LC, Zamanian JL, Christopherson KS, et al. A Transcriptome Database for Astrocytes, Neurons, and Oligodendrocytes: A New Resource for Understanding Brain Development and Function. J Neurosci. 2 janv 2008;28(1):264-78.

64. Srinivasan R, Lu TY, Chai H, Xu J, Huang BS, Golshani P, et al. New Transgenic Mouse Lines for Selectively Targeting Astrocytes and Studying Calcium Signals in Astrocyte Processes In Situ and In Vivo. Neuron. déc 2016;92(6):1181-95.

65. Yang Y, Vidensky S, Jin L, Jie C, Lorenzini I, Frankl M, et al. Molecular comparison of GLT1+ and ALDH1L1+ astrocytes in vivo in astroglial reporter mice. Glia. févr 2011;59(2):200-7.
66. Kamphuis W, Mamber C, Moeton M, Kooijman L, Sluijs JA, Jansen AHP, et al. GFAP Isoforms in Adult Mouse Brain with a Focus on Neurogenic Astrocytes and Reactive Astrogliosis in Mouse Models of Alzheimer Disease. Ikezu T, éditeur. PLoS ONE. 13 août 2012;7(8):e42823.
67. Olsen M, Aguilar X, Sehlin D, Fang XT, Antoni G, Erlandsson A, et al. Astroglial Responses to Amyloid-Beta Progression in a Mouse Model of Alzheimer's Disease. Mol Imaging Biol. août 2018;20(4):605-14.
68. Simpson JE, Ince PG, Lace G, Forster G, Shaw PJ, Matthews F, et al. Astrocyte phenotype in relation to Alzheimer-type pathology in the ageing brain. Neurobiol Aging. avr 2010;31(4):578-90.
69. Phillips JM, Winfree RL, Seto M, Schneider JA, Bennett DA, Dumitrescu LC, et al. Pathologic and clinical correlates of region-specific brain GFAP in Alzheimer's disease. Acta Neuropathol (Berl). 24 nov 2024;148(1):69.
70. Livingston NR, Calsolaro V, Hinz R, Nowell J, Raza S, Gentleman S, et al. Relationship between astrocyte reactivity, using novel 11C-BU99008 PET, and glucose metabolism, grey matter volume and amyloid load in cognitively impaired individuals. Mol Psychiatry. avr 2022;27(4):2019-29.
71. Mohamed MA, Zeng Z, Gennaro M, Lao-Kaim NP, Myers JFM, Calsolaro V, et al. Astrogliosis in aging and Parkinson's disease dementia: a new clinical study with 11C-BU99008 PET. Brain Commun. 1 sept 2022;4(5):fcac199.
72. Huang Y, Wang M, Ni H, Zhang J, Li A, Hu B, et al. Regulation of cell distancing in peri-plaque glial nets by Plexin-B1 affects glial activation and amyloid compaction in Alzheimer's disease. Nat Neurosci. août 2024;27(8):1489-504.
73. Mallach A, Zielonka M, Van Lieshout V, An Y, Khoo JH, Vanheusden M, et al. Microglia-astrocyte crosstalk in the amyloid plaque niche of an Alzheimer's disease mouse model, as revealed by spatial transcriptomics. Cell Rep. juin 2024;43(6):114216.
74. Nagelhus EA, Ottersen OP. Physiological Roles of Aquaporin-4 in Brain. Physiol Rev. oct 2013;93(4):1543-62.
75. Kress BT, Iliff JJ, Xia M, Wang M, Wei HS, Zeppenfeld D, et al. Impairment of paravascular clearance pathways in the aging brain. Ann Neurol. déc 2014;76(6):845-61.
76. Hsiao WC, Chang HI, Hsu SW, Lee CC, Huang SH, Cheng CH, et al. Association of Cognition and Brain Reserve in Aging and Glymphatic Function Using Diffusion Tensor Image-along the Perivascular Space (DTI-ALPS). Neuroscience. août 2023;524:11-20.

77. McKnight CD, Trujillo P, Lopez AM, Petersen K, Considine C, Lin YC, et al. Diffusion along perivascular spaces reveals evidence supportive of glymphatic function impairment in Parkinson disease. Parkinsonism Relat Disord. août 2021;89:98-104.

78. Liu S, Sun X, Ren Q, Chen Y, Dai T, Yang Y, et al. Glymphatic dysfunction in patients with early-stage amyotrophic lateral sclerosis. Brain. 4 janv 2024;147(1):100-8.

79. Carotenuto A, Cacciaguerra L, Pagani E, Preziosa P, Filippi M, Rocca MA. Glymphatic system impairment in multiple sclerosis: relation with brain damage and disability. Brain. 27 août 2022;145(8):2785-95.

80. Zeppenfeld DM, Simon M, Haswell JD, D'Abreo D, Murchison C, Quinn JF, et al. Association of Perivascular Localization of Aquaporin-4 With Cognition and Alzheimer Disease in Aging Brains. JAMA Neurol. 1 janv 2017;74(1):91.

81. Ishida K, Yamada K, Nishiyama R, Hashimoto T, Nishida I, Abe Y, et al. Glymphatic system clears extracellular tau and protects from tau aggregation and neurodegeneration. J Exp Med. 7 mars 2022;219(3):e20211275.

82. Xu Z, Xiao N, Chen Y, Huang H, Marshall C, Gao J, et al. Deletion of aquaporin-4 in APP/PS1 mice exacerbates brain Aβ accumulation and memory deficits. Mol Neurodegener. déc 2015;10(1):58.

83. Pedersen TJ, Keil SA, Han W, Wang MX, Iliff JJ. The effect of aquaporin-4 mis-localization on Aβ deposition in mice. Neurobiol Dis. juin 2023;181:106100.

84. MohanaSundaram A, Mofatteh M, Ashraf GM, Praticò D. Glymphotherapeutics for Alzheimer's disease: Time to move the needle. Ageing Res Rev. nov 2024;101:102478.

85. Bou Ghanem A, Hussayni Y, Kadbey R, Ratel Y, Yehya S, Khouzami L, et al. Exploring the complexities of 1C metabolism: implications in aging and neurodegenerative diseases. Front Aging Neurosci. 4 janv 2024;15:1322419.

86. Doddaballapur DB, Heyes DJ, Miyan JA. Multiple Hits on Cerebral Folate, Tetrahydrobiopterin and Dopamine Metabolism in the Pathophysiology of Parkinson's Disorder: A Limited Study of Post-Mortem Human Brain Tissues. Metabolites. 5 mai 2025;15(5):307.

87. Yan J, Wu J, Xu M, Wang M, Guo W. Disrupted de novo pyrimidine biosynthesis impairs adult hippocampal neurogenesis and cognition in pyridoxine-dependent epilepsy. Sci Adv. 5 avr 2024;10(14):eadl2764.

88. Coughlin CR, Gospe SM. Pyridoxine-dependent epilepsy: Current perspectives and questions for future research. Ann Child Neurol Soc. mars 2023;1(1):24-37.

89. Salih MA, AlBakheet A, Almass R, Hamed AAA, AlOdaib A, Kaya N. Case report: Clinical and genetic characterization of a novel ALDH7A1 variant causing pyridoxine-dependent epilepsy, developmental delay, and intellectual disability in two siblings. Front Psychiatry. 23 déc 2024;15:1501238.

90. Jansen LA, Hevner RF, Roden WH, Hahn SH, Jung S, Gospe SM. Glial localization of antiquitin: Implications for pyridoxine-dependent epilepsy. Ann Neurol. janv 2014;75(1):22-32.

91. Wu J, Qin D, Liang Z, Liu Q, Wang M, Guo Y, et al. Dysregulation of astrocyte-derived matrix gla protein impairs dendritic spine development in pyridoxine-dependent epilepsy. Mol Ther. avr 2025;33(4):1785-802.

92. Jones EV, Bouvier DS. Astrocyte-Secreted Matricellular Proteins in CNS Remodelling during Development and Disease. Neural Plast. 2014;2014:1-12.

93. Yang Q, Yan C, Sun Y, Xie Z, Yang L, Jiang M, et al. Extracellular Matrix Remodeling Alleviates Memory Deficits in Alzheimer's Disease by Enhancing the Astrocytic Autophagy-Lysosome Pathway. Adv Sci. août 2024;11(31):2400480.

94. Jacobson KR, Song H. Changes in the Extracellular Matrix with Aging: A Larger Role in Alzheimer's Disease. J Neurosci. 29 mai 2024;44(22):e0081242024.

95. Song YJC, Halliday GM, Holton JL, Lashley T, O'Sullivan SS, McCann H, et al. Degeneration in Different Parkinsonian Syndromes Relates to Astrocyte Type and Astrocyte Protein Expression. J Neuropathol Exp Neurol. oct 2009;68(10):1073-83.

96. van den Berge SA, Kevenaar JT, Sluijs JA, Hol EM. Dementia in Parkinson's Disease Correlates with α-Synuclein Pathology but Not with Cortical Astrogliosis. Park Dis. 2012;2012:420957.

97. Filmus J, Capurro M, Rast J. Glypicans. Genome Biol. 2008;9(5):224.

98. Marsan E, Velmeshev D, Ramsey A, Patel RK, Zhang J, Koontz M, et al. Astroglial toxicity promotes synaptic degeneration in the thalamocortical circuit in frontotemporal dementia with GRN mutations. J Clin Invest. 15 mars 2023;133(6):e164919.

99. Schirmer L, Velmeshev D, Holmqvist S, Kaufmann M, Werneburg S, Jung D, et al. Neuronal vulnerability and multilineage diversity in multiple sclerosis. Nature. sept 2019;573(7772):75-82.

100. Lau SF, Cao H, Fu AKY, Ip NY. Single-nucleus transcriptome analysis reveals dysregulation of angiogenic endothelial cells and neuroprotective glia in Alzheimer's disease. Proc Natl Acad Sci. 13 oct 2020;117(41):25800-9.

101. Saliu IO, Zhao G. New insights into astrocyte diversity from the lens of transcriptional regulation and their implications for neurodegenerative disease treatments. Neural Regen Res. nov 2024;19(11):2335-6.

102. Dai DL, Li M, Lee EB. Human Alzheimer's disease reactive astrocytes exhibit a loss of homeostastic gene expression. Acta Neuropathol Commun. 2 août 2023;11(1):127.
103. Bouvier DS, Jones EV, Quesseveur G, Davoli MA, A. Ferreira T, Quirion R, et al. High Resolution Dissection of Reactive Glial Nets in Alzheimer's Disease. Sci Rep. 19 avr 2016;6:24544.
104. Williamson TG, Mok SS, Henry A, Cappai R, Lander AD, Nurcombe V, et al. Secreted Glypican Binds to the Amyloid Precursor Protein of Alzheimer's Disease (APP) and Inhibits APP-induced Neurite Outgrowth. J Biol Chem. déc 1996;271(49):31215-21.
105. Van Horssen J, Kleinnijenhuis J, Maass CN, Rensink AAM, Otte-Höller I, David G, et al. Accumulation of heparan sulfate proteoglycans in cerebellar senile plaques. Neurobiol Aging. juill 2002;23(4):537-45.
106. Levites Y, Dammer EB, Ran Y, Tsering W, Duong D, Abreha M, et al. Integrative proteomics identifies a conserved Aβ amyloid responsome, novel plaque proteins, and pathology modifiers in Alzheimer's disease. Cell Rep Med. août 2024;5(8):101669.
107. Serrano-Pozo A, Li H, Li Z, Muñoz-Castro C, Jaisa-aad M, Healey MA, et al. Astrocyte transcriptomic changes along the spatiotemporal progression of Alzheimer's disease. Nat Neurosci. déc 2024;27(12):2384-400.
108. Derevyanko A, Tao T, Allen NJ. Common alterations to astrocytes across neurodegenerative disorders. Curr Opin Neurobiol. févr 2025;90:102970.

2. Manuscript II

1. Jahn H. Memory loss in Alzheimer's disease. Dialogues Clin Neurosci. 31 déc 2013;15(4):445-54.
2. Olivieri P, Lagarde J, Lehericy S, Valabrègue R, Michel A, Macé P, et al. Early alteration of the locus coeruleus in phenotypic variants of Alzheimer's disease. Ann Clin Transl Neurol. juill 2019;6(7):134551.
3. Gilvesy A, Husen E, Magloczky Z, Mihaly O, Hortobágyi T, Kanatani S, et al. Spatiotemporal characterization of cellular tau pathology in the human locus coeruleus–pericoerulear complex by three- dimensional imaging. Acta Neuropathol (Berl). oct 2022;144(4):651-76.
4. Flores-Aguilar L, Hall H, Orciani C, Foret MK, Kovecses O, Ducatenzeiler A, et al. Early loss of locus coeruleus innervation promotes cognitive and neuropathological changes before amyloid plaque deposition in a transgenic rat model of Alzheimer's disease. Neuropathol Appl Neurobiol. oct 2022;48(6):e12835.
5. Bertrand E, Lechowicz W, Szpak GM, Dymecki J. Qualitative and quantitative analysis of locus coeruleus neurons in Parkinson's disease. Folia Neuropathol. 1997;35(2):80-6.

6. Sun J, Ma J, Gao L, Wang J, Zhang D, Chen L, et al. Disruption of locus coeruleus-related functional networks in Parkinson's disease. Npj Park Dis. 30 mai 2023;9(1):81.

7. Jacobs HI, Priovoulos N, Poser BA, Pagen LH, Ivanov D, Verhey FR, et al. Dynamic behavior of the locus coeruleus during arousal-related memory processing in a multi-modal 7T fMRI paradigm. eLife. 24 juin 2020;9:e52059.

8. Matchett BJ, Grinberg LT, Theofilas P, Murray ME. The mechanistic link between selective vulnerability of the locus coeruleus and neurodegeneration in Alzheimer's disease. Acta Neuropathol (Berl) [Internet]. 11 janv 2021 [cité 30 janv 2021]; Disponible sur: https://doi.org/10.1007/s00401-020-02248-1

9. Holland N, Robbins TW, Rowe JB. The role of noradrenaline in cognition and cognitive disorders. Brain. 4 sept 2021;144(8):2243-56.

10. Theofilas P, Ehrenberg AJ, Dunlop S, Di Lorenzo Alho AT, Nguy A, Leite REP, et al. Locus coeruleus volume and cell population changes during Alzheimer's disease progression: A stereological study in human postmortem brains with potential implication for early-stage biomarker discovery. Alzheimers Dement. mars 2017;13(3):236-46.

11. Gutiérrez IL, Dello Russo C, Novellino F, Caso JR, García-Bueno B, Leza JC, et al. Noradrenaline in Alzheimer's Disease: A New Potential Therapeutic Target. Int J Mol Sci. 30 mai 2022;23(11):6143.

12. Mercan D, Heneka MT. The Contribution of the Locus Coeruleus–Noradrenaline System Degeneration during the Progression of Alzheimer's Disease. Biology. 14 déc 2022;11(12):1822.

13. Marien MR, Colpaert FC, Rosenquist AC. Noradrenergic mechanisms in neurodegenerative diseases: a theory. Brain Res Rev. avr 2004;45(1):38-78.

14. Vizi E, Fekete A, Karoly R, Mike A. Non-synaptic receptors and transporters involved in brain functions and targets of drug treatment. Br J Pharmacol. juin 2010;160(4):785-809.

15. Bélanger M, Allaman I, Magistretti PJ. Brain Energy Metabolism: Focus on Astrocyte-Neuron Metabolic Cooperation. Cell Metab. déc 2011;14(6):724-38.

16. Mulligan SJ, MacVicar BA. Calcium transients in astrocyte endfeet cause cerebrovascular constrictions. Nature. sept 2004;431(7005):195-9.

17. Díaz-Castro B, Robel S, Mishra A. Astrocyte Endfeet in Brain Function and Pathology: Open Questions. Annu Rev Neurosci. 10 juill 2023;46(1):101-21.

18. Eroglu C, Barres BA. Regulation of synaptic connectivity by glia. Nature. nov 2010;468(7321):223-31. 19. Sancho L, Contreras M, Allen NJ. Glia as sculptors of synaptic plasticity. Neurosci Res. juin 2021;167:17- 29.

20. Perea G, Navarrete M, Araque A. Tripartite synapses: astrocytes process and control synaptic information. Trends Neurosci. août 2009;32(8):421-31.
21. Bekar LK, He W, Nedergaard M. Locus Coeruleus α-Adrenergic–Mediated Activation of Cortical Astrocytes In Vivo. Cereb Cortex. déc 2008;18(12):2789-95.
22. Hertz L, Lovatt D, Goldman SA, Nedergaard M. Adrenoceptors in brain: Cellular gene expression and effects on astrocytic metabolism and [Ca2+]i. Neurochem Int. nov 2010;57(4):411-20.
23. Ding F, O'Donnell J, Thrane AS, Zeppenfeld D, Kang H, Xie L, et al. α1-Adrenergicreceptorsmediate coordinated Ca2+ signaling of cortical astrocytes in awake, behaving mice. Cell Calcium. Déc 2013;54(6):387-94.
24. Wahis J, Holt MG. Astrocytes, Noradrenaline, α1-Adrenoreceptors, and Neuromodulation: Evidence and Unanswered Questions. Front Cell Neurosci. 25 févr 2021;15:645691.
25. Oe Y, Wang X, Patriarchi T, Konno A, Ozawa K, Yahagi K, et al. Distinct temporal integration of noradrenaline signaling by astrocytic second messengers during vigilance. Nat Commun. 24 janv 2020;11(1):471.
26. Mu Y, Bennett DV, Rubinov M, Narayan S, Yang CT, Tanimoto M, et al. Glia Accumulate Evidence that Actions Are Futile and Suppress Unsuccessful Behavior. Cell. juin 2019;178(1):27-43.e19.
27. Paukert M, Agarwal A, Cha J, Doze VA, Kang JU, Bergles DE. Norepinephrine Controls Astroglial Responsiveness to Local Circuit Activity. Neuron. juin 2014;82(6):1263-70.
28. Reitman ME, Tse V, Mi X, Willoughby DD, Peinado A, Aivazidis A, et al. Norepinephrine links astrocytic activity to regulation of cortical state. Nat Neurosci. avr 2023;26(4):579-93.
29. Guttenplan KA, Maxwell I, Santos E, Borchardt LA, Manzo E, Abalde-Atristain L, et al. GPCR signaling gates astrocyte responsiveness to neurotransmitters and control of neuronal activity. Science. 15 mai 2025;388(6748):763-8.
30. Lefton KB, Wu Y, Dai Y, Okuda T, Zhang Y, Yen A, et al. Norepinephrine signals through astrocytes to modulate synapses. Science. 15 mai 2025;388(6748):776-83.
31. Chen AB, Duque M, Rymbek A, Dhanasekar M, Wang VM, Mi X, et al. Norepinephrine changes behavioral state through astroglial purinergic signaling. Science. 15 mai 2025;388(6748):769-75.
32. Hauglund NL, Andersen M, Tokarska K, Radovanovic T, Kjaerby C, Sørensen FL, et al. Norepinephrine- mediated slow vasomotion drives glymphatic clearance during sleep. Cell. févr 2025;188(3):606-622.e17.
33. Bouvier DS, Fixemer S, Heurtaux T, Jeannelle F, Frauenknecht KBM, Mittelbronn M. The Multifaceted Neurotoxicity of Astrocytes in Ageing and Age-Related Neurodegenerative Diseases:

A Translational Perspective. Front Physiol [Internet]. 2022;13. Disponible sur: https://www.frontiersin.org/articles/10.3389/fphys.2022.814889

34. Zorec R, Parpura V, Verkhratsky A. Preventing neurodegeneration by adrenergic astroglial excitation. FEBS J. oct 2018;285(19):3645-56.

35. Heneka MT, Nadrigny F, Regen T, Martinez-Hernandez A, Dumitrescu-Ozimek L, Terwel D, et al. Locus ceruleus controls Alzheimer's disease pathology by modulating microglial functions through norepinephrine. Proc Natl Acad Sci U S A. 30 mars 2010;107(13):6058-63.

36. Frohman EM, Vayuvegula B, Gupta S, VanDenNoort S. Norepinephrine inhibits gamma-interferon-induced major histocompatibility class II (Ia) antigen expression on cultured astrocytes via beta-2-adrenergic signal transduction mechanisms. Proc Natl Acad Sci. févr 1988;85(4):1292-6.

37. Vay SU, Olschewski DN, Petereit H, Lange F, Nazarzadeh N, Gross E, et al. Osteopontin regulates proliferation, migration, and survival of astrocytes depending on their activation phenotype. J Neurosci Res. nov 2021;99(11):2822-43.

38. Martin M. Cutadapt removes adapter sequences from high-throughput sequencing reads. EMBnet.journal. 2 mai 2011;17(1):10.

39. Dobin A, Davis CA, Schlesinger F, Drenkow J, Zaleski C, Jha S, et al. STAR: ultrafast universal RNA-seq aligner. Bioinformatics. 1 janv 2013;29(1):15-21.

40. Mölder F, Jablonski KP, Letcher B, Hall MB, Tomkins-Tinch CH, Sochat V, et al. Sustainable data analysis with Snakemake. F1000Research. 19 avr 2021;10:33.

41. Love MI, Huber W, Anders S. Moderated estimation of fold change and dispersion for RNA-seq data with DESeq2. Genome Biol. 5 déc 2014;15(12):550.

42. Braak H, Braak E. Neuropathological stageing of Alzheimer-related changes. Acta Neuropathol (Berl). sept 1991;82(4):239-59.

43. Braak H, Tredici KD, Rüb U, De Vos RAI, Jansen Steur ENH, Braak E. Staging of brain pathology related to sporadic Parkinson's disease. Neurobiol Aging. mars 2003;24(2):197-211.

44. Montine TJ, Phelps CH, Beach TG, Bigio EH, Cairns NJ, Dickson DW, et al. National Institute on Aging–Alzheimer's Association guidelines for the neuropathologic assessment of Alzheimer's disease: a practical approach. Acta Neuropathol (Berl). janv 2012;123(1):1-11.

45. McKeith IG. Consensus guidelines for the clinical and pathologic diagnosis of dementia with Lewy bodies (DLB): Report of the Consortium on DLB International Workshop. J Alzheimers Dis. 27 juill 2006;9(s3):417-23.

46. Fixemer S, Miranda De La Maza M, Hammer GP, Jeannelle F, Schreiner S, Gérardy JJ, et al. Microglia

aggregates define distinct immune and neurodegenerative niches in Alzheimer's disease hippocampus. Acta Neuropathol (Berl). 15 févr 2025;149(1):19.

47. Mai JK, Majtanik M, Paxinos G. Atlas of the human brain. 4th edition. Amsterdam Boston Heidelberg: Academic Press; 2016. 448 p. (Elsevier science & technology books).

48. CorkrumM,AraqueA.Astrocyte-neuronsignalinginthemesolimbicdopaminesystem:thehidden stars of dopamine signaling. Neuropsychopharmacology. oct 2021;46(11):1864-72.

49. Requie LM, Gómez-Gonzalo M, Speggiorin M, Managò F, Melone M, Congiu M, et al. Astrocytes mediate long-lasting synaptic regulation of ventral tegmental area dopamine neurons. Nat Neurosci. déc 2022;25(12):1639-50.

50. MacVicar BA, Newman EA. Astrocyte Regulation of Blood Flow in the Brain. Cold Spring Harb Perspect Biol. mai 2015;7(5):a020388.

51. Schiera G, Di Liegro CM, Schirò G, Sorbello G, Di Liegro I. Involvement of Astrocytes in the Formation, Maintenance, and Function of the Blood–Brain Barrier. Cells. 12 janv 2024;13(2):150.

52. Metea MR, Newman EA. Glial Cells Dilate and Constrict Blood Vessels: A Mechanism of Neurovascular Coupling. J Neurosci. 15 mars 2006;26(11):2862-70.

53. Gordon GRJ, Choi HB, Rungta RL, Ellis-Davies GCR, MacVicar BA. Brain metabolism dictates the polarity of astrocyte control over arterioles. Nature. déc 2008;456(7223):745-9.

54. Singh SK, Kordula T, Spiegel S. Neuronal contact upregulates astrocytic sphingosine-1-phosphate receptor 1 to coordinate astrocyte-neuron cross communication. Glia. avr 2022;70(4):712-27.

55. ChristophersonKS,UllianEM,StokesCCA,MullowneyCE,HellJW,AgahA,etal.Thrombospondins Are Astrocyte-Secreted Proteins that Promote CNS Synaptogenesis. Cell. févr 2005;120(3):421-33.

56. Kucukdereli H, Allen NJ, Lee AT, Feng A, Ozlu MI, Conatser LM, et al. Control of excitatory CNS synaptogenesis by astrocyte-secreted proteins Hevin and SPARC. Proc Natl Acad Sci [Internet]. 9 août 2011 [cité 26 juin 2025];108(32). Disponible sur: https://pnas.org/doi/full/10.1073/pnas.1104977108

57. ClarkeLE,BarresBA.Emergingrolesofastrocytesinneuralcircuitdevelopment.NatRevNeurosci. mai 2013;14(5):311-21.

58. Bosworth A, Contreras M, Weiser Novak S, Sancho L, Salas I, Manor U, et al. Astrocyte glypican 5 regulates synapse maturation and stabilization [Internet]. Neuroscience; 2023 [cité 3 févr 2025]. Disponible sur: http://biorxiv.org/lookup/doi/10.1101/2023.03.02.529949

59. Salas IH, Paumier A, Tao T, Derevyanko A, Switzler C, Burgado J, et al. Astrocyte transcriptomic analysis identifies glypican 5 downregulation as a contributor to synaptic dysfunction in Alzheimer's

disease models [Internet]. Neuroscience; 2024 [cité 21 janv 2025]. Disponible sur: http://biorxiv.org/lookup/doi/10.1101/2024.10.30.621182

60. Tsetsenis T, Broussard JI, Dani JA. Dopaminergic regulation of hippocampal plasticity, learning, and memory. Front Behav Neurosci. 27 janv 2023;16:1092420.

61. Guidolin D, Tortorella C, Marcoli M, Cervetto C, De Caro R, Maura G, et al. Modulation of Neuron and Astrocyte Dopamine Receptors via Receptor–Receptor Interactions. Pharmaceuticals. 8 oct 2023;16(10):1427.

62. Hinojosa AE, Caso JR, García-Bueno B, Leza JC, Madrigal JL. Dual effects of noradrenaline on astroglial production of chemokines and pro-inflammatory mediators. J Neuroinflammation. déc 2013;10(1):852.

63. RostamiJ,FotakiG,SiroisJ,MzezewaR,BergströmJ,EssandM,etal.Astrocyteshavethecapacity to act as antigen-presenting cells in the Parkinson's disease brain. J Neuroinflammation. déc 2020;17(1):119.

64. Horng S, Villavicencio J, Amatruda M. Astrocytic MHC-I but Not MHC-II Regulates EAE Disease Severity (S17.009). Neurology. 9 avr 2024;102(7_supplement_1):6365.

65. Fisher TM, Liddelow SA. Emerging roles of astrocytes as immune effectors in the central nervous system. Trends Immunol. sept 2024;S1471490624001947.

66. Cao S, Fisher DW, Rodriguez G, Yu T, Dong H. Comparisons of neuroinflammation, microglial activation, and degeneration of the locus coeruleus-norepinephrine system in APP/PS1 and aging mice. J Neuroinflammation. 6 janv 2021;18(1):10.

67. Dey A, Pramanik PK, Dwivedi SKD, Neizer-Ashun F, Kiss T, Ganguly A, et al. A role for the cystathionine- β-synthase /H2S axis in astrocyte dysfunction in the aging brain. Redox Biol. déc 2023;68:102958.

68. Lee M, Schwab C, Yu S, McGeer E, McGeer PL. Astrocytes produce the antiinflammatory and neuroprotective agent hydrogen sulfide. Neurobiol Aging. oct 2009;30(10):1523-34.

69. Tawfik A, Elsherbiny NM, Zaidi Y, Rajpurohit P. Homocysteine and Age-Related Central Nervous System Diseases: Role of Inflammation. Int J Mol Sci. 10 juin 2021;22(12):6259.

70. Lin WZ, Yu D, Xiong LY, Zebarth J, Wang R, Fischer CE, et al. Homocysteine, neurodegenerative biomarkers, and APOE ε4 in neurodegenerative diseases. Alzheimers Dement. janv 2025;21(1):e14376.

71. Smith AD, Smith SM, De Jager CA, Whitbread P, Johnston C, Agacinski G, et al. Homocysteine-Lowering by B Vitamins Slows the Rate of Accelerated Brain Atrophy in Mild Cognitive Impairment: A Randomized Controlled Trial. Bush AI, éditeur. PLoS ONE. 8 sept 2010;5(9):e12244.

72. PeriñánMT,Macías-GarcíaD,JesúsS,Martín-RodríguezJF,Muñoz-DelgadoL,Jimenez-JarabaMV, et al. Homocysteine levels, genetic background, and cognitive impairment in Parkinson's disease. J Neurol. janv 2023;270(1):477-85.

73. McGovern KE, Nance JP, David CN, Harrison RES, Noor S, Worth D, et al. SPARC coordinates extracellular matrix remodeling and efficient recruitment to and migration of antigen-specific T cells in the brain following infection. Sci Rep. 25 févr 2021;11(1):4549.

74. Yang Q, Yan C, Sun Y, Xie Z, Yang L, Jiang M, et al. Extracellular Matrix Remodeling Alleviates Memory Deficits in Alzheimer's Disease by Enhancing the Astrocytic Autophagy-Lysosome Pathway. Adv Sci. août 2024;11(31):2400480.

75. Jones EV, Bouvier DS. Astrocyte-Secreted Matricellular Proteins in CNS Remodelling during Development and Disease. Neural Plast. 2014;2014:1-12.

76. Strunz M, Jarrell JT, Cohen DS, Rosin ER, Vanderburg CR, Huang X. Modulation of SPARC/Hevin Proteins in Alzheimer's Disease Brain Injury. J Alzheimers Dis. 29 mars 2019;68(2):695-710.

77. Yang H, Xiang Y, Wang J, Ke Z, Zhou W, Yin X, et al. Modulating the blood-brain barrier in CNS disorders: A review of the therapeutic implications of secreted protein acidic and rich in cysteine (SPARC). Int J Biol Macromol. févr 2025;288:138747.

3. Manuscript III

Adolfsson, R., Gottfries, C. G., Roos, B. E., and Winblad, B. (1979). Changes in the brain catecholamines in patients with dementia of Alzheimer type. Br. J. Psychiatry 135, 216–223. doi: 10.1192/bjp.135.3.216

Agarwal, D., Sandor, C., Volpato, V., Caffrey, T. M., Monzón-Sandoval, J., Bowden, R., et al. (2020). A single- cell atlas of the human substantia nigra reveals cell-specific pathways associated with neurological disorders. Nat. Commun. 11:4183. doi: 10.1038/s41467-020-17876-0

Akama, K. T., Albanese, C., Pestell, R. G., and Van Eldik, L. J. (1998). Amyloid β-peptide stimulates nitric oxide production in astrocytes through an NFκb- dependent mechanism. Proc. Natl. Acad. Sci. U. S. A. 95, 5795–5800. doi: 10.1073/pnas.95.10.5795

Allen, N. J., and Eroglu, C. (2017). Cell biology of astrocyte-synapse interactions. Neuron 96, 697–708. doi: 10.1016/j.neuron.2017.09.056

Almad, A. A., Doreswamy, A., Gross, S. K., Richard, J. P., Huo, Y., Haughey, N., et al. (2016). Connexin 43 in astrocytes contributes to motor neuron toxicity in amyotrophic lateral sclerosis. Glia 64, 1154– 1169. doi: 10.1002/glia.22989

Amenta, F., Bronzetti, E., Sabbatini, M., and Vega, J. A. (1998). Astrocyte changes in cerebral cortex and hippocampus: A quantitative immunohistochemical study. Microsc. Res. Tech. 43, 29–33. doi: 10.1002/(SI CI)1097-0029(19981001)43:1<29::AID-JEMT5>3.0.CO;2-H

Arai, T., Hasegawa, M., Akiyama, H., Ikeda, K., Nonaka, T., Mori, H., et al. (2006). TDP-43 is a component of ubiquitin-positive tau-negative inclusions in frontotemporal lobar degeneration and amyotrophic lateral sclerosis. Biochem. Biophys. Res. Commun. 351, 602–611. doi: 10.1016/j.bbrc.2006.10.093

Araque, A., Carmignoto, G., Haydon, P. G., Oliet, S. H. R., Robitaille, R., and Volterra, A. (2014). Gliotransmitters travel in time and space. Neuron 81, 728–739. doi: 10.1016/j.neuron.2014.02.007

Arias-Carrián, O., Stamelou, M., Murillo-Rodríguez, E., Menéndez-Gonzlez, M., and Pöppel, E. (2010). Dopaminergic reward system: a short integrative review. Int. Arch. Med. 3:24. doi: 10.1186/1755-7682-3- 24

Baker, D. J., Childs, B. G., Durik, M., Wijers, M. E., Sieben, C. J., Zhong, J., et al. (2016). Naturally occurring p16 Ink4a-positive cells shorten healthy lifespan. Nature 530, 184–189. doi: 10.1038/nature16932

Balu, D. T., Pantazopoulos, H., Huang, C. C. Y., Muszynski, K., Harvey, T. L., Uno, Y., et al. (2019). Neurotoxic astrocytes express the D-serine synthesizing enzyme, serine racemase, in Alzheimer's disease. Neurobiol. Dis. 130:104511. doi: 10.1016/j.nbd.2019.104511

Baptista, P., and Andrade, J. P. (2018). Adult hippocampal neurogenesis: regulation and possible functional and clinical correlates. Front. Neuroanat. 12:44. doi: 10.3389/fnana.2018.00044

Batarseh, Y. S., Duong, Q. V., Mousa, Y. M., Al Rihani, S. B., Elfakhri, K., and Kaddoumi, A. (2016). Amyloid- β and astrocytes interplay in amyloid-β related disorders. Int. J. Mol. Sci. 17:338. doi: 10.3390/ijms17030338

Batiuk, M. Y., Martirosyan, A., Wahis, J., de Vin, F., Marneffe, C., Kusserow, C., et al. (2020). Identification of region-specific astrocyte subtypes at single cell resolution. Nat. Commun. 11:1220. doi: 10.1038/s41467-019-14198-8

Beardmore, R., Hou, R., Darekar, A., Holmes, C., and Boche, D. (2021). The locus coeruleus in aging and Alzheimer's disease: a postmortem and brain imaging review. J. Alzheimers Dis. 83, 5–22. doi: 10.3233/JAD-210191

Bell, A. M., and Robinson, G. E. (2011). Behavior and the dynamic genome. Science 332, 1161–1162. doi: 10.1126/science.1203295

Bernal, G. M., and Peterson, D. A. (2011). Phenotypic and gene expression modification with normal brain aging in GFAP-positive astrocytes and neural stem cells. Aging Cell 10, 466–482. doi: 10.1111/j.1474- 9726.2011.00694.x

Bhat, R., Crowe, E. P., Bitto, A., Moh, M., Katsetos, C. D., Garcia, F. U., et al. (2012). Astrocyte senescence as a component of Alzheimer's disease. PLoS One 7:e45069. doi: 10.1371/journal.pone.0045069

Bi, F., Huang, C., Tong, J., Qiu, G., Huang, B., Wu, Q., et al. (2013). Reactive astrocytes secrete lcn2 to promote neuron death. Proc. Natl. Acad. Sci. U. S. A. 110, 4069–4074. doi: 10.1073/pnas.1218497110

Biondetti, E., Santin, M. D., Valabrègue, R., Mangone, G., Gaurav, R., Pyatigorskaya, N., et al. (2021). The spatiotemporal changes in dopamine, neuromelanin and iron characterizing Parkinson's disease. Brain 144, 3114–3125. doi: 10.1093/brain/awab191

Birch, J., and Gil, J. (2020). Senescence and the SASP: many therapeutic avenues. Genes Dev. 34, 1565–1576. doi: 10.1101/gad.343129.120

Birger, A., Ben-Dor, I., Ottolenghi, M., Turetsky, T., Gil, Y., Sweetat, S., et al. (2019). Human iPSC-derived astrocytes from ALS patients with mutated C9ORF72 show increased oxidative stress and neurotoxicity. EBioMedicine 50, 274–289. doi: 10.1016/j.ebiom.2019.11.026

Bitto, A., Sell, C., Crowe, E., Lorenzini, A., Malaguti, M., Hrelia, S., et al. (2010). Stress-induced senescence in human and rodent astrocytes. Exp. Cell Res. 316, 2961–2968. doi: 10.1016/j.yexcr.2010.06.021

Björklund, A., and Dunnett, S. B. (2007). Dopamine neuron systems in the brain: an update. Trends Neurosci. 30, 194–202. doi: 10.1016/j.tins.2007.03.006 Boisvert, M. M., Erikson, G. A., Shokhirev, M. N., and Allen, N. J. (2018). The aging astrocyte transcriptome from multiple regions of the mouse brain. Cell Rep. 22, 269–285. doi: 10.1016/j.celrep.2017.12.039

Boldrini, M., Fulmore, C. A., Tartt, A. N., Simeon, L. R., Pavlova, I., Poposka, V., et al. (2018). Human hippocampal neurogenesis persists throughout aging. Cell Stem Cell 22, 589–599.e5. doi: 10.1016/j.stem.2018.03.015

Bonzano, S., Crisci, I., Podlesny-Drabiniok, A., Rolando, C., Krezel, W., Studer, M., et al. (2018). Neuron-astroglia cell fate decision in the adult mouse hippocampal neurogenic niche is cell-intrinsically controlled by COUP-TFI in vivo. Cell Rep. 24, 329–341. doi: 10.1016/j.celrep.2018.06.044

Bouvier, D. S., Jones, E. V., Quesseveur, G., Davoli, M. A., Ferreira, T. A., Quirion, R., et al. (2016). High resolution dissection of reactive glial nets in Alzheimer's disease. Sci. Rep. 6:24544. doi: 10.1038/srep24544

Bouvier, D. S., and Murai, K. K. (2015). Synergistic actions of microglia and astrocytes in the progression of Alzheimer's disease. J. Alzheimers Dis. 45, 1001–1014. doi: 10.3233/JAD-143156

Briel, N., Pratsch, K., Roeber, S., Arzberger, T., and Herms, J. (2021). Contribution of the astrocytic tau pathology to synapse loss in progressive supranuclear palsy and corticobasal degeneration. Brain Pathol. 31:e12914. doi: 10.1111/ bpa.12914

Bronzuoli, M. R., Facchinetti, R., Valenza, M., Cassano, T., Steardo, L., and Scuderi, C. (2019). Astrocyte function is affected by aging and not Alzheimer's disease: a preliminary investigation in hippocampi of 3xTg-AD mice. Front. Pharmacol. 10:644. doi: 10.3389/fphar.2019.00644

Buendia, I., Michalska, P., Navarro, E., Gameiro, I., Egea, J., and León, R. (2016). Nrf2-ARE pathway: an emerging target against oxidative stress and neuroinflammation in neurodegenerative diseases. Pharmacol. Ther. 157, 84–104. doi: 10.1016/j.pharmthera.2015.11.003

Bushong, E. A., Martone, M. E., and Ellisman, M. H. (2004). Maturation of astrocyte morphology and the establishment of astrocyte domains during postnatal hippocampal development. Int. J. Dev. Neurosci. 22, 73–86. doi: 10.1016/j.ijdevneu.2003.12.008

Bushong, E. A., Martone, M. E., Jones, Y. Z., and Ellisman, M. H. (2002). Protoplasmic astrocytes in CA1 stratum radiatum occupy separate anatomical domains. J. Neurosci. 22, 183–192. doi: 10.1523/JNEUROSCI.22-01-00183.2002

Bussian, T. J., Aziz, A., Meyer, C. F., Swenson, B. L., van Deursen, J. M., and Baker, D. J. (2018). Clearance of senescent glial cells prevents tau-dependent pathology and cognitive decline. Nature 562, 578–582. doi: 10.1038/ s41586-018-0543-y

Caldeira, C., Oliveira, A. F., Cunha, C., Vaz, A. R., Falcão, A. S., Fernandes, A., et al. (2014). Microglia change from a reactive to an age-like phenotype with the time in culture. Front. Cell. Neurosci. 8:152. doi: 10.3389/ fncel.2014.00152

Calsolaro, V., Matthews, P. M., Donat, C. K., Livingston, N. R., Femminella, G. D., Guedes, S. S., et al. (2021). Astrocyte reactivity with late-onset cognitive impairment assessed in vivo using 11C-BU99008 PET and its relationship with amyloid load. Mol. Psychiatry 26, 5848–5855. doi: 10.1038/ s41380-021-01193-z

Carnevale, D., De Simone, R., and Minghetti, L. (2007). Microglia-neuron interaction in inflammatory and degenerative diseases: role of cholinergic and noradrenergic systems. CNS Neurol. Disord. Drug Targets 6, 388–397. doi: 10.2174/187152707783399193

Carter, S. F., Herholz, K., Rosa-Neto, P., Pellerin, L., Nordberg, A., and Zimmer, E. R. (2019). Astrocyte biomarkers in Alzheimer's disease. Trends Mol. Med. 25, 77–95. doi: 10.1016/j.molmed.2018.11.006

Carter, S. F., Schöll, M., Almkvist, O., Wall, A., Engler, H., Långström, B., et al. (2012). Evidence for astrocytosis in prodromal alzheimer disease provided by 11C-deuterium-L-deprenyl: a multitracer PET

paradigm combining 11C-Pittsburgh compound B and 18F-FDG. J. Nucl. Med. 53, 37–46. doi: 10.2967/jnumed.110.087031

Cerbai, F., Lana, D., Nosi, D., Petkova-Kirova, P., Zecchi, S., Brothers, H. M., et al. (2012). The neuron-astrocyte-microglia triad in normal brain ageing and in a model of neuroinflammation in the rat hippocampus. PLoS One 7:e45250. doi: 10.1371/journal.pone.0045250

Ceyzériat, K., Ben Haim, L., Denizot, A., Pommier, D., Matos, M., Guillemaud, O., et al. (2018). Modulation of astrocyte reactivity improves functional deficits in mouse models of Alzheimer's disease. Acta Neuropathol. Commun. 6:104. doi: 10.1186/s40478-018-0606-1

Chalermpalanupap, T., Kinkead, B., Hu, W. T., Kummer, M. P., Hammerschmidt, T., Heneka, M. T., et al. (2013). Targeting norepinephrine in mild cognitive impairment and Alzheimer's disease. Alzheimers Res. Ther. 5:21. doi: 10.1186/ alzrt175

Chatterjee, P., Pedrini, S., Stoops, E., Goozee, K., Villemagne, V. L., Asih, P. R., et al. (2021). Plasma glial fibrillary acidic protein is elevated in cognitively normal older adults at risk of Alzheimer's disease. Transl. Psychiatry 11:27. doi: 10.1038/s41398-020-01137-1

Chavarría, C., Rodríguez-Bottero, S., Quijano, C., Cassina, P., and Souza, J. M. (2018). Impact of monomeric, oligomeric and fibrillar alpha-synuclein on astrocyte reactivity and toxicity to neurons. Biochem. J. 475, 3153–3169. doi: 10.1042/BCJ20180297

Chen, P. S., Peng, G. S., Li, G., Yang, S., Wu, X., Wang, C. C., et al. (2006). Valproate protects dopaminergic neurons in midbrain neuron/glia cultures by stimulating the release of neurotrophic factors from astrocytes. Mol. Psychiatry 11, 1116–1125. doi: 10.1038/sj.mp.4001893 Chinta, S. J., Woods, G., Demaria, M., Rane, A., Zou, Y., McQuade, A., et al. (2018). Cellular senescence is induced by the environmental neurotoxin paraquat and contributes to neuropathology linked to parkinson's disease. Cell Rep. 22, 930– 940. doi: 10.1016/j.celrep.2017.12.092

Chisholm, N. C., Henderson, M. L., Selvamani, A., Park, M. J., Dindot, S., Miranda, R. C., et al. (2015). Histone methylation patterns in astrocytes are influenced by age following ischemia. Epigenetics 10, 142–152. doi: 10.1080/15592294.2014.1001219

Chou, T. W., Chang, N. P., Krishnagiri, M., Patel, A. P., Lindman, M., Angel, J. P., et al. (2021). Fibrillar α-synuclein induces neurotoxic astrocyte activation via RIP kinase signaling and NF-κB. Cell Death Dis. 12:756. doi: 10.1038/ s41419-021-04049-0

Christopherson, K. S., Ullian, E. M., Stokes, C. C. A., Mullowney, C. E., Hell, J. W., Agah, A., et al. (2005). Thrombospondins are astrocyte-secreted proteins that promote CNS synaptogenesis. Cell 120, 421–433. doi: 10.1016/j. cell.2004.12.020

Chun, H., Im, H., Kang, Y. J., Kim, Y., Shin, J. H., Won, W., et al. (2020). Severe reactive astrocytes precipitate pathological hallmarks of Alzheimer's disease via H2O2− production. Nat. Neurosci. 23, 1555–1566. doi: 10.1038/ s41593-020-00735-y

Chung, W. S., Clarke, L. E., Wang, G. X., Stafford, B. K., Sher, A., Chakraborty, C., et al. (2013). Astrocytes mediate synapse elimination through MEGF10 and MERTK pathways. Nature 504, 394–400. doi: 10.1038/nature12776

Chung, D. E. C., Roemer, S., Petrucelli, L., and Dickson, D. W. (2021). Cellular and pathological heterogeneity of primary tauopathies. Mol. Neurodegener. 16:57. doi: 10.1186/s13024-021-00476-x

Cicognola, C., Janelidze, S., Hertze, J., Zetterberg, H., Blennow, K., Mattsson-Carlgren, N., et al. (2021). Plasma glial fibrillary acidic protein detects Alzheimer pathology and predicts future conversion to Alzheimer dementia in patients with mild cognitive impairment. Alzheimers Res. Ther. 13:68. doi: 10.1186/s13195-021-00804-9

Clarke, L. E., Liddelow, S. A., Chakraborty, C., Münch, A. E., Heiman, M., and Barres, B. A. (2018). Normal aging induces A1-like astrocyte reactivity. Proc. Natl. Acad. Sci. U. S. A. 115, E1896–E1905. doi: 10.1073/pnas. 1800165115

Colodner, K. J., Montana, R. A., Anthony, D. C., Folkerth, R. D., De Girolami, U., and Feany, M. B. (2005). Proliferative potential of human astrocytes. J. Neuropathol. Exp. Neurol. 64, 163–169. doi: 10.1093/jnen/64.2.163

Colombo, J. (2018). Interlaminar glia and other glial themes revisited: pending answers following three decades of glial research. Neuroglia 1, 7–20. doi: 10.3390/neuroglia1010003

Coppedè, F. (2014). The potential of epigenetic therapies in neurodegenerative diseases. Front. Genet. 5:220. doi: 10.3389/fgene.2014.00220

Coppieters, N., Dieriks, B. V., Lill, C., Faull, R. L. M., Curtis, M. A., and Dragunow, M. (2014). Global changes in DNA methylation and hydroxymethylation in Alzheimer's disease human brain. Neurobiol. Aging 35, 1334–1344. doi: 10.1016/j.neurobiolaging.2013.11.031

Corkrum, M., Covelo, A., Lines, J., Bellocchio, L., Pisansky, M., Loke, K., et al. (2020). Dopamine-evoked synaptic regulation in the nucleus accumbens requires astrocyte activity. Neuron 105, 1036–1047.e5. doi: 10.1016/j. neuron.2019.12.026

Crowe, E. P., Tuzer, F., Gregory, B. D., Donahue, G., Gosai, S. J., Cohen, J., et al. (2016). Changes in the transcriptome of human astrocytes accompanying oxidative stress-induced senescence. Front. Aging Neurosci. 8:208. doi: 10.3389/ fnagi.2016.00208

Cui, Z., Zhong, Z., Yang, Y., Wang, B., Sun, Y., Sun, Q., et al. (2016). Ferrous iron induces Nrf2 expression in mouse brain astrocytes to prevent neurotoxicity. J. Biochem. Mol. Toxicol. 30, 396–403. doi: 10.1002/jbt.21803

Dai, X., Hong, L., Shen, H., Du, Q., Ye, Q., Chen, X., et al. (2020). Estradiol- induced senescence of hypothalamic astrocytes contributes to aging-related reproductive function declines in female mice. Aging 12, 6089–6108. doi: 10.18632/aging.103008

David, J. P., Ghozali, F., Fallet-Bianco, C., Wattez, A., Delaine, S., Boniface, B., et al. (1997). Glial reaction in the hippocampal formation is highly correlated with aging in human brain. Neurosci. Lett. 235, 53–56. doi: 10.1016/ S0304-3940(97)00708-8

Davis, N., Mota, B. C., Stead, L., Palmer, E. O., Lombardero, L., Rodriguez-Puertas, R., et al. (2020). Ablation of astrocytes affects Aβ degradation, microglia activation and synaptic connectivity in an ex vivo model of Alzheimer's disease. Alzheimers Dement. 16, 1–12. doi: 10.1002/ alz.047419

De Strooper, B., and Karran, E. (2016). The cellular phase of Alzheimer's disease. Cell 164, 603–615. doi: 10.1016/j.cell.2015.12.056

De Zeeuw, C. I., and Hoogland, T. M. (2015). Reappraisal of Bergmann glial cells as modulators of cerebellar circuit function. Front. Cell. Neurosci. 9:246. doi: 10.3389/fncel.2015.00246

Deitmer, J. W., Theparambil, S. M., Ruminot, I., Noor, S. I., and Becker, H. M. (2019). Energy dynamics in the brain: contributions of astrocytes to metabolism and pH homeostasis. Front. Neurosci. 13:1301. doi: 10.3389/ fnins.2019.01301

Deora, V., Lee, J. D., Albornoz, E. A., McAlary, L., Jagaraj, C. J., Robertson, A. A. B., et al. (2020). The microglial NLRP3 inflammasome is activated by amyotrophic lateral sclerosis proteins. Glia 68, 402–421. doi: 10.1002/glia.23728

Di Micco, R., Krizhanovsky, V., Baker, D., and d'Adda di Fagagna, F. (2021). Cellular senescence in ageing: from mechanisms to therapeutic opportunities. Nat. Rev. Mol. Cell Biol. 22, 75–95. doi: 10.1038/s41580- 020-00314-w

Ding, F., O'Donnell, J., Thrane, A. S., Zeppenfeld, D., Kang, H., Xie, L., et al. (2013). α1-adrenergic receptors mediate coordinated Ca2+ signaling of cortical astrocytes in awake, behaving mice. Cell Calcium 54, 387– 394. doi: 10.1016/j. ceca.2013.09.001

Escartin, C., Galea, E., Lakatos, A., O'Callaghan, J. P., Petzold, G. C., Serrano-Pozo, A., et al. (2021). Reactive astrocyte nomenclature, definitions, and future directions. Nat. Neurosci. 24, 312–325. doi: 10.1038/ s41593-020-00783-4

Flanary, B. E., and Streit, W. J. (2004). Progressive telomere shortening occurs in cultured rat microglia, but not astrocytes. Glia 45, 75–88. doi: 10.1002/ glia.10301

Fonseca, M. I., Chu, S. H., Berci, A. M., Benoit, M. E., Peters, D. G., Kimura, Y., et al. (2011). Contribution of complement activation pathways to neuropathology differs among mouse models of Alzheimer's disease. J. Neuroinflammation 8:4. doi: 10.1186/1742-2094-8-4

Forman, M. S., Lal, D., Zhang, B., Dabir, D. V., Swanson, E., Lee, V. M. Y., et al. (2005). Transgenic mouse model of tau pathology in astrocytes leading to nervous system degeneration. J. Neurosci. 25, 3539–3550. doi: 10.1523/ JNEUROSCI.0081-05.2005

Francis, Y. I., Fà, M., Ashraf, H., Zhang, H., Staniszewski, A., Latchman, D. S., et al. (2009). Dysregulation of histone acetylation in the APP/PS1 mouse model of Alzheimer's disease. J. Alzheimers Dis. 18, 131–139. doi: 10.3233/ JAD-2009-1134

Frost, G. R., and Li, Y. M. (2017). The role of astrocytes in amyloid production and Alzheimer's disease. Open Biol. 7:170228. doi: 10.1098/rsob.170228 Fuchs, M., Luthold, C., Guilbert, S. M., Varlet, A. A., Lambert, H., Jetté, A., et al. (2015). A role for the chaperone complex BAG3-HSPB8 in actin dynamics, spindle orientation and proper chromosome segregation during mitosis. PLoS Genet. 11:e1005582. doi: 10.1371/journal.pgen.1005582

Fuchs, M., Poirier, D. J., Seguin, S. J., Lambert, H., Carra, S., Charette, S. J., et al. (2010). Identification of the key structural motifs involved in HspB8/ HspB6-Bag3 interaction. Biochem. J. 425, 245–255. doi: 10.1042/BJ20 090907

Furman, J. L., Sama, D. M., Gant, J. C., Beckett, T. L., Murphy, M. P., Bachstetter, A. D., et al. (2012). Targeting astrocytes ameliorates neurologic changes in a mouse model of Alzheimer's disease. J. Neurosci. 32, 16129–16140. doi: 10.1523/JNEUROSCI.2323-12.2012

Gaikwad, S., Puangmalai, N., Bittar, A., Montalbano, M., Garcia, S., McAllen, S., et al. (2021). Tau oligomer induced HMGB1 release contributes to cellular senescence and neuropathology linked to Alzheimer's disease and frontotemporal dementia. Cell Rep. 36:109419. doi: 10.1016/j.celrep.2021.109419

Galloway, A., Adeluyi, A., O'donovan, B., Fisher, M. L., Rao, C. N., Critchfield, P., et al. (2018). Dopamine triggers CTCF-dependent morphological and genomic remodeling of astrocytes. J. Neurosci. 38, 4846–4858. doi: 10.1523/ JNEUROSCI.3349-17.2018

Gao, V., Suzuki, A., Magistretti, P. J., Lengacher, S., Pollonini, G., Steinman, M. Q., et al. (2016). Astrocytic β2-adrenergic receptors mediate hippocampal long- term memory consolidation. Proc. Natl. Acad. Sci. U. S. A. 113, 8526–8531. doi: 10.1073/pnas.1605063113

Garwood, C. J., Pooler, A. M., Atherton, J., Hanger, D. P., and Noble, W. (2011). Astrocytes are important mediators of Aβ-induced neurotoxicity and tau phosphorylation in primary culture. Cell Death Dis. 2, 1–9. doi: 10.1038/ cddis.2011.50

Gate, D., Saligrama, N., Yang, A., Middeldorp, J., Levanthal, O., Chen, K., et al. (2019). O4-09-06: clonally expanded Cd8 T cells patrol Alzheimer's cerebrospinal fluid. Alzheimers Dement. 15, P1257–P1258. doi: 10.1016/j. jalz.2019.06.4793

Gerovska, D., Irizar, H., Otaegi, D., Ferrer, I., López de Munain, A., and Araúzo-Bravo, M. J. (2020). Genealogy of the neurodegenerative diseases based on a meta-analysis of age-stratified incidence data. Sci. Rep. 10:18923. doi: 10.1038/s41598-020-75014-8

Gerrits, E., Brouwer, N., Kooistra, S. M., Woodbury, M. E., Vermeiren, Y., Lambourne, M., et al. (2021). Distinct amyloid-β and tau-associated microglia profiles in Alzheimer's disease. Acta Neuropathol. 141, 681–696. doi: 10.1007/ s00401-021-02263-w

Gibney, E. R., and Nolan, C. M. (2010). Epigenetics and gene expression. Heredity 105, 4–13. doi: 10.1038/hdy.2010.54

Goetzl, E. J., Schwartz, J. B., Abner, E. L., Jicha, G. A., and Kapogiannis, D. (2018). High complement levels in astrocyte-derived exosomes of Alzheimer disease. Ann. Neurol. 83, 544–552. doi: 10.1002/ana.25172

Golde, T. E., Borchelt, D. R., Giasson, B. I., and Lewis, J. (2013). Thinking laterally about neurodegenerative proteinopathies. J. Clin. Invest. 123, 1847–1855. doi: 10.1172/JCI66029

Gorter, R. P., Stephenson, J., Nutma, E., Anink, J., de Jonge, J. C., Baron, W., et al. (2019). Rapidly progressive amyotrophic lateral sclerosis is associated with microglial reactivity and small heat shock protein expression in reactive astrocytes. Neuropathol. Appl. Neurobiol. 45, 459–475. doi: 10.1111/nan.12525

Grubman, A., Chew, G., Ouyang, J. F., Sun, G., Choo, X. Y., McLean, C., et al. (2019). A single-cell atlas of entorhinal cortex from individuals with Alzheimer's disease reveals cell-type-specific gene expression regulation. Nat. Neurosci. 22, 2087–2097. doi: 10.1038/s41593-019-0539-4

Gu, X. L., Long, C. X., Sun, L., Xie, C., Lin, X., and Cai, H. (2010). Astrocytic expression of Parkinson's disease- related A53T-synuclein causes neurodegeneration in mice. Mol. Brain 3:12. doi: 10.1186/1756-6606-3-12

Guerra-Gomes, S., Sousa, N., Pinto, L., and Oliveira, J. F. (2018). Functional roles of astrocyte calcium elevations: From synapses to behavior. Front. Cell. Neurosci. 11:427. doi: 10.3389/fncel.2017.00427

Guttikonda, S. R., Sikkema, L., Tchieu, J., Saurat, N., Walsh, R. M., Harschnitz, O., et al. (2021). Fully defined human pluripotent stem cell-derived microglia and tri-culture system model C3 production in Alzheimer's disease. Nat. Neurosci. 24, 343–354. doi: 10.1038/s41593-020-00796-z

Habib, N., McCabe, C., Medina, S., Varshavsky, M., Kitsberg, D., Dvir-Szternfeld, R., et al. (2020). Disease- associated astrocytes in Alzheimer's disease and aging. Nat. Neurosci. 23, 701–706. doi: 10.1038/s41593- 020-0624-8

Haidet-Phillips, A. M., Hester, M. E., Miranda, C. J., Meyer, K., Braun, L., Frakes, A., et al. (2011). Astrocytes from familial and sporadic ALS patients are toxic to motor neurons. Nat. Biotechnol. 29, 824–828. doi: 10.1038/nbt.1957

Haim, L. B., Ceyzériat, K., de Sauvage, M. A. C., Aubry, F., Auregan, G., Guillermier, M., et al. (2015). The JAK/STAT3 pathway is a common inducer of astrocyte reactivity in Alzheimer's and Huntington's diseases. J. Neurosci. 35, 2817–2829. doi: 10.1523/JNEUROSCI.3516-14.2015

Hansen, N. (2017). The longevity of hippocampus-dependent memory is orchestrated by the locus Coeruleus-noradrenergic system. Neural Plast. 2017:2727602. doi: 10.1155/2017/2727602

Hasel, P., Rose, I. V. L., Sadick, J. S., Kim, R. D., and Liddelow, S. A. (2021). Neuroinflammatory astrocyte subtypes in the mouse brain. Nat. Neurosci. 24, 1475–1487. doi: 10.1038/s41593-021-00905-6

Haslbeck, M., Weinkauf, S., and Buchner, J. (2015). "Regulation of the chaperone function of small Hsps," in The Big Book on Small Heat Shock Proteins. eds. R. M. Tanguay and L. E. Hightower (Springer: Switzerland), 155–178.

Hatada, I., Namihira, M., Morita, S., Kimura, M., Horii, T., and Nakashima, K. (2008). Astrocyte-specific genes are generally demethylated in neural precursor cells prior to astrocytic differentiation. PLoS One 3:e3189. doi: 10.1371/ journal.pone.0003189

Heneka, M. T. (2019). Microglia take Centre stage in neurodegenerative disease. Nat. Rev. Immunol. 19, 79–80. doi: 10.1038/s41577-018-0112-5

Heneka, M. T., Galea, E., Gavriluyk, V., Dumitrescu-Ozimek, L., Daeschner, J. A., O'Banion, M. K., et al. (2002). Noradrenergic depletion potentiates β-amyloid-induced cortical inflammation: implications for Alzheimer's disease. J. Neurosci. 22, 2434–2442. doi: 10.1523/ JNEUROSCI.22-07-02434.2002

Heneka, M. T., Nadrigny, F., Regen, T., Martinez-Hernandez, A., Dumitrescu-Ozimek, L., Terwel, D., et al. (2010). Locus ceruleus controls Alzheimer's disease pathology by modulating microglial functions through norepinephrine. Proc. Natl. Acad. Sci. U. S. A. 107, 6058–6063. doi: 10.1073/ pnas.0909586107

Heneka, M. T., Ramanathan, M., Jacobs, A. H., Dumitrescu-Ozimek, L., Bilkei-Gorzo, A., Debeir, T., et al. (2006). Locus ceruleus degeneration promotes Alzheimer pathogenesis in amyloid precursor protein 23 transgenic mice. J. Neurosci. 26, 1343–1354. doi: 10.1523/JNEUROSCI.4236- 05.2006

Heneka, M. T., Sastre, M., Dumitrescu-Ozimek, L., Dewachter, I., Walter, J., Klockgether, T., et al. (2005). Focal glial activation coincides with increased BACE1 activation and precedes amyloid plaque deposition in APP[V717I] transgenic mice. J. Neuroinflammation 2:22. doi: 10.1186/1742-2094-2-22

Heneka, M. T., Wiesinger, H., Dumitrescu-Ozimek, L., Riederer, P., Feinstein, D. L., and Klockgether, T. (2001). Neuronal and glial coexpression of argininosuccinate synthetase and inducible nitric oxide synthase in Alzheimer disease. J. Neuropathol. Exp. Neurol. 60, 906–916. doi: 10.1093/jnen/60.9.906

Heurtaux, T., Kirchmeyer, M., Koncina, E., Felten, P., Richart, L., Uriarte Huarte, O., et al. (2021). Apomorphine reduces A53T α-synuclein-induced microglial reactivity through activation of NRF2 signalling pathway. Cell. Mol. Neurobiol. doi:10.1007/s10571-021-01131-1 [Epub ahead of print].

Hishikawa, N., Hashizume, Y., Yoshida, M., Niwa, J. I., Tanaka, F., and Sobue, G. (2005). Tuft-shaped astrocytes in Lewy body disease. Acta Neuropathol. 109, 373–380. doi: 10.1007/s00401-004-0967-3

Holland, N., Robbins, T. W., and Rowe, J. B. (2021). The role of noradrenaline in cognition and cognitive disorders. Brain 144, 2243–2256. doi: 10.1093/ brain/awab111

Huang, C., Huang, B., Bi, F., Yan, L. H., Tong, J., Huang, J., et al. (2014). Profiling the genes affected by pathogenic TDP-43 in astrocytes. J. Neurochem. 129, 932–939. doi: 10.1111/jnc.12660

Huang, X., Su, Y., Wang, N., Li, H., Li, Z., Yin, G., et al. (2021). Astroglial connexins in neurodegenerative diseases. Front. Mol. Neurosci. 14:657514. doi: 10.3389/fnmol.2021.657514

Hummel, C., Leylamian, O., Pösch, A., Weis, J., Aronica, E., Beyer, C., et al. (2021). Expression and cell type- specific localization of Inflammasome sensors in the spinal cord of SOD1(G93A) mice and sporadic amyotrophic lateral sclerosis patients. Neuroscience 463, 288–302. doi: 10.1016/j. neuroscience.2021.03.023

Inoue, Y., Ayaki, T., Ishimoto, T., Yamakado, H., Maki, T., Matsuzawa, S., et al. (2021). The stimulator of interferon genes (STING) pathway is upregulated in striatal astrocytes of patients with multiple system atrophy. Neurosci. Lett. 757:135972. doi: 10.1016/j.neulet.2021.135972

Izrael, M., Slutsky, S. G., and Revel, M. (2020). Rising stars: astrocytes as a therapeutic target for ALS disease. Front. Neurosci. 14:824. doi: 10.3389/ fnins.2020.00824

Jäkel, S., Agirre, E., Mendanha Falcão, A., van Bruggen, D., Lee, K. W., Knuesel, I., et al. (2019). Altered human oligodendrocyte heterogeneity in multiple sclerosis. Nature 566, 543–547. doi: 10.1038/s41586- 019-0903-2

Jaya, N., Garcia, V., and Vierling, E. (2009). Substrate binding site flexibility of the small heat shock protein molecular chaperones. Proc. Natl. Acad. Sci. U. S. A. 106, 15604–15609. doi: 10.1073/pnas.0902177106

Johann, S., Heitzer, M., Kanagaratnam, M., Goswami, A., Rizo, T., Weis, J., et al. (2015). NLRP3 inflammasome is expressed by astrocytes in the SOD1 mouse model of ALS and in human sporadic ALS patients. Glia 63, 2260–2273. doi: 10.1002/glia.22891

Johnson, J. A., Johnson, D. A., Kraft, A. D., Calkins, M. J., Jakel, R. J., Vargas, M. R., et al. (2008). The Nrf2-ARE pathway: an indicator and modulator of oxidative stress in neurodegeneration. Ann. N. Y. Acad. Sci. 1147, 61–69. doi: 10.1196/annals.1427.036

Jones, E. V., and Bouvier, D. S. (2014). Astrocyte-secreted matricellular proteins in CNS remodelling during development and disease. Neural Plast. 2014:321209. doi: 10.1155/2014/321209

Joshi, A. U., Minhas, P. S., Liddelow, S. A., Haileselassie, B., Andreasson, K. I., Dorn, G. W., et al. (2019). Fragmented mitochondria released from microglia trigger A1 astrocytic response and propagate inflammatory neurodegeneration. Nat. Neurosci. 22, 1635–1648. doi: 10.1038/s41593-019-0486-0

Kalinin, S., Gavrilyuk, V., Polak, P. E., Vasser, R., Zhao, J., Heneka, M. T., et al. (2007). Noradrenaline deficiency in brain increases β-amyloid plaque burden in an animal model of Alzheimer's disease. Neurobiol. Aging 28, 1206–1214. doi: 10.1016/j.neurobiolaging.2006.06.003

Katsipis, G., Tzekaki, E. E., Tsolaki, M., and Pantazaki, A. A. (2021). Salivary GFAP as a potential biomarker for diagnosis of mild cognitive impairment and Alzheimer's disease and its correlation with neuroinflammation and apoptosis. J. Neuroimmunol. 361:577744. doi: 10.1016/j.jneuroim.2021.577744

Katsouri, L., Birch, A. M., Renziehausen, A. W. J., Zach, C., Aman, Y., Steeds, H., et al. (2020). Ablation of reactive astrocytes exacerbates disease pathology in a model of Alzheimer's disease. Glia 68, 1017–1030. doi: 10.1002/glia.23759

Katsuse, O., Iseki, E., and Kosaka, K. (2003). Immunohistochemical study of the expression of cytokines and nitric oxide synthases in brains of patients with dementia with Lewy bodies. Neuropathology 23, 9–15. doi: 10.1046/j. 1440-1789.2003.00483.x

Kazama, M., Kato, Y., Kakita, A., Noguchi, N., Urano, Y., Masui, K., et al. (2020). Astrocytes release glutamate via cystine/glutamate antiporter upregulated in response to increased oxidative stress related to sporadic amyotrophic lateral sclerosis. Neuropathology 40, 587–598. doi: 10.1111/ neup.12716

Khan, Z. U., Koulen, P., Rubinstein, M., Grandy, D. K., and Goldman-Rakic, P. S. (2001). An astroglia-linked dopamine D2-receptor action in prefrontal cortex. Proc. Natl. Acad. Sci. U. S. A. 98, 1964–1969. doi: 10.1073/pnas.98.4.1964

Kia, A., McAvoy, K., Krishnamurthy, K., Trotti, D., and Pasinelli, P. (2018). Astrocytes expressing ALS-linked mutant FUS induce motor neuron death through release of tumor necrosis factor-alpha. Glia 66, 1016– 1033. doi: 10.1002/glia.23298

Kim, B., and Hong, J. (2014). An overview of naturally occurring histone deacetylase inhibitors. Curr. Top. Med. Chem. 14, 2759–2782. doi: 10.217 4/1568026615666141208105614

King, A., Szekely, B., Calapkulu, E., Ali, H., Rios, F., Jones, S., et al. (2020). The increased densities, but different distributions, of both C3 and S100A10 immunopositive astrocyte-like cells in alzheimer's disease brains suggest possible roles for both A1 and A2 astrocytes in the disease pathogenesis. Brain Sci. 10:503. doi: 10.3390/brainsci10080503

Kobayashi, E., Nakano, M., Kubota, K., Himuro, N., Mizoguchi, S., Chikenji, T., et al. (2018). Activated forms of astrocytes with higher GLT-1 expression are associated with cognitive normal subjects with Alzheimer pathology in human brain. Sci. Rep. 8:1712. doi: 10.1038/s41598-018-19442-7

Konsoula, Z., and Barile, F. A. (2012). Epigenetic histone acetylation and deacetylation mechanisms in experimental models of neurodegenerative disorders. J. Pharmacol. Toxicol. Methods 66, 215–220. doi: 10.1016/j. vascn.2012.08.001

Kovacs, G. G., Ferrer, I., Grinberg, L. T., Alafuzoff, I., Attems, J., Budka, H., et al. (2016). Aging-related tau astrogliopathy (ARTAG): harmonized evaluation strategy. Acta Neuropathol. 131, 87–102. doi: 10.1007/s00401- 015-1509-x

Kovacs, G. G., Xie, S. X., Robinson, J. L., Lee, E. B., Smith, D. H., Schuck, T., et al. (2018). Sequential stages and distribution patterns of aging-related tau astrogliopathy (ARTAG) in the human brain. Acta Neuropathol. Commun. 6:50. doi: 10.1186/s40478-018-0552-y

Kraft, A. W., Hu, X., Yoon, H., Yan, P., Xiao, Q., Wang, Y., et al. (2013). Attenuating astrocyte activation accelerates plaque pathogenesis in APP/PS1 mice. FASEB J. 27, 187–198. doi: 10.1096/fj.12-208660

Kwon, H. S., and Koh, S. H. (2020). Neuroinflammation in neurodegenerative disorders: the roles of microglia and astrocytes. Transl. Neurodegener. 9:42. doi: 10.1186/s40035-020-00221-2

Lagier-Tourenne, C., Baughn, M., Rigo, F., Sun, S., Liu, P., Li, H. R., et al. (2013). Targeted degradation of sense and antisense C9orf72 RNA foci as therapy for ALS and frontotemporal degeneration. Proc. Natl. Acad. Sci. U. S. A. 110, E4530–E4539. doi: 10.1073/pnas.1318835110

Lake, B. B., Chen, S., Sos, B. C., Fan, J., Kaeser, G. E., Yung, Y. C., et al. (2018). Integrative single-cell analysis of transcriptional and epigenetic states in the human adult brain. Nat. Biotechnol. 36, 70–80. doi: 10.1038/ nbt.4038

Lau, S. F., Cao, H., Fu, A. K. Y., and Ip, N. Y. (2020). Single-nucleus transcriptome analysis reveals dysregulation of angiogenic endothelial cells and neuroprotective glia in Alzheimer's disease. Proc. Natl. Acad. Sci. U. S. A. 117, 25800–25809. doi: 10.1073/pnas.2008762117

Lee, S., Kim, S., Kang, H. Y., Lim, H. R., Kwon, Y., Jo, M., et al. (2020). The overexpression of TDP-43 in astrocytes causes neurodegeneration via a PTP1B-mediated inflammatory response. J. Neuroinflammation 17, 1–22. doi: 10.1186/s12974-020-01963-6

Li, J., Pan, L., Pembroke, W. G., Rexach, J. E., Godoy, M. I., Condro, M. C., et al. (2021). Conservation and divergence of vulnerability and responses to stressors between human and mouse astrocytes. Nat. Commun. 12:3958. doi: 10.1038/s41467-021-24232-3

Lian, H., Litvinchuk, A., Chiang, A. C. A., Aithmitti, N., Jankowsky, J. L., and Zheng, H. (2016). Astrocyte-microglia cross talk through complement activation modulates amyloid pathology in mouse models of alzheimer's disease. J. Neurosci. 36, 577–589. doi: 10.1523/JNEUROSCI.2117-15.2016

Liddelow, S. A., Guttenplan, K. A., Clarke, L. E., Bennett, F. C., Bohlen, C. J., Schirmer, L., et al. (2017). Neurotoxic reactive astrocytes are induced by activated microglia. Nature 541, 481–487. doi: 10.1038/nature21029

Limbad, C., Oron, T. R., Alimirah, F., Davalos, A. R., Tracy, T. E., Gan, L., et al. (2020). Astrocyte senescence promotes glutamate toxicity in cortical neurons. PLoS One 15:e0227887. doi: 10.1371/journal.pone.0227887

Lochs, S. J. A., Kefalopoulou, S., and Kind, J. (2019). Lamina associated domains and gene regulation in development and cancer. Cell 8:271. doi: 10.3390/ cells8030271

Lomen-Hoerth, C. (2011). Clinical phenomenology and neuroimaging correlates in ALS-FTD. J. Mol. Neurosci. 45, 656–662. doi: 10.1007/s12031-011- 9636-x

Lü, L., Li, J., Zhu, Y., Mak, Y. T., and Yew, D. T. (2008). H2O2-induced changes in astrocytic cultures from control and rapidly aging strains of mouse. Int. J. Neurosci. 118, 1239–1250. doi: 10.1080/00207450601059429

Lüth, H. J., Münch, G., and Arendt, T. (2002). Aberrant expression of NOS isoforms in Alzheimer's disease is structurally related to nitrotyrosine formation. Brain Res. 953, 135–143. doi: 10.1016/S0006-8993(02)03280-8

Lyra e Silva, N. M., Gonçalves, R. A., Pascoal, T. A., Lima-Filho, R. A. S., Resende, E. D. P. F., Vieira, E. L. M., et al. (2021). Pro-inflammatory interleukin-6 signaling links cognitive impairments and peripheral metabolic alterations in Alzheimer's disease. Transl. Psychiatry 11:251. doi: 10.1038/ s41398-021-01349- z

Madill, M., McDonagh, K., Ma, J., Vajda, A., McLoughlin, P., O'Brien, T., et al. (2017). Amyotrophic lateral sclerosis patient iPSC-derived astrocytes impair autophagy via non-cell autonomous mechanisms. Mol. Brain 10:22. doi: 10.1186/s13041-017-0300-4

Maegawa, S., Hinkal, G., Kim, H. S., Shen, L., Zhang, L., Zhang, J., et al. (2010). Widespread and tissue specific age-related DNA methylation changes in mice. Genome Res. 20, 332–340. doi: 10.1101/gr.096826.109

Manaye, K. F., McIntire, D. D., Mann, D. M. A., and German, D. C. (1995). Locus coeruleus cell loss in the aging human brain: A non-random process. J. Comp. Neurol. 358, 79–87. doi: 10.1002/cne.903580105

Månberg, A., Skene, N., Sanders, F., Trusohamn, M., Remnestål, J., Szczepińska, A., et al. (2021). Altered perivascular fibroblast activity precedes ALS disease onset. Nat. Med. 27:1308. doi: 10.1038/ s41591-021- 01414-6

Martínez-Cué, C., and Rueda, N. (2020). Cellular senescence in neurodegenerative diseases. Front. Cell. Neurosci. 14:16. doi: 10.3389/fncel.2020.00016

Matchett, B. J., Grinberg, L. T., Theofilas, P., and Murray, M. E. (2021). The mechanistic link between selective vulnerability of the locus coeruleus and neurodegeneration in Alzheimer's disease. Acta Neuropathol. 141, 631–650. doi: 10.1007/s00401-020-02248-1

Matejuk, A., and Ransohoff, R. M. (2020). Crosstalk Between astrocytes and microglia: An overview. Front. Immunol. 11:1416. doi: 10.3389/ fimmu.2020.01416

Mathys, H., Davila-Velderrain, J., Peng, Z., Gao, F., Mohammadi, S., Young, J. Z., et al. (2019). Single- cell transcriptomic analysis of Alzheimer's disease. Nature 570, 332–337. doi: 10.1038/s41586-019- 1195-2

McAlpine, C. S., Park, J., Griciuc, A., Kim, E., Choi, S. H., Iwamoto, Y., et al. (2021). Astrocytic interleukin-3 programs microglia and limits Alzheimer's disease. Nature 595, 701–706. doi: 10.1038/s41586-021-03734-6

McCann, H., Durand, B., and Shepherd, C. E. (2021). Aging-related tau astrogliopathy in aging and neurodegeneration. Brain Sci. 11:927. doi: 10.3390/ brainsci11070927

Meiser, J., Weindl, D., and Hiller, K. (2013). Complexity of dopamine metabolism. Cell Commun. Signal 11:34. doi: 10.1186/1478-811X-11-34

Mirza, B., Hadberg, H., Thomsen, P., and Moos, T. (1999). The absence of reactive astrocytosis is indicative of a unique inflammatory process in Parkinson's disease. Neuroscience 95, 425–432. doi: 10.1016/ S0306- 4522(99)00455-8

Miyazaki, I., Asanuma, M., Diaz-Corrales, F. J., Miyoshi, K., and Ogawa, N. (2004). Direct evidence for expression of dopamine receptors in astrocytes from basal ganglia. Brain Res. 1029, 120–123. doi: 10.1016/j.brainres.2004.09.014

Miyazaki, K., Ohta, Y., Nagai, M., Morimoto, N., Kurata, T., Takehisa, Y., et al. (2011). Disruption of neurovascular unit prior to motor neuron degeneration in amyotrophic lateral sclerosis. J. Neurosci. Res. 89, 718–728. doi: 10.1002/ jnr.22594

Munger, E. L., Edler, M. K., Hopkins, W. D., Ely, J. J., Erwin, J. M., Perl, D. P., et al. (2019). Astrocytic changes with aging and Alzheimer's disease-type pathology in chimpanzees. J. Comp. Neurol. 527, 1179–1195. doi: 10.1002/ cne.24610

Muñoz, Y., Cuevas-Pacheco, F., Quesseveur, G., and Murai, K. K. (2021). Light microscopic and heterogeneity analysis of astrocytes in the common marmoset brain. J. Neurosci. Res. 99, 1–27. doi: 10.1002/jnr.24967

Narayan, P., and Dragunow, M. (2010). Pharmacology of epigenetics in brain disorders. Br. J. Pharmacol. 159, 285–303. doi: 10.1111/j.1476-5381.2009. 00526.x

Narayan, P., Holmström, K. M., Kim, D. H., Whitcomb, D. J., Wilson, M. R., St. George-Hyslop, P., et al. (2014). Rare individual amyloid-β oligomers act on astrocytes to initiate neuronal damage. Biochemistry 53, 2442–2453. doi: 10.1021/bi401606f

Nelson, P. T., Dickson, D. W., Trojanowski, J. Q., Jack, C. R., Boyle, P. A., Arfanakis, K., et al. (2019). Limbic- predominant age-related TDP-43 encephalopathy (LATE): consensus working group report. Brain 142, 1503–1527. doi: 10.1093/brain/awz099

Neumann, M., Sampathu, D. M., Kwong, L. K., Truax, A. C., Micsenyi, M. C., Chou, T. T., et al. (2006). Ubiquitinated TDP-43 in frontotemporal lobar degeneration and amyotrophic lateral sclerosis. Science 314, 130–133. doi: 10.1126/science.1134108

Nichols, N. R., Day, J. R., Laping, N. J., Johnson, S. A., and Finch, C. E. (1993). GFAP mRNA increases with age in rat and human brain. Neurobiol. Aging 14, 421–429. doi: 10.1016/0197-4580(93)90100-P

Nuutinen, T., Suuronen, T., Kauppinen, A., and Salminen, A. (2010). Valproic acid stimulates clusterin expression in human astrocytes: implications for Alzheimer's disease. Neurosci. Lett. 475, 64–68. doi: 10.1016/j.neulet.2010. 03.041

O'Donnell, J., Zeppenfeld, D., McConnell, E., Pena, S., and Nedergaard, M. (2012). Norepinephrine: A neuromodulator that boosts the function of multiple cell types to optimize CNS performance. Neurochem. Res. 37, 2496–2512. doi: 10.1007/s11064-012-0818-x

Oberheim, N. A., Takano, T., Han, X., He, W., Lin, J. H. C., Wang, F., et al. (2009). Uniquely hominid features of adult human astrocytes. J. Neurosci. 29, 3276–3287. doi: 10.1523/JNEUROSCI.4707-08.2009

Oberheim, N. A., Wang, X., Goldman, S., and Nedergaard, M. (2006). Astrocytic complexity distinguishes the human brain. Trends Neurosci. 29, 547–553. doi: 10.1016/j.tins.2006.08.004

Oe, Y., Wang, X., Patriarchi, T., Konno, A., Ozawa, K., Yahagi, K., et al. (2020). Distinct temporal integration of noradrenaline signaling by astrocytic second messengers during vigilance. Nat. Commun. 24:471. doi: 10.1038/ s41467-020-14378-x

Oeckl, P., Halbgebauer, S., Anderl-Straub, S., Steinacker, P., Hussa, A. M., Neugebauer, H., et al. (2019). Glial fibrillary acidic protein in serum is increased in Alzheimer's disease and correlates with cognitive impairment. J. Alzheimers Dis. 67, 481–488. doi: 10.3233/JAD-180325

Ogrodnik, M., Evans, S. A., Fielder, E., Victorelli, S., Kruger, P., Salmonowicz, H., et al. (2021). Whole-body senescent cell clearance alleviates age-related brain inflammation and cognitive impairment in mice. Aging Cell 20:e13296. doi: 10.1111/acel.13296

Pan, J., Ma, N., Yu, B., Zhang, W., and Wan, J. (2020). Transcriptomic profiling of microglia and astrocytes throughout aging. J. Neuroinflammation 17:97. doi: 10.1186/s12974-020-01774-9

Park, J. S., Kam, T. I., Lee, S., Park, H., Oh, Y., Kwon, S. H., et al. (2021). Blocking microglial activation of reactive astrocytes is neuroprotective in models of Alzheimer's disease. Acta Neuropathol. Commun. 9:78. doi: 10.1186/s40478-021-01180-z

Pellegrini, C., Pirazzini, C., Sala, C., Sambati, L., Yusipov, I., Kalyakulina, A., et al. (2021). A meta-analysis of brain DNA methylation across sex, age, and alzheimer's disease points for accelerated epigenetic aging in neurodegeneration. Front. Aging Neurosci. 13:639428. doi: 10.3389/ fnagi.2021.639428

Pereira, J. B., Janelidze, S., Smith, R., Mattsson-Carlgren, N., Palmqvist, S., Teunissen, C. E., et al. (2021). Plasma GFAP is an early marker of amyloid-β but not tau pathology in Alzheimer's disease. Brain 144, 3505–3516. doi: 10.1093/brain/awab223

Pestana, F., Edwards-Faret, G., Belgard, T. G., Martirosyan, A., and Holt, M. G. (2020). No longer underappreciated: the emerging concept of astrocyte heterogeneity in neuroscience. Brain Sci. 10:168. doi: 10.3390/brainsci10030168

Peters, O. M., Ghasemi, M., and Brown, R. H. (2015). Emerging mechanisms of molecular pathology in ALS. J. Clin. Invest. 125, 1767–1779. doi: 10.1172/ JCI71601

Phipps, A. J., Vickers, J. C., Taberlay, P. C., and Woodhouse, A. (2016). Neurofilament-labeled pyramidal neurons and astrocytes are deficient in DNA methylation marks in Alzheimer's disease. Neurobiol. Aging 45, 30–42. doi: 10.1016/j.neurobiolaging.2016.05.003

Porchet, R., Probst, A., Bouras, C., Dráberová, E., Dráber, P., and Riederer, B. M. (2003). Analysis of gial acidic fibrillary protein in the human entorhinal cortex during aging and in Alzheimer's disease. Proteomics 3, 1476–1485. doi: 10.1002/pmic.200300456

Radford, R., Rcom-H'cheo-Gauthier, A., Wong, M. B., Eaton, E. D., Quilty, M., Blizzard, C., et al. (2015). The degree of astrocyte activation in multiple system atrophy is inversely proportional to the distance to α- synuclein inclusions. Mol. Cell. Neurosci. 65, 68–81. doi: 10.1016/j.mcn.2015.02.015

Reichenbach, N., Delekate, A., Plescher, M., Schmitt, F., Krauss, S., Blank, N., et al. (2019). Inhibition of Stat3-mediated astrogliosis ameliorates pathology in an Alzheimer's disease model. EMBO Mol. Med. 11:e9665. doi: 10.15252/ emmm.201809665

Richetin, K., Steullet, P., Pachoud, M., Perbet, R., Parietti, E., Maheswaran, M., et al. (2020). Tau accumulation in astrocytes of the dentate gyrus induces neuronal dysfunction and memory deficits in Alzheimer's disease. Nat. Neurosci. 23, 1567–1579. doi: 10.1038/s41593-020-00728-x

Rivers-Auty, J., Mather, A. E., Peters, R., Lawrence, C. B., and Brough, D. (2020). Anti-inflammatories in Alzheimer's disease—potential therapy or spurious correlate? Brain Commun. 2:fcaa109. doi: 10.1093/braincomms/ fcaa109

Robinson, J. L., Lee, E. B., Xie, S. X., Rennert, L., Suh, E., Bredenberg, C., et al. (2018). Neurodegenerative disease concomitant proteinopathies are prevalent, age-related and APOE4-associated. Brain 141, 2181– 2193. doi: 10.1093/brain/awy146

Robledinos-Antón, N., Fernández-Ginés, R., Manda, G., and Cuadrado, A. (2019). Activators and inhibitors of NRF2: a review of their potential for clinical development. Oxidative Med. Cell. Longev. 2019:9372182. doi: 10.1155/2019/9372182

Rose, J., Brian, C., Pappa, A., Panayiotidis, M. I., and Franco, R. (2020). Mitochondrial metabolism in astrocytes regulates brain bioenergetics, neurotransmission and redox balance. Front. Neurosci. 14:536682. doi: 10.3389/ fnins.2020.536682

Rostami, J., Fotaki, G., Sirois, J., Mzezewa, R., Bergström, J., Essand, M., et al. (2020). Astrocytes have the capacity to act as antigen-presenting cells in the Parkinson's disease brain. J. Neuroinflammation 17:119. doi: 10.1186/ s12974-020-01776-7

Rothhammer, V., and Quintana, F. J. (2015). Control of autoimmune CNS inflammation by astrocytes. Semin. Immunopathol. 37, 625–638. doi: 10.1007/ s00281-015-0515-3

Rothstein, J. D., Van Kammen, M., Levey, A. I., Martin, L. J., and Kuncl, R. W. (1995). Selective loss of glial glutamate transporter GLT-1 in amyotrophic lateral sclerosis. Ann. Neurol. 38, 73–84. doi: 10.1002/ana.410380114

Rueda-Carrasco, J., Martin-Bermejo, M. J., Pereyra, G., Mateo, M. I., Borroto, A., Brosseron, F., et al. (2021). SFRP1 modulates astrocyte-to-microglia crosstalk in acute and chronic neuroinflammation. EMBO Rep. 22:e51696. doi: 10.15252/ embr.202051696

Russ, K., Teku, G., Bousset, L., Redeker, V., Piel, S., Savchenko, E., et al. (2021). TNF-α and α-synuclein fibrils differently regulate human astrocyte immune reactivity and impair mitochondrial respiration. Cell Rep. 34:108895. doi: 10.1016/j.celrep.2021.108895

Salter, M. W., and Stevens, B. (2017). Microglia emerge as central players in brain disease. Nat. Med. 23, 1018–1027. doi: 10.1038/nm.4397

Sanfilippo, C., Longo, A., Lazzara, F., Cambria, D., Distefano, G., Palumbo, M., et al. (2017). CHI3L1 and CHI3L2 overexpression in motor cortex and spinal cord of sALS patients. Mol. Cell. Neurosci. 85, 162–169. doi: 10.1016/j. mcn.2017.10.001

Sathe, G., Na, C. H., Renuse, S., Madugundu, A. K., Albert, M., Moghekar, A., et al. (2019). Quantitative proteomic profiling of cerebrospinal fluid to identify candidate biomarkers for alzheimer's disease. Proteomics Clin. Appl. 13:e1800105. doi: 10.1002/prca.201800105

Schiffer, D., Cordera, S., Cavalla, P., and Migheli, A. (1996). Reactive astrogliosis of the spinal cord in amyotrophic lateral sclerosis. J. Neurol. Sci. 139, 27–33. doi: 10.1016/0022-510X(96)00073-1

Schirmer, L., Velmeshev, D., Holmqvist, S., Kaufmann, M., Werneburg, S., Jung, D., et al. (2019). Neuronal vulnerability and multilineage diversity in multiple sclerosis. Nature 573, 75–82. doi: 10.1038/s41586-019- 1404-z

Serrano-Pozo, A., Gómez-Isla, T., Growdon, J. H., Frosch, M. P., and Hyman, B. T. (2013). A phenotypic change but not proliferation underlies glial responses in Alzheimer disease. Am. J. Pathol. 182, 2332–2344. doi: 10.1016/j. ajpath.2013.02.031

Sharma, K. K., Kaur, H., and Kester, K. (1997). Functional elements in molecular chaperone α-crystallin: identification of binding sites in αB- crystallin. Biochem. Biophys. Res. Commun. 239, 217–222. doi: 10.1006/ bbrc.1997.7460

Shih, A. Y., Johnson, D. A., Wong, G., Kraft, A. D., Jiang, L., Erb, H., et al. (2003). Coordinate regulation of glutathione biosynthesis and release by Nrf2-expressing glia potently protects neurons from oxidative stress. J. Neurosci. 23, 3394–3406. doi: 10.1523/JNEUROSCI.23-08-03394.2003

Shukla, S., and Tekwani, B. L. (2020). Histone deacetylases inhibitors in neurodegenerative diseases, neuroprotection and neuronal differentiation. Front. Pharmacol. 11:537. doi: 10.3389/fphar.2020.00537

Sidoryk-Wegrzynowicz, M., Gerber, Y. N., Ries, M., Sastre, M., Tolkovsky, A. M., and Spillantini, M. G. (2017). Astrocytes in mouse models of tauopathies acquire early deficits and lose neurosupportive functions. Acta Neuropathol. Commun. 5:89. doi: 10.1186/s40478-017-0478-9

Sigfridsson, E., Marangoni, M., Johnson, J. A., Hardingham, G. E., Fowler, J. H., and Horsburgh, K. (2018). Astrocyte-specific overexpression of Nrf2 protects against optic tract damage and behavioural alterations in a mouse model of cerebral hypoperfusion. Sci. Rep. 8:12552. doi: 10.1038/s41598-018-30675-4

Singh, D., Agrawal, A., Singal, C. M. S., Pandey, H. S., Seth, P., and Sharma, S. K. (2020). Sinomenine inhibits amyloid beta-induced astrocyte activation and protects neurons against indirect toxicity. Mol. Brain 13:30. doi: 10.1186/ s13041-020-00569-6

Sivandzade, F., Prasad, S., Bhalerao, A., and Cucullo, L. (2019). NRF2 and NF-ĸB interplay in cerebrovascular and neurodegenerative disorders: molecular mechanisms and possible therapeutic approaches. Redox Biol. 21:101059. doi: 10.1016/j.redox.2018.11.017

Smethurst, P., Risse, E., Tyzack, G. E., Mitchell, J. S., Taha, D. M., Chen, Y. R., et al. (2020). Distinct responses of neurons and astrocytes to TDP-43 proteinopathy in amyotrophic lateral sclerosis. Brain 143, 430–440. doi: 10.1093/brain/awz419

Smith, H. L., Freeman, O. J., Butcher, A. J., Holmqvist, S., Humoud, I., Schätzl, T., et al. (2020). Astrocyte unfolded protein response induces a specific reactivity state that causes non-cell-autonomous neuronal degeneration. Neuron 105, 855–866.e5. doi: 10.1016/j.neuron.2019.12.014

Smith, M. A., Richey Harris, P. L., Sayre, L. M., Beckman, J. S., and Perry, G. (1997). Widespread peroxynitrite-mediated damage in Alzheimer's disease. J. Neurosci. 17, 2653–2657. doi: 10.1523/JNEUROSCI.17-08-02653.1997

Sofroniew, M. V. (2015). Astrocyte barriers to neurotoxic inflammation. Nat. Rev. Neurosci. 16, 249–263. doi: 10.1038/nrn3898

Sofroniew, M. V., and Vinters, H. V. (2010). Astrocytes: biology and pathology. Acta Neuropathol. 119, 7– 35. doi: 10.1007/s00401-009-0619-8

Soreq, L., Rose, J., Soreq, E., Hardy, J., Trabzuni, D., Cookson, M. R., et al. (2017). Major shifts in glial regional identity are a transcriptional hallmark of human brain aging. Cell Rep. 18, 557–570. doi: 10.1016/j.celrep.2016. 12.011

Sorrells, S. F., Paredes, M. F., Cebrian-Silla, A., Sandoval, K., Qi, D., Kelley, K. W., et al. (2018). Human hippocampal neurogenesis drops sharply in children to undetectable levels in adults. Nature 555, 377–381. doi: 10.1038/nature25975

Sorrentino, Z. A., Giasson, B. I., and Chakrabarty, P. (2019). α-Synuclein and astrocytes: tracing the pathways from homeostasis to neurodegeneration in Lewy body disease. Acta Neuropathol. 138, 1–21. doi: 10.1007/s00401-019- 01977-2

Spanos, F., and Liddelow, S. A. (2020). An overview of astrocyte responses in genetically induced alzheimer's disease mouse models. Cell 9:2415. doi: 10.3390/cells9112415

Stojiljkovic, M. R., Ain, Q., Bondeva, T., Heller, R., Schmeer, C., and Witte, O. W. (2019). Phenotypic and functional differences between senescent and aged murine microglia. Neurobiol. Aging 74, 56–69. doi: 10.1016/j. neurobiolaging.2018.10.007

Swenson, B. L., Meyer, C. F., Bussian, T. J., and Baker, D. J. (2019). Senescence in aging and disorders of the central nervous system. Transl. Med. Aging 3, 17–25. doi: 10.1016/j.tma.2019.01.002

Szebeni, A., Szebeni, K., DiPeri, T., Chandley, M. J., Crawford, J. D., Stockmeier, C. A., et al. (2014). Shortened telomere length in white matter oligodendrocytes in major depression: potential role of oxidative stress. Int. J. Neuropsychopharmacol. 17, 1579–1589. doi: 10.1017/S1461145714000698

Takeda, T., Hosokawa, M., and Higuchi, K. (1997). Senescence-accelerated mouse (SAM): a novel murine model of senescence. Exp. Gerontol. 32, 105–109. doi: 10.1016/S0531-5565(96)00036-8

Tong, J., Ang, L. C., Williams, B., Furukawa, Y., Fitzmaurice, P., Guttman, M., et al. (2015). Low levels of astroglial markers in Parkinson's disease: relationship to α-synuclein accumulation. Neurobiol. Dis. 82, 243–253. doi: 10.1016/j. nbd.2015.06.010

Tong, J., Huang, C., Bi, F., Wu, Q., Huang, B., Liu, X., et al. (2013). Expression of ALS-linked TDP-43 mutant in astrocytes causes non-cell-autonomous motor neuron death in rats. EMBO J. 32, 1917–1926. doi: 10.1038/emboj.2013.122

Van Den Berge, S. A., Kevenaar, J. T., Sluijs, J. A., and Hol, E. M. (2012). Dementia in Parkinson's disease correlates with α-synuclein pathology but not with cortical astrogliosis. Parkinson. Dis. 2012:420957. doi: 10.1155/2012/ 420957

Van Montfort, R. L. M., Basha, E., Friedrich, K. L., Slingsby, C., and Vierling, E. (2001). Crystal structure and assembly of a eukaryotic small heat shock protein. Nat. Struct. Biol. 8, 1025–1030. doi: 10.1038/nsb722

Velebit, J., Horvat, A., Smolič, T., Prpar Mihevc, S., Rogelj, B., Zorec, R., et al. (2020). Astrocytes with TDP- 43 inclusions exhibit reduced noradrenergic cAMP and Ca2+ signaling and dysregulated cell metabolism. Sci. Rep. 10:6003. doi: 10.1038/s41598-020-62864-5

Verberk, I. M. W., Thijssen, E., Koelewijn, J., Mauroo, K., Vanbrabant, J., De Wilde, A., et al. (2020). Combination of plasma amyloid beta(1-42/1-40) and glial fibrillary acidic protein strongly associates with cerebral amyloid pathology. Alzheimers Res. Ther. 12:118. doi: 10.1186/s13195-020-00682-7

Verkhratsky, A., and Nedergaard, M. (2018). Physiology of astroglia. Physiol. Rev. 98, 239–389. doi: 10.1152/physrev.00042.2016

Verma, M., and Kumar, V. (2018). "Epigenetic drugs for cancer and precision medicine," in Epigenetics of Aging and Longevity. Vol. 4. eds. A. Moskalev and A. M. Vaiserman 439–451.

Viejo, L., Noori, A., Merrill, E., Das, S., Hyman, B. T., and Serrano-Pozo, A. (2021). Systematic review of human post-mortem immunohistochemical studies and bioinformatics analyses unveil the complexity of

astrocyte reaction in Alzheimer's disease. Neuropathol. Appl. Neurobiol. 48:e12753. doi: 10.1111/ nan.12753

Vodovotz, Y., Lucia, M. S., Flanders, K. C., Chesler, L., Xie, Q. W., Smith, T. W., et al. (1996). Inducible nitric oxide synthase in tangle-bearing neurons of patients with Alzheimer's disease. J. Exp. Med. 184, 1425– 1433. doi: 10.1084/ jem.184.4.1425

Vojta, A., Dobrinic, P., Tadic, V., Bockor, L., Korac, P., Julg, B., et al. (2016). Repurposing the CRISPR-Cas9 system for targeted DNA methylation. Nucleic Acids Res. 44, 5615–5628. doi: 10.1093/nar/gkw159

Volk, A. E., Weishaupt, J. H., Andersen, P. M., Ludolph, A. C., and Kubisch, C. (2018). Current knowledge and recent insights into the genetic basis of amyotrophic lateral sclerosis. Med. Genet. 30, 252–258. doi: 10.1007/ s11825-018-0185-3

Volkow, N. D., Gur, R. C., Wang, G. J., Fowler, J. S., Moberg, P. J., Ding, Y. S., et al. (1998). Association between decline in brain dopamine activity with age and cognitive and motor impairment in healthy individuals. Am. J. Psychiatry 155, 344–349. doi: 10.1176/ajp.155.3.344

Volterra, A., Liaudet, N., and Savtchouk, I. (2014). Astrocyte Ca2+ signalling: An unexpected complexity. Nat. Rev. Neurosci. 15, 327–335. doi: 10.1038/nrn3725 von Kobbe, C. (2019). Targeting senescent cells: approaches, opportunities, challenges. Aging 11, 12844–12861. doi: 10.18632/aging.102557

Vu, L., An, J., Kovalik, T., Gendron, T., Petrucelli, L., and Bowser, R. (2020). Cross-sectional and longitudinal measures of chitinase proteins in amyotrophic lateral sclerosis and expression of CHI3L1 in activated astrocytes. J. Neurol. Neurosurg. Psychiatry 91, 350–358. doi: 10.1136/jnnp-2019-321916

Wahis, J., and Holt, M. G. (2021). Astrocytes, noradrenaline, α1-adrenoreceptors, and neuromodulation: evidence and unanswered questions. Front. Cell. Neurosci. 15:645691. doi: 10.3389/fncel.2021.645691

Walker, L. C. (2020). Aβ Plaques. Free Neuropathol. 1:31. doi: 10.17879/ freeneuropathology-2020-3025

Wang, J. C., Ramaswami, G., and Geschwind, D. H. (2021). Gene co-expression network analysis in human spinal cord highlights mechanisms underlying amyotrophic lateral sclerosis susceptibility. Sci. Rep. 11:5748. doi: 10.1038/ s41598-021-85061-4

Wang, P., and Ye, Y. (2021). Filamentous recombinant human tau activates primary astrocytes via an integrin receptor complex. Nat. Commun. 12:95. doi: 10.1038/s41467-020-20322-w

Waters, S., Swanson, M. E. V., Dieriks, B. V., Zhang, Y. B., Grimsey, N. L., Murray, H. C., et al. (2021). Blood- spinal cord barrier leakage is independent of motor neuron pathology in ALS. Acta Neuropathol. Commun. 9:144. doi: 10.1186/s40478-021-01244-0

Weinshenker, D. (2018). Long road to ruin: noradrenergic dysfunction in neurodegenerative disease. Trends Neurosci. 41, 211–223. doi: 10.1016/j. tins.2018.01.010

Wheeler, M. A., Clark, I. C., Tjon, E. C., Li, Z., Zandee, S. E. J., Couturier, C. P., et al. (2020). MAFG-driven astrocytes promote CNS inflammation. Nature 578, 593–599. doi: 10.1038/s41586-020-1999-0

Wu, T., Dejanovic, B., Gandham, V. D., Gogineni, A., Edmonds, R., Schauer, S., et al. (2019). Complement C3 is activated in human AD brain and is required for neurodegeneration in mouse models of amyloidosis and tauopathy. Cell Rep. 28, 2111–2123.e6. doi: 10.1016/j.celrep.2019.07.060

Xin, W., Schuebel, K. E., Jair, K. W., Cimbro, R., De Biase, L. M., Goldman, D., et al. (2019). Ventral midbrain astrocytes display unique physiological features and sensitivity to dopamine D2 receptor signaling. Neuropsychopharmacology 44, 344–355. doi: 10.1038/s41386-018-0151-4

Xu, X., Shen, X., Wang, J., Feng, W., Wang, M., Miao, X., et al. (2021). YAP prevents premature senescence of astrocytes and cognitive decline of Alzheimer's disease through regulating CDK6 signaling. Aging Cell 20:e13465. doi: 10.1111/ acel.13465

Yao, S., He, Z., and Chen, C. (2015). CRISPR/Cas9-mediated genome editing of epigenetic factors for cancer therapy. Hum. Gene Ther. 26, 463–471. doi: 10.1089/hum.2015.067

Yu, H. M., Zhao, Y. M., Luo, X. G., Feng, Y., Ren, Y., Shang, H., et al. (2012). Repeated lipopolysaccharide stimulation induces cellular senescence in BV2 cells. Neuroimmunomodulation 19, 131–136. doi: 10.1159/000330254

Zamanian, J. L., Xu, L., Foo, L. C., Nouri, N., Zhou, L., Giffard, R. G., et al. (2012). Genomic analysis of reactive astrogliosis. J. Neurosci. 32, 6391–6410. doi: 10.1523/JNEUROSCI.6221-11.2012

Zanetti, O., Pasqualetti, P., Bonomini, C., Forno, G. D., Paulon, L., Sinforiani, E., et al. (2009). A randomized controlled study on effects of ibuprofen on cognitive progression of Alzheimer's disease. Aging Clin. Exp. Res. 21, 102–110. doi: 10.1007/BF03325217

Zhang, P., Kishimoto, Y., Grammatikakis, I., Gottimukkala, K., Cutler, R. G., Zhang, S., et al. (2019). Senolytic therapy alleviates Aβ-associated oligodendrocyte progenitor cell senescence and cognitive deficits in an Alzheimer's disease model. Nat. Neurosci. 22, 719–728. doi: 10.1038/ s41593-019-0372-9

Zhao, C., Devlin, A. C., Chouhan, A. K., Selvaraj, B. T., Stavrou, M., Burr, K., et al. (2020). Mutant C9orf72 human iPSC-derived astrocytes cause non-cell autonomous motor neuron pathophysiology. Glia 68, 1046– 1064. doi: 10.1002/ glia.23761

Zhou, Y., Song, W. M., Andhey, P. S., Swain, A., Levy, T., Miller, K. R., et al. (2020b). Human and mouse single-nucleus transcriptomics reveal TREM2-dependent and TREM2-independent cellular responses in Alzheimer's disease. Nat. Med. 26, 131–142. doi: 10.1038/s41591-019-0695-9

Zhou, H., Wang, Y., You, Q., and Jiang, Z. (2020a). Recent progress in the development of small molecule Nrf2 activators: a patent review (2017-present). Expert Opin. Ther. Pat. 30, 209–225. doi: 10.1080/13543776.2020.1715365

Zhu, Y., Tchkonia, T., Fuhrmann-Stroissnigg, H., Dai, H. M., Ling, Y. Y., Stout, M. B., et al. (2016). Identification of a novel senolytic agent, navitoclax, targeting the Bcl-2 family of anti-apoptotic factors. Aging Cell 15, 428–435. doi: 10.1111/acel.12445

Part IX: Annex of original publications

1. Supplementary data of Manuscript I

1.1. Figure 1 – Quantification data – all markers

Table 10: Statistical analysis of HALO quantification for GFAP, ALDH1L1 and AQP4 in healthy brains.

marker	group1	group2	p	p.adj	p.signif	method	n1	mean1	median1	n2	mean2	median2
GFAP	CA1/CA2	SUBICULUM	0.65	1.00	ns	Wilcoxon	8	56.81	56.71	8	52.52	48.96
GFAP	CA3	CA1/CA2	0.23	1.00	ns	Wilcoxon	8	69.49	74.47	8	56.81	56.71
GFAP	CA3	SUBICULUM	0.08	1.00	ns	Wilcoxon	8	69.49	74.47	8	52.52	48.96
GFAP	CA4	CA1/CA2	0.16	1.00	ns	Wilcoxon	8	71.48	72.26	8	56.81	56.71
GFAP	CA4	CA3	0.96	1.00	ns	Wilcoxon	8	71.48	72.26	8	69.49	74.47
GFAP	CA4	SUBICULUM	0.10	1.00	ns	Wilcoxon	8	71.48	72.26	8	52.52	48.96
GFAP	DG	CA1/CA2	0.33	1.00	ns	Wilcoxon	8	65.28	71.27	8	56.81	56.71
GFAP	DG	CA3	0.57	1.00	ns	Wilcoxon	8	65.28	71.27	8	69.49	74.47
GFAP	DG	CA4	0.57	1.00	ns	Wilcoxon	8	65.28	71.27	8	71.48	72.26
GFAP	DG	SUBICULUM	0.19	1.00	ns	Wilcoxon	8	65.28	71.27	8	52.52	48.96
ALDH1L1	CA1/CA2	SUBICULUM	0.72	1.00	ns	Wilcoxon	8	70.92	78.07	8	74.35	76.38
ALDH1L1	CA3	CA1/CA2	0.80	1.00	ns	Wilcoxon	8	73.97	73.47	8	70.92	78.07
ALDH1L1	CA3	SUBICULUM	0.88	1.00	ns	Wilcoxon	8	73.97	73.47	8	74.35	76.38
ALDH1L1	CA4	CA1/CA2	0.51	1.00	ns	Wilcoxon	8	77.76	79.32	8	70.92	78.07
ALDH1L1	CA4	CA3	0.57	1.00	ns	Wilcoxon	8	77.76	79.32	8	73.97	73.47
ALDH1L1	CA4	SUBICULUM	0.65	1.00	ns	Wilcoxon	8	77.76	79.32	8	74.35	76.38
ALDH1L1	DG	CA1/CA2	0.38	1.00	ns	Wilcoxon	8	78.93	80.06	8	70.92	78.07
ALDH1L1	DG	CA3	0.44	1.00	ns	Wilcoxon	8	78.93	80.06	8	73.97	73.47
ALDH1L1	DG	CA4	0.96	1.00	ns	Wilcoxon	8	78.93	80.06	8	77.76	79.32
ALDH1L1	DG	SUBICULUM	0.51	1.00	ns	Wilcoxon	8	78.93	80.06	8	74.35	76.38
AQP4	CA1/CA2	SUBICULUM	0.12	1.00	ns	Wilcoxon	8	73.69	70.98	7	86.18	87.76
AQP4	CA3	CA1/CA2	0.13	1.00	ns	Wilcoxon	8	87.48	89.40	8	73.69	70.98
AQP4	CA3	SUBICULUM	0.54	1.00	ns	Wilcoxon	8	87.48	89.40	7	86.18	87.76
AQP4	CA4	CA1/CA2	0.01	0.20	**	Wilcoxon	8	95.95	97.36	8	73.69	70.98
AQP4	CA4	CA3	0.03	0.73	*	Wilcoxon	8	95.95	97.36	8	87.48	89.40
AQP4	CA4	SUBICULUM	0.00	0.06	**	Wilcoxon	8	95.95	97.36	7	86.18	87.76
AQP4	DG	CA1/CA2	0.01	0.40	*	Wilcoxon	8	94.11	94.54	8	73.69	70.98
AQP4	DG	CA3	0.10	1.00	ns	Wilcoxon	8	94.11	94.54	8	87.48	89.40
AQP4	DG	CA4	0.19	1.00	ns	Wilcoxon	8	94.11	94.54	8	95.95	97.36
AQP4	DG	SUBICULUM	0.00	0.11	**	Wilcoxon	8	94.11	94.54	7	86.18	87.76

1.2. Figure 2 – Quantification data

Table 11: Statistical analysis of HALO quantification for GPC5 in healthy brains.

marker	group1	group2	p	p.adj	p.signif	method	n1	mean1	median1	n2	mean2	median2
GPC5	CA1/CA2	SUBICULUM	0.51	1.00	ns	Wilcoxon	8	1,54	1,63	8	1,08	1,15
GPC5	CA3	CA1/CA2	0.80	1.00	ns	Wilcoxon	8	1,62	0.86	8	1,54	1,63
GPC5	CA3	SUBICULUM	0.96	1.00	ns	Wilcoxon	8	1,62	0.86	8	1,08	1,15
GPC5	CA4	CA1/CA2	0.16	1.00	ns	Wilcoxon	8	0.69	0.53	8	1,54	1,63
GPC5	CA4	CA3	0.38	1.00	ns	Wilcoxon	8	0.69	0.53	8	1,62	0.86
GPC5	CA4	SUBICULUM	0.38	1.00	ns	Wilcoxon	8	0.69	0.53	8	1,08	1,15
GPC5	DG	CA1/CA2	0.44	1.00	ns	Wilcoxon	8	5,56	1,72	8	1,54	1,63
GPC5	DG	CA3	0.16	1.00	ns	Wilcoxon	8	5,56	1,72	8	1,62	0.86
GPC5	DG	CA4	0.04	0.38	*	Wilcoxon	8	5,56	1,72	8	0.69	0.53
GPC5	DG	SUBICULUM	0.16	1.00	ns	Wilcoxon	8	5,56	1,72	8	1,08	1,15

1.3. Figure 4 – Quantification data – GFAP

Table 12: Statistical analysis of HALO quantification for GFAP in disease conditions.

Analysis.region	group1	group2	p	p.adj	p.signif	method	n1	mean1	median1	n2	mean2	median2
DG	AD	PDD	0.00	0.05	**	Wilcoxon	9	38.95	40.74	11	60.87	57.97
DG	CTL	AD	0.01	0.16	*	Wilcoxon	8	65.28	71.27	9	38.95	40.74
DG	CTL	PDD	0.35	1.00	ns	Wilcoxon	8	65.28	71.27	11	60.87	57.97
CA4	AD	PDD	0.00	0.00	***	Wilcoxon	9	50.38	57.33	11	77.44	78.15
CA4	CTL	AD	0.03	0.36	*	Wilcoxon	8	71.48	72.26	9	50.38	57.33
CA4	CTL	PDD	0.35	1.00	ns	Wilcoxon	8	71.48	72.26	11	77.44	78.15
CA3	AD	PDD	0.00	0.04	**	Wilcoxon	9	46.26	47.50	11	71.83	73.52
CA3	CTL	AD	0.01	0.08	**	Wilcoxon	8	69.49	74.47	9	46.26	47.50
CA3	CTL	PDD	0.90	1.00	ns	Wilcoxon	8	69.49	74.47	11	71.83	73.52
CA1/CA2	AD	PDD	0.94	1.00	ns	Wilcoxon	9	39.97	43.59	11	40.27	40.95
CA1/CA2	CTL	AD	0.07	0.82	ns	Wilcoxon	8	56.81	56.71	9	39.97	43.59
CA1/CA2	CTL	PDD	0.04	0.49	*	Wilcoxon	8	56.81	56.71	11	40.27	40.95
SUBICULUM	AD	PDD	0.37	1.00	ns	Wilcoxon	9	44.98	48.24	11	47.82	50.71
SUBICULUM	CTL	AD	0.61	1.00	ns	Wilcoxon	8	52.52	48.96	9	44.98	48.24
SUBICULUM	CTL	PDD	0.90	1.00	ns	Wilcoxon	8	52.52	48.96	11	47.82	50.71
PHC	AD	PDD	0.10	0.95	ns	Wilcoxon	9	39.19	33.43	11	53.91	55.38
PHC	CTL	AD	0.17	1.00	ns	Wilcoxon	8	57.47	55.35	9	39.19	33.43
PHC	CTL	PDD	0.84	1.00	ns	Wilcoxon	8	57.47	55.35	11	53.91	55.38

1.4. Figure 4 – Quantification data – AQP4

Table 13: Statistical analysis of HALO quantification for AQP4 in disease conditions.

Analysis.region	group1	group2	p	p.adj	p.signif	method	n1	mean1	median1	n2	mean2	median2
DG	AD	PDD	0.07	0.65	ns	Wilcoxon	9	94.80	95.36	10	91.67	91.62
DG	CTL	AD	0.61	1.00	ns	Wilcoxon	8	94.11	94.54	9	94.80	95.36
DG	CTL	PDD	0.24	1.00	ns	Wilcoxon	8	94.11	94.54	10	91.67	91.62
CA4	AD	PDD	0.00	0.06	**	Wilcoxon	9	96.88	96.69	10	91.97	94.25
CA4	CTL	AD	0.96	1.00	ns	Wilcoxon	8	95.95	97.36	9	96.88	96.69
CA4	CTL	PDD	0.03	0.29	*	Wilcoxon	8	95.95	97.36	10	91.97	94.25
CA3	AD	PDD	0.00	0.02	***	Wilcoxon	9	96.11	96.56	10	86.56	91.73
CA3	CTL	AD	0.02	0.20	*	Wilcoxon	8	87.48	89.40	9	96.11	96.56
CA3	CTL	PDD	0.97	1.00	ns	Wilcoxon	8	87.48	89.40	10	86.56	91.73
CA1/CA2	AD	PDD	0.00	0.02	**	Wilcoxon	9	92.08	92.66	10	62.32	59.58
CA1/CA2	CTL	AD	0.02	0.20	*	Wilcoxon	8	73.69	70.98	9	92.08	92.66
CA1/CA2	CTL	PDD	0.32	1.00	ns	Wilcoxon	8	73.69	70.98	10	62.32	59.58
SUBICULUM	AD	PDD	0.00	0.03	**	Wilcoxon	9	93.58	93.52	10	70.73	76.30
SUBICULUM	CTL	AD	0.00	0.03	**	Wilcoxon	7	86.18	87.76	9	93.58	93.52
SUBICULUM	CTL	PDD	0.36	1.00	ns	Wilcoxon	7	86.18	87.76	10	70.73	76.30
PHC	AD	PDD	0.40	1.00	ns	Wilcoxon	9	91.68	92.28	10	78.42	81.67
PHC	CTL	AD	0.09	0.83	ns	Wilcoxon	8	84.09	89.47	9	91.68	92.28
PHC	CTL	PDD	0.97	1.00	ns	Wilcoxon	8	84.09	89.47	10	78.42	81.67

1.5. Figure 4 – Quantification data – ALDH1L1

Table 14: Statistical analysis of HALO quantification for ALDH1L1 in disease conditions.

Analysis.region	group1	group2	p	p.adj	p.signif	method	n1	mean1	median1	n2	mean2	median2
DG	AD	PDD	0.66	1.00	ns	Wilcoxon	9	42.63	41.40	10	50.48	55.05
DG	CTL	AD	0.01	0.08	**	Wilcoxon	8	78.93	80.06	9	42.63	41.40
DG	CTL	PDD	0.00	0.05	**	Wilcoxon	8	78.93	80.06	10	50.48	55.05
CA4	AD	PDD	0.78	1.00	ns	Wilcoxon	9	37.34	33.27	10	43.11	45.23
CA4	CTL	AD	0.01	0.08	**	Wilcoxon	8	77.76	79.32	9	37.34	33.27
CA4	CTL	PDD	0.00	0.02	**	Wilcoxon	8	77.76	79.32	10	43.11	45.23
CA3	AD	PDD	0.18	1.00	ns	Wilcoxon	9	49.54	53.34	10	37.27	44.16
CA3	CTL	AD	0.04	0.32	*	Wilcoxon	8	73.97	73.47	9	49.54	53.34

CA3	CTL	PDD	0.00	0.02	***	Wilcoxon	8	73.97	73.47	10	37.27	44.16
CA1/CA2	AD	PDD	0.24	1.00	ns	Wilcoxon	9	52.52	60.94	10	44.06	43.46
CA1/CA2	CTL	AD	0.07	0.60	ns	Wilcoxon	8	70.92	78.07	9	52.52	60.94
CA1/CA2	CTL	PDD	0.01	0.13	*	Wilcoxon	8	70.92	78.07	10	44.06	43.46
SUBICULUM	AD	PDD	0.50	1.00	ns	Wilcoxon	9	51.03	54.91	10	46.60	50.34
SUBICULUM	CTL	AD	0.09	0.65	ns	Wilcoxon	8	74.35	76.38	9	51.03	54.91
SUBICULUM	CTL	PDD	0.00	0.03	**	Wilcoxon	8	74.35	76.38	10	46.60	50.34
PHC	AD	PDD	0.72	1.00	ns	Wilcoxon	9	56.96	69.16	10	58.72	60.94
PHC	CTL	AD	0.02	0.21	*	Wilcoxon	8	80.64	84.10	9	56.96	69.16
PHC	CTL	PDD	0.01	0.08	**	Wilcoxon	8	80.64	84.10	10	58.72	60.94

1.6. Figure 4 – Quantification data – ALDH7A1

Table 15: Statistical analysis of HALO quantification for ALDH7A1 in disease conditions.

Analysis.region	group1	group2	p	p.adj	p.signif	method	n1	mean1	median1	n2	mean2	median2
DG	AD	PDD	0.54	1.00	ns	Wilcoxon	9	22,43	21,32	8	20,11	16,51
DG	CTL	AD	0.09	0.83	ns	Wilcoxon	8	39,62	35,19	9	22,43	21,32
DG	CTL	PDD	0.06	0.78	ns	Wilcoxon	8	39,62	35,19	8	20,11	16,51
CA4	AD	PDD	0.81	1.00	ns	Wilcoxon	9	18,93	19,11	8	19,19	15,47
CA4	CTL	AD	0.14	0.97	ns	Wilcoxon	8	41,39	33,22	9	18,93	19,11
CA4	CTL	PDD	0.08	0.83	ns	Wilcoxon	8	41,39	33,22	8	19,19	15,47
CA3	AD	PDD	0.24	1.00	ns	Wilcoxon	9	16,07	12,68	8	11,55	9,51
CA3	CTL	AD	0.11	0.91	ns	Wilcoxon	8	23,45	21,17	9	16,07	12,68
CA3	CTL	PDD	0.01	0.17	*	Wilcoxon	8	23,45	21,17	8	11,55	9,51
CA1/CA2	AD	PDD	0.07	0.82	ns	Wilcoxon	9	18,52	18,03	8	10,10	8,40
CA1/CA2	CTL	AD	0.74	1.00	ns	Wilcoxon	8	20,49	19,25	9	18,52	18,03
CA1/CA2	CTL	PDD	0.05	0.65	*	Wilcoxon	8	20,49	19,25	8	10,10	8,40
SUBICULUM	AD	PDD	0.37	1.00	ns	Wilcoxon	9	13,89	12,92	8	11,24	9,24
SUBICULUM	CTL	AD	0.02	0.29	*	Wilcoxon	8	25,23	22,51	9	13,89	12,92
SUBICULUM	CTL	PDD	0.00	0.08	**	Wilcoxon	8	25,23	22,51	8	11,24	9,24
PHC	AD	PDD	0.96	1.00	ns	Wilcoxon	9	7,73	7,76	8	13,23	6,54
PHC	CTL	AD	0.00	0.00	***	Wilcoxon	8	30,29	26,04	9	7,73	7,76
PHC	CTL	PDD	0.01	0.22	*	Wilcoxon	8	30,29	26,04	8	13,23	6,54

1.7. Figure 4 – Quantification data – GPC5

Table 16: Statistical analysis of HALO quantification for GPC5 in disease conditions.

Analysis.region	group1	group2	p	p.adj	p.signif	method	n1	mean1	median1	n2	mean2	median2
DG	AD	PDD	0.24	1.00	ns	Wilcoxon	9	2,08	0.51	10	6,57	1,63
DG	CTL	AD	0.07	1.00	ns	Wilcoxon	8	5,56	1,72	9	2,08	0.51
DG	CTL	PDD	0.70	1.00	ns	Wilcoxon	8	5,56	1,72	10	6,57	1,63
CA4	AD	PDD	0.66	1.00	ns	Wilcoxon	9	0.43	0.24	10	1,31	0.11
CA4	CTL	AD	0.81	1.00	ns	Wilcoxon	8	0.69	0.53	9	0.43	0.24
CA4	CTL	PDD	0.83	1.00	ns	Wilcoxon	8	0.69	0.53	10	1,31	0.11
CA3	AD	PDD	0.09	1.00	ns	Wilcoxon	9	1,65	0.58	10	0.46	0.21
CA3	CTL	AD	0.89	1.00	ns	Wilcoxon	8	1,62	0.86	9	1,65	0.58
CA3	CTL	PDD	0.27	1.00	ns	Wilcoxon	8	1,62	0.86	10	0.46	0.21
CA1/CA2	AD	PDD	0.45	1.00	ns	Wilcoxon	9	1,23	0.61	10	1,16	0.38
CA1/CA2	CTL	AD	0.67	1.00	ns	Wilcoxon	8	1,54	1,63	9	1,23	0.61
CA1/CA2	CTL	PDD	0.46	1.00	ns	Wilcoxon	8	1,54	1,63	10	1,16	0.38
SUBICULUM	AD	PDD	0.04	0.78	*	Wilcoxon	9	1,14	0.51	10	0.41	0.08
SUBICULUM	CTL	AD	0.89	1.00	ns	Wilcoxon	8	1,08	1,15	9	1,14	0.51
SUBICULUM	CTL	PDD	0.05	0.93	ns	Wilcoxon	8	1,08	1,15	10	0.41	0.08
PHC	AD	PDD	0.55	1.00	ns	Wilcoxon	9	0.86	0.34	10	0.41	0.24
PHC	CTL	AD	0.81	1.00	ns	Wilcoxon	8	0.97	0.26	9	0.86	0.34
PHC	CTL	PDD	0.27	1.00	ns	Wilcoxon	8	0.97	0.26	10	0.41	0.24

1.8. Supplementary Figure 1 – Quantification data

Table 17: Statistical analysis of HALO quantification for GFAP, ALDH1L1, AQP4 and GPC5 in the PHC of healty brains.

Analysis.region	group1	group2	p	p.adj	p.signif	method	n1	mean1	median1	n2	mean2	median2
PHC	ALDH1L1	AQP4	0.51	0.51	ns	Wilcoxon	8	80.64	84.10	8	84.09	89.47
PHC	GFAP	ALDH1L1	0.03	0.08	*	Wilcoxon	8	57.47	55.35	8	80.64	84.10
PHC	GFAP	AQP4	0.03	0.08	*	Wilcoxon	8	57.47	55.35	8	84.09	89.47
PHC	GFAP	GPC5	0.00	0.00	***	Wilcoxon	8	57.47	55.35	8	0.97	0.26
PHC	GPC5	ALDH1L1	0.00	0.00	***	Wilcoxon	8	0.97	0.26	8	80.64	84.10
PHC	GPC5	AQP4	0.00	0.00	***	Wilcoxon	8	0.97	0.26	8	84.09	89.47

2. Supplementary data of Manuscript II

2.1. Figure 4 – Quantification data

Table 18: Statistical analysis of HALO quantification for VMAT2 in disease conditions.

Analysis.region	group1	group2	p	p.adj	p.signif	method	n1	mean1	median1	n2	mean2	median2
DG	AD	PDD	0.47	1.00	ns	Wilcoxon	8	7.40	6.51	14	11.02	9.17
DG	CTL	AD	0.54	1.00	ns	Wilcoxon	7	14.78	15.08	8	7.40	6.51
DG	CTL	PDD	0.79	1.00	ns	Wilcoxon	7	14.78	15.08	14	11.02	9.17
CA4	AD	PDD	0.00	0.07	**	Wilcoxon	8	7.09	2.17	14	22.68	23.00
CA4	CTL	AD	0.61	1.00	ns	Wilcoxon	7	22.11	14.93	8	7.09	2.17
CA4	CTL	PDD	0.53	1.00	ns	Wilcoxon	7	22.11	14.93	14	22.68	23.00
CA3	AD	PDD	0.23	1.00	ns	Wilcoxon	8	13.66	12.90	14	22.73	15.72
CA3	CTL	AD	0.96	1.00	ns	Wilcoxon	7	21.44	13.50	8	13.66	12.90
CA3	CTL	PDD	0.48	1.00	ns	Wilcoxon	7	21.44	13.50	14	22.73	15.72
CA1/CA2	AD	PDD	0.00	0.06	**	Wilcoxon	8	5.63	1.55	14	21.77	23.77
CA1/CA2	CTL	AD	0.40	1.00	ns	Wilcoxon	7	31.63	43.34	8	5.63	1.55
CA1/CA2	CTL	PDD	0.74	1.00	ns	Wilcoxon	7	31.63	43.34	14	21.77	23.77
SUBICULUM	AD	PDD	0.00	0.00	****	Wilcoxon	8	0.63	0.66	13	8.11	2.66
SUBICULUM	CTL	AD	0.09	1.00	ns	Wilcoxon	7	11.63	12.35	8	0.63	0.66
SUBICULUM	CTL	PDD	1.00	1.00	ns	Wilcoxon	7	11.63	12.35	13	8.11	2.66
PHC	AD	PDD	0.00	0.00	****	Wilcoxon	8	0.25	0.22	13	1.71	1.27
PHC	CTL	AD	0.02	0.29	*	Wilcoxon	7	3.13	2.85	8	0.25	0.22
PHC	CTL	PDD	0.76	1.00	ns	Wilcoxon	7	3.13	2.85	13	1.71	1.27

2.2. Figure 5 – Quantification data

Table 19: Statistical analysis of HALO quantification for CBS in disease conditions.

Analysis.region	group1	group2	p	p.adj	p.signif	method	n1	mean1	median1	n2	mean2	median2
DG	AD	PDD	0.78	1.00	ns	Wilcoxon	9	24.61	32.11	10	27.10	19.94
DG	CTL	AD	0.00	0.01	***	Wilcoxon	7	79.05	86.53	9	24.61	32.11
DG	CTL	PDD	0.00	0.01	**	Wilcoxon	7	79.05	86.53	10	27.10	19.94
CA4	AD	PDD	0.90	1.00	ns	Wilcoxon	9	22.85	20.01	10	22.09	14.34
CA4	CTL	AD	0.00	0.01	***	Wilcoxon	7	85.75	92.24	9	22.85	20.01
CA4	CTL	PDD	0.00	0.00	***	Wilcoxon	7	85.75	92.24	10	22.09	14.34
CA3	AD	PDD	0.90	1.00	ns	Wilcoxon	9	26.06	29.38	10	24.72	17.37
CA3	CTL	AD	0.00	0.02	**	Wilcoxon	7	74.10	75.74	9	26.06	29.38
CA3	CTL	PDD	0.00	0.02	**	Wilcoxon	7	74.10	75.74	10	24.72	17.37
CA1/CA2	AD	PDD	0.45	1.00	ns	Wilcoxon	9	18.94	21.08	10	15.52	12.41
CA1/CA2	CTL	AD	0.00	0.01	***	Wilcoxon	7	64.92	76.05	9	18.94	21.08
CA1/CA2	CTL	PDD	0.00	0.01	***	Wilcoxon	7	64.92	76.05	10	15.52	12.41
SUBICULUM	AD	PDD	0.97	1.00	ns	Wilcoxon	9	11.99	16.60	12	15.26	8.02
SUBICULUM	CTL	AD	0.00	0.00	***	Wilcoxon	7	61.16	60.85	9	11.99	16.60
SUBICULUM	CTL	PDD	0.00	0.01	***	Wilcoxon	7	61.16	60.85	12	15.26	8.02
PHC	AD	PDD	0.46	1.00	ns	Wilcoxon	9	3.16	3.09	12	9.75	6.61
PHC	CTL	AD	0.00	0.01	***	Wilcoxon	7	45.48	31.75	9	3.16	3.09
PHC	CTL	PDD	0.01	0.05	**	Wilcoxon	7	45.48	31.75	12	9.75	6.61

2.3. Supplementary Figure 3 – Quantification data – SPARC

Table 20: *Statistical analysis of HALO quantification for SPARC in disease conditions.*

Analysis.region	group1	group2	p	p.adj	p.signif	method	n1	mean1	median1	n2	mean2	median2
DG	AD	PDD	0.42	1.00	ns	Wilcoxon	5	48.02	47.75	5	25.99	21.52
DG	CTL	AD	1.00	1.00	ns	Wilcoxon	3	47.64	46.14	5	48.02	47.75
DG	CTL	PDD	0.25	1.00	ns	Wilcoxon	3	47.64	46.14	5	25.99	21.52
CA4	AD	PDD	0.55	1.00	ns	Wilcoxon	5	53.30	50.85	5	35.11	38.36
CA4	CTL	AD	0.57	1.00	ns	Wilcoxon	3	69.87	66.88	5	53.30	50.85
CA4	CTL	PDD	0.14	1.00	ns	Wilcoxon	3	69.87	66.88	5	35.11	38.36
CA3	AD	PDD	0.10	1.00	ns	Wilcoxon	5	46.26	52.07	5	24.31	24.32
CA3	CTL	AD	0.14	1.00	ns	Wilcoxon	3	66.88	68.04	5	46.26	52.07
CA3	CTL	PDD	0.04	0.61	*	Wilcoxon	3	66.88	68.04	5	24.31	24.32
CA1/CA2	AD	PDD	0.15	1.00	ns	Wilcoxon	5	34.34	30.79	5	13.92	13.81
CA1/CA2	CTL	AD	0.25	1.00	ns	Wilcoxon	3	55.99	53.45	5	34.34	30.79
CA1/CA2	CTL	PDD	0.04	0.61	*	Wilcoxon	3	55.99	53.45	5	13.92	13.81
SUBICULUM	AD	PDD	0.06	0.72	ns	Wilcoxon	5	26.21	30.70	5	7.91	5.95
SUBICULUM	CTL	AD	0.57	1.00	ns	Wilcoxon	3	33.73	33.66	5	26.21	30.70
SUBICULUM	CTL	PDD	0.04	0.61	*	Wilcoxon	3	33.73	33.66	5	7.91	5.95
PHC	AD	PDD	0.03	0.57	*	Wilcoxon	5	14.42	10.79	5	5.59	4.79
PHC	CTL	AD	0.25	1.00	ns	Wilcoxon	3	25.33	31.52	5	14.42	10.79
PHC	CTL	PDD	0.04	0.61	*	Wilcoxon	3	25.33	31.52	5	5.59	4.79

2.4. Supplementary Figure 3 – Quantification data – BACE2

Table 21: *Statistical analysis of HALO quantification for BACE2 in disease conditions.*

Analysis.region	group1	group2	p	p.adj	p.signif	method	n1	mean1	median1	n2	mean2	median2
DG	AD	PDD	0.15	1.00	ns	Wilcoxon	5	0.52	0.15	5	0.60	0.75
DG	CTL	AD	0.79	1.00	ns	Wilcoxon	3	0.12	0.04	5	0.52	0.15
DG	CTL	PDD	0.07	1.00	ns	Wilcoxon	3	0.12	0.04	5	0.60	0.75
CA4	AD	PDD	0.03	0.57	*	Wilcoxon	5	0.08	0.02	5	0.51	0.56
CA4	CTL	AD	1.00	1.00	ns	Wilcoxon	3	0.04	0.04	5	0.08	0.02
CA4	CTL	PDD	0.07	1.00	ns	Wilcoxon	3	0.04	0.04	5	0.51	0.56
CA3	AD	PDD	0.31	1.00	ns	Wilcoxon	5	4,17	3,39	5	1,35	0.69
CA3	CTL	AD	0.25	1.00	ns	Wilcoxon	3	0.76	0.86	5	4,17	3,39
CA3	CTL	PDD	1.00	1.00	ns	Wilcoxon	3	0.76	0.86	5	1,35	0.69
CA1/CA2	AD	PDD	0.15	1.00	ns	Wilcoxon	5	2,91	3,73	5	1,08	0.86
CA1/CA2	CTL	AD	1.00	1.00	ns	Wilcoxon	3	3,79	2,31	5	2,91	3,73
CA1/CA2	CTL	PDD	0.25	1.00	ns	Wilcoxon	3	3,79	2,31	5	1,08	0.86
SUBICULUM	AD	PDD	1.00	1.00	ns	Wilcoxon	5	0.97	1,19	5	0.85	0.59
SUBICULUM	CTL	AD	1.00	1.00	ns	Wilcoxon	3	0.91	0.98	5	0.97	1,19
SUBICULUM	CTL	PDD	1.00	1.00	ns	Wilcoxon	3	0.91	0.98	5	0.85	0.59
PHC	AD	PDD	0.10	1.00	ns	Wilcoxon	5	1,26	0.59	5	2,73	1,91
PHC	CTL	AD	0.79	1.00	ns	Wilcoxon	3	1,79	2,43	5	1,26	0.59
PHC	CTL	PDD	1.00	1.00	ns	Wilcoxon	3	1,79	2,43	5	2,73	1,91

2.5. Supplementary Figure 3 – Quantification data – VIM

Table 22: Statistical analysis of HALO quantification for VIM in disease conditions.

Analysis.region	group1	group2	p	p.adj	p.signif	method	n1	mean1	median1	n2	mean2	median2
DG	AD	PDD	0.69	1.00	ns	Wilcoxon	5	5.29	3.74	5	7.55	5.40
DG	CTL	AD	1.00	1.00	ns	Wilcoxon	3	4.48	3.47	5	5.29	3.74
DG	CTL	PDD	0.57	1.00	ns	Wilcoxon	3	4.48	3.47	5	7.55	5.40
CA4	AD	PDD	0.42	1.00	ns	Wilcoxon	5	3.26	2.45	5	3.86	3.85
CA4	CTL	AD	0.57	1.00	ns	Wilcoxon	3	2.61	2.33	5	3.26	2.45
CA4	CTL	PDD	0.25	1.00	ns	Wilcoxon	3	2.61	2.33	5	3.86	3.85
CA3	AD	PDD	0.55	1.00	ns	Wilcoxon	5	12.36	6.53	5	9.04	4.73
CA3	CTL	AD	1.00	1.00	ns	Wilcoxon	3	19.55	5.74	5	12.36	6.53
CA3	CTL	PDD	0.79	1.00	ns	Wilcoxon	3	19.55	5.74	5	9.04	4.73
CA1/CA2	AD	PDD	0.42	1.00	ns	Wilcoxon	5	14.75	15.69	5	10.84	8.68
CA1/CA2	CTL	AD	1.00	1.00	ns	Wilcoxon	3	19.89	8.44	5	14.75	15.69
CA1/CA2	CTL	PDD	0.79	1.00	ns	Wilcoxon	3	19.89	8.44	5	10.84	8.68
SUBICULUM	AD	PDD	0.84	1.00	ns	Wilcoxon	5	5.75	6.27	5	5.68	5.17
SUBICULUM	CTL	AD	1.00	1.00	ns	Wilcoxon	2	5.25	5.25	5	5.75	6.27
SUBICULUM	CTL	PDD	0.86	1.00	ns	Wilcoxon	2	5.25	5.25	5	5.68	5.17
PHC	AD	PDD	0.55	1.00	ns	Wilcoxon	5	8.20	4.77	5	6.91	6.04
PHC	CTL	AD	0.25	1.00	ns	Wilcoxon	3	13.03	13.03	5	8.20	4.77
PHC	CTL	PDD	0.04	0.64	*	Wilcoxon	3	13.03	13.03	5	6.91	6.04

2.6. Summary RNA-sequencing data NA-/CM-exposed astrocytes compared to non-exposed astrocytes.

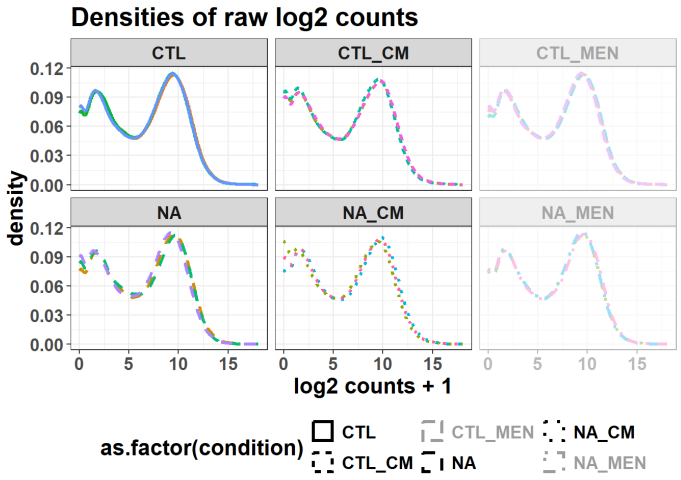

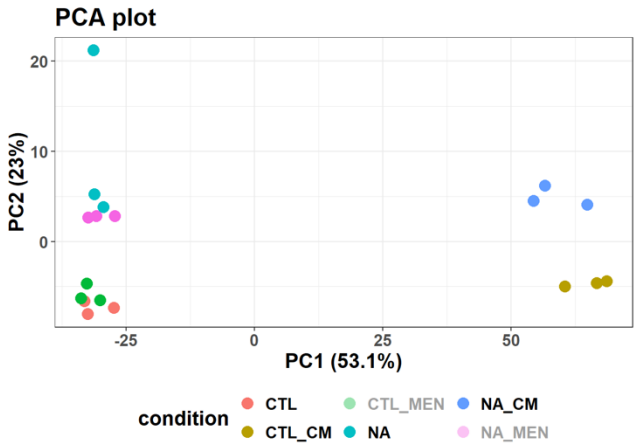

Mean gene expression:

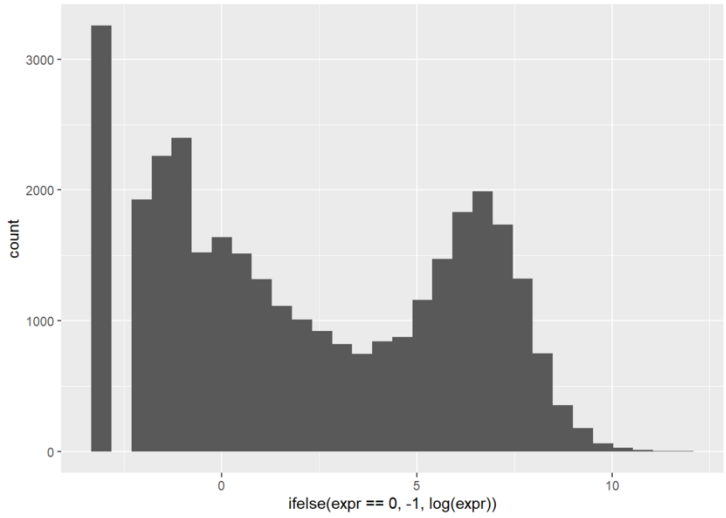

Overview of DESeq2 comparisons

Overview of DESeq2 comparisons

ref	comp	n
CTL	CTL_CM	25361
CTL	CTL_MEN	26095
CTL	NAD	27706
CTL_CM	NAD_CM	22904
CTL_MEN	NAD_MEN	23470
NAD	NAD_CM	25531
NAD	NAD_MEN	26111

Contrast	no. of DEG
CTL_CM_vs_CTL	8263
CTL_MEN_vs_CTL	93
NAD_CM_vs_CTL_CM	1397
NAD_CM_vs_NAD	7296
NAD_MEN_vs_CTL_MEN	905
NAD_MEN_vs_NAD	739
NAD_vs_CTL	2385

Venn diagram of differentially expressed genes

The total number of genes in DESeq2 analysis is 31562.

The total number of genes differentially expressed at least once (FDR < 0.1) is 10803.

Number of differentially expressed genes in the 7 comparisons with FDR < 0.1 and p_value < 0.05

	Comparison							
Reference	CTL	CTL_CM	CTL_MEN	NAD	NAD_CM	NAD_MEN	DA	CM
CTL	0	8263	93	23850	0	0	0	0
CTL_CM	0	0	0	0	1397	0	0	0
CTL_MEN	0	0	0	0	0	905	0	0
NAD	0	0	0	0	7296	739	0	0
NAD_CM	0	0	0	0	0	0	0	0
NAD_MEN	0	0	0	0	0	0	0	0
DA	0	0	0	0	0	0	0	0
CM	0	0	0	0	0	0	0	0

Table 23: Top 100 DEGs in each contrast according to padj.overall.

(NAD= NA)

Ref	Contrast	Mgi_symbol	Log2foldchange	Pvalue	Padj.by_comparison	Padj.overall
CTL	NAD_vs_CTL	Sod3	3,39301403	1,1446E-63	1,803E-59	5,301E-61
CTL	NAD_vs_CTL	Scg2	5,4399094	8,5675E-59	6,7482E-55	3,5311E-56
CTL	NAD_vs_CTL	Npy	-2,4745872	3,686E-37	1,9355E-33	8,2196E-35
CTL	NAD_vs_CTL	Dapk2	3,70947445	1,5519E-24	6,1119E-21	2,0275E-22
CTL	NAD_vs_CTL	Sat1	1,45487963	3,9613E-22	1,248E-18	4,4964E-20
CTL	NAD_vs_CTL	Crem	1,03201988	2,6627E-21	6,991E-18	2,8921E-19
CTL	NAD_vs_CTL	Npffr1	4,14811375	3,5789E-20	8,054E-17	3,6123E-18
CTL	NAD_vs_CTL	S1pr1	1,37639014	7,1971E-20	1,4172E-16	7,1088E-18
CTL	NAD_vs_CTL	Nck2	-0,9691544	7,8124E-19	1,3674E-15	7,2077E-17
CTL	NAD_vs_CTL	Tacr1	2,6218442	1,016E-17	1,6005E-14	8,5424E-16
CTL	NAD_vs_CTL	Cartpt	9,02725622	3,4333E-17	4,9167E-14	2,761E-15
CTL	NAD_vs_CTL	Klhl25	-0,9558294	5,0665E-17	6,6511E-14	4,023E-15
CTL	NAD_vs_CTL	Maff	1,90564016	6,8722E-17	8,3276E-14	5,395E-15
CTL	NAD_vs_CTL	Itpr3	2,05615326	9,0877E-17	1,0226E-13	7,0305E-15
CTL	NAD_vs_CTL	Zswim6	0,84525047	1,7581E-16	1,8463E-13	1,3239E-14
CTL	NAD_vs_CTL	Sik1	2,66717834	1,914E-16	1,8845E-13	1,4358E-14
CTL	NAD_vs_CTL	Trh	4,36848354	6,9921E-16	6,4792E-13	5,0222E-14
CTL	NAD_vs_CTL	Igsf1	-2,0363889	7,6397E-16	6,686E-13	5,445E-14
CTL	NAD_vs_CTL	Ptprn	1,68240502	1,2715E-15	1,0542E-12	8,9109E-14
CTL	NAD_vs_CTL	Ttl	-0,7561391	1,5216E-15	1,1985E-12	1,0573E-13
CTL	NAD_vs_CTL	Arntl	-1,6965532	1,7191E-15	1,2895E-12	1,1891E-13
CTL	NAD_vs_CTL	Nr4a3	1,81204166	2,0289E-15	1,4528E-12	1,3902E-13
CTL	NAD_vs_CTL	Per1	0,9194199	2,2097E-15	1,5024E-12	1,5081E-13
CTL	NAD_vs_CTL	Pcyox1l	0,77234472	2,2889E-15	1,5024E-12	1,5599E-13
CTL	NAD_vs_CTL	Slc6a17	1,19671591	3,8896E-15	2,4509E-12	2,5834E-13
CTL	NAD_vs_CTL	Ace	-2,2434294	4,8295E-15	2,9261E-12	3,1711E-13
CTL	NAD_vs_CTL	Tmem41a	2,0864472	5,6328E-15	3,2864E-12	3,6673E-13
CTL	NAD_vs_CTL	Pde4d	2,6103938	6,704E-15	3,7717E-12	4,3443E-13
CTL	NAD_vs_CTL	Ap1s3	2,54199336	6,981E-15	3,7921E-12	4,5153E-13
CTL	NAD_vs_CTL	Ace2	-1,9180123	5,0882E-14	2,6718E-11	3,0228E-12
CTL	NAD_vs_CTL	Ciart	1,52095909	5,6307E-14	2,8613E-11	3,3322E-12
CTL	NAD_vs_CTL	Syt1	-1,4478653	8,0849E-14	3,9801E-11	4,7102E-12
CTL	NAD_vs_CTL	Procr	1,54896987	1,2875E-13	6,1462E-11	7,3133E-12
CTL	NAD_vs_CTL	Pea15a	-0,9187842	1,435E-13	6,6486E-11	8,1274E-12
CTL	NAD_vs_CTL	Igsf9b	-1,4998229	2,3514E-13	1,0583E-10	1,3046E-11
CTL	NAD_vs_CTL	Avpi1	1,49236905	2,4881E-13	1,0888E-10	1,3755E-11
CTL	NAD_vs_CTL	Tcim	2,65549519	3,2517E-13	1,3844E-10	1,7777E-11
CTL	NAD_vs_CTL	Tcerg1l	-2,3179998	5,4291E-13	2,2507E-10	2,8883E-11
CTL	NAD_vs_CTL	Arid5a	1,17056639	1,937E-12	7,824E-10	9,7755E-11

CTL	NAD_vs_CTL	Camk4	-2,6658832	2,5077E-12	9,8761E-10	1,2487E-10
CTL	NAD_vs_CTL	Srl	-1,2273335	3,5754E-12	1,3737E-09	1,7397E-10
CTL	NAD_vs_CTL	Net1	1,25476975	1,3725E-11	5,1477E-09	6,2872E-10
CTL	NAD_vs_CTL	Hdc	-2,0766359	2,9682E-11	1,0874E-08	1,3049E-09
CTL	NAD_vs_CTL	Snta1	-0,5588213	4,2078E-11	1,5065E-08	1,8068E-09
CTL	NAD_vs_CTL	Vamp1	0,73285708	1,1986E-10	4,196E-08	4,8563E-09
CTL	NAD_vs_CTL	Nkain2	-2,7907611	2,223E-10	7,613E-08	8,6889E-09
CTL	NAD_vs_CTL	Atp6ap2	0,42770884	2,656E-10	8,9022E-08	1,0277E-08
CTL	NAD_vs_CTL	Sh3bp5	-1,0525093	4,2383E-10	1,391E-07	1,6028E-08
CTL	NAD_vs_CTL	Jade1	0,74703179	6,1977E-10	1,992E-07	2,2924E-08
CTL	NAD_vs_CTL	Crabp2	1,96189923	6,3226E-10	1,992E-07	2,3354E-08
CTL	NAD_vs_CTL	Rnf122	1,37204515	6,6924E-10	2,0672E-07	2,4648E-08
CTL	NAD_vs_CTL	Slc22a17	-0,6442929	8,3458E-10	2,5283E-07	3,0271E-08
CTL	NAD_vs_CTL	Osr1	-1,1037263	9,5625E-10	2,8422E-07	3,4369E-08
CTL	NAD_vs_CTL	Habp4	-0,522213	1,1745E-09	3,4263E-07	4,1673E-08
CTL	NAD_vs_CTL	Tubb4b	-0,5807446	1,2174E-09	3,487E-07	4,3129E-08
CTL	NAD_vs_CTL	Calca	2,39124762	1,2521E-09	3,5221E-07	4,4254E-08
CTL	NAD_vs_CTL	Hspa4l	-0,3628781	1,4928E-09	4,1256E-07	5,2137E-08
CTL	NAD_vs_CTL	Slco1c1	2,36449346	1,767E-09	4,7992E-07	6,1189E-08
CTL	NAD_vs_CTL	Adap1	-0,7238539	1,9381E-09	5,1748E-07	6,6615E-08
CTL	NAD_vs_CTL	Ankrd40	-0,5895781	2,3829E-09	6,2564E-07	8,092E-08
CTL	NAD_vs_CTL	Acp5	1,60790063	3,1439E-09	8,0225E-07	1,0488E-07
CTL	NAD_vs_CTL	Fam167a	0,63093702	3,2075E-09	8,0225E-07	1,0687E-07
CTL	NAD_vs_CTL	Gm10635	-2,4484046	3,2408E-09	8,0225E-07	1,0791E-07
CTL	NAD_vs_CTL	Mest	1,61107943	3,2593E-09	8,0225E-07	1,0847E-07
CTL	NAD_vs_CTL	Mgst1	0,63106981	3,4184E-09	8,2847E-07	1,1355E-07
CTL	NAD_vs_CTL	Erc2	-1,7428587	3,5278E-09	8,4202E-07	1,1693E-07
CTL	NAD_vs_CTL	Chgb	2,05490324	3,6788E-09	8,6496E-07	1,215E-07
CTL	NAD_vs_CTL	Ifi27l2a	1,64859841	4,5089E-09	1,0445E-06	1,4692E-07
CTL	NAD_vs_CTL	Tfcp2l1	-1,4945995	4,8263E-09	1,1019E-06	1,5645E-07
CTL	NAD_vs_CTL	Nrg2	-1,152936	5,6031E-09	1,2609E-06	1,8041E-07
CTL	NAD_vs_CTL	Ldhd	1,10555307	5,9082E-09	1,3109E-06	1,8983E-07
CTL	NAD_vs_CTL	Sugct	-1,422212	5,9994E-09	1,3126E-06	1,9258E-07
CTL	NAD_vs_CTL	Psd2	-0,9520328	6,7673E-09	1,4604E-06	2,1573E-07
CTL	NAD_vs_CTL	Cmya5	-2,383231	6,9907E-09	1,4882E-06	2,225E-07
CTL	NAD_vs_CTL	Nr4a1	2,66514843	7,3192E-09	1,5373E-06	2,3205E-07
CTL	NAD_vs_CTL	Pde4b	1,11579912	7,4881E-09	1,5521E-06	2,3707E-07
CTL	NAD_vs_CTL	Tbcel	-0,309829	7,9625E-09	1,629E-06	2,5146E-07
CTL	NAD_vs_CTL	Scap	-0,5247261	1,0007E-08	2,0211E-06	3,1114E-07
CTL	NAD_vs_CTL	Il11	3,25193514	1,0351E-08	2,0641E-06	3,2114E-07
CTL	NAD_vs_CTL	Plekhf1	-0,6411019	1,0998E-08	2,1656E-06	3,3958E-07
CTL	NAD_vs_CTL	Mark3	-0,3261497	1,1268E-08	2,1915E-06	3,4716E-07
CTL	NAD_vs_CTL	Mmp28	0,70672514	1,2234E-08	2,3503E-06	3,7481E-07

CTL	NAD_vs_CTL	Wwox	-1,2705339	1,2865E-08	2,4417E-06	3,9336E-07
CTL	NAD_vs_CTL	Fhit	-2,8303251	1,5024E-08	2,8176E-06	4,5398E-07
CTL	NAD_vs_CTL	Bcan	-1,2575878	1,5769E-08	2,9225E-06	4,7499E-07
CTL	NAD_vs_CTL	Slc31a2	0,66879809	1,6516E-08	3,0254E-06	4,9614E-07
CTL	NAD_vs_CTL	Rit2	-3,3421487	1,7835E-08	3,2294E-06	5,3264E-07
CTL	NAD_vs_CTL	Dio2	2,83064298	1,8557E-08	3,322E-06	5,5253E-07
CTL	NAD_vs_CTL	Ttc39c	1,20937862	2,0026E-08	3,5446E-06	5,927E-07
CTL	NAD_vs_CTL	Timp2	-0,6113965	2,0365E-08	3,5607E-06	6,0208E-07
CTL	NAD_vs_CTL	Usp40	0,4168766	2,0569E-08	3,5607E-06	6,0773E-07
CTL	NAD_vs_CTL	Cdk6	-1,0413126	2,0873E-08	3,5741E-06	6,1592E-07
CTL	NAD_vs_CTL	Fmod	-1,7339651	2,257E-08	3,8231E-06	6,6162E-07
CTL	NAD_vs_CTL	Bhlhe40	0,83134245	2,2948E-08	3,8457E-06	6,7213E-07
CTL	NAD_vs_CTL	Anxa5	-0,7543103	2,4363E-08	4,0399E-06	7,1102E-07
CTL	NAD_vs_CTL	Nr4a2	1,55844902	2,4873E-08	4,0815E-06	7,2546E-07
CTL	NAD_vs_CTL	Bbip1	-0,4394485	2,7297E-08	4,4331E-06	7,9131E-07
CTL	NAD_vs_CTL	G6pdx	0,77646298	2,8157E-08	4,5262E-06	8,1421E-07
CTL	NAD_vs_CTL	Coq10b	0,76691271	2,9677E-08	4,7223E-06	8,5477E-07

Ref	Contrast	Mgi_symbol	Log2foldchange	Pvalue	Padj.by_comparison	Padj.overall
CTL	CTL_CM_vs_CTL	Tap2	3,89885814	-inf	-inf	-inf
CTL	CTL_CM_vs_CTL	Gbp2	5,65035494	-inf	-inf	-inf
CTL	CTL_CM_vs_CTL	Wars	4,09792223	-inf	-inf	-inf
CTL	CTL_CM_vs_CTL	Irgm1	6,11325864	-inf	-inf	-inf
CTL	CTL_CM_vs_CTL	Gbp6	7,74782057	-inf	-inf	-inf
CTL	CTL_CM_vs_CTL	H2-Q4	5,51105076	-inf	-inf	-inf
CTL	CTL_CM_vs_CTL	Igtp	7,55288133	-inf	-inf	-inf
CTL	CTL_CM_vs_CTL	Tap1	4,92730765	-inf	-inf	-inf
CTL	CTL_CM_vs_CTL	Irf1	5,90086026	-inf	-inf	-inf
CTL	CTL_CM_vs_CTL	Psme1	3,38991606	-inf	-inf	-inf
CTL	CTL_CM_vs_CTL	Gbp10	8,95687018	5,201E-298	1,018E-294	4,001E-294
CTL	CTL_CM_vs_CTL	Nlrc5	6,06414265	1,718E-294	3,081E-291	1,19E-290
CTL	CTL_CM_vs_CTL	Gbp11	9,21923346	1,867E-293	3,091E-290	1,231E-289
CTL	CTL_CM_vs_CTL	Cd274	6,37624393	3,604E-293	5,54E-290	2,268E-289
CTL	CTL_CM_vs_CTL	Tapbp	3,72959193	5,394E-278	7,739E-275	3,112E-274
CTL	CTL_CM_vs_CTL	Gbp7	5,37625454	5,584E-271	7,512E-268	3,093E-267
CTL	CTL_CM_vs_CTL	Psmb10	4,77890171	4,356E-264	5,515E-261	2,154E-260
CTL	CTL_CM_vs_CTL	Cd74	9,97987509	3,039E-258	3,634E-255	1,275E-254
CTL	CTL_CM_vs_CTL	H2-Ab1	7,84976639	3,748E-258	4,246E-255	1,527E-254
CTL	CTL_CM_vs_CTL	Irgm2	6,56168474	9,294E-242	1E-238	3,478E-238
CTL	CTL_CM_vs_CTL	Ly6e	5,23945838	2,078E-238	2,13E-235	7,378E-235
CTL	CTL_CM_vs_CTL	B2m	4,25772485	5,411E-236	5,293E-233	1,873E-232
CTL	CTL_CM_vs_CTL	Ifi204	6,44978437	4,686E-228	4,385E-225	1,509E-224
CTL	CTL_CM_vs_CTL	Parp12	3,45646867	1,611E-225	1,445E-222	5,071E-222
CTL	CTL_CM_vs_CTL	Psmb8	5,81166972	1,311E-223	1,129E-220	3,947E-220
CTL	CTL_CM_vs_CTL	Ifit3	4,54146724	1,375E-222	1,139E-219	4,053E-219
CTL	CTL_CM_vs_CTL	Dtx3l	4,23511632	1,73E-215	1,379E-212	4,99E-212
CTL	CTL_CM_vs_CTL	Ciita	7,38122458	1,097E-187	8,434E-185	2,814E-184
CTL	CTL_CM_vs_CTL	H2-K1	4,47192893	1,11E-180	8,241E-178	2,698E-177
CTL	CTL_CM_vs_CTL	Irf8	7,67853581	5,177E-177	3,714E-174	1,236E-173
CTL	CTL_CM_vs_CTL	Tapbpl	3,79918195	3,328E-174	2,311E-171	7,681E-171
CTL	CTL_CM_vs_CTL	Snx10	2,80263139	1,63E-172	1,096E-169	3,701E-169
CTL	CTL_CM_vs_CTL	Gbp3	5,74732689	6,265E-167	4,086E-164	1,377E-163
CTL	CTL_CM_vs_CTL	Kars	1,85536542	2,563E-164	1,623E-161	5,461E-161
CTL	CTL_CM_vs_CTL	Gbp9	5,50128949	7,331E-164	4,508E-161	1,538E-160
CTL	CTL_CM_vs_CTL	Nampt	2,61220374	6,007E-163	3,592E-160	1,242E-159
CTL	CTL_CM_vs_CTL	Psmb9	5,70814968	1,285E-161	7,476E-159	2,617E-158
CTL	CTL_CM_vs_CTL	Trim21	3,29244587	1,642E-161	9,301E-159	3,296E-158
CTL	CTL_CM_vs_CTL	Vcam1	5,48419522	9,146E-161	5,048E-158	1,809E-157
CTL	CTL_CM_vs_CTL	Psme2	3,13052635	3,954E-156	2,127E-153	7,604E-153
CTL	CTL_CM_vs_CTL	Dhx58	5,65645301	1,874E-154	9,839E-152	3,556E-151
CTL	CTL_CM_vs_CTL	Slfn8	8,35009769	1,705E-153	8,736E-151	3,19E-150

CTL	CTL_CM_vs_CTL	Il18bp	6,04643567	2,048E-152	1,025E-149	3,781E-149
CTL	CTL_CM_vs_CTL	Asap3	3,1574632	4,016E-152	1,964E-149	7,129E-149
CTL	CTL_CM_vs_CTL	Gm4841	10,8880891	1,992E-151	9,527E-149	3,492E-148
CTL	CTL_CM_vs_CTL	Trafd1	2,54319613	9,003E-148	4,212E-145	1,52E-144
CTL	CTL_CM_vs_CTL	Iigp1	9,68755806	3,459E-145	1,584E-142	5,703E-142
CTL	CTL_CM_vs_CTL	H2-Aa	8,4700753	4,899E-144	2,197E-141	7,888E-141
CTL	CTL_CM_vs_CTL	Parp9	4,06132442	9,111E-142	4,002E-139	1,434E-138
CTL	CTL_CM_vs_CTL	H2-Q6	6,63975426	7,731E-140	3,328E-137	1,164E-136
CTL	CTL_CM_vs_CTL	Parp14	5,66128388	1,492E-139	6,298E-137	2,222E-136
CTL	CTL_CM_vs_CTL	Myd88	2,68192137	3,683E-139	1,524E-136	5,368E-136
CTL	CTL_CM_vs_CTL	Gbp5	9,07378264	8,836E-139	3,588E-136	1,275E-135
CTL	CTL_CM_vs_CTL	Samhd1	4,01829389	1,335E-137	5,321E-135	1,906E-134
CTL	CTL_CM_vs_CTL	Ifi35	3,71668171	4,009E-134	1,569E-131	5,608E-131
CTL	CTL_CM_vs_CTL	Ptx3	6,50765496	9,067E-132	3,485E-129	1,231E-128
CTL	CTL_CM_vs_CTL	Rnd1	4,58144051	3,891E-131	1,469E-128	5,232E-128
CTL	CTL_CM_vs_CTL	C1s1	6,79934255	1,175E-126	4,362E-124	1,536E-123
CTL	CTL_CM_vs_CTL	Rsad2	6,56853537	1,61E-123	5,873E-121	2,009E-120
CTL	CTL_CM_vs_CTL	Gbp8	9,31673353	1,087E-122	3,899E-120	1,344E-119
CTL	CTL_CM_vs_CTL	Stat1	4,85715606	3,557E-121	1,255E-118	4,284E-118
CTL	CTL_CM_vs_CTL	Ube2l6	4,90605514	5,236E-120	1,818E-117	6,094E-117
CTL	CTL_CM_vs_CTL	Lap3	1,72558622	9,903E-119	3,383E-116	1,124E-115
CTL	CTL_CM_vs_CTL	Plaat3	2,61621694	1,152E-118	3,873E-116	1,297E-115
CTL	CTL_CM_vs_CTL	Bst2	5,23879038	1,648E-118	5,457E-116	1,84E-115
CTL	CTL_CM_vs_CTL	H2-D1	4,45293058	2,716E-117	8,857E-115	3,009E-114
CTL	CTL_CM_vs_CTL	Ripk2	4,9743274	1,151E-115	3,696E-113	1,255E-112
CTL	CTL_CM_vs_CTL	Slc31a2	2,62511262	2,25E-115	7,122E-113	2,434E-112
CTL	CTL_CM_vs_CTL	Mlkl	7,89549151	7,343E-115	2,29E-112	7,883E-112
CTL	CTL_CM_vs_CTL	Nod1	2,85486175	1,658E-114	5,096E-112	1,766E-111
CTL	CTL_CM_vs_CTL	Casp1	4,07592583	4,907E-114	1,487E-111	5,148E-111
CTL	CTL_CM_vs_CTL	Gm12185	8,63530851	7,587E-113	2,268E-110	7,783E-110
CTL	CTL_CM_vs_CTL	Irf7	7,19878988	8,478E-113	2,499E-110	8,632E-110
CTL	CTL_CM_vs_CTL	Zbp1	9,22773562	2,166E-112	6,3E-110	2,174E-109
CTL	CTL_CM_vs_CTL	Apol6	9,41502713	1,348E-110	3,869E-108	1,333E-107
CTL	CTL_CM_vs_CTL	Parp11	2,82597155	1,523E-110	4,314E-108	1,496E-107
CTL	CTL_CM_vs_CTL	Ifit3b	3,6331033	1,945E-110	5,437E-108	1,897E-107
CTL	CTL_CM_vs_CTL	Casp4	7,32104094	2,721E-110	7,509E-108	2,635E-107
CTL	CTL_CM_vs_CTL	Rnf213	4,69037569	1,2E-108	3,269E-106	1,146E-105
CTL	CTL_CM_vs_CTL	Tlr2	7,64872339	1,825E-108	4,91E-106	1,719E-105
CTL	CTL_CM_vs_CTL	Tnfaip2	7,57487289	2,785E-108	7,401E-106	2,606E-105
CTL	CTL_CM_vs_CTL	Litaf	3,48531333	4,889E-108	1,283E-105	4,544E-105
CTL	CTL_CM_vs_CTL	Ifi211	5,62869798	8,846E-108	2,294E-105	8,113E-105
CTL	CTL_CM_vs_CTL	Coch	5,81251442	9,227E-108	2,364E-105	8,406E-105
CTL	CTL_CM_vs_CTL	C1rb	5,50488485	1,641E-107	4,155E-105	1,485E-104

CTL	CTL_CM_vs_CTL	Nfkbia	4,43070518	1,97E-106	4,93E-104	1,771E-103
CTL	CTL_CM_vs_CTL	Nfkbiz	4,84326291	1,567E-105	3,876E-103	1,391E-102
CTL	CTL_CM_vs_CTL	Mpeg1	8,02257236	1,408E-103	3,444E-101	1,211E-100
CTL	CTL_CM_vs_CTL	Arrdc4	4,06856429	3,613E-103	8,737E-101	3,07E-100
CTL	CTL_CM_vs_CTL	Gbp2b	7,18083094	3,818E-103	9,131E-101	3,224E-100
CTL	CTL_CM_vs_CTL	Slc2a6	7,04585023	7,847E-103	1,856E-100	6,586E-100
CTL	CTL_CM_vs_CTL	Ttc9c	1,6877691	5,269E-102	1,233E-99	4,396E-99
CTL	CTL_CM_vs_CTL	C1s2	6,89526646	3,49E-101	8,076E-99	2,8764E-98
CTL	CTL_CM_vs_CTL	Slfn2	8,09789242	1,128E-100	2,5827E-98	9,2426E-98
CTL	CTL_CM_vs_CTL	Plekhf1	2,15139419	1,008E-99	2,2845E-97	8,2139E-97
CTL	CTL_CM_vs_CTL	Mx2	5,70345134	1,643E-99	3,6835E-97	1,3305E-96
CTL	CTL_CM_vs_CTL	Znfx1	3,32273566	4,482E-99	9,9444E-97	3,5875E-96
CTL	CTL_CM_vs_CTL	Erap1	2,48138448	4,918E-99	1,08E-96	3,9137E-96
CTL	CTL_CM_vs_CTL	Cxcl16	6,23445425	6,3887E-98	1,3889E-95	5,0268E-95

Ref	Contrast	Mgi_symbol	Log2foldchange	Pvalue	Padj.by_comparison	Padj.overall
CTL_CM	NAD_CM_vs_CTL_CM	Scg2	5,06094444	6,2721E-50	9,4783E-46	2,0879E-47
CTL_CM	NAD_CM_vs_CTL_CM	Coch	-3,3557645	6,9178E-45	5,2271E-41	1,9917E-42
CTL_CM	NAD_CM_vs_CTL_CM	H2-Ab1	-1,190089	7,2522E-18	3,6532E-14	6,165E-16
CTL_CM	NAD_CM_vs_CTL_CM	Cartpt	6,36588647	8,9872E-16	3,3954E-12	6,3693E-14
CTL_CM	NAD_CM_vs_CTL_CM	Il1rn	-4,2657542	2,2953E-15	6,9372E-12	1,5634E-13
CTL_CM	NAD_CM_vs_CTL_CM	Gbp6	-0,9064783	2,8014E-15	7,0557E-12	1,885E-13
CTL_CM	NAD_CM_vs_CTL_CM	Slc6a17	1,19938827	6,8695E-14	1,483E-10	4,0326E-12
CTL_CM	NAD_CM_vs_CTL_CM	Tmem35a	1,22489964	1,9118E-13	3,6114E-10	1,071E-11
CTL_CM	NAD_CM_vs_CTL_CM	Gabarapl1	-0,5249764	2,7333E-12	4,5896E-09	1,3543E-10
CTL_CM	NAD_CM_vs_CTL_CM	Madcam1	-2,2312609	4,4902E-12	6,7855E-09	2,1628E-10
CTL_CM	NAD_CM_vs_CTL_CM	Lamp1	-0,5260712	6,0175E-12	8,267E-09	2,8567E-10
CTL_CM	NAD_CM_vs_CTL_CM	Gm38398	-1,927833	9,7582E-12	1,2289E-08	4,5514E-10
CTL_CM	NAD_CM_vs_CTL_CM	Tmem200c	-0,9937291	1,3247E-11	1,5399E-08	6,0844E-10
CTL_CM	NAD_CM_vs_CTL_CM	Basp1	0,61723653	1,6752E-11	1,8082E-08	7,5959E-10
CTL_CM	NAD_CM_vs_CTL_CM	Mest	1,83527202	2,1608E-11	2,1769E-08	9,6557E-10
CTL_CM	NAD_CM_vs_CTL_CM	Tmem171	3,03718716	4,3136E-11	3,9269E-08	1,8477E-09
CTL_CM	NAD_CM_vs_CTL_CM	Pdlim4	1,08363678	4,4175E-11	3,9269E-08	1,8895E-09
CTL_CM	NAD_CM_vs_CTL_CM	Pcyox1l	0,71106412	4,9735E-11	4,1755E-08	2,114E-09
CTL_CM	NAD_CM_vs_CTL_CM	Itih3	-2,4474718	1,8458E-10	1,4681E-07	7,2988E-09
CTL_CM	NAD_CM_vs_CTL_CM	Itpr3	1,52578431	2,084E-10	1,5746E-07	8,1896E-09
CTL_CM	NAD_CM_vs_CTL_CM	Mmp3	-3,7274922	2,9316E-10	2,1096E-07	1,1286E-08
CTL_CM	NAD_CM_vs_CTL_CM	Fktn	-0,6038424	3,3257E-10	2,2844E-07	1,274E-08
CTL_CM	NAD_CM_vs_CTL_CM	Kif1c	-0,4402022	4,5337E-10	2,9788E-07	1,706E-08
CTL_CM	NAD_CM_vs_CTL_CM	Psap	-0,5664126	6,5718E-10	4,138E-07	2,423E-08
CTL_CM	NAD_CM_vs_CTL_CM	Cnn1	1,22580759	9,2453E-10	5,5886E-07	3,3272E-08
CTL_CM	NAD_CM_vs_CTL_CM	Odc1	-0,7111568	1,1607E-09	6,7461E-07	4,1244E-08
CTL_CM	NAD_CM_vs_CTL_CM	Dlg2	-2,5596278	1,2457E-09	6,9722E-07	4,4074E-08
CTL_CM	NAD_CM_vs_CTL_CM	Timp2	-0,6605022	1,4697E-09	7,8725E-07	5,1355E-08
CTL_CM	NAD_CM_vs_CTL_CM	Mbd1	-0,6896648	1,5161E-09	7,8725E-07	5,2859E-08
CTL_CM	NAD_CM_vs_CTL_CM	BC023105	-0,8529926	1,5629E-09	7,8725E-07	5,4408E-08
CTL_CM	NAD_CM_vs_CTL_CM	Gm4841	-0,9286378	1,6149E-09	7,8725E-07	5,6176E-08
CTL_CM	NAD_CM_vs_CTL_CM	Igsf1	-1,5974624	2,4847E-09	1,1734E-06	8,417E-08
CTL_CM	NAD_CM_vs_CTL_CM	Tom1	-0,757091	3,1875E-09	1,4597E-06	1,0623E-07
CTL_CM	NAD_CM_vs_CTL_CM	Ciita	-0,8159633	3,3003E-09	1,4669E-06	1,0978E-07
CTL_CM	NAD_CM_vs_CTL_CM	Tcerg1l	-2,1702496	3,9232E-09	1,6939E-06	1,2911E-07
CTL_CM	NAD_CM_vs_CTL_CM	Fmod	-1,7915456	9,2295E-09	3,8743E-06	2,8897E-07
CTL_CM	NAD_CM_vs_CTL_CM	Ldhd	1,22923081	9,9672E-09	4,0709E-06	3,1003E-07
CTL_CM	NAD_CM_vs_CTL_CM	Lingo3	1,49619541	1,2496E-08	4,9696E-06	3,826E-07
CTL_CM	NAD_CM_vs_CTL_CM	Sat1	0,84802752	1,5304E-08	5,93E-06	4,6192E-07
CTL_CM	NAD_CM_vs_CTL_CM	Ltbp2	-1,6946488	1,7082E-08	6,3676E-06	5,1136E-07
CTL_CM	NAD_CM_vs_CTL_CM	Tcim	2,1401528	1,7327E-08	6,3676E-06	5,1801E-07
CTL_CM	NAD_CM_vs_CTL_CM	Liph	1,81823025	1,7697E-08	6,3676E-06	5,2874E-07

CTL_CM	NAD_CM_vs_CTL_CM	Plppr4	-0,7335164	1,8852E-08	6,6253E-06	5,6034E-07
CTL_CM	NAD_CM_vs_CTL_CM	Ampd3	-0,9596787	2,1421E-08	7,3572E-06	6,2982E-07
CTL_CM	NAD_CM_vs_CTL_CM	Apoe	-0,5442055	2,6549E-08	8,9157E-06	7,7092E-07
CTL_CM	NAD_CM_vs_CTL_CM	Rida	-0,5600988	2,7344E-08	8,9832E-06	7,9253E-07
CTL_CM	NAD_CM_vs_CTL_CM	Xrn2	0,32701068	3,0482E-08	9,8011E-06	8,7614E-07
CTL_CM	NAD_CM_vs_CTL_CM	Pspc1	0,80305981	4,6497E-08	1,4639E-05	1,2977E-06
CTL_CM	NAD_CM_vs_CTL_CM	Peg10	0,74302332	4,8744E-08	1,5033E-05	1,356E-06
CTL_CM	NAD_CM_vs_CTL_CM	Aldh1a3	-2,4585369	5,6945E-08	1,7211E-05	1,5663E-06
CTL_CM	NAD_CM_vs_CTL_CM	Flnc	0,9418043	7,4805E-08	2,21E-05	2,0229E-06
CTL_CM	NAD_CM_vs_CTL_CM	Sh3bp5	-0,895845	7,6045E-08	2,21E-05	2,0548E-06
CTL_CM	NAD_CM_vs_CTL_CM	Snta1	-0,4700778	9,7558E-08	2,7817E-05	2,5941E-06
CTL_CM	NAD_CM_vs_CTL_CM	Zfp36l1	0,33006218	1,0484E-07	2,934E-05	2,7754E-06
CTL_CM	NAD_CM_vs_CTL_CM	Msln	3,15670233	1,1029E-07	3,0303E-05	2,9063E-06
CTL_CM	NAD_CM_vs_CTL_CM	H2-Aa	-0,9177737	1,2543E-07	3,3848E-05	3,2699E-06
CTL_CM	NAD_CM_vs_CTL_CM	S1pr1	0,79554727	1,2838E-07	3,4035E-05	3,3379E-06
CTL_CM	NAD_CM_vs_CTL_CM	Slc36a2	-3,2614101	1,4284E-07	3,7216E-05	3,6862E-06
CTL_CM	NAD_CM_vs_CTL_CM	Clspn	2,20451783	1,5003E-07	3,8429E-05	3,8597E-06
CTL_CM	NAD_CM_vs_CTL_CM	Ifi27	-1,1350454	1,6817E-07	4,2357E-05	4,2912E-06
CTL_CM	NAD_CM_vs_CTL_CM	Pcyox1	-0,3177938	1,7189E-07	4,2382E-05	4,3755E-06
CTL_CM	NAD_CM_vs_CTL_CM	Cntnap1	-1,1302263	1,7388E-07	4,2382E-05	4,4247E-06
CTL_CM	NAD_CM_vs_CTL_CM	Npy	-1,099789	2,4977E-07	5,8571E-05	6,1665E-06
CTL_CM	NAD_CM_vs_CTL_CM	Adap1	-0,6144447	2,518E-07	5,8571E-05	6,2122E-06
CTL_CM	NAD_CM_vs_CTL_CM	Calca	1,81669045	2,5227E-07	5,8571E-05	6,2207E-06
CTL_CM	NAD_CM_vs_CTL_CM	Timeless	1,46136225	2,558E-07	5,8571E-05	6,2998E-06
CTL_CM	NAD_CM_vs_CTL_CM	Umps	0,72059676	4,1211E-07	9,2951E-05	9,7989E-06
CTL_CM	NAD_CM_vs_CTL_CM	Sox21	0,8835928	4,486E-07	9,9695E-05	1,061E-05
CTL_CM	NAD_CM_vs_CTL_CM	Faap20	-0,5932677	4,9129E-07	0,0001076	1,1535E-05
CTL_CM	NAD_CM_vs_CTL_CM	Map1lc3b	-0,3208565	5,1834E-07	0,0001119	1,2125E-05
CTL_CM	NAD_CM_vs_CTL_CM	Pclaf	1,89345621	5,4227E-07	0,00011542	1,2634E-05
CTL_CM	NAD_CM_vs_CTL_CM	Gm12185	-0,6454266	5,9618E-07	0,00012513	1,3774E-05
CTL_CM	NAD_CM_vs_CTL_CM	Prdx1	-0,7248906	6,1673E-07	0,00012767	1,4227E-05
CTL_CM	NAD_CM_vs_CTL_CM	Hmgn3	-0,5687805	6,5127E-07	0,00013202	1,4979E-05
CTL_CM	NAD_CM_vs_CTL_CM	4833439L19Rik	-0,3461368	6,552E-07	0,00013202	1,5064E-05
CTL_CM	NAD_CM_vs_CTL_CM	Net1	0,93076181	7,1786E-07	0,00014274	1,638E-05
CTL_CM	NAD_CM_vs_CTL_CM	Ggcx	0,57791455	7,4839E-07	0,0001451	1,6996E-05
CTL_CM	NAD_CM_vs_CTL_CM	Klk8	2,8822085	7,4893E-07	0,0001451	1,7005E-05
CTL_CM	NAD_CM_vs_CTL_CM	Crym	1,22564456	8,0525E-07	0,00015372	1,817E-05
CTL_CM	NAD_CM_vs_CTL_CM	Lamb3	-2,0861529	8,1436E-07	0,00015372	1,8361E-05
CTL_CM	NAD_CM_vs_CTL_CM	Lrrn3	1,01466429	8,2396E-07	0,00015372	1,855E-05
CTL_CM	NAD_CM_vs_CTL_CM	Ctsh	0,64042901	8,5672E-07	0,00015789	1,9216E-05
CTL_CM	NAD_CM_vs_CTL_CM	Sirt2	-0,5362765	9,9611E-07	0,00018136	2,2067E-05
CTL_CM	NAD_CM_vs_CTL_CM	Otud1	0,76901364	1,0294E-06	0,00018519	2,2714E-05
CTL_CM	NAD_CM_vs_CTL_CM	Zfp984	-0,6588571	1,1303E-06	0,00020096	2,4713E-05

CTL_CM	NAD_CM_vs_CTL_CM	Sall1	0,34406658	1,2019E-06	0,00021119	2,6136E-05
CTL_CM	NAD_CM_vs_CTL_CM	Glb1l2	1,14044517	1,2833E-06	0,0002229	2,7732E-05
CTL_CM	NAD_CM_vs_CTL_CM	Pon2	-0,3957687	1,3288E-06	0,00022819	2,8609E-05
CTL_CM	NAD_CM_vs_CTL_CM	Thbs2	1,30575526	1,507E-06	0,00025407	3,2122E-05
CTL_CM	NAD_CM_vs_CTL_CM	C1rb	-0,6235284	1,5131E-06	0,00025407	3,2222E-05
CTL_CM	NAD_CM_vs_CTL_CM	Sox1	0,63379406	1,6727E-06	0,00027777	3,5337E-05
CTL_CM	NAD_CM_vs_CTL_CM	Npc2	-0,5453077	1,7715E-06	0,00028844	3,7293E-05
CTL_CM	NAD_CM_vs_CTL_CM	Snx8	-0,5776498	1,7751E-06	0,00028844	3,7358E-05
CTL_CM	NAD_CM_vs_CTL_CM	Nr4a3	1,14348875	1,9399E-06	0,00031186	4,0512E-05
CTL_CM	NAD_CM_vs_CTL_CM	Tmem260	-0,4676975	2,1302E-06	0,00033885	4,4074E-05
CTL_CM	NAD_CM_vs_CTL_CM	Stc2	-1,8579781	2,1736E-06	0,00034216	4,4878E-05
CTL_CM	NAD_CM_vs_CTL_CM	Zyg11b	-0,3392642	2,3657E-06	0,00036856	4,8476E-05
CTL_CM	NAD_CM_vs_CTL_CM	Ccdc93	-0,5695617	2,4607E-06	0,00037945	5,0297E-05
CTL_CM	NAD_CM_vs_CTL_CM	Celrr	-1,5044089	2,4985E-06	0,00038067	5,1024E-05

Ref	Contrast	Mgi_symbol	Log2foldchange	Pvalue	Padj.by_comparison	Padj.overall
NAD	NAD_CM_vs_NAD	Irf1	5,53229255	-inf	-inf	-inf
NAD	NAD_CM_vs_NAD	Irgm1	5,50713908	-inf	-inf	-inf
NAD	NAD_CM_vs_NAD	Tap1	4,93499853	-inf	-inf	-inf
NAD	NAD_CM_vs_NAD	Gbp6	6,7923992	-inf	-inf	-inf
NAD	NAD_CM_vs_NAD	Wars	3,93094112	-inf	-inf	-inf
NAD	NAD_CM_vs_NAD	H2-Q4	5,91061025	-inf	-inf	-inf
NAD	NAD_CM_vs_NAD	Igtp	7,14559649	-inf	-inf	-inf
NAD	NAD_CM_vs_NAD	Tap2	3,60680677	1,194E-297	3,117E-294	8,704E-294
NAD	NAD_CM_vs_NAD	Nlrc5	6,00003434	1,508E-292	3,499E-289	9,08E-289
NAD	NAD_CM_vs_NAD	Gbp10	8,79036817	2,418E-266	5,048E-263	1,288E-262
NAD	NAD_CM_vs_NAD	Ly6e	5,55993752	3,341E-266	6,343E-263	1,714E-262
NAD	NAD_CM_vs_NAD	Cd274	5,91948015	7,794E-264	1,356E-260	3,722E-260
NAD	NAD_CM_vs_NAD	Gbp2	4,98461913	1,028E-259	1,651E-256	4,745E-256
NAD	NAD_CM_vs_NAD	Tapbp	3,59946282	4,056E-259	6,05E-256	1,812E-255
NAD	NAD_CM_vs_NAD	Psmb10	4,68519457	2,149E-258	2,992E-255	9,299E-255
NAD	NAD_CM_vs_NAD	Psme1	2,96435728	1,388E-256	1,811E-253	5,491E-253
NAD	NAD_CM_vs_NAD	Gbp11	8,08844005	2,28E-243	2,801E-240	8,771E-240
NAD	NAD_CM_vs_NAD	Parp12	3,55547442	5,199E-240	6,031E-237	1,895E-236
NAD	NAD_CM_vs_NAD	Psmb8	5,97287244	1,28E-231	1,407E-228	4,323E-228
NAD	NAD_CM_vs_NAD	Gbp7	4,95612094	2,867E-230	2,994E-227	9,453E-227
NAD	NAD_CM_vs_NAD	Ifit3	4,56163844	9,633E-225	9,579E-222	2,964E-221
NAD	NAD_CM_vs_NAD	Irgm2	6,11312862	6,989E-210	6,633E-207	1,975E-206
NAD	NAD_CM_vs_NAD	Ifi204	5,53119942	1,483E-197	1,346E-194	4,107E-194
NAD	NAD_CM_vs_NAD	B2m	3,88005661	3,66E-196	3,184E-193	9,937E-193
NAD	NAD_CM_vs_NAD	Dtx3l	3,98722107	2,26E-194	1,887E-191	6,018E-191
NAD	NAD_CM_vs_NAD	H2-K1	4,64657209	4,032E-194	3,239E-191	1,054E-190
NAD	NAD_CM_vs_NAD	H2-Ab1	6,7975594	6,223E-183	4,813E-180	1,567E-179
NAD	NAD_CM_vs_NAD	Irf8	6,91642995	1,652E-182	1,232E-179	4,086E-179
NAD	NAD_CM_vs_NAD	Cd74	10,3705845	2,345E-176	1,689E-173	5,505E-173
NAD	NAD_CM_vs_NAD	Psmb9	5,86252605	1,954E-167	1,36E-164	4,365E-164
NAD	NAD_CM_vs_NAD	Dhx58	5,62920055	2,411E-164	1,624E-161	5,216E-161
NAD	NAD_CM_vs_NAD	Ciita	6,27064172	1,482E-156	9,673E-154	2,891E-153
NAD	NAD_CM_vs_NAD	Il18bp	6,02411358	2,089E-152	1,322E-149	3,806E-149
NAD	NAD_CM_vs_NAD	Iigp1	10,7274006	2,789E-152	1,713E-149	5,017E-149
NAD	NAD_CM_vs_NAD	Kars	1,77309585	4,625E-151	2,759E-148	8,006E-148
NAD	NAD_CM_vs_NAD	Psme2	3,04342761	1,158E-149	6,719E-147	1,98E-146
NAD	NAD_CM_vs_NAD	Gbp9	5,1666817	1,114E-146	6,285E-144	1,858E-143
NAD	NAD_CM_vs_NAD	Nampt	2,44413104	4,874E-144	2,678E-141	7,888E-141
NAD	NAD_CM_vs_NAD	Slfn8	8,60249527	5,18E-144	2,774E-141	8,246E-141
NAD	NAD_CM_vs_NAD	Trim21	3,05362873	9,847E-142	5,141E-139	1,532E-138
NAD	NAD_CM_vs_NAD	Gbp5	9,24767359	3,524E-141	1,795E-138	5,422E-138
NAD	NAD_CM_vs_NAD	Plekhf1	2,67851674	2,668E-140	1,327E-137	4,06E-137

NAD	NAD_CM_vs_NAD	Asap3	3,03283288	1,912E-139	9,285E-137	2,817E-136
NAD	NAD_CM_vs_NAD	Tapbpl	3,32275905	3,635E-136	1,725E-133	5,136E-133
NAD	NAD_CM_vs_NAD	Gbp3	5,11230774	7,291E-134	3,383E-131	1,01E-130
NAD	NAD_CM_vs_NAD	Ifi35	3,61752929	9,19E-134	4,172E-131	1,26E-130
NAD	NAD_CM_vs_NAD	H2-Q6	6,50872259	1,875E-127	8,329E-125	2,496E-124
NAD	NAD_CM_vs_NAD	Trafd1	2,34778019	3,215E-127	1,399E-124	4,24E-124
NAD	NAD_CM_vs_NAD	Rnf213	5,06489529	3,076E-126	1,311E-123	3,981E-123
NAD	NAD_CM_vs_NAD	Mlkl	7,49932886	2,076E-124	8,669E-122	2,662E-121
NAD	NAD_CM_vs_NAD	Rnd1	4,47332118	7,99E-124	3,271E-121	1,015E-120
NAD	NAD_CM_vs_NAD	Samhd1	3,80105492	1,607E-123	6,452E-121	2,009E-120
NAD	NAD_CM_vs_NAD	Parp14	5,27523333	1,154E-121	4,546E-119	1,414E-118
NAD	NAD_CM_vs_NAD	Gbp8	10,3521436	1,265E-121	4,892E-119	1,537E-118
NAD	NAD_CM_vs_NAD	Parp9	3,72751994	4,613E-121	1,752E-118	5,507E-118
NAD	NAD_CM_vs_NAD	Ube2l6	4,92696182	8,888E-121	3,314E-118	1,052E-117
NAD	NAD_CM_vs_NAD	Arel1	2,55746209	1,225E-120	4,486E-118	1,437E-117
NAD	NAD_CM_vs_NAD	Stat1	4,8501585	7,282E-120	2,622E-117	8,404E-117
NAD	NAD_CM_vs_NAD	Rsad2	6,44631955	1,029E-119	3,643E-117	1,178E-116
NAD	NAD_CM_vs_NAD	Plaat3	2,60643148	5,742E-116	1,998E-113	6,311E-113
NAD	NAD_CM_vs_NAD	Bst2	5,14919311	1,753E-114	5,999E-112	1,853E-111
NAD	NAD_CM_vs_NAD	Mx2	5,85213456	6,303E-114	2,123E-111	6,563E-111
NAD	NAD_CM_vs_NAD	Myd88	2,37770676	8,75E-114	2,9E-111	9,042E-111
NAD	NAD_CM_vs_NAD	Tnfaip2	7,8031917	1,145E-112	3,736E-110	1,158E-109
NAD	NAD_CM_vs_NAD	C1s1	6,38146032	9,315E-112	2,993E-109	9,281E-109
NAD	NAD_CM_vs_NAD	Vcam1	4,49985928	2,254E-109	7,131E-107	2,168E-106
NAD	NAD_CM_vs_NAD	Erap1	2,61077688	1,336E-108	4,165E-106	1,267E-105
NAD	NAD_CM_vs_NAD	Ifit3b	3,58088523	6,849E-108	2,103E-105	6,323E-105
NAD	NAD_CM_vs_NAD	H2-D1	4,23117621	5,126E-106	1,551E-103	4,579E-103
NAD	NAD_CM_vs_NAD	Mpeg1	8,25467603	1,734E-105	5,172E-103	1,529E-102
NAD	NAD_CM_vs_NAD	Znfx1	3,42084776	4,104E-105	1,207E-102	3,597E-102
NAD	NAD_CM_vs_NAD	Zbp1	9,88716034	8,22E-105	2,384E-102	7,159E-102
NAD	NAD_CM_vs_NAD	Irf7	6,91380368	1,495E-104	4,276E-102	1,294E-101
NAD	NAD_CM_vs_NAD	Snx10	2,14346777	2,441E-103	6,889E-101	2,087E-100
NAD	NAD_CM_vs_NAD	Ifi211	4,92398301	6,604E-102	1,839E-99	5,477E-99
NAD	NAD_CM_vs_NAD	Ripk2	4,58897266	1,898E-99	5,2162E-97	1,5285E-96
NAD	NAD_CM_vs_NAD	Parp11	2,66616916	5,772E-99	1,5652E-96	4,5671E-96
NAD	NAD_CM_vs_NAD	Casp4	7,65996469	7,1884E-98	1,9245E-95	5,624E-95
NAD	NAD_CM_vs_NAD	Tlr2	7,37902678	7,8296E-98	2,0696E-95	6,0913E-95
NAD	NAD_CM_vs_NAD	Nfkbiz	4,59934125	8,9294E-98	2,3308E-95	6,8698E-95
NAD	NAD_CM_vs_NAD	Lap3	1,55788737	1,0237E-96	2,6392E-94	7,8324E-94
NAD	NAD_CM_vs_NAD	Slc2a6	6,66825457	7,0323E-96	1,7908E-93	5,3508E-93
NAD	NAD_CM_vs_NAD	Ptx3	5,43282183	4,0417E-93	1,0168E-90	3,0418E-90
NAD	NAD_CM_vs_NAD	Gbp2b	7,1085792	1,4369E-92	3,5721E-90	1,0756E-89
NAD	NAD_CM_vs_NAD	Nod1	2,57035617	6,7811E-92	1,6659E-89	5,0486E-89

NAD	NAD_CM_vs_NAD	Herc6	4,22515136	2,131E-91	5,1743E-89	1,5697E-88
NAD	NAD_CM_vs_NAD	Nfkbia	4,07079458	5,2821E-91	1,2678E-88	3,8702E-88
NAD	NAD_CM_vs_NAD	Rmdn3	2,07926389	2,4793E-90	5,8832E-88	1,7882E-87
NAD	NAD_CM_vs_NAD	Cd47	1,98111714	1,9444E-89	4,5622E-87	1,3668E-86
NAD	NAD_CM_vs_NAD	C1s2	6,4490882	9,5313E-89	2,2115E-86	6,5667E-86
NAD	NAD_CM_vs_NAD	Lgals3bp	4,0188811	4,2755E-88	9,8112E-86	2,9166E-85
NAD	NAD_CM_vs_NAD	Gm4951	8,84732937	5,2658E-88	1,1952E-85	3,5746E-85
NAD	NAD_CM_vs_NAD	C1rb	4,31040586	1,804E-87	4,0507E-85	1,2187E-84
NAD	NAD_CM_vs_NAD	Slc31a2	2,1884908	2,5238E-85	5,6067E-83	1,6564E-82
NAD	NAD_CM_vs_NAD	Slfn2	8,10776265	8,3693E-85	1,8397E-82	5,467E-82
NAD	NAD_CM_vs_NAD	Trim25	2,79533862	5,8619E-84	1,2751E-81	3,7756E-81
NAD	NAD_CM_vs_NAD	Isg15	6,60316558	1,3065E-83	2,8127E-81	8,3764E-81
NAD	NAD_CM_vs_NAD	Uaca	1,4783408	2,1E-82	4,4747E-80	1,334E-79
NAD	NAD_CM_vs_NAD	Ifi44	8,2445365	7,0078E-82	1,4781E-79	4,4312E-79

2.7. Summary RNA-sequencing data DA-exposed astrocytes compared to non-exposed astrocytes.

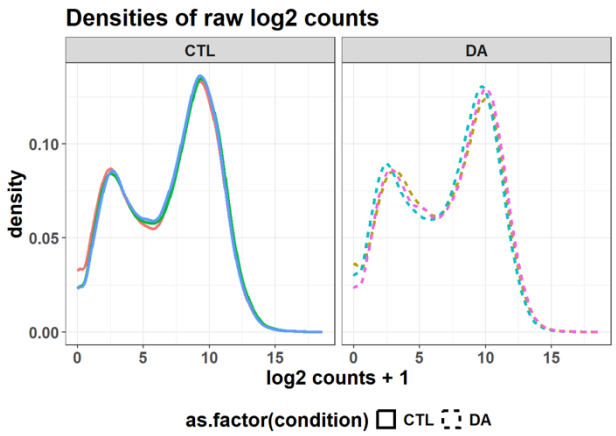

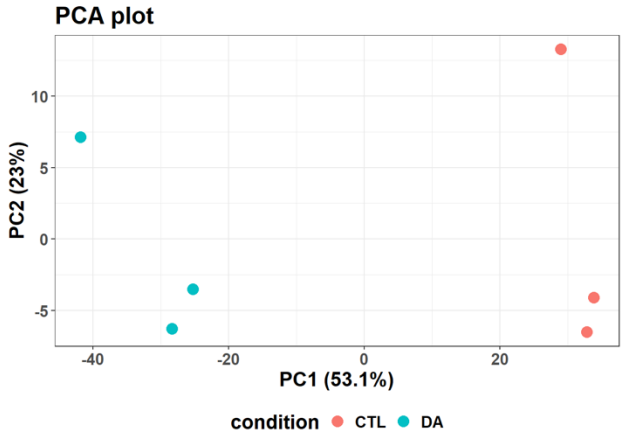

Mean gene expression:

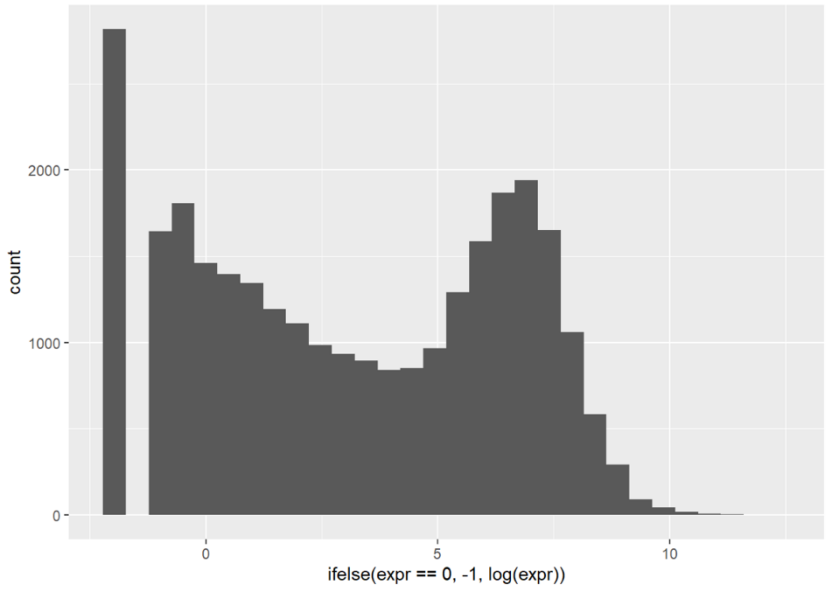

Overview of DESeq2 comparisons

Overview of DESeq2 comparisons

ref	comp	n
CTL	DA	23458

	no. of DEG
DA_vs_CTL	9661

Table 24: Top 100 DEGs in DA versus CTL according to padj.overall.

Ref	Contrast	Gene	Log2foldchange	Pvalue	Padj.by_comparison	Padj.overall
CTL	DA vs. CTL	Ctnna2	-6,8721339	2,18E-163	4,219E-159	4,219E-159
CTL	DA vs. CTL	Sorcs1	-5,9162946	1,007E-159	9,744E-156	9,744E-156
CTL	DA vs. CTL	C3	-3,6701415	3,659E-152	2,361E-148	2,361E-148
CTL	DA vs. CTL	Vps13b	-5,5887562	3,249E-144	1,572E-140	1,572E-140
CTL	DA vs. CTL	Gpc6	-6,5189884	2,127E-143	8,233E-140	8,233E-140
CTL	DA vs. CTL	Adra2a	-4,4183803	8,912E-136	2,875E-132	2,875E-132
CTL	DA vs. CTL	Cpq	-2,8067336	6,113E-130	1,69E-126	1,69E-126
CTL	DA vs. CTL	Atrnl1	-3,8835255	4,6E-129	1,113E-125	1,113E-125
CTL	DA vs. CTL	Slc38a3	-3,3069891	1,073E-127	2,308E-124	2,308E-124
CTL	DA vs. CTL	Pard3b	-7,5408981	1,489E-126	2,881E-123	2,881E-123
CTL	DA vs. CTL	Ptprd	-6,5653826	3,127E-125	5,502E-122	5,502E-122
CTL	DA vs. CTL	Gabrb1	-6,4289484	1,203E-114	1,94E-111	1,94E-111
CTL	DA vs. CTL	Ptprm	-5,0182357	6,513E-114	9,697E-111	9,697E-111
CTL	DA vs. CTL	Cfap54	-3,3039918	1,649E-112	2,279E-109	2,279E-109
CTL	DA vs. CTL	Nebl	-3,4528993	2,123E-110	2,739E-107	2,739E-107
CTL	DA vs. CTL	Exoc4	-4,6255879	2,336E-106	2,825E-103	2,825E-103
CTL	DA vs. CTL	Cadps	-5,8429573	4,911E-103	5,591E-100	5,591E-100
CTL	DA vs. CTL	Diaph2	-5,4853128	3,913E-102	4,207E-99	4,207E-99
CTL	DA vs. CTL	Lpp	-5,7903995	3,013E-101	3,0692E-98	3,0692E-98
CTL	DA vs. CTL	Srxn1	2,40295136	6,418E-101	6,2104E-98	6,2104E-98
CTL	DA vs. CTL	Bcas3	-4,5972279	5,662E-99	5,2178E-96	5,2178E-96
CTL	DA vs. CTL	Rsrc1	-4,9381029	7,382E-99	6,4944E-96	6,4944E-96
CTL	DA vs. CTL	Gria1	-4,7451311	1,0937E-98	9,203E-96	9,203E-96
CTL	DA vs. CTL	Pacrg	-4,7486527	7,7338E-96	6,2367E-93	6,2367E-93
CTL	DA vs. CTL	Dennd1a	-5,2722434	3,877E-95	3,0014E-92	3,0014E-92
CTL	DA vs. CTL	Npas3	-5,8626688	2,7322E-94	2,0338E-91	2,0338E-91
CTL	DA vs. CTL	Ctnnd2	-4,7270486	1,1936E-91	8,5561E-89	8,5561E-89
CTL	DA vs. CTL	Robo2	-5,7335644	2,5078E-91	1,7334E-88	1,7334E-88
CTL	DA vs. CTL	Ptprk	-4,4361627	3,4867E-91	2,327E-88	2,327E-88
CTL	DA vs. CTL	Cdh4	-6,2623428	5,6489E-90	3,6443E-87	3,6443E-87
CTL	DA vs. CTL	Adk	-4,3643497	4,8994E-89	3,0588E-86	3,0588E-86
CTL	DA vs. CTL	Slc39a11	-3,83719	3,6402E-88	2,2016E-85	2,2016E-85
CTL	DA vs. CTL	Ptprg	-5,2298753	4,3189E-88	2,533E-85	2,533E-85
CTL	DA vs. CTL	Prkce	-5,7637696	3,6581E-86	2,0823E-83	2,0823E-83
CTL	DA vs. CTL	Sod3	2,08122664	8,0956E-86	4,4766E-83	4,4766E-83
CTL	DA vs. CTL	Dgki	-4,1952692	1,8461E-84	9,9249E-82	9,9249E-82
CTL	DA vs. CTL	Slc35f1	-4,4434739	7,0753E-83	3,701E-80	3,701E-80
CTL	DA vs. CTL	Megf11	-4,624729	8,786E-82	4,4749E-79	4,4749E-79
CTL	DA vs. CTL	Tmem117	-5,0740497	3,2344E-80	1,6051E-77	1,6051E-77
CTL	DA vs. CTL	Scaper	-4,4482852	5,7199E-79	2,7676E-76	2,7676E-76

CTL	DA vs. CTL	Mdga2	-4,0387511	2,7779E-78	1,3113E-75	1,3113E-75
CTL	DA vs. CTL	Dner	-3,1294594	3,0104E-78	1,3872E-75	1,3872E-75
CTL	DA vs. CTL	Ccdc148	-4,0563292	9,8636E-78	4,4396E-75	4,4396E-75
CTL	DA vs. CTL	Igsf1	-3,4514488	2,6057E-77	1,1461E-74	1,1461E-74
CTL	DA vs. CTL	Bace2	-2,7333503	7,9605E-77	3,4237E-74	3,4237E-74
CTL	DA vs. CTL	Fbxl17	-4,122938	2,757E-76	1,16E-73	1,16E-73
CTL	DA vs. CTL	Adamtsl1	-3,8992614	7,616E-76	3,1362E-73	3,1362E-73
CTL	DA vs. CTL	Vti1a	-3,2680757	1,717E-75	6,9232E-73	6,9232E-73
CTL	DA vs. CTL	Nlgn1	-4,8348587	4,5099E-75	1,7813E-72	1,7813E-72
CTL	DA vs. CTL	Cadm2	-7,0195249	7,1513E-75	2,7681E-72	2,7681E-72
CTL	DA vs. CTL	Cep128	-5,3071711	1,2849E-74	4,876E-72	4,876E-72
CTL	DA vs. CTL	Arsb	-2,2261436	2,5953E-74	9,6593E-72	9,6593E-72
CTL	DA vs. CTL	Nkain2	-5,4710936	2,7228E-72	9,9427E-70	9,9427E-70
CTL	DA vs. CTL	Vwa8	-3,2991465	3,0919E-72	1,1082E-69	1,1082E-69
CTL	DA vs. CTL	Negr1	-7,6983257	1,3411E-71	4,7191E-69	4,7191E-69
CTL	DA vs. CTL	Dok6	-6,0243637	4,4635E-71	1,5426E-68	1,5426E-68
CTL	DA vs. CTL	Dab1	-5,3911503	9,7953E-71	3,3259E-68	3,3259E-68
CTL	DA vs. CTL	Igfbp5	-3,9102531	7,6843E-69	2,5642E-66	2,5642E-66
CTL	DA vs. CTL	Dock1	-3,5780451	1,4949E-67	4,9038E-65	4,9038E-65
CTL	DA vs. CTL	Galnt17	-5,3769798	3,5997E-67	1,1612E-64	1,1612E-64
CTL	DA vs. CTL	Lrba	-4,6347985	1,257E-66	3,9883E-64	3,9883E-64
CTL	DA vs. CTL	Trappc9	-5,0766928	1,6828E-66	5,2529E-64	5,2529E-64
CTL	DA vs. CTL	Thsd7a	-4,6814139	2,1477E-66	6,5979E-64	6,5979E-64
CTL	DA vs. CTL	Adgrl3	-6,3193394	2,8716E-66	8,6839E-64	8,6839E-64
CTL	DA vs. CTL	Nbea	-4,381578	3,443E-66	1,0252E-63	1,0252E-63
CTL	DA vs. CTL	Hmox1	2,60861986	4,0649E-66	1,192E-63	1,192E-63
CTL	DA vs. CTL	Exoc6b	-3,7542073	5,4845E-66	1,561E-63	1,561E-63
CTL	DA vs. CTL	Tmtc1	-4,4691903	5,4156E-66	1,561E-63	1,561E-63
CTL	DA vs. CTL	Nalcn	-4,4975945	2,152E-65	6,0363E-63	6,0363E-63
CTL	DA vs. CTL	Lama2	-4,4197308	4,8499E-65	1,3409E-62	1,3409E-62
CTL	DA vs. CTL	Fam172a	-3,6445548	9,8471E-65	2,6842E-62	2,6842E-62
CTL	DA vs. CTL	Cux1	-2,9342135	7,6583E-64	2,0586E-61	2,0586E-61
CTL	DA vs. CTL	App	-2,4116218	1,2625E-63	3,3471E-61	3,3471E-61
CTL	DA vs. CTL	Erbb4	-7,2422789	1,3159E-63	3,4416E-61	3,4416E-61
CTL	DA vs. CTL	Large1	-5,5829594	1,028E-62	2,6527E-60	2,6527E-60
CTL	DA vs. CTL	Plxna4	-6,4338411	3,1818E-62	8,1028E-60	8,1028E-60
CTL	DA vs. CTL	Itih5	-3,984928	2,6023E-61	6,541E-59	6,541E-59
CTL	DA vs. CTL	Samd12	-5,0268527	1,633E-60	4,052E-58	4,052E-58
CTL	DA vs. CTL	Msi2	-3,0672437	5,3747E-60	1,3167E-57	1,3167E-57
CTL	DA vs. CTL	Ppp1r9a	-2,904564	1,9898E-59	4,8138E-57	4,8138E-57
CTL	DA vs. CTL	Mt2	-2,4688067	4,5164E-59	1,0791E-56	1,0791E-56
CTL	DA vs. CTL	B3galt1	-6,7775477	1,6272E-58	3,8406E-56	3,8406E-56
CTL	DA vs. CTL	Rbms3	-6,6839584	1,7613E-58	4,1071E-56	4,1071E-56

CTL	DA vs. CTL	Snd1	-4,6430284	1,8911E-58	4,3571E-56	4,3571E-56
CTL	DA vs. CTL	Cacna1d	-5,3686009	2,8176E-58	6,4155E-56	6,4155E-56
CTL	DA vs. CTL	Slit3	-4,4758395	3,399E-58	7,6494E-56	7,6494E-56
CTL	DA vs. CTL	Gphn	-5,6105135	4,7982E-58	1,0674E-55	1,0674E-55
CTL	DA vs. CTL	Babam2	-4,1946999	8,3271E-58	1,8314E-55	1,8314E-55
CTL	DA vs. CTL	Slc9a9	-6,6672442	1,5772E-57	3,4298E-55	3,4298E-55
CTL	DA vs. CTL	Dnah11	-3,7818039	2,4438E-57	5,2552E-55	5,2552E-55
CTL	DA vs. CTL	Astn1	-4,5730301	8,3098E-57	1,7673E-54	1,7673E-54
CTL	DA vs. CTL	Pdia4	-1,4675308	2,5615E-56	5,3886E-54	5,3886E-54
CTL	DA vs. CTL	Ndrg1	-2,8910612	8,1083E-56	1,6874E-53	1,6874E-53
CTL	DA vs. CTL	Efcab2	-2,5361114	1,0516E-55	2,1652E-53	2,1652E-53
CTL	DA vs. CTL	Reck	-2,0712624	8,5904E-55	1,7501E-52	1,7501E-52
CTL	DA vs. CTL	Rgs7	-5,0944622	1,2736E-54	2,5676E-52	2,5676E-52
CTL	DA vs. CTL	Ccdc9b	1,87041675	2,743E-54	5,4729E-52	5,4729E-52
CTL	DA vs. CTL	Cacna2d1	-3,9880335	3,1017E-54	6,1256E-52	6,1256E-52
CTL	DA vs. CTL	Rian	-2,7815961	3,4165E-54	6,6791E-52	6,6791E-52